

Reliability Analysis of Soil Slopes

Sahithi Arukonda

A Dissertation Submitted to
Indian Institute of Technology Hyderabad
In Partial Fulfillment of the Requirements for
The Degree of Master of Technology



भारतीय प्रौद्योगिकी संस्थान हैदराबाद
Indian Institute of Technology Hyderabad

Department of Civil Engineering

July, 2015

Declaration

I declare that this written submission represents my ideas in my own words, and where others' ideas or words have been included, I have adequately cited and referenced the original sources. I also declare that I have adhered to all principles of academic honesty and integrity and have not misrepresented or fabricated or falsified any idea/data/fact/source in my submission. I understand that any violation of the above will be a cause for disciplinary action by the Institute and can also evoke penal action from the sources that have thus not been properly cited, or from whom proper permission has not been taken when needed.

Sahithi D

(Signature)

Sahithi Arukonda

CE13M1013

Approval Sheet

This thesis entitled Reliability Analysis of Soil Slopes by Sahithi Arukonda is approved for the degree of Master of Technology from IIT Hyderabad.



Dr. C. Viswanath

Assistant Professor

Department of Mechanical and Aerospace Engineering

Indian Institute of Technology Hyderabad

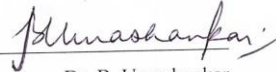


Dr. S. Sireesh

Associate Professor

Department of civil Engineering

Indian Institute of Technology Hyderabad

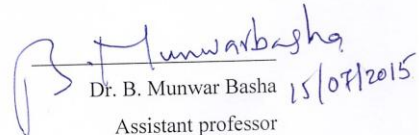


Dr. B. Umashankar

Assistant professor

Department of civil Engineering

Indian Institute of Technology Hyderabad



Dr. B. Munwar Basha

Assistant professor

Department of civil Engineering

Indian Institute of Technology Hyderabad

Acknowledgements

The research presented in this thesis is the result of the work carried out during the years 2014 - 2015 at the Indian Institute of Technology, Hyderabad.

Behind this work there are important contributions and the significant support of a certain number of persons, whom I would like to thank sincerely.

I wish to express first of all my deep gratitude to Dr. B. Munwar Basha for his extensive, invaluable and steadfast guidance, for his support and patience, sharing his knowledge and experience, throughout my Masters studies.

I would like to thank all the people who contributed in some way to the work described in this thesis. Every result described in this thesis was accomplished with the help and support of fellow lab mates and friends and I they will forever have my gratitude.

I would like to acknowledge the Department of Civil Engineering at IIT Hyderabad. My graduate experience benefitted greatly from the courses I took, the opportunities serve as a teaching assistant, and the high-quality seminars that the department organized.

Finally, I would like to acknowledge friends and family who supported me during my time here and without whom this work wouldn't have been possible. I thank my parents, my sister, my friends and all the people I have met during my stay here who gave me indispensable support through their company and advice.

Sahithi Arukonda

July, 2015

Dedicated to

My Parents

Abstract

Slope stability analysis is a classical problem of geotechnical engineering characterized by many sources of uncertainty. Some of these sources are connected to the uncertainties of soil properties involved in the analysis. Current practice of slope stability analysis relies in the deterministic characterization and assessment of performance of embankments, excavations and Municipal Solid Waste (MSW) landfills. These slopes have been evaluated in terms of the factor of safety, where the shear strength mobilized along the failure envelop is compared with the shear stresses generated due to self-weight of the soil mass and surcharge loading on the slope. The significant uncertainties associated with the shear strength and shear stresses render deterministic modeling potentially misleading. For example, two slopes with the same factor of safety can have significantly different probabilities of failure.

The traditional engineering approaches like method of slices used for evaluating the slope stability are frequently questionable because they do not adequately account for uncertainties included in analytical modeling and natural variability. The present work builds on probabilistic assessment approaches to develop reliability based design optimization (RBDO) methodology. Moreover, Reliability Based Design Optimization (RBDO) quantifies the variability associated with the shear parameters of the soil and thereby produce a more accurate and informative method in geotechnical sustainability of slopes. The reliability index or probability of occurrence or probability of failure is directly influenced by how well the slope mechanism is understood, and how much uncertainty exists with the performance of sliding limit states. Therefore, a probabilistic slope stability analysis should account for inherent uncertainty and modeling uncertainty.

The mean and standard deviations associated with unit weight, cohesion and angle of internal friction of the soil are taken into account in the probabilistic optimization. Reliability analysis of soil slopes is presented using first order reliability method (FORM) i.e Hasofer-Lind-Rackwitz-Fiessler (HL-RF) method. The results of these methods are compared using five recognized methods of slope stability. These are

Ordinary method of slices, simplified Bishop's method, Janbu's Simplified Method, Spencer Method and Morgenstern & Price Method. A limit state function is formulated against sliding failure. Reliability indices against sliding failure using the various method of slices have been computed. Moreover, a procedure is presented for locating the surface of minimum reliability index for slopes.

Design Charts have been presented for the calculation of reliability indices using different deterministic methods. The influence of the variable parameters on the location of the critical center and there by the critical slip surface is observed and significant conclusions have been drawn.

An attempt has been made to apply the RBDO to soil lopes in the presence of water table and for heterogeneous soil slopes with layered soils.

Nomenclature

f_r	probability density function of stresses (r)
f_s	probability density function of strengths (s)
$P(x)$	probability of occurrence of the event x
s	The available shear strength
τ	The equilibrium shear stress
FS	factor of safety
τ_m	mobilized shear strength
τ_f	ultimate shear strength
COV	co-efficient of variation
β	Reliability Index
c	cohesion at the base of the slice
ϕ	angle of internal friction at the base of the slice
γ	unit weight of soil
α	The inclination of the slope with respect to horizontal in degrees
H	Height of the soil slope in meters
x_o	x-coordinate of the center of the slip circle
y_o	y-coordinate of the center of the slip circle
R	Radius of the slip circle
(p,q)	crest point of the slope
(p_1,q_1)	entry point of the slip circle
(p_2,q_2)	exit point of the slip circle
b	base width of the slice
z	average height of the slice
x_i	x-coordinates of points on the slip circle
y_i	y-coordinates of points on the slip circle
E, X	normal and shear interslice forces

N	normal forces acting at the base of the slice
F_f, F_m	force (f) and moment (m) factor of safety
w	weight of a slice
θ	base angle of a slice
dl	length of slice along the base
FS_{OMS}	factor of safety from Ordinary Method of Slices
FS_{Bishop}	factor of safety from Bishop's Simplified Method
FS_{Janbu}	factor of safety from Janbu's simplified Method
$FS_{Spencer}$	factor of safety from Spencer Method
FS_{MP}	factor of safety from Morgenstern – Price Method
$G(x)$	The performance function
β_c	Cornell Reliability Index
β_{HL}	Hasofer – Lind Reliability Index
β_{OMS}	Reliability Index from Ordinary Method of Slices
β_{Bishop}	Reliability Index from Bishop's Simplified Method
$\beta_{Spencer}$	Reliability Index from Spencer Method
β_{MP}	Reliability Index from Morgenstern – Price Method
u	pore water pressure
U	resultant pore water pressure at the base of the slice
H_w	height of the water table
α_w	inclination of water table with the horizontal
x_{wt}	x- coordinate point of intersection of the water table and the slip circle
mbx	x-coordinate of the midpoint of the base of the slice
mby	y-coordinate of the midpoint of the base of the slice
h_w	average height of the water table for a given slice
h_t	height of top layer in a three-layered soil slope
c_t	cohesion of the soil in top layer in a three-layered soil slope

ϕ_t	angle of internal friction of soil in the top layer in a three-layered soil slope
h_m	height of middle layer in a three-layered soil slope
c_m	cohesion of the soil in middle layer in a three-layered soil slope
ϕ_m	angle of internal friction of soil in the middle layer in a three-layered soil slope
c_b	cohesion of the soil in the base in a three-layered soil slope
ϕ_b	angle of internal friction of soil in the base a three-layered soil slope
x_m	x- coordinate of the point of intersection of the middle layer and the slip circle
x_s	x – coordinate of the point of intersection of the middle layer with the slope
x_b	x- coordinate of the point of intersection of the base of the slope and the slip circle

List of Figures

- 1.1 Graphical representation of stress and strength interference region
- 3.1 Geometry showing the parameters used and moment arms for circular slip surface
- 3.2 The forces acting on a slice
- 3.3 Geometry and parameters used for the calculation of factor of safety
- 3.4 The parameters for the i^{th} slice
- 3.5 The grid for centres
- 3.6 The grid for radius
- 3.7 The matrices showing the critical factors of safety for Ordinary method of slices and Bishop's simplified method for corresponding points in user defined centre grid (a 10 by 10 grid was used for ease of viewing)
- 3.8 The matrices showing the radii of critical factors of safety for Ordinary method of slices and Bishop's simplified method for corresponding points in user defined centre grid (a 10 by 10 grid was used for ease of viewing)
- 3.9 The matrices showing the critical factors of safety for Ordinary method of slices and Bishop's simplified method for corresponding points in the generalized centre grid (a 10 by 10 grid was used for ease of viewing)
- 3.10 The matrices showing the critical factors of safety for Janbu's Simplified Method for corresponding points in the generalized centre grid (a 10 by 10 grid was used for ease of viewing)
- 3.11 The matrices showing the critical factors of safety for Spencer Method for corresponding points in the generalized centre grid (a 10 by 10 grid was used for ease of viewing)
- 3.12 The interslice force function as it varies along the base of the slip surface
- 3.13 The matrices showing the critical factors of safety for Spencer Method for corresponding points in the generalized centre grid (a 10 by 10 grid was used for ease of viewing)
- 3.14 Distribution of safety margin, $Z = R - S$ (Melchers 2002)

- 3.15 Two dimensional representation of design point on the failure boundary for the linear limit state function
- 3.16 Identification of MPP in the reliability analysis (FORM)
- 3.17 Critical Reliability Indices for Ordinary Method of Slices
- 3.18 Critical Reliability Indices for Bishop's Simplified Method
- 3.19 Critical Reliability Indices for Janbu Simplified Method
- 3.20 Critical Reliability Indices for Spencer Method
- 3.21 Critical Reliability Indices for Morgenstern-Price Method
- 4.1 The geometry and soil properties of the slope from Bolton et al. (2003)
- 4.2 The geometry and soil properties of the slope from Zolfaghari et al. (2005)
- 4.3 The geometry and soil properties of the slope from Malkawi et al. (2000)
- 4.4 The geometry and soil properties of the slope from Zhao et al. (2008)
- 4.5 The effect of change in slope angle α on the critical slip surfaces for Ordinary Method of Slices
- 4.6 The effect of change in slope angle α on the shear bands for Ordinary Method of Slices
- 4.7 The effect of change in slope angle α on the critical slip surfaces for Bishop's Simplified Method
- 4.8 The effect of change in slope angle α on the shear bands for Bishop's Simplified Method
- 4.9 The effect of change in slope angle α on the critical slip surfaces for Spencer Method
- 4.10 The effect of change in slope angle α on the shear bands for Spencer Method
- 4.11 The effect of change in slope angle α on the critical slip surfaces for Morgenstern-Price Method

- 4.12 The effect of change in slope angle α on the shear bands for Morgenstern-Price Method
- 4.13 The effect of change in $c/\gamma H$ on the critical slip surfaces for Ordinary Method of Slices
- 4.14 The effect of change in $c/\gamma H$ on the shear bands for Ordinary Method of Slices
- 4.15 The effect of change in $c/\gamma H$ on the critical slip surfaces for Bishop's Simplified Method
- 4.16 The effect of change in $c/\gamma H$ on the shear bands for Bishop's Simplified Method
- 4.17 The effect of change in $c/\gamma H$ on the critical slip surfaces for Spencer Method
- 4.18 The effect of change in $c/\gamma H$ on the shear bands for Spencer Method
- 4.19 The effect of change in $c/\gamma H$ on the critical slip surfaces for Morgenstern-Price Method
- 4.20 The effect of change in $c/\gamma H$ on the shear bands for Morgenstern-Price Method
- 4.21 The effect of change in COV of $c/\gamma H$ on the critical slip surfaces for Ordinary Method of Slices
- 4.22 The effect of change in COV of $c/\gamma H$ on the shear bands for Ordinary Method of Slices
- 4.23 The effect of change in COV of $c/\gamma H$ on the critical slip surfaces for Bishop's Simplified Method
- 4.24 The effect of change in COV of $c/\gamma H$ on the shear bands for Bishop's Simplified Method
- 4.25 The effect of change in COV of $c/\gamma H$ on the critical slip surfaces for Spencer Method
- 4.26 The effect of change in COV of $c/\gamma H$ on the shear bands for Spencer Method

- 4.27 The effect of change in COV of $c/\gamma H$ on the critical slip surfaces for Morgenstern-Price Method
- 4.28 The effect of change in COV of $c/\gamma H$ on the shear bands for Morgenstern-Price Method
- 4.29 The effect of change in ϕ on the critical slip surfaces for Ordinary Method of Slices
- 4.30 The effect of change in ϕ on the shear bands for Ordinary Method of Slices
- 4.31 The effect of change in ϕ on the critical slip surfaces for Bishop's Simplified, Spencer and Morgenstern-Price Method
- 4.32 The effect of change in ϕ on the shear bands Bishop's Simplified, Spencer and Morgenstern-Price Method
- 4.33 The effect of change in COV of ϕ on the critical slip surfaces for Ordinary Method of Slices
- 4.34 The effect of change in COV of ϕ on the shear bands for Ordinary Method of Slices
- 4.35 The effect of change in COV of ϕ on the critical slip surfaces for Bishop's Simplified Method
- 4.36 The effect of change in COV of ϕ on the shear bands for Bishop's Simplified Method
- 4.37 The effect of change in COV of ϕ on the critical slip surfaces for Spencer Method
- 4.38 The effect of change in COV of ϕ on the shear bands for Spencer Method
- 4.39 The effect of change in COV of ϕ on the critical slip surfaces for Morgenstern-Price Method
- 4.40 The effect of change in COV of ϕ on the shear bands for Morgenstern-Price Method

- 4.41 Design charts for $c/\gamma H=0.1$ and $\phi=10^0$ for Ordinary Method of Slices
- 4.42 Design charts for $c/\gamma H=0.1$ and $\phi=20^0$ for Ordinary Method of Slices
- 4.43 Design charts for $c/\gamma H=0.1$ and $\phi=30^0$ for Ordinary Method of Slices
- 4.44 Design charts for $c/\gamma H=0.1$ and $\phi=40^0$ for Ordinary Method of Slices
- 4.45 Design charts for $c/\gamma H=0.2$ and $\phi=10^0$ for Ordinary Method of Slices
- 4.46 Design charts for $c/\gamma H=0.2$ and $\phi=20^0$ for Ordinary Method of Slices
- 4.47 Design charts for $c/\gamma H=0.2$ and $\phi=30^0$ for Ordinary Method of Slices
- 4.48 Design charts for $c/\gamma H=0.2$ and $\phi=40^0$ for Ordinary Method of Slices
- 4.49 Design charts for $c/\gamma H=0.3$ and $\phi=10^0$ for Ordinary Method of Slices
- 4.50 Design charts for $c/\gamma H=0.3$ and $\phi=20^0$ for Ordinary Method of Slices
- 4.51 Design charts for $c/\gamma H=0.3$ and $\phi=30^0$ for Ordinary Method of Slices
- 4.52 Design charts for $c/\gamma H=0.3$ and $\phi=40^0$ for Ordinary Method of Slices
- 4.53 Design charts for $c/\gamma H=0.4$ and $\phi=10^0$ for Ordinary Method of Slices
- 4.54 Design charts for $c/\gamma H=0.4$ and $\phi=20^0$ for Ordinary Method of Slices
- 4.55 Design charts for $c/\gamma H=0.4$ and $\phi=30^0$ for Ordinary Method of Slices
- 4.56 Design charts for $c/\gamma H=0.4$ and $\phi=40^0$ for Ordinary Method of Slices
- 4.57 Design charts for $c/\gamma H=0.5$ and $\phi=10^0$ for Ordinary Method of Slices
- 4.58 Design charts for $c/\gamma H=0.5$ and $\phi=20^0$ for Ordinary Method of Slices
- 4.59 Design charts for $c/\gamma H=0.5$ and $\phi=30^0$ for Ordinary Method of Slices
- 4.60 Design charts for $c/\gamma H=0.5$ and $\phi=40^0$ for Ordinary Method of Slice
- 4.61 Design charts for $c/\gamma H=0.1$ and $\phi=10^0$ for Bishop's Simplified Method
- 4.62 Design charts for $c/\gamma H=0.1$ and $\phi=20^0$ for Bishop's Simplified Method
- 4.63 Design charts for $c/\gamma H=0.1$ and $\phi=30^0$ for Bishop's Simplified Method

- 4.64 Design charts for $c/\gamma H=0.1$ and $\phi=40^0$ for Bishop's Simplified Method
- 4.65 Design charts for $c/\gamma H=0.2$ and $\phi=10^0$ for Bishop's Simplified Method
- 4.66 Design charts for $c/\gamma H=0.2$ and $\phi=20^0$ for Bishop's Simplified Method
- 4.67 Design charts for $c/\gamma H=0.2$ and $\phi=30^0$ for Bishop's Simplified Method
- 4.68 Design charts for $c/\gamma H=0.2$ and $\phi=40^0$ for Bishop's Simplified Method
- 4.69 Design charts for $c/\gamma H=0.3$ and $\phi=10^0$ for Bishop's Simplified Method
- 4.70 Design charts for $c/\gamma H=0.3$ and $\phi=20^0$ for Bishop's Simplified Method
- 4.71 Design charts for $c/\gamma H=0.3$ and $\phi=30^0$ for Bishop's Simplified Method
- 4.72 Design charts for $c/\gamma H=0.3$ and $\phi=40^0$ for Bishop's Simplified Method
- 4.73 Design charts for $c/\gamma H=0.4$ and $\phi=10^0$ for Bishop's Simplified Method
- 4.74 Design charts for $c/\gamma H=0.4$ and $\phi=20^0$ for Bishop's Simplified Method
- 4.75 Design charts for $c/\gamma H=0.4$ and $\phi=30^0$ for Bishop's Simplified Method
- 4.76 Design charts for $c/\gamma H=0.4$ and $\phi=40^0$ for Bishop's Simplified Method
- 4.77 Design charts for $c/\gamma H=0.5$ and $\phi=10^0$ for Bishop's Simplified Method
- 4.78 Design charts for $c/\gamma H=0.5$ and $\phi=20^0$ for Bishop's Simplified Method
- 4.79 Design charts for $c/\gamma H=0.5$ and $\phi=30^0$ for Bishop's Simplified Method
- 4.80 Design charts for $c/\gamma H=0.5$ and $\phi=40^0$ for Bishop's Simplified Method
- 4.81 Design charts for $c/\gamma H=0.1$ and $\phi=10^0$ for Spencer Method
- 4.82 Design charts for $c/\gamma H=0.1$ and $\phi=20^0$ for Spencer Method
- 4.83 Design charts for $c/\gamma H=0.1$ and $\phi=30^0$ for Spencer Method
- 4.84 Design charts for $c/\gamma H=0.1$ and $\phi=40^0$ for Spencer Method
- 4.85 Design charts for $c/\gamma H=0.2$ and $\phi=10^0$ for Spencer Method
- 4.86 Design charts for $c/\gamma H=0.2$ and $\phi=20^0$ for Spencer Method

- 4.87 Design charts for $c/\gamma H=0.2$ and $\phi=30^0$ for Spencer Method
- 4.88 Design charts for $c/\gamma H=0.2$ and $\phi=40^0$ for Spencer Method
- 4.89 Design charts for $c/\gamma H=0.3$ and $\phi=10^0$ for Spencer Method
- 4.90 Design charts for $c/\gamma H=0.3$ and $\phi=20^0$ for Spencer Method
- 4.91 Design charts for $c/\gamma H=0.3$ and $\phi=30^0$ for Spencer Method
- 4.92 Design charts for $c/\gamma H=0.3$ and $\phi=40^0$ for Spencer Method
- 4.93 Design charts for $c/\gamma H=0.4$ and $\phi=10^0$ for Spencer Method
- 4.94 Design charts for $c/\gamma H=0.4$ and $\phi=20^0$ for Spencer Method
- 4.95 Design charts for $c/\gamma H=0.4$ and $\phi=30^0$ for Spencer Method
- 4.96 Design charts for $c/\gamma H=0.4$ and $\phi=40^0$ for Spencer Method
- 4.97 Design charts for $c/\gamma H=0.5$ and $\phi=10^0$ for Spencer Method
- 4.98 Design charts for $c/\gamma H=0.5$ and $\phi=20^0$ for Spencer Method
- 4.99 Design charts for $c/\gamma H=0.5$ and $\phi=30^0$ for Spencer Method
- 4.100 Design charts for $c/\gamma H=0.5$ and $\phi=40^0$ for Spencer Method
- 4.101 Design charts for $c/\gamma H=0.1$ and $\phi=10^0$ for Morgenstern-Price Method
- 4.102 Design charts for $c/\gamma H=0.1$ and $\phi=20^0$ for Morgenstern-Price Method
- 4.103 Design charts for $c/\gamma H=0.1$ and $\phi=30^0$ for Morgenstern-Price Method
- 4.104 Design charts for $c/\gamma H=0.1$ and $\phi=40^0$ for Morgenstern-Price Method
- 4.105 Design charts for $c/\gamma H=0.2$ and $\phi=10^0$ for Morgenstern-Price Method
- 4.106 Design charts for $c/\gamma H=0.2$ and $\phi=20^0$ for Morgenstern-Price Method
- 4.107 Design charts for $c/\gamma H=0.2$ and $\phi=30^0$ for Morgenstern-Price Method
- 4.108 Design charts for $c/\gamma H=0.2$ and $\phi=40^0$ for Morgenstern-Price Method
- 4.109 Design charts for $c/\gamma H=0.3$ and $\phi=10^0$ for Morgenstern-Price Method

- 4.110 Design charts for $c/\gamma H=0.3$ and $\phi=20^0$ for Morgenstern-Price Method
- 4.111 Design charts for $c/\gamma H=0.3$ and $\phi=30^0$ for Morgenstern-Price Method
- 4.112 Design charts for $c/\gamma H=0.3$ and $\phi=40^0$ for Morgenstern-Price Method
- 4.113 Design charts for $c/\gamma H=0.4$ and $\phi=10^0$ for Morgenstern-Price Method
- 4.114 Design charts for $c/\gamma H=0.4$ and $\phi=20^0$ for Morgenstern-Price Method
- 4.115 Design charts for $c/\gamma H=0.4$ and $\phi=30^0$ for Morgenstern-Price Method
- 4.116 Design charts for $c/\gamma H=0.4$ and $\phi=40^0$ for Morgenstern-Price Method
- 4.117 Design charts for $c/\gamma H=0.5$ and $\phi=10^0$ for Morgenstern-Price Method
- 4.118 Design charts for $c/\gamma H=0.5$ and $\phi=20^0$ for Morgenstern-Price Method
- 4.119 Design charts for $c/\gamma H=0.5$ and $\phi=30^0$ for Morgenstern-Price Method
- 4.120 Design charts for $c/\gamma H=0.5$ and $\phi=40^0$ for Morgenstern-Price Method
- 5.1 The geometry and parameters used for factor of safety using pore water pressure calculations
- 5.2 The forces acting on a slice in presence of water table
- 5.3 The calculation of the water head for a slice
- 5.4 Three Layered soil slope showing the parameters used in determination of factor of safety
- 5.5 Three Layered soil slope showing the division of the slices to determine corresponding c and ϕ

List of Tables

- 2.1 Values of Coefficient of Variation (COV) for Geotechnical Properties
- 3.1 Random variables considered in the present study
- 4.1 The comparison of factors of safety obtained from the study with Bolton et al. (2003)
- 4.2 The comparison of factors of safety obtained from the study with Zolfaghari et al. (2005)
- 4.3 The comparison of factors of safety obtained from the study with Malkawi et al. (2001)
- 4.4 The comparison of factors of safety obtained from the study with Zhao et al. (2008) with a height of 10 m and an inclination of 1V:3H
- 4.5 The comparison of factors of safety obtained from the study with GeoStudio examples
- 4.6 The comparison of reliability indices (β_{Bishop} , β_{Spencer}) obtained from Zhao et al. (2008) and calculated from the present study
- 4.7 The ranges of the values used for the various parameters involved in the present study
- 4.8 The classification of Reliability Indices as given by USACE (1997)
- 5.1 The comparison of the values obtained from GeoStudio to those calculated by the present study for the presence of water table
- 5.2 The comparison of the values obtained from GeoStudio to those calculated by the present study for three layered soil slope

Contents

Declaration	ii
Approval Sheet.....	iii
Acknowledgements	iv
Abstract	vi
Nomenclature	viii
List of figures	xi
List of tables.....	xix
1 Introduction.....	1
1.1 Uncertainty.....	1
1.2 Reliability and Probability	2
1.1.1 Reliability Based Design Optimization (RBDO)	3
1.1.2 Reliability Calculation Methods.....	4
1.3 Slope Stability	16
1.4 Deterministic Methods and Factor of safety	16
1.5 Limit Equilibrium Methods.....	7
2 Review of Literature.....	10
2.1 Studies pertaining to soil variability	10
2.2 Slope Stability	13
2.3 Studies pertaining to Reliability based slope stability	16
2.4 Observations from the review of the literature.....	19
2.5 Objectives of the present study	20
3 Formulation of Optimization Methodology	21
3.1 Methods of Slices.....	21
3.2 Factor of Safety	21
3.3 Derivation of the Factor of Safety.....	22
3.4 Inter-slice force function	26
3.5 Ordinary Method of Slices	26
3.6 Grid and Radius search technique.....	31
3.7 Bishops' Simplified Method of Slices Using Grid and Radius.....	35
3.8 Generalization of the Grid points for Centre and Radius	36

3.9	Normalization with respect to H	39
3.10	Janbu's Simplified Method	40
3.11	Spencer Method	42
3.12	Morgenstern-Price Method	43
3.13	Normalization of the equations	46
3.14	First order reliability method (FORM)	47
3.15	Correlated Gaussian random variables.....	50
3.16	Calculation of reliability index.....	52
3.17	Non-Gaussian random variables	54
3.18	Most probable point of failure (MPP).....	55
3.19	Random variables considered in the present study	56
4	Results and Discussion	60
4.1	Validation of the formulation.....	60
4.2	Slip Circle Study	65
4.3	Design Charts	86
4.4	Design Charts for Ordinary Method of Slices.....	87
4.5	Design Charts for Bishop's Simplified Method.....	98
4.6	Design Charts for Spencer Method	108
4.7	Design Charts for Morgenstern-Price Method.....	118
4.8	Design Example	128
5	Pore Water Pressure and Layered soil slope	129
5.1	Pore Water Pressure	129
5.2	Layered Soil Slope	134
	References.....	138

Chapter 1

Introduction

1.1. Uncertainty

Unlike structural and mechanical engineers whose work composes with dealing with components which have fixed dimensions and pre-defined behavioral properties, geotechnical engineer have to deal with materials and geometries provide by the nature.

These conditions are not predefined and hence must be inferred via intense observational and experimental studies which are often costly. Uncertainties arise when we look for accuracy of these experiments, in modelling in-situ conditions of the soils perfectly in a laboratory and in prediction of the resistances that the materials will be able to mobilize.

In structural and mechanical engineering, the uncertainties are largely deductive i.e. they start from known conditions and models can be employed to deduce their behavior from the pre-defined specifications. Whereas the uncertainties in geotechnical engineering are inductive i.e. there are limited observations to begin with, the judgment of the engineer isn't reliable, and the limited knowledge of geology, and the statistical reasoning's that are employed to infer the behavior undefined naturally occurring materials.

Decisions have to be made on the basis of information which is limited or incomplete. For instance, there might exist spatial variability in the strength of soil in a slope, the measurement of parameters might not be perfect and there is a possibility that the samples collected do not correctly represent the entirety of the slope material. Hence there is a considerable uncertainty in regards to our knowledge of the input parameters.

Geotechnical engineers deal with uncertainties by recognizing that risk and uncertainty are inevitable and by applying the observational method (Peck 1969) [1] to maintain control over them. However, the observational method is applicable only when the design can be changed during construction on the basis of observed behavior. In those cases in which the critical behavior cannot be observed until too late to make changes, the designer must rely on a calculated risk.

It is, therefore, desirable to use methods and concepts in engineering planning and design which facilitate the evaluation and analysis of uncertainty. Traditional deterministic methods of analysis, which use the factor of safety as a measure of safety, must be supplemented by methods which use the principles of statistics and probability. These latter methods, often called probabilistic methods, enable a logical analysis of uncertainty to be made and provide a quantitative basis for assessing the reliability of foundations and retaining structures. Consequently, these methods provide a sound basis for the development and exercise of engineering judgment.

In this study, we are mainly concerned about the uncertainties involved in slope failure mechanism and their influence on the overall slope stability.

1.2. Reliability and Probability

Over the years, a more formal way of dealing with the uncertainties has been developed by applying the Reliability Theory to geotechnical engineering.

Reliability studies provide a way of quantifying those uncertainties and handling them consistently.

As discussed above, the deterministic method do not take into account the variation or the uncertainty in the various factors that are involved in the calculation of the stability. When uncertainty in the factors exists, the factor of safety, which is dependent on these factors will not be a consistent measure of the stability of slopes, as slopes with same factor of safety can have different levels of failure probability depending on the variability of those factors. As deterministic slope models do not take into consideration these uncertainties and use only average input parameters, may provide misleading results for slope reliability. Reliability calculations provide a means of evaluating the combined effects of uncertainties, and a means of distinguishing between conditions where uncertainties are particularly high or low.

Reliability, accounts for the heterogeneity of the system under consideration. The effect of the various parameters which vary continuously across the system are called the random variables. In the probabilistic approach to slope stability, the input parameters which are essentially the properties of the material, are considered as random variables.

Reliability is theoretically defined as the probability of success i.e.

$$R = 1 - P(x) \quad (1.1)$$

where $P(x)$ is the probability of the event x , which is the failure.

Slope reliability analysis provide a means of evaluating the combined effects of uncertainties in the parameters involved in the calculations. The computational effort that goes into probabilistic analysis is much more than that required for deterministic analysis. As stated before, experience and engineering judgement are required to establish an order of magnitude of the acceptable failure probability which depend on the importance and service time of a slope as well as the consequences of failure, if and when failure occurs. Both deterministic and probabilistic methods should be performed and these alternative methods can be considered as complementary to each.

1.2.1. Reliability Based Design Optimization (RBDO)

The above literature clearly indicating the fact that there is a high degree of variability and uncertainty involved in the material properties of soil slope which have not been incorporated in the calculations of factor of safety. As the traditional factor of safety based design does not include uncertainties of in the soil properties, there is a need to apply Reliability Based Design Optimization (RBDO).

A target reliability based design optimization method developed by (Basha and Babu 2010 [2]) is used in this work to obtain a reliability index considering the variability associated with cohesion of soil, the unit weight of the soil and the angle of internal friction of the soil. Reliability based design optimization has been carried in order to study the influence of uncertainties associated with soil properties and geometry of the slope on the critical slip surfaces.

1.2.2. Reliability Calculations Method

The factor of safety is the index that is considered for the assessment of slope stability within a deterministic framework. Similarly, within a probabilistic framework, the probability of failure is considered as an index of instability. Alternatively we can say that the probability of failure is when the stress coming onto the soil slope (s) is more than the strength possessed by the soil slope. Stress is used to indicate any component or equipment that tends to induce failure, while strength indicates any component or equipment that resists failure. Let the probability density function for the stress(es) be denoted by f_s and that for strength (r) by f_r as shown in Fig. 1.1.

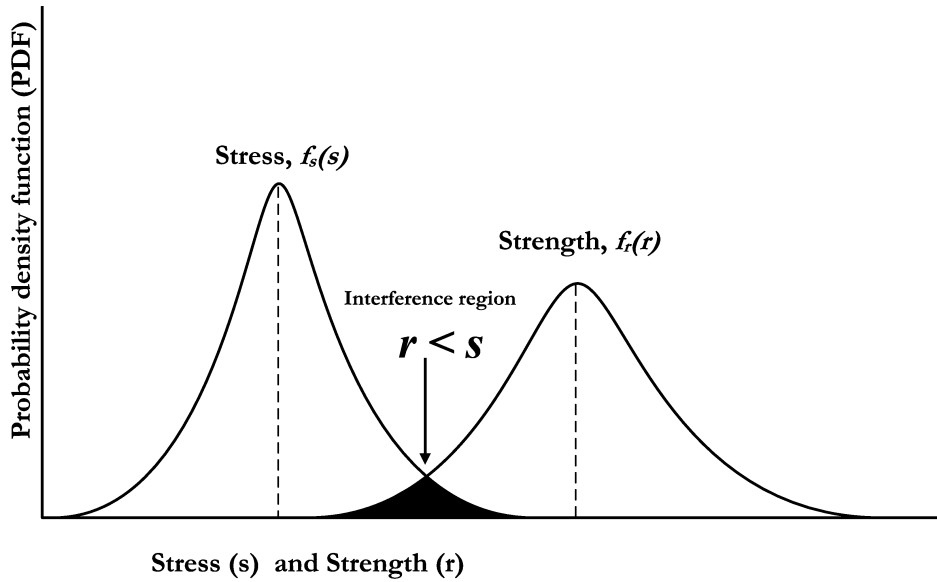


Figure 1.1: Graphical representation of stress and strength interference region

The reliability is defined as the probability that the stress will not exceed the strength as follows:

$$\text{Reliability} = P(r > s) = P(r - s > 0) \quad (1.2)$$

where P is the probability of failure. The shaded region in Fig. 1.1 is the interference region, which indicates a finite probability of failure and its converse denotes the probability of safety or reliability. The magnitude of the failure probability is a function of the degree of overlap of the two distributions. The greater the shaded area, the greater is the probability of failure.

The probability of failure (P_f) for this example can be calculated from the following integral:

$$P_f = \iint_{\Omega} f_r(r) f_s(s) dr ds \quad (1.3)$$

However, despite that the integral of Eq. (1.3) can have a direct analytical solution for some special cases, or can be performed numerically for some other cases, in most real life situations the integral cannot be evaluated directly. In many cases the failure domain may not have an analytical expression and

the problem gets more complicated as the number of random variables increases. Thus, other methods such as the simulation-based reliability methods (Monte-Carlo simulation methods), or the analytical reliability approximation methods (e.g. the first and second order reliability methods, and the advanced mean value method) must be employed, and are presented in the following sub-sections. Based on the level of complexity involved in the probability theory used, the international standards organization (Madsen et al., 1986 [3]) categorized the design procedures into three groups

Level I: Semi probabilistic method

Reliability methods that employ only one characteristic value of each uncertain parameter are called Level I methods. Load and resistance factor formats including the allowable stress formats are examples of Level I methods.

Level II: Approximate probabilistic method

Reliability methods that employ two values of each uncertain parameter (mean and variance), supplemented with measure of the correlation between the parameters are called Level II methods. Reliability methods are examples of Level II methods. One of the approximate probabilistic methods is the first order second moment (FOSM) method, which uses the first two so called moments, the mean and coefficient of variation. A Taylor series expansion is used to approximate the first two moments and only the first order terms in the series considered.

Level III: Fully probabilistic method

The Level III reliability method requires the exact shape of probability distributions of each random variable. Reliability methods that employ probability of failure as a measure and therefore require a knowledge of the joint distribution of all uncertain parameters. Since the fully probabilistic method is too complex and the exact information about loads and resistance is hardly available.

1.3. Slope Stability

Evaluating the stability of slopes in soil is an important aspect in civil engineering. The quest for solving problems in slope stability have led to important advances in understanding the behavior of soils. Extensive research and advances in engineering over the past 80 years provide us with a sound set of soil mechanics principles with which to attack practical problems of slope stability.

With the passage of time, the experiences with the behavior of slopes and their pattern of failure, have paved way for the development of increased understanding of the changes in properties of the soil that can occur over time, to recognize the limitations of laboratory and in situ testing for evaluating soil strengths, improved understanding of the principles of soil mechanics which connect behavior of soil to slope stability, and improved analytical procedures strengthened by extensive examination of the mechanics of slope stability analyses, and the usage of computers to perform complex analyses.

Slope stability analysis is performed to assess the safety of a human-made or natural slopes (e.g. embankments, road cuts, excavations, landfills etc.) and the equilibrium conditions. Slope stability is the resistance offered by the curvilinear surface to failure. The objective of slope stability analysis is to locate critical failure surfaces, investigate potential failure mechanisms, optimal design of slopes with due consideration to safety, reliability and economics.

1.4. Deterministic Methods and Factor of safety

Slopes are can be highly unstable structures due to the lack of lateral confining pressure on the slope side. Thus it is essential to determine how stable a slope is in order to optimize the geometry of the slope in such that an effective use of space and

efficient functioning is assured. Slope stability calculations need to be performed to ensure that the resisting forces are sufficiently greater than the forces tending to cause a slope to fail. The computation of factor of safety (FS) is the most commonly measured quantity to depict the stability of the slope.

The factor of safety, FS in general is defined as ratio of the forces which contribute in resisting the failure of the slope to the forces causing it, is defined with respect to the shear strength of the soil as

$$FS = \frac{s}{\tau} \quad (1.4)$$

where s is the available shear strength and τ is the equilibrium shear stress.

Factor of safety (FS) is usually calculated using limit equilibrium procedures of analysis. The equations of static equilibrium are used to compute F in these procedures. Various deterministic calculation methods are in practice based on the characteristics of the slope material, the area of usage of the slope, the shape of the failure of the slope surface etc., There are several models developed by researchers and geotechnical engineers for assessing slope stability, like Bishop (1955), Janbu (1954), Lowe and Karafiath (1960), Spencer (1967) and Morgenstern & Price (1965) [4-8].

1.5. Limit Equilibrium methods

In the present investigation, the concepts of reliability are applied in the calculation of the reliability indices, which measure the reliability by using the limit equilibrium technique of method of slices.

The common features of the methods of slices have been summarized by Zhu et al., (2003) [9] as:

- The sliding body over the failure surface is divided into a finite number of slices. The slices are usually cut vertically, but horizontal as well as inclined cuts have also been used by various researchers. In general, the differences between different methods of cutting are not major, and the vertical cut is preferred by most engineers at present.

- The strength of the slip surface is mobilized to the same degree to bring the sliding body into a limit state. That means there is only a single factor of safety which is applied throughout the whole failure mass.
- Assumptions regarding inter-slice forces are employed to render the problem determinate.
- The factor of safety is computed from force and/or moment equilibrium equations.

In the conventional limiting equilibrium method, the shear strength τ_m which can be mobilized along the failure surface is given by:

$$\tau_m = \frac{\tau_f}{FS} \quad (1.5)$$

where FS is the factor of safety with respect to the ultimate shear strength τ_f which is given by the Mohr–Coulomb relation as

$$\tau_f = c' + \sigma'_n \tan \phi' \text{ or } c_u \quad (1.6)$$

where c' is the cohesion, σ'_n is the effective normal stress, ϕ' is the angle of internal friction and c_u is the undrained shear strength.

In the stability analysis, FS assumed to be constant along the entire failure surface. Hence, an average value of FS along the slip surface is obtained instead of the actual factor of safety which varies along the failure surface as in a progressive failure. The factor of safety is taken as the performance function while searching for the critical slip surface (i.e. with the minimum factor of safety) in slopes.

1.5.1. Methods of Slices

The limit equilibrium methods, when applied to slope stability in two dimensions, a general formulation can be obtained and all the common methods of finding factors of safety such as

- i. The Ordinary method
- ii. The Simplified Bishop method

- iii. The Spencer method
- iv. The Janbu simplified and the Janbu generalized methods
- v. The Morgenstern-Price method

In these methods, the elements of statics are used to derive the factor of safety. It takes into account the summation of forces in two directions, (here horizontal and vertical) and the summation of moments about a chosen point of rotation.

These basics of theory of statics, along with the failure criteria, are insufficient to make the slope stability problem determinate. Hence, additional elements in regards to physics of the problem or an assumptions with respect to the direction or magnitude of the forces involved is required to make the problem determinate.

Theoretical studies have shown that factor of safety equations can be independently derived to satisfy moment equilibrium and force equilibrium of the slices contained above an assumed slip surface (Fredlund and Krahn, 1977 [10]). In addition, an assumed functional relationship is used to specify the direction of the interslice forces.

In view of the above, the published works on the reliability analysis of soil slopes is presented in the following chapter.

Chapter 2

Review of Literature

2.1 Studies pertaining to soil variability

Considerable variability in soil properties is inevitable, i.e. not just from site to site and stratum to stratum, but even within apparently homogeneous deposits at a single site.

As discussed earlier, confidence in the values of soil properties used for design purposes is affected by a series of uncertainties arising from several sources such as: inherent random heterogeneity (also referred to as spatial variability), measurement errors, statistical errors (due to small sample) and the uncertainty in transforming the index soil properties obtained from soil tests into desired geotechnical properties. (Phoon and Khulhawy (1999) [11])

The inputs to be given in the reliability analysis of slopes in addition to the general characteristics of the soil will be the means, standard deviations and the coefficient of variations of the parameters with which the uncertainty is associated. These are derived from the statistical analysis of experimental data and are mainly affected by the type of the soil and the conditions in which it exists. There are several works which give the range of values of means and COV's for different parameters associated with soil.

Laboratory test results on natural soils indicate that most soil properties can be considered as random variables conforming to the normal distribution function (Lumb (1966), Tan et al., (1993) [12,13])

Lambe and Whitman (1979) [14], suggested that variability often observed in comparatively homogenous soil formations. The bore hole profile of Mexico City

showed different kinds of clays present along its length the properties of which were are more or less uniform with depth but have coefficients of variation ranging from about 20% to as much as 50%, depending on the property.

Many authors since then have published various works in which they have compiled reported coefficients of variation, which are used to quantify the variability, for a broad variety of soil properties. The ranges of these reported values are sometimes quite wide and can only be considered as suggestive of conditions on any specific project. The following are some of the works done on coefficients of variation for soil engineering test.

The variation in angle of internal friction of sands was reported by Lumb (1974), Hoeg and Murarka (1974), Singh (1971), Schultze (1975) [15-18] etc. and can be summarized to have a COV in the range of 5-15%.

The angle of friction in clays was studied by Lumb (1974), Singh (1971), Schultze (1975) [15, 17, 18] and it's reported COV ranges from 12% to 56% which is quite wide.

The clay content and its COV were studied by Lumb (1974), Inges and Noble (1975), Minty et al., (1979), Corotis et al., (1975), Stamatopoulos and Kotzias (1975) [15,19-22] etc, and is reported to have a range of 9-70% with a standard value of 25%.

The cohesion of undrained sands and clays was studied by Lumb (1974) and Singh (1971) [15,17].

Apparent or true density was report to have a COV of 1-10% and was reported by Sherwood (1970) [23] among others.

The unconfined compressive strength is reported to have a COV of 6-100% with a standard value of 40% as reported by Otte (1978), Morse (1971) and Stamatopoulos and Kotzias (1975) [24,25,22]etc.

Seed and Idriss (1970) [26] presented an experimental data on the variation of shear modulus and damping ratio with cyclic strain amplitude, and used the data to develop their widely used modulus reduction and damping curves for sands and clays.

Uncertainties in the modelling were studied by Ditlevsen (1982), Tang (1989), Der Kiureghian (1989) [37-39] who used statistical approach or consistent Bayesian updating for assessment of model uncertainty.

Harr (1987) and Phoon and Kulhawy (1999) [27,28] also reported on the characterization of geotechnical variability.

Lacasse and Nadim (1996) and Wolff et al. (1996) [29,30] suggested that the probability density function for friction angle, ϕ , is normally distributed in sands. They also suggested that a lognormal pdf must be used for undrained shear strength, s_u , in clays, and that a normal probability density function be used for s_u in clayey silts.

Lacasse and Nadim (1997) [31] presented a review of the uncertainties in characterizing soil properties, including spatial variability and measurement methods. They suggest the probability density function for unit weight is normally distributed for all soil types.

Studies have also been conducted to investigate the effect of uncertainty of soil parameters on soil-structure interaction, its propagation to the response of structural and/or nonstructural systems by Chakraborty and Dey (1988) and Lutes et al (2000) [32,33] etc.

Popescu et al., (1998) [34] gave the coefficients of variation, and correlation distances exhibited by the soil properties in the two cases, one of a natural soil deposit in the Tokyo Bay area, Japan and of an artificial island in the Canadian Beaufort Sea.

Duncan (2000) [35] gave a rough guide for estimating values of COV for any given case.

The effect of the variability of strength properties in improved soils was studied by Larsson (2005) [36] and is very high owing to variations in geology and the complex mixing processes.

Eze et al., (2014) [40] gave the geotechnical characterization of samples of three lateritic sub-base soils along Ibadan-Oyo highway which were executed to establish the variability in properties of the soils. The COV of various parameters such as California Bearing Ratio (CBR), plasticity index, optimum moisture content (OMC), Specific gravity, activity etc. were given.

All these studies stresses the importance of characterizing the uncertainties in the soil properties for design.

In the present study the parameters which are considered to be varying are the cohesion of the soil (c), the angle of internal friction (ϕ) and the unit weight of the soil (γ). Their results required for this study are summarized in Table 2.1.

Table 2.1: Values of Coefficient of Variation (COV) for Geotechnical Properties

Property	COV (%)	Source
Unit weight (γ)	3–7%	Harr (1984), Kulhawy (1992)
Effective stress friction angle (ϕ')	2–13%	Harr (1984), Kulhawy (1992)
Undrained shear strength (c_u)	13–40%	Harr (1984), Kulhawy (1992), Lacasse and Nadim (1997), Duncan (2000)

2.2 Slope Stability

Slope stability is one of the most important aspects of geotechnical engineering. There has been immense research in this field for decades which has given us many a literature in order to understand the mechanism of slope failures and their consequent behavior of interaction with the soil involved.

In limit equilibrium analysis of slope stability, the soil involved in failure can be considered to be divide into several slices or can be treated as a wedge. For the purpose of this study, the method of slices is used to arrive at the factors of safety of the soil slopes, which will be later involved in the calculations of the reliability indices.

There are several limit equilibrium methods that have been developed for the analysis of slope stability. The ones include in the study are discussed below.

Fellenius (1936) [41] was the first to introduce the method, referred to as the ordinary or the Swedish method, for a circular slip surface for drained analysis considers only the global moment equilibrium and neglects all the internal force between slices. The left and right inter-slice forces are assumed to be equal and acting opposite of each other such that they cancel out and the base normal forces become known. The factor of safety can be obtained easily without the need of iteration analysis. It gives the most conservative values for the factor of safety (FS_{OMS}) and is used mainly for demonstrative purposes.

The Bishop Simplified method (1955) [4] is one of the most popular slope stability analysis methods which is used extensively worldwide. It is the first advanced method which introduces a new relationship for the base normal forces but neglects the interslice shear forces. This method satisfies only the moment equilibrium, where moment is taken as the center of the slip circle, but not the horizontal force equilibrium and it applies only for a circular failure surface. The factor of safety is given by

$$FS_{Bishop} = \frac{\sum \left[\frac{cdl_i + W_i \cos \theta_i \tan \phi}{m} \right]}{\sum W_i \sin \theta_i} \quad (2.1)$$

where

$$m = \cos \theta_i + \frac{\sin \theta_i \tan \phi}{FS_{Bishop}}$$

The computation requires an iterative procedure because of the nonlinear relationship as the factor of safety appears on both sides of the equation.

The more rigorous form is the Bishop's generalized method which considers both, the interslice normal forces as well as the interslice shear forces.

At the same time, Janbu (1954a) [5] developed a simplified method for non-circular failure surfaces, in which the potential sliding mass is divided into several vertical slices. Later, Morgenstern-Price (1965), Spencer (1967) [8,7], and several others made further contributions with different assumptions for the interslice forces.

In the derivation of the Janbu Simplified Method, the interslice shear forces are assumed to be zero the factor of safety is determined by horizontal force equilibrium (Janbu (1956) [42]). The Janbu Simplified Method thus satisfies the force equilibrium but not the moment equilibrium.

The Janbu generalized method included the effect of interslice forces by making an assumption regarding the point of action of interslice forces which is generally assumed to center of the base of each slice. According to Janbu (1973 [43]), a state of limit equilibrium exists when the mobilized shear stress (τ) is expressed as a fraction of the shear strength. In this study the simplified method was used.

Hence, the factor of safety by Janbu's Simplified Method is calculated using the equation

$$FS_{Janbu} = \frac{\sum_{i=1}^n T_{i,lim}}{\sum_{i=1}^n T_i} = \frac{\sum_{i=1}^n (cdl_i + N_i \tan \phi) \times \cos \theta_i}{\sum_{i=1}^n N_i \sin \theta_i} \quad (2.2)$$

where,

$$N_i = \frac{w_i - \frac{cdl_i \sin \theta_i}{FS_{Janbu}}}{\cos \theta_i + \frac{\tan \phi \sin \theta_i}{FS_{Janbu}}}$$

Spencer (1967) [7] proposed an analysis in which the factor of safety is computed for both equilibriums and a constant relationship is assumed between the magnitude of the interslice shear and the normal forces

$$\frac{X}{E} = \tan \delta \quad (2.3)$$

where δ = angle of the resultant interslice force with the horizontal.

Hence the Spencer method considers both the interslice forces, assumes a constant interslice force function, and satisfies both moment and force equilibrium, and computes factor of safety for force and moment equilibrium iteratively till they converge.

The Morgenstern-Price (1965) [8] originally gives the factor of safety forces tangential and normal to the base of a slice and the summation of the moments about the center of the base of each slice. These equations which were written for a slice of infinitesimal thickness, were combined and a modified Newton-Raphson numerical technique was used to solve for the FS . Any arbitrary assumption can be made with respect to the direction of the resultant of the interslice and normal forces in order to arrive at the solution.

Slope stability analysis have since then been improved upon by the addition of robust search techniques which are very efficient in calculating the location of the critical slip surfaces using various optimization techniques.

Fredlund and Krahn (1977) [10] presented a 'best-fit regression' solution for solving the Morgenstern-Price method, which is readily comprehended giving a complete understanding of the variation of the factor of safety with interslice force factor λ .

Fredlund (1981) [44] states how the different method of slices can be considered as a subset of the General Limit Equilibrium method.

Fredlund (1984) [45] used the variational calculus method to directly compute the most critical slip surface.

Yamagami and Ueta (1988), Farias and Naylor (1998), Zou and Williams (1995) [46-48] etc., developed some technical algorithms for locating the critical slip surfaces associated with the *FS*.

Greco (1996) [49] reported a search technique for the critical slip surface in slope-stability analysis by means of a minimization of the *FS*. Monte-Carlo method for locating the critical slip surface is also presented in the study.

Malkawei et al., (2001) [50] gave the robust and effective optimization techniques using Monte- Carlo Simulations to solve problems that involve extremely complicated slope geometry.

Zhu et al., (2001, 2005[54,55]) gave an algorithm to for the calculation of the factor of safety of a slope using the Morgenstern–Price method which has the advantages of simplicity and efficiency and easy to implement into a computer program.

Cheng et al., (2007 and 2008 [51,52]) used particle swarm optimization and artificial fish swarm optimization to find the location of the slip surfaces.

Van der Meij and Sellmeijer (2010) [53], presented an alternative genetic algorithm which eliminates the need of grid search technique for finding the critical slip surface.

Cheng et al., (2010) [56] evaluates the interslice force function by eliminating the need for assumptions made in to different methods which give different factors of safety to the same problem.

2.3 Studies pertaining to Reliability based slope stability

As Duncan stated, reliability calculations provide a means of evaluating the combined effects of uncertainties and a means of distinguishing between conditions where uncertainties are particularly high or low. The reliability of a slope is the probability that the slope will remain stable under specified design conditions. Christian et al., (1994), Tang et al., (1995), Duncan (2000) [57,58,35] and others have described examples of the use of reliability for slope stability.

The results of simple reliability analyses are neither more accurate nor less accurate than factors of safety calculated using the same types of data, judgments, and

approximations. Although neither deterministic nor reliability analyses are precise, they both have value, and each enhances the value of the other.

Once the range of uncertainties associated with the varying parameters are known, there are several ways to approach the reliability analysis based on the method in which the level of probability and the way the reliability index is calculated. Some of the studies are summarized below.

Wu and Kraft (1970) [59] were amongst the first to incorporate reliability with slope stability. Uncertainties from various publications were used to calculate the probability of failure using conventional methods. Statistical decision theory was used to obtain the optimum safety factor and the expected cost.

Yong et al. (1977) [60] used the method of slices, in conjunction to reliability, in which, the different sources of error have been incorporated into a first-order probability analysis of the simplified Bishop model in order to arrive at quantitative information concerning the probability of failure.

Li and Lumb (1987) [61] discussed the advantaged of the Hasofer-Lind reliability index (β_{HL}) approach. The authors highlighted the importance of the correlation structure of soil properties and its effect on the reliability index β_{HL} .

Oka and Wu (1990) [62] stated that in stability problems, the failure probability associated with the critical slip surface is known to be smaller than that for the system that comprises all potential slip surfaces. Calculation were made for Congress Street cut, in Chicago to differentiate this reliability and it was observed that the probability failure of the system is twice that of the probability of failure of the critical slip surface.

Chowdary and Xu (1995) [63] addressed the system reliability for inexplicit and non-linear performance functions as well as for linear and explicit ones. It is shown that the upper bound system failure probability is higher than the failure probability associated with a critical slip surface. The difference increases as the coefficient of variation of the shear strength parameters increases.

Hassan & Wolff (1999) [64] proposed an algorithm to search for the minimum reliability index for soil slopes. The existing deterministic slope stability programs were utilized. Using specific combinations of soil parameter values, searches were conducted for the critical surfaces. It was determined that the critical probabilistic

surface was found to, in general, coincide with that obtained by setting one dominant parameter to a low value.

Malkawi and Abdulla (2000) [65] used the first-order second-moment method (FOSM) and Monte Carlo simulation method (MCSM) of measuring uncertainty associated with the cohesion of the soil c , the angle of internal friction ϕ and the unit weight of the soil (γ) for the reliability analysis of the soil slopes, and compared their values to those obtained by the method of slices mentioned previously. Conclusion were made regarding the relative difference between the reliability indices obtain by FOSM and MCSM methods and their dependence on the method of slices used.

El-Ramly et al., (2002) [66] gave the probabilistic analysis of the dykes of the James Bay hydroelectric project in spreadsheet form using MCSM. The results are compared with those obtained using the FOSM and the deficiencies of simple probability analysis are pointed out.

Low (2003) [67] implemented Spencer's method of slices with varying side force inclination for probabilistic approach to slope stability. Noncircular critical slip surfaces were determined using spreadsheet-automated constrained optimization.

Bhattacharya et al., (2003) [68] proposed a numerical procedure for locating the surface of minimum reliability index for earthen slope which utilizes an existing deterministic slope stability algorithm with the addition of a simple module for the calculation of the reliability index.

Xue and Gavin (2007) [69] gave a method to calculate the minimum reliability index with the uncertainty associated with the soil properties. The determination of the reliability index using FOSM and Hasofer-Lind reliability Index and associated slip surface is formulated as a nonlinear programming problem and solved using an efficient genetic algorithm for slope stability analysis (GASSA) environment. The results of the method are compared to existing reliability approaches applied to case histories of slope failures from the geotechnical literature and was found to be consistent and reasonable.

In order to eliminate the cumbersome calculation involved in determining the reliability indices by FOSM when the performance function are implicit, Zhao (2008) [70] presented a support vector machine (SVM)-based reliability analysis method which combines the SVM with the FOSM. The SVM method uses a small set of the

actual values of the performance functions to approximate the implicit performance functions, thus arriving at SVM-based explicit performance functions. The method was compared to the examples compared in the literature and was determined to be a good way to approach is implicit performance functions based reliability analysis of slope.

Cho (2009) [71] presented a numerical procedure for integrating a commercial finite difference method into a probabilistic analysis of slope stability using an artificial neural network (ANN)-based response surface. The limit state function which is implicit, thereby reducing the number of stability analysis calculations. A trained ANN model is used to calculate the probability of failure through the first- and second-order reliability methods and a Monte Carlo simulation technique.

Bhattacharya and Dey (2010) [72] coupled FORM with the Ordinary Method of Slices for evaluation of factor of safety. Numerical example problems are presented which are solved using both FORM and Mean-Value First-Order Second-Moment method (MVFOSM) based on the Taylor series expansion of the factor of safety and the results compared to enable to conclude that the effect of the distributions used to define the variability of the parameters on the reliability indices is very significant.

Wang et al., (2010) [73] developed a probabilistic failure analysis approach that makes use of the failure samples generated in MCS and analyzes these failure samples to assess the effects of various uncertainties on slope failure probability.

Griffiths et al., (2011) [74] developed a method to analyze infinite slopes using probability methods which can be applied to landslide conditions. It demonstrates how “first order” methods that may not properly account for spatial variability can lead to un-conservative estimates of the probability of slope failure.

2.4 Observations from the review of the literature

Review of the literature clearly indicates a fact that no observations on how the critical centres and the critical slip surfaces change with change in the co-efficient of variation of the parameters involved and their effect on the value of reliability index (β) as a combination.

Also, in each of the studies, the reliability indices have been mentioned for a few example problems which leaves a range of values of the variable parameters unexplored. Therefore, the present study has been focussed on to develop an analytical

study to combine the method of slices and FORM to develop a methodology to compute reliability indices. Perhaps this is the first analytical study to propose a formulation which computes the factors of safety as well as reliability indices. Therefore, the efforts have been made in this direction. The objectives and scope of the present investigation are presented in the next section.

2.5 Objectives of the present study

In view of the above, the objectives of the present study are summarized as:

- a) The formulation of factors of safety computed using various methods of slices using MATLAB
- b) The determination of reliability indices using target based reliability approach (Bash and Babu (2010) [2]) using various methods of slices considering the variability associated with the soil parameters, i.e. cohesion of the soil (c), the angle of internal friction (ϕ) and the unit weight of the soil (γ)
- c) Determination of the influence of the geometric properties of the soil slope i.e., the height and the angle the slope makes with the horizontal on the values of the reliability indices
- d) To observe the changes in the positions of the critical centers and slip surfaces associated with critical factors of safety and reliability indices.
- e) To assess the changes in way the critical slip surfaces are formed with varying values of the uncertainties of soil parameters as well as the geometric parameters.

Chapter 3

Formulation of Optimization

Methodology

3.1 Methods of Slices

The most commonly used method of slices to determine the factors of safety of slopes are

- i. The Ordinary method
- ii. The Simplified Bishop method
- iii. The Spencer method
- iv. The Janbu simplified method
- v. The Morgenstern-Price method

3.2 Factor of Safety

In the limit equilibrium methods, the elements of statics are used to derive the factor of safety. It takes into account the summation of forces in two directions, (here horizontal and vertical) and the summation of moments about a chosen point of rotation.

The factor of safety for slope stability analysis is usually defined as the ratio of the ultimate shear strength divided by the mobilized shear stress at incipient failure. There are several ways in formulating the factor of safety FS . The most common formulation for FS assumes the factor of safety to be constant along the slip surface, and it is defined with respect to the force or moment equilibrium:

1. Moment equilibrium: generally used for the analysis of rotational landslides. Considering a slip surface, the factor of safety FS_m defined with respect to moment is given by:

$$FS_m = \frac{M_r}{M_d} \quad (3.1)$$

where M_r is the sum of the resisting moments and M_d is the sum of the driving moment. For a circular failure surface, the center of the circle is usually taken as the moment point for convenience.

2. Force equilibrium: generally applied to translational or rotational failures composed of planar or polygonal slip surfaces. The factor of safety FS_f defined with respect to force is given by:

$$FS_f = \frac{F_r}{F_d} \quad (3.2)$$

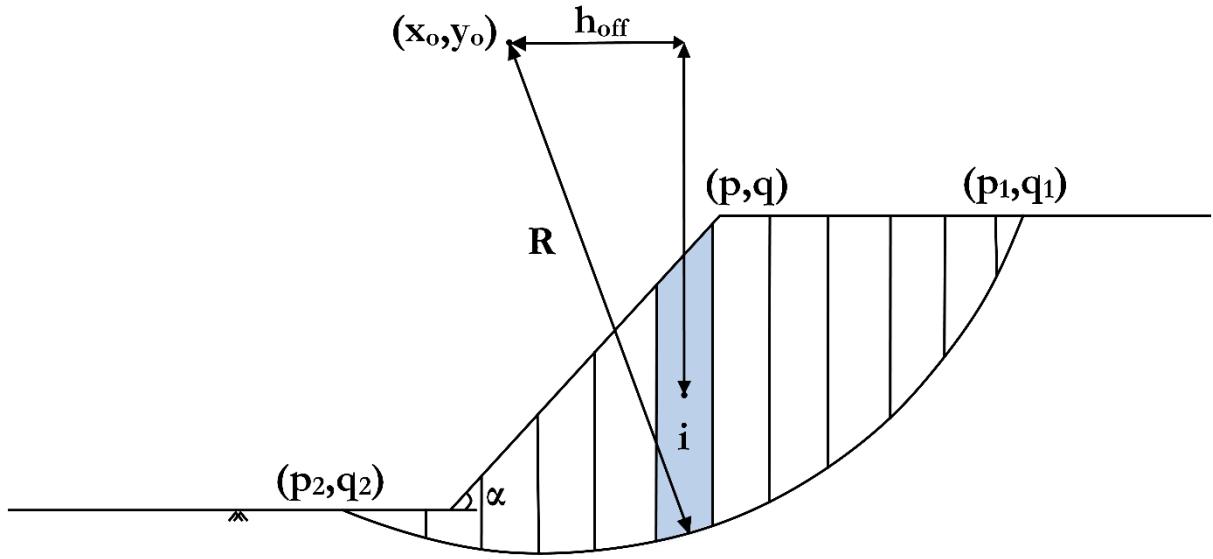


Figure 3.1: Geometry showing the parameters used and moment arms for circular slip surface

where FS_r is the sum of the resisting forces and FS_d is the sum of the driving forces.

3.3 Derivation of the Factor of Safety

The following are the notations for the variables associated with each slice and shall be used throughout the study in conjunction with the parameters defines before.

N = the total normal force on the base of a slice

T = the shear force mobilized on the base of each slice

E = the horizontal interslice normal forces

X = the vertical interslice shear forces

h_{off} = the horizontal distance from the centroid of each slice to the center of rotation
(as shown in Fig. 3.1)

θ = the angle between the tangent to the center of the base of each slice and the horizontal.

The notations ‘i’ are as same as used before to compute the factor of safety i.e. from right to left in the direction of failure which is also the direction in which the interslice function will be applied.

The distribution of the inclination of the inter-slice forces within the sliding mass is defined through a function $f(x_i)$ and a scalar coefficient λ as:

$$\frac{X_i}{E_i} = \lambda \times f(x_i) \quad (3.3)$$

In the above equation x_i is the abscissa of the i^{th} slice of the slope, $f(x_i)$ describes the variation of the inter-slice shear (X_i) and normal (E_i) forces across the slope; the coefficient λ represents the percentage of $f(x_i)$ used in the solution.

Imposing horizontal force (f) and moment (m) equilibrium of the whole soil mass and solving for the factor of safety, the following two equations can be derived:

$$FS_f = \frac{\sum_{i=1}^n T_{i,\text{lim}}}{\sum_{i=1}^n T_i} = \frac{\sum_{i=1}^n (cdl_i + N_i \tan \phi) \times \cos \theta_i}{\sum_{i=1}^n N_i \sin \theta_i} \quad (3.4)$$

$$FS_m = \frac{\sum_{i=1}^n (cdl_i + N_i \tan \phi)R}{\sum_{i=1}^n w_i h_{off_i}} \quad (3.5)$$

where

$$h_{off_i} = R \sin \theta_i \quad (3.6)$$

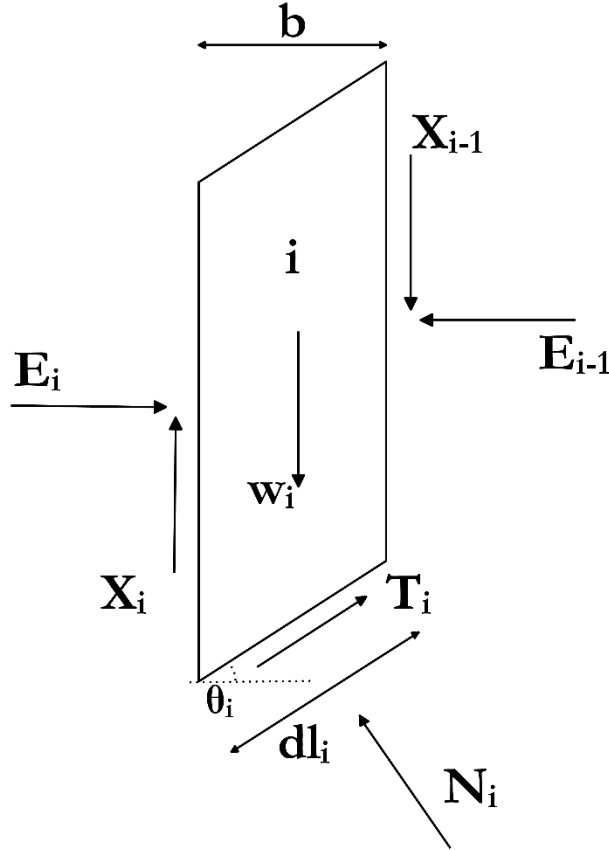


Figure 3.2: The forces acting on a slice

Now considering the equilibrium of an individual slice, the magnitude of the shear force mobilized at the base of a slice, T_i can be written in terms of the Mohr-Coulomb failure criterion as

$$T_i = \tau_i dl = \frac{\tau_{fi} dl_i}{FS} = \frac{(c + \sigma \tan \phi) dl_i}{FS} \quad (3.7)$$

where τ_i and τ_{fi} are the shear stress and shear stress at failure for the i^{th} slice.

also,

$$\sigma = \frac{N_i}{dl} \quad (3.8)$$

Which gives

$$T_i = \frac{c dl_i + N_i dl_i \tan \phi}{FS} \quad (3.9)$$

Considering force equilibrium in the vertical direction we get

$$w_i + X_i - X_{i-1} - N_i \cos \theta_i - T_i \sin \theta_i = 0 \quad (3.10)$$

Substituting the value of T_i in the above equation and solving for N_i , we get,

$$N_i = \frac{w_i + X_i - X_{i-1} - \frac{c dl_i \sin \theta_i}{FS}}{\cos \theta_i + \frac{\tan \phi \sin \theta_i}{FS}} \quad (3.11)$$

Now, consider the equilibrium of the slice in the horizontal direction, we get

$$E_{i-1} - E_i - N_i \sin \theta_i + T_i \cos \theta_i = 0 \quad (3.12)$$

$$E_i = E_{i-1} - N_i \sin \theta_i + T_i \cos \theta_i \quad (3.13)$$

All the above equations are then collectively used to determine the factor of safety FS which satisfies either one or both, the moment and force equilibrium based on the method being followed.

3.4 Inter-slice force function

The inter-slice shear force X is assumed to be related to the inter-slice normal force E by the relation

$$X = \lambda f(x) E \quad (3.14)$$

where, λ is an unknown scaling factor that is solved for as part of the unknowns, and $f(x)$ is an assumed function that has prescribed values at each slice boundary. There is no theoretical basis to determine $f(x)$ for a general problem, as the slope stability problem is statically indeterminate by nature.

3.5 Ordinary Method of Slices

The ordinary method of slices is the most popular and simplest method for determining the factor of safety of a slope. It considers a circular slip surface which is divide into n number of vertical slices and uses moment equilibrium about the center of the slip surface to calculate the factor of safety. The interslice forces and normal forces are ignored.

The expression for FS_{OMS} in this method is

$$FS_{OMS} = \frac{\sum (cdl_i + W_i \cos \theta_i \tan \phi)}{\sum W_i \sin \theta_i} \quad (3.15)$$

where c = cohesion of soil

ϕ = angle of internal friction of soil

γ = unit weight of soil

H = height of the slope and

α = the angle the slope makes with the horizontal.

W_i = is the weight of i^{th} slice = $\gamma b z_i$

b = base length of each slice

dl_i = length along slip surface of i^{th} slice = $b \sec \theta_i$

z_i = average height of i^{th} slice

θ_i = the inclination of the base of the slice measured between the base of the slice and the horizontal

The MATLAB program which implements this method to find FS_{OMS} was created by considering the toe as the origin $(0, 0)$ for the entire slope geometry. The inputs include the center of the circular slip surface for which the FS has to be calculated (x_o, y_o) , the geometric parameters H and α , the soil properties γ , c and ϕ and the number of slices, n the user wants to divide the slip surface into. The geometry and various parameters used are as shown in Figure 3.3.

The crest point (p, q) can be calculated using

$$p = H \cot \alpha \quad (3.16)$$

$$q = H \quad (3.17)$$

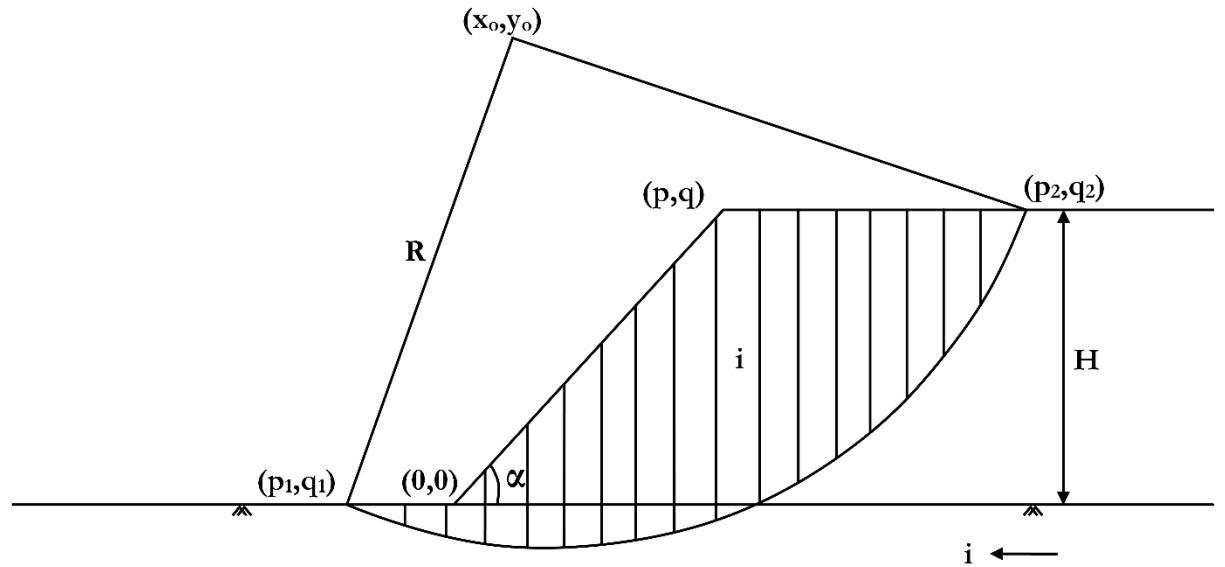


Figure 3.3: Geometry and parameters used for the calculation of factor of safety

This makes the equation of the slope as

$$y = \frac{q}{p} x \quad (3.18)$$

Thus knowing the radius of the slip surface, the general equation of the circle can be given as

$$(x - x_o)^2 + (y - y_o)^2 = R^2 \quad (3.19)$$

To find the entry point we initially substitute the ground level i.e $y = 0$ in eq.(3.19). we get

$$x_1 = x_o - \sqrt{R^2 - y_o^2} \quad (3.20)$$

$$x_2 = x_o + \sqrt{R^2 - y_o^2} \quad (3.21)$$

Three cases arise:

- a) If both x_1 and x_2 are less than zero, the slip circle doesn't cut the slope.
- b) If $x_1 < 0$ and $x_2 > 0$, the entry point is $(x_1, 0)$
- c) If both x_1 and x_2 are greater than zero, the entry point is along the slope.

In case of c, the equation of the circle and the equation of the slope are solved simultaneously and get two x-coordinates, say xx_1 and xx_2 which are as follows

$$xx_1 = \frac{-m - \sqrt{m^2 - 4lk}}{2l} \quad (3.22)$$

$$xx_2 = \frac{-m + \sqrt{m^2 - 4lk}}{2l} \quad (3.23)$$

where $m = -2(x_o + \frac{q}{p} y_o)$

$$l = 1 + \frac{q^2}{p^2}$$

$$k = x_o^2 + y_o^2 - R^2$$

If

1) xx_1 and xx_2 are imaginary, the circle doesn't cut the slope

2) $xx_1 > 0$ and $xx_2 < 0$, the entry point is (xx_1, yy_1) and the exit point is (xx_2, yy_2)

where

$$yy_1 = \frac{q}{p} xx_1 \quad (3.24)$$

$$yy_2 = \frac{q}{p} xx_2 \quad (3.26)$$

3) $xx_1 > 0$ and $xx_2 > p$, entry point is (xx_1, yy_1) where

$$yy_1 = \frac{q}{p} xx_1 \quad (3.27)$$

For easy understanding the entry point is referred to as (p_1, q_1) further on.

In exception to case 2, the exit point yet to be determined for cases b and 3.

In order to find the exit point we substitute the crest level i.e. $y = q$ in eq.(3.19) . We get

$$x_3 = x_o - \sqrt{R^2 - (q - y_o)^2} \quad (3.28)$$

$$x_4 = x_o + \sqrt{R^2 - (q - y_o)^2} \quad (3.29)$$

As $x_3 < x_4$ the defining point will be x_4 and determines the exit point. If $x_3 < x_4$, the circle cuts the crest i.e., (x_4, H) .

For easy understanding the exit point is referred to as (p_2, q_2) further on.

Now the distance between entry (p_1, q_1) and exit $((p_2, q_2))$ has to be divided into n slices each of width b given as

$$b = \frac{p_2 - p_1}{n} \quad (3.31)$$

The x co-ordinates of the i^{th} slice on the slip surface x_i can be found using

$$x_i = p_2 - ib \quad (3.32)$$

We can substitute these x_i 's in eq.(3.19) to get corresponding y_i 's such that $y_i < q$ (as they should lie within the geometry of the slope)

To determine the heights of each slice, an additional parameter $h1_i$ is used such that if $0 < x_i < p$, then

$$h1_i = \frac{q}{p} x_i \quad (3.33)$$

else

$$h1_i = q_2 \quad (3.34)$$

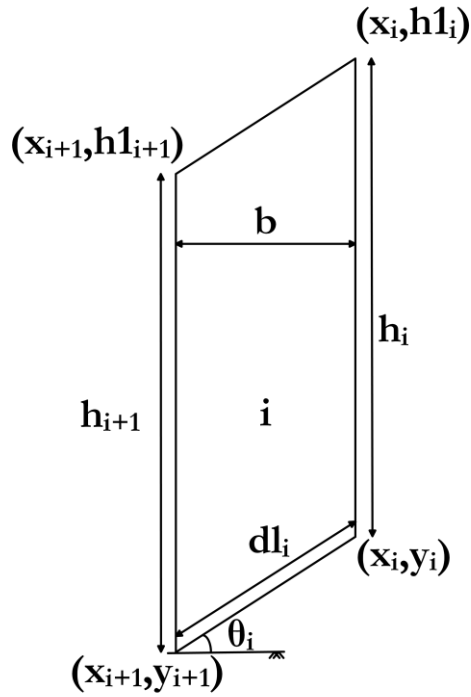


Figure 3.4: The parameters for the i^{th} slice

Thus heights of slices can be determined as

$$h_i = h1_i - y_i \quad (3.35)$$

The area of each slice can then be determined using

$$z_i = \frac{1}{2}(h_{i+1} + h_i) \quad (3.36)$$

$$a_i = bz_i \quad (3.37)$$

The weights are given by

$$W_i = \gamma bz_i \quad (3.38)$$

The inclinations of each slice θ_i are calculated using

$$\theta_i = \tan^{-1} \left(\frac{y_i - y_{i+1}}{x_i - x_{i+1}} \right) \quad (3.39)$$

Hence all the parameters for the geometry and the slices (Fig.3.4) are determined and the factor of safety is then calculated using eq.(3.15).

3.6 Grid and Radius search technique

In order to find the global critical factor of safety, a range of areas which will cover several points and different radii has to be generated. One of the ways to do this is to use the Grid and Radius method of search as in GeoStudio. The idea is to create a grids which cover the possible positions of the centre and radii of the slip surfaces, divide them into desired number of parts and search each possibility. The co-ordinates of these grids are given manually in the initial stages.

Grid: For the grid, say (x_1, y_1) , (x_2, y_2) , (x_3, y_3) and (x_4, y_4) are the top left, bottom left, bottom right and top left co-ordinates respectively as shown in Figure 3. If n_l and n_b are the number of parts the grid has to be divided into lengthwise and breadthwise respectively, then the co-ordinates of various points on the grid can be given as a combination of x_i 's and y_i 's as follows.

$$x_i = x_1 + [(i-1)m_l] \quad (3.40)$$

$$y_i = y_1 - [(i-1)m_b] \quad (3.41)$$

Where i shall vary from 1 to n_l+1 for x_i and 1 to n_b+1 for y_i and m_l and m_b are as follows

$$m_l = abs\left(\frac{x_4 - x_1}{n_l}\right) \quad (3.42)$$

$$m_b = abs\left(\frac{y_4 - y_3}{n_b}\right) \quad (3.43)$$

Radius: The radius grid is generated similarly as (X_1, Y_1) , (X_2, Y_2) , (X_3, Y_3) and (X_4, Y_4) and is divided into n_r parts breadthwise as shown in Figure 3.4. The sides of the grid are assumed to be at an angle so as to provide some diversification in the calculation of the radius values. The corresponding co-ordinates along the both breadths are then joined to make lines. The radius of the slip circle will be the perpendicular distance to this line from the centre under consideration. This can be determined as follows

$$ny_1 = \left(\frac{Y_1 - Y_2}{n_r}\right) \quad (3.45)$$

$$ny_2 = \left(\frac{Y_4 - Y_3}{n_r}\right) \quad (3.46)$$

$$d_1 = \left(\frac{Y_1 - Y_2}{X_1 - X_2}\right) \quad (3.47)$$

$$nx_1 = \frac{ny_1}{d_1} \quad (3.48)$$

$$nx_2 = \frac{ny_2}{d_2} \quad (3.49)$$

$$xx_{1i} = X_2 + [(i-1)nx_1] \quad (3.50)$$

$$yy_{1i} = Y_3 + [(i-1)ny_1] \quad (3.51)$$

$$xx_{2i} = X_3 + [(i-1)nx_1] \quad (3.52)$$

$$yy_{2i} = Y_3 + [(i-1)ny_2] \quad (3.53)$$

$$m_i = \frac{yy_{2i} - yy_{1i}}{xx_{2i} - xx_{1i}} \quad (3.54)$$

$$d_2 = \left(\frac{Y_3 - Y_4}{X_3 - X_4} \right) \quad (3.56)$$

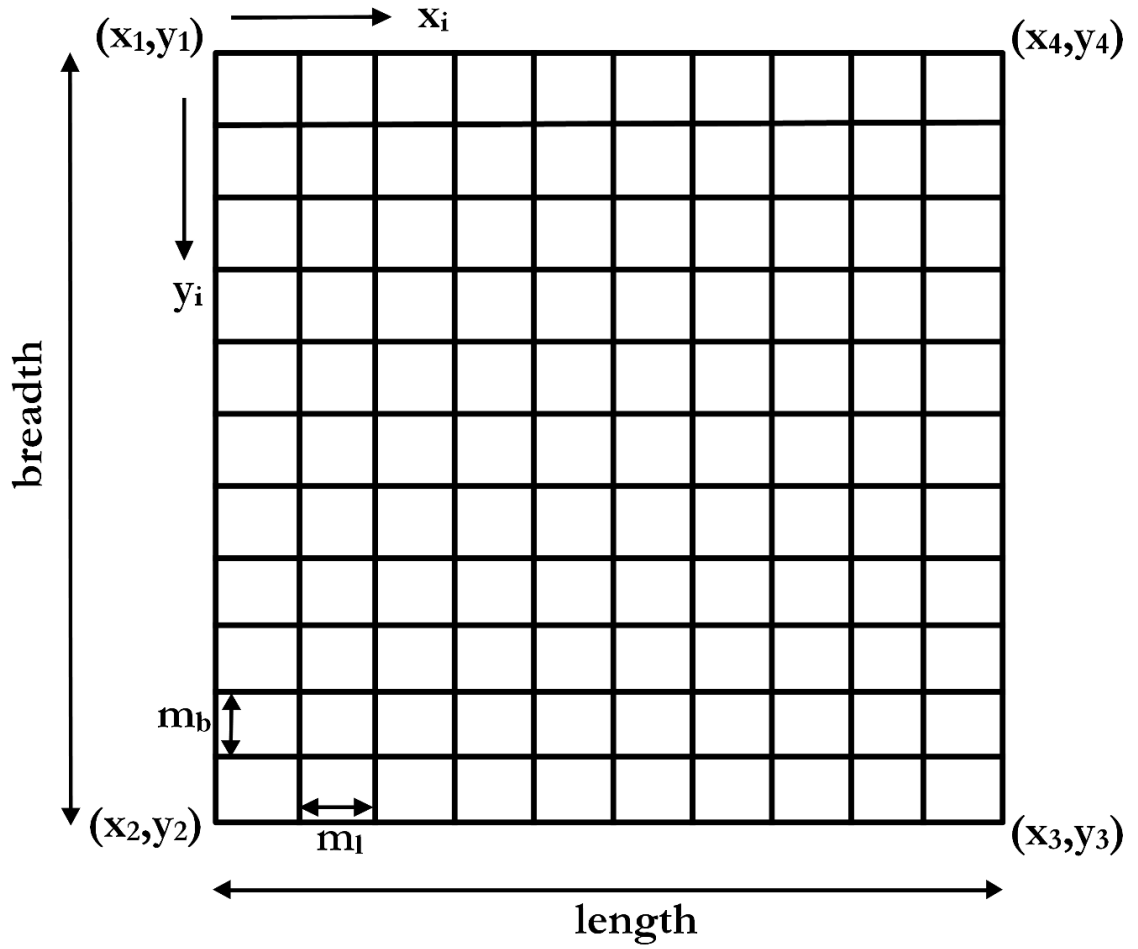


Figure 3.5: The grid for centers

$$cc_i = yy_{1i} - m_i xx_{1i} \quad (3.57)$$

$$R_i = \frac{abs[y_o - m_i x_o - cc_i]}{\sqrt{1 + m_i^2}} \quad (3.58)$$

The individual combinations of the points of the grid and their corresponding radii are calculated and fed into the above program to get the individual factors of safety. Once

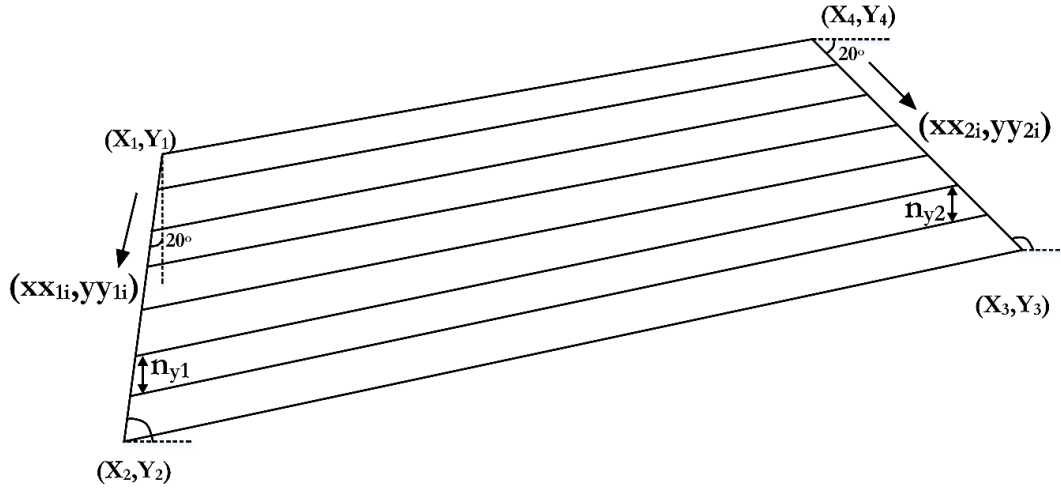


Figure 3.6: The grid for radius

the factors for a single point and different radii combination is calculated, the least of these values will be assigned as a value to the position in a matrix which constitutes FS_{OMS}'s equal to the point co-ordinates.

This will thus result in a matrix, FS_{OMS} which has the minimum values of factor of safety corresponding to the points of the grid as shown in Figure 3.7.

Whenever the given center and point combination fails to touch the slope, as in cases (a) and (1) as stated previously, is taken as a non-feasible value.

The minimum value among the entire matrix FS_{OMS}, which is the critical factor of safety, is then identified and its position determined, from which we can calculate the co-ordinates of the point.

Hence, given the grid for the centers and the grid for the radii of the slip circles, the critical factor of safety can be calculated.

3.7 Bishops' Simplified Method of Slices Using Grid and Radius

The Modified (or Simplified) Bishop's Method proposed by Alan W. Bishop (1995) [4] is a method for calculating the stability of slopes. It is an extension of the Method of Slices. By making some simplifying assumptions, the problem becomes statically determinate and suitable for hand calculations. The assumption made is forces on the sides of each slice are horizontal.

1.77	1.72	1.67	1.63	1.90	1.83	1.78	1.73	1.69	1.65	1.63
1.89	1.83	1.77	1.72	1.68	1.64	1.60	1.57	1.77	1.73	1.70
1.75	1.70	1.66	1.62	1.78	1.73	1.68	1.65	1.62	1.59	1.58
1.86	1.81	1.76	1.71	1.67	1.64	1.61	1.58	1.56	1.67	1.65
2.01	1.94	1.88	1.82	1.77	1.73	1.69	1.66	1.63	1.62	1.60
2.22	2.12	2.03	1.96	1.90	1.84	1.79	1.75	1.72	1.70	1.68
2.51	2.37	2.25	2.15	2.06	1.99	1.93	1.87	1.83	1.80	1.77
2.96	2.74	2.56	2.42	2.30	2.19	2.11	2.04	1.98	1.93	1.89
3.78	3.37	3.07	2.83	2.64	2.49	2.37	2.26	2.18	2.11	2.06
5.85	4.72	4.04	3.57	3.22	2.96	2.76	2.60	2.47	2.37	2.29
NF	10.43	6.84	5.30	4.43	3.86	3.46	3.16	2.94	2.77	2.64

1.82	1.77	1.73	1.69	1.94	1.88	1.83	1.78	1.75	1.73	1.71
1.94	1.87	1.82	1.78	1.74	1.70	1.68	1.66	1.84	1.80	1.78
1.80	1.76	1.73	1.70	1.83	1.79	1.76	1.73	1.71	1.70	1.70
1.92	1.87	1.82	1.78	1.75	1.73	1.71	1.69	1.69	1.77	1.77
2.07	2.00	1.94	1.89	1.85	1.82	1.79	1.77	1.76	1.75	1.76
2.27	2.18	2.10	2.03	1.98	1.93	1.89	1.86	1.84	1.84	1.84
2.56	2.42	2.31	2.22	2.14	2.08	2.03	1.98	1.96	1.94	1.94
3.00	2.79	2.62	2.49	2.37	2.28	2.21	2.15	2.10	2.07	2.06
3.82	3.42	3.13	2.90	2.72	2.58	2.46	2.37	2.31	2.26	2.23
5.99	4.78	4.10	3.63	3.30	3.05	2.86	2.71	2.60	2.52	2.47
NF	10.69	7.01	5.43	4.51	3.95	3.57	3.29	3.08	2.93	2.83

*NF – Not feasible

Figure 3.7: The matrices showing the critical factors of safety for Ordinary method of slices and Bishop's simplified method for corresponding points in user defined centre grid (a 10 by 10 grid was used for ease of viewing)

The expression for factor of safety in this method (without accounting to pore water pressure is

$$FS_{Bishop} = \frac{\sum \left[\frac{cdl_i + W_i \cos \theta_i \tan \phi}{m} \right]}{\sum W_i \sin \theta_i} \quad (3.59)$$

where $m = \cos \theta_i + \frac{\sin \theta_i \tan \phi}{FS_{Bishop}}$

The other parameters are same as before.

In order to calculate FS_{Bishop} , as it is present on both sides of the equation, an iterative search technique was used with an initial guess value. The starting value as per Rickard and Sitar (2001) [75] was recommended as $1.2 \times FS_{OMS}$.

This initial guess value was used and the Newton Raphson Iteration technique was used to obtain the FS_{Bishop} , once FS_{OMS} was calculated. This led to satisfactory results.

However, various examples were tested with varying initial guess values of FS_{OMS} , $1.025 \times FS_{OMS}$, $1.05 \times FS_{OMS}$, $1.1 \times FS_{OMS}$ and $1.2 \times FS_{OMS}$. Error between the GeoStudio values and the MATLAB program were calculated and were least and efficient in the case of $1.05 \times FS_{OMS}$. Hence, this was deemed to be a good initial guess value and the calculation of FS_{Bishop} was proceeded with.

Thus with an initial guess of $1.05 \times FS_{OMS}$ and an allowable error of 10^{-7} , the FS_{Bishop} , for each corresponding FS_{OMS} was calculated and matrices, FS_{Bishop} (Figure 3.8) and R_{Bishop} are obtained.

3.8 Generalization of the Grid points for Centre and Radius

In an effort to generalize the co-ordinates of the grids for radius and centres, so that they can be applied to any given problem, the initial search areas used for some examples which were in accordance to GeoStudio, were converted in terms of p and H .

The guidelines given in Duncan & Wright (2005) [76] as to the search areas for critical centre and the radius, were kept in mind and the grid points were generalized as follows.

27.05	25.92	24.78	23.64	20.81	19.64	18.48	17.32	16.16	14.99	13.83
26.49	25.35	24.21	23.08	21.94	20.80	19.66	18.53	15.62	14.46	13.29
27.47	26.35	25.24	24.12	21.37	20.23	19.10	17.96	16.82	15.69	14.55
26.88	25.76	24.65	23.53	22.42	21.31	20.19	19.08	17.96	15.12	13.98
26.29	25.17	24.06	22.94	21.83	20.72	19.60	18.49	17.37	16.26	15.14
25.70	24.58	23.47	22.36	21.24	20.13	19.01	17.90	16.78	15.67	14.55
25.11	24.00	22.88	21.77	20.65	19.54	18.42	17.31	16.19	15.08	13.96
24.52	23.41	22.29	21.18	20.06	18.95	17.83	16.72	15.60	14.49	13.37
23.93	22.82	21.70	20.59	19.47	18.36	17.24	16.13	15.01	13.90	12.78
23.34	22.23	21.11	20.00	18.88	17.77	16.65	15.54	14.42	13.31	12.19
NF	21.64	20.52	19.41	18.29	17.18	16.06	14.95	13.83	12.72	11.60

27.05	25.92	24.78	23.64	20.81	19.64	18.48	17.32	16.16	14.99	13.83
26.49	25.35	24.21	23.08	21.94	20.80	19.66	18.53	15.62	14.46	13.29
27.47	26.35	25.24	24.12	21.37	20.23	19.10	17.96	16.82	15.69	14.55
26.88	25.76	24.65	23.53	22.42	21.31	20.19	19.08	17.96	15.12	13.98
26.29	25.17	24.06	22.94	21.83	20.72	19.60	18.49	17.37	16.26	15.14
25.70	24.58	23.47	22.36	21.24	20.13	19.01	17.90	16.78	15.67	14.55
25.11	24.00	22.88	21.77	20.65	19.54	18.42	17.31	16.19	15.08	13.96
24.52	23.41	22.29	21.18	20.06	18.95	17.83	16.72	15.60	14.49	13.37
23.93	22.82	21.70	20.59	19.47	18.36	17.24	16.13	15.01	13.90	12.78
23.34	22.23	21.11	20.00	18.88	17.77	16.65	15.54	14.42	13.31	12.19
NF	21.64	20.52	19.41	18.29	17.18	16.06	14.95	13.83	12.72	11.60

Figure 3.8: The matrices showing the radii of critical factors of safety for Ordinary method of slices and Bishop's simplified method for corresponding points in user defined centre grid (a 10 by 10 grid was used for ease of viewing)

For the centre grid,

$$x_1 = p - 3.5H \quad (3.60)$$

$$y_1 = 5H \quad (3.61)$$

$$x_2 = x_1 \quad (3.62)$$

$$y_2 = H \quad (3.63)$$

$$x_3 = p + 2H \quad (3.64)$$

$$y_3 = y_2 \quad (3.65)$$

$$x_4 = x_1 + (x_3 - x_2) \quad (3.66)$$

$$y_4 = y_3 + (y_1 - y_2) \quad (3.67)$$

For the radius grid,

$$X_1 = -0.667H \quad (3.68)$$

$$Y_1 = 0 \quad (3.69)$$

$$Y_2 = -3H \quad (3.70)$$

$$X_2 = 1.5X_1 + \tan(20)Y_2 \quad (3.70)$$

$$Y_3 = 0.5H \quad (3.72)$$

$$X_4 = p \quad (3.73)$$

$$Y_4 = H \quad (3.74)$$

$$X_3 = 3X_4 + \tan(70)Y_3 \quad (3.75)$$

This generalization was proven to be very efficient when tested with additional examples.

And hence, the grid points were generalized successfully and the critical factor of safety and radii matrices are obtained as shown in Figure 3.10 and Figure 3.011 respectively

NF	NF	NF	NF	NF	NF	NF	NF	NF	NF	NF	NF
NF	NF	NF	NF	NF	NF	NF	NF	NF	NF	NF	NF
NF	NF	NF	NF	NF	NF	NF	NF	NF	NF	NF	NF
1.823	1.745	1.676	1.616	1.570	1.543	NF	NF	NF	NF	NF	NF
2.286	2.151	2.026	1.912	1.809	1.718	1.643	1.595	1.603	1.746	1.978	
2.027	1.944	1.863	1.787	1.715	1.647	1.585	1.532	1.495	1.494	1.611	
2.173	2.118	2.067	2.021	1.980	1.947	1.924	1.918	1.941	2.026	2.110	
2.479	2.454	2.437	2.427	2.429	2.448	2.491	2.574	2.728	2.643	3.121	
2.916	2.931	2.959	3.005	3.076	3.182	3.344	3.597	4.020	4.822	6.859	
4.489	4.592	4.739	4.948	5.248	5.694	6.397	7.546	9.830	15.721	54.001	
8.729	9.303	10.126	11.365	13.183	16.286	22.825	38.444	NF	NF	NF	

NF	NF	NF	NF	NF	NF	NF	NF	NF	NF	NF	NF
NF	NF	NF	NF	NF	NF	NF	NF	NF	NF	NF	NF
NF	NF	NF	NF	NF	NF	NF	NF	NF	NF	NF	NF
1.833	1.757	1.689	1.632	1.587	1.563	NF	NF	NF	NF	NF	NF
2.296	2.162	2.039	1.928	1.826	1.738	1.668	1.625	1.639	1.786	2.030	
2.054	1.973	1.897	1.825	1.758	1.696	1.643	1.601	1.580	1.605	1.758	
2.228	2.179	2.135	2.098	2.067	2.047	2.042	2.060	2.119	2.260	2.476	
2.577	2.563	2.558	2.564	2.586	2.631	2.709	2.841	3.070	3.109	3.789	
3.075	3.108	3.158	3.232	3.339	3.493	3.721	4.072	4.653	5.747	8.504	
4.731	4.869	5.060	5.326	5.706	6.266	7.147	8.593	11.477	18.986	55.351	
9.192	9.855	10.805	12.231	14.334	17.934	25.537	43.881	NF	NF	NF	

Figure 3.9: The matrices showing the critical factors of safety for Ordinary method of slices and Bishop's simplified method for corresponding points in the generalized centre grid (a 10 by 10 grid was used for ease of viewing)

Thus, a MATLAB program was written which will give us the critical factor of safety using OMS and Bishop's methods given the characteristic soil properties and the geometrical properties of a homogeneous soil slope.

3.9 Normalization with respect to H

$c/\gamma H$ is the stability number and is a quantity popularly used to in the stability analysis of slopes. Dividing both FSOMS and FSBishop will change the expressions as

$$\text{follows } FS_{OMS} = \frac{\sum \left(\frac{c}{\gamma H} \frac{dl_i}{H} + \frac{W_i}{\gamma H^2} \cos \theta_i \tan \phi \right)}{\sum \frac{W_i}{\gamma H^2} \sin \theta_i} \quad (3.76)$$

$$FS_{Bishop} = \frac{\sum \left[\frac{\frac{c}{\gamma H} \frac{dl_i}{H} + \frac{W_i}{\gamma H^2} \cos \theta_i \tan \phi}{\cos \theta_i + \frac{\sin \theta_i \tan \phi}{F_b}} \right]}{\sum \frac{W_i}{\gamma H^2} \sin \theta_i} \quad (3.77)$$

But,

$$W_i = \gamma b z_i$$

Hence,

$$FS_{OMS} = \frac{\sum \left(\frac{c}{\gamma H} \frac{dl_i}{H} + \frac{b}{H} \frac{z_i}{H} \cos \theta_i \tan \phi \right)}{\sum \frac{b}{H} \frac{z_i}{H} \sin \theta_i} \quad (3.78)$$

$$FS_{Bishop} = \frac{\sum \left[\frac{\frac{c}{\gamma H} \frac{dl_i}{H} + \frac{b}{H} \frac{z_i}{H} \cos \theta_i \tan \phi}{\cos \theta_i + \frac{\sin \theta_i \tan \phi}{F_b}} \right]}{\sum \frac{b}{H} \frac{z_i}{H} \sin \theta_i} \quad (3.79)$$

It is clear that by simply dividing the entire geometric system with the height H, the change of the parameter $c/\gamma H$ can be observed with respect to change in other quantities. The code was modified accordingly and the results were calculated.

3.10 Janbu's Simplified Method

Janbu is a general method of slices developed on the basis of limit equilibrium and was first presented by Janbu (1954) [5]. It is required to satisfy the equilibrium of forces and moments acting on individual blocks or slices (only moment equilibrium at last uppermost slices is not satisfied).

In Janbu simplified method, the interslice shear forces are assumed to be zero (i.e. $\lambda=0$) but the normal forces are taken into consideration (Janbu et al, 1956) [42]. The normal force equation will now be same as before but with the interslice shear forces set to zero. The horizontal force equilibrium equation is then considered to calculate the factor of safety.

Then an empirical correction factor is multiplied by the computed factor of safety in an attempt to account for the effect of the interslice shear forces. The empirical correction factor is related to the shear strength properties and the shape of the slip surface. Moment equilibrium is not satisfied.

NF	NF	NF	NF	NF	NF	NF	NF	NF	NF	NF
NF	NF	NF	NF	NF	NF	NF	NF	NF	NF	NF
NF	NF	NF	NF	NF	NF	NF	NF	NF	NF	NF
1.810	1.731	1.659	1.597	1.546	1.515	NF	NF	NF	NF	NF
2.275	2.138	2.011	1.895	1.788	1.693	1.613	1.557	1.557	1.713	1.958
2.007	1.921	1.839	1.761	1.686	1.614	1.548	1.490	1.447	1.443	1.612
2.135	2.077	2.023	1.972	1.925	1.885	1.853	1.834	1.842	1.908	1.996
2.413	2.382	2.357	2.337	2.326	2.328	2.348	2.398	2.501	2.388	2.776
2.808	2.810	2.821	2.847	2.890	2.959	3.065	3.235	3.517	NF	NF
4.275	4.346	4.449	4.598	4.813	5.130	NF	NF	NF	NF	NF
8.182	NF	NF	NF	NF	NF	NF	NF	NF	NF	NF

Figure 3.10: The matrices showing the critical factors of safety for Janbu's Simplified Method for corresponding points in the generalized centre grid (a 10 by 10 grid was used for ease of viewing)

Here, no correction factor is applied and the Janbu's Simplified Method results are reported without any correction towards the influence of the interslice forces.

Hence, the factor of safety by Janbu's Simplified Method is calculated using the equation

$$FS_{Janbu} = \frac{\sum_{i=1}^n T_{i,lim}}{\sum_{i=1}^n T_i} = \frac{\sum_{i=1}^n (cdl_i + N_i \tan \phi) \times \cos \theta_i}{\sum_{i=1}^n N_i \sin \theta_i} \quad (3.80)$$

where,

$$N_i = \frac{w_i - \frac{cdl_i \sin \theta_i}{FS_{Janbu}}}{\cos \theta_i + \frac{\tan \phi \sin \theta_i}{FS_{Janbu}}}$$

3.11 Spencer Method

Spencer (1967) [7] proposed an analysis in which a constant relationship is assumed between the magnitude of the interslice shear and the normal forces

$$\frac{X}{E} = \tan \delta \quad (3.81)$$

where δ = angle of the resultant interslice force with the horizontal

The above equation is similar to the generalized interslice equation in which $f(x)$ is equal to 1; then λ is equal to $\tan \delta$.

Originally Spencer summed the forces perpendicular to the interslice forces to derive the normal force equation but the same can also be done by summing the forces in the horizontal and vertical directions. He derived two factor of safety equations, one of which satisfies the force equilibrium. These equations are fundamentally same as the one's proposed in the limit equilibrium method when the interslice force function is a constant.

$$FS_{Spencer,f} = \frac{\sum_{i=1}^n T_{i,\lim}}{\sum_{i=1}^n T_i} = \frac{\sum_{i=1}^n (cdl_i + N_i \tan \phi) \times \cos \theta_i}{\sum_{i=1}^n N_i \sin \theta_i} \quad (3.82)$$

$$FS_{Spencer,m} = \frac{\sum_{i=1}^n (cdl_i + N_i \tan \phi) R}{\sum_{i=1}^n w_i h_{off_i}} \quad (3.83)$$

In order to solve for Spencer method according to Nash (1987) [77], we initially set , $X_i - X_{i-1} = 0$. The equations of $FS_{Spencer,f}$ and $FS_{Spencer,m}$ are then calculated to obtain a first set. Also for the first slice, X_i is equal to 0. Then a trial value of δ to obtain new estimates for the values of X and E . Having these values in hand $FS_{Spencer,f}$ and $FS_{Spencer,m}$ are recalculated to obtain the new estimates of the factors of safety. This computation is then repeated until the values of the interslice force function converge.

NF	NF	NF	NF	NF	NF	NF	NF	NF	NF	NF
NF	NF	NF	NF	NF	NF	NF	NF	NF	NF	NF
NF	NF	NF	NF	NF	NF	NF	NF	NF	NF	NF
1.832	1.756	1.688	1.630	1.586	1.561	NF	NF	NF	NF	NF
2.295	2.161	2.038	1.926	1.825	1.737	1.666	1.623	1.637	1.785	2.031
2.054	1.973	1.896	1.824	1.757	1.695	1.642	1.601	1.581	1.606	1.766
2.228	2.179	2.135	2.097	2.067	2.047	2.042	2.060	2.119	2.262	2.480
2.576	2.563	2.558	2.564	2.586	2.630	2.708	2.841	3.070	3.109	3.789
3.074	3.107	3.158	3.232	3.339	3.493	3.721	4.071	4.651	5.744	8.502
4.731	4.869	5.060	5.326	5.705	6.265	7.145	8.591	11.474	NF	NF
9.192	9.855	10.804	12.230	14.333	17.933	NF	NF	NF	NF	NF

Figure 3.11: The matrices showing the critical factors of safety for Spencer Method for corresponding points in the generalized centre grid (a 10 by 10 grid was used for ease of viewing)

The values of $FS_{Spencer,f}$ and $FS_{Spencer,m}$ are which are obtained are not necessarily equal. If $FS_{Spencer,f} \neq FS_{Spencer,m}$ means that the moment and force equilibrium aren't satisfied simultaneously. Hence the computation must be repeated with various trial values of δ until $FS_{Spencer,f}$ and $FS_{Spencer,m}$. When the convergence is obtained, that value is then taken as the factor of safety $FS_{Spencer}$ for the slope.

3.12 Morgenstern-Price Method

Morgenstern and Price (1965) [8] obtained the factor of safety using the summation of forces tangential and normal to the base of a slice and the summation of the moments about the center of the base of each slice. The equations which were written for a slice of infinitesimal thickness, were combined and a modified Newton-Raphson numerical technique was used to solve for the safety factor. An

arbitrary assumption is required to be made with respect to the direction of the resultant of the interslice and normal forces in order to arrive at the solution.

The Morgenstern-Price procedure assumes that the shear forces between slices are related to the normal forces in many ways depending on the preference of the user. In this method, $f(x_i)$, which describes the variation of the inter-slice shear (X_i) and normal (E_i) forces across the slope can be assumed to be a constant or a geometrical function as shown in the figure.

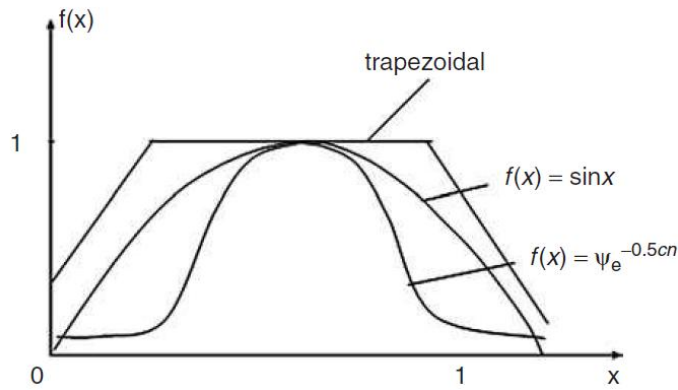


Figure 3.12: The interslice force function as it varies along the base of the slip surface

As stated by Duncan [80], in the original formulation of the Morgenstern and Price, stresses were integrated across each slice assuming that $f(x)$ varied linearly across the slice. This implicitly fixed the distribution of the normal stresses, including the location of the normal force on the base of the slice. In recent implementations, discrete formulations are used for slices and the location of the normal force has been assumed. Typically, it is assumed to act at the midpoint of the base of the slice or at a point on the base of the slice that is directly below the center of gravity.

$$FS_{MP,f} = \frac{\sum_{i=1}^n T_{i,lim}}{\sum_{i=1}^n T_i} = \frac{\sum_{i=1}^n (cdl_i + N_i \tan \phi) \times \cos \theta_i}{\sum_{i=1}^n N_i \sin \theta_i} \quad (3.84)$$

$$FS_{MP,m} = \frac{\sum_{i=1}^n (cdl_i + N_i \tan \phi) R}{\sum_{i=1}^n w_i h_{off_i}} \quad (3.85)$$

The unknowns that are solved for in the Morgenstern and Price procedure are the factor of safety FS_{MP} , the scaling parameter λ , the normal forces on the base of the slice (N), the horizontal interslice force (E), and the location of the interslice forces (line of thrust). The vertical component of the interslice force, X , is known from the interslice relation; that is, once the unknowns are calculated using the equilibrium equations, the vertical component of the interslice forces is calculated from the independent equation.

NF	NF	NF	NF	NF	NF	NF	NF	NF	NF	NF
NF	NF	NF	NF	NF	NF	NF	NF	NF	NF	NF
NF	NF	NF	NF	NF	NF	NF	NF	NF	NF	NF
1.828	1.751	1.683	1.625	1.580	1.555	NF	NF	NF	NF	NF
2.292	2.157	2.034	1.922	1.820	1.731	1.660	1.616	1.630	1.777	2.023
2.049	1.968	1.891	1.819	1.751	1.689	1.636	1.594	1.573	1.598	1.757
2.222	2.173	2.129	2.091	2.061	2.041	2.035	2.053	2.112	2.255	2.477
2.571	2.557	2.552	2.558	2.579	2.624	2.701	2.834	3.063	3.104	3.787
3.068	3.NF5	3.151	3.225	3.331	3.485	3.713	4.063	4.643	5.736	8.489
4.723	4.861	5.051	5.317	5.695	6.255	7.134	8.578	11.459	18.957	NF
9.182	9.845	10.794	12.219	14.320	17.918	25.518	NF	NF	NF	NF

Figure 3.13: The matrices showing the critical factors of safety for Morgenstern Price Method for corresponding points in the generalized centre grid (a 10 by 10 grid was used for ease of viewing)

In this study the interslice force function is taken according to Morgenstern Price method as

$$f(x_i) = \tan \delta \left(\sin \left(\frac{i}{n} \eta \right) \right)^\mu \quad (3.86)$$

Where 'i' is the slice under consideration and 'n' is the total number of slices that the geometry is divided into.

The initial values of $\tan \delta$ is taken as equal to 1 as given in Zhu et al., (2001) [54] and iterated until the convergence of FS_{MP} .

3.13 Normalization of the equations

When the above formulation is normalized with respect to H, the factor of safety equations can be normalized by dividing the equations with γH^2 which results in the following changes

$$T_i = \frac{\left(\frac{c}{\gamma H} + N_i \tan \phi \right) dl_i}{F} \quad (3.87)$$

$$F_f = \frac{\sum_{i=1}^n T_{i, \lim}}{\sum_{i=1}^n T_i} = \frac{\sum_{i=1}^n \left(\frac{c}{\gamma H} dl_i + N_i \tan \phi \right) \cos \theta_i}{\sum_{i=1}^n N_i \sin \theta_i} \quad (3.88)$$

$$F_m = \frac{\sum_{i=1}^n \left(\frac{c}{\gamma H} dl_i + N_i \tan \phi \right)}{\sum_{i=1}^n w_i h_{off_i}} \quad (3.89)$$

$$N_i = \frac{w_i + X_i - X_{i-1} - \frac{c}{\gamma H} dl_i \sin \theta_i}{\cos \theta_i + \frac{\tan \phi \sin \theta_i}{F}} \quad (3.90)$$

where w_i and dl_i are also normalized values.

Once all the above values are plugged into the MATLAB code, FS_{Janbu} , $FS_{Spencer}$ and FS_{MP} can be calculated.

This will thus result in the corresponding matrices, FS_{Janbu} , $FS_{Spencer}$ and FS_{MP} which have the minimum values of factor of safety corresponding to the points of the grid as

shown in Fig.3.10, Fig.3.11 and Fig 3.13 respectively. In addition to these matrices showing the interslice force parameter λ are also obtained for Spencer and Morgenstern Price Method.

Thus the factors of safety using the ordinary method of slices, Bishops Simplified method, Janbu's simplified method, Spencer method and Morgenstern-Price method are obtained.

The performance functions for the reliability analysis are given below:

$$g_{OMS}(X) = FS_{OMS} - 1 \quad (3.91)$$

$$g_{Bishop}(X) = FS_{Bishop} - 1 \quad (3.92)$$

$$g_{Spencer}(X) = FS_{Spencer} - 1 \quad (3.93)$$

$$g_{MP}(X) = FS_{MP} - 1 \quad (3.94)$$

3.14 First order reliability method (FORM)

The name first order reliability method comes from approximating the performance function $G(X)$ by a first order Taylor series. Also, the methods which consider the first two moments of the random variables (for normally distributed random variables, the first moment is mean value, and the second is the variance) and ignoring the higher moments (i.e. skewness, kurtosis etc.), are called the first-order second-moment methods (FOSM). However, before presenting some of the FORM methods, it is appropriate to define the Cornell reliability index (β_c).

Cornell reliability index (β_c)

The Cornell reliability index was the first analytical approximation method to calculate the probability of failure, and it paved the way for other methods that have a wider domain of application (Ang and Tang (1984) [78]).

The limit state function or performance function can be written as

$$g(X) = R - S \quad (3.95)$$

Where R = resistance of the structures and S = load applied on the structure. Assuming that R and S are statistically independent and normally distributed random variables, we may define a new random variable Z with the following properties (Ang and Tang (1984) [78]):

$$Z = R - S \quad (3.96)$$

$$\mu_Z = \mu_R - \mu_S \quad (3.97)$$

$$\sigma_Z^2 = \sigma_R^2 + \sigma_S^2 \quad (3.98)$$

where, μ_Z and σ_Z are the mean value and the standard deviation of the random variable Z respectively (Fig. 3.14). Then the probability of failure can be calculated from

$$P_f = P[Z < 0] = \Phi\left(-\frac{\mu_Z}{\sigma_Z}\right) = \Phi(-\beta_c) \quad (3.99)$$

where $\Phi(\cdot)$ is the cumulative distribution function for a standard normal variable, and β_c is the safety index. The same concept can be generalized to the case of more than two random variables and to the case of nonlinear performance function and this can be done by Taylor series expansion of the performance function around the mean values of the random variables as shown below:

$$Z = g(\mu_X) + \sum_{i=1}^n \frac{\partial g}{\partial x_i} (x_i - \mu_{x_i}) + \frac{1}{2} \sum_{i=1}^n \sum_{j=1}^n \frac{\partial^2 g}{\partial x_i \partial x_j} (x_i - \mu_{x_i}) (x_j - \mu_{x_j}) + \dots \quad (3.100)$$

where $g(\mu_X)$ is the performance function evaluated at the mean values of the random variables, and μ_{x_i} is the mean value of the random variable x_i . Then, if we truncate the series at the linear terms, the first approximate mean value and the variance of Z will be given by

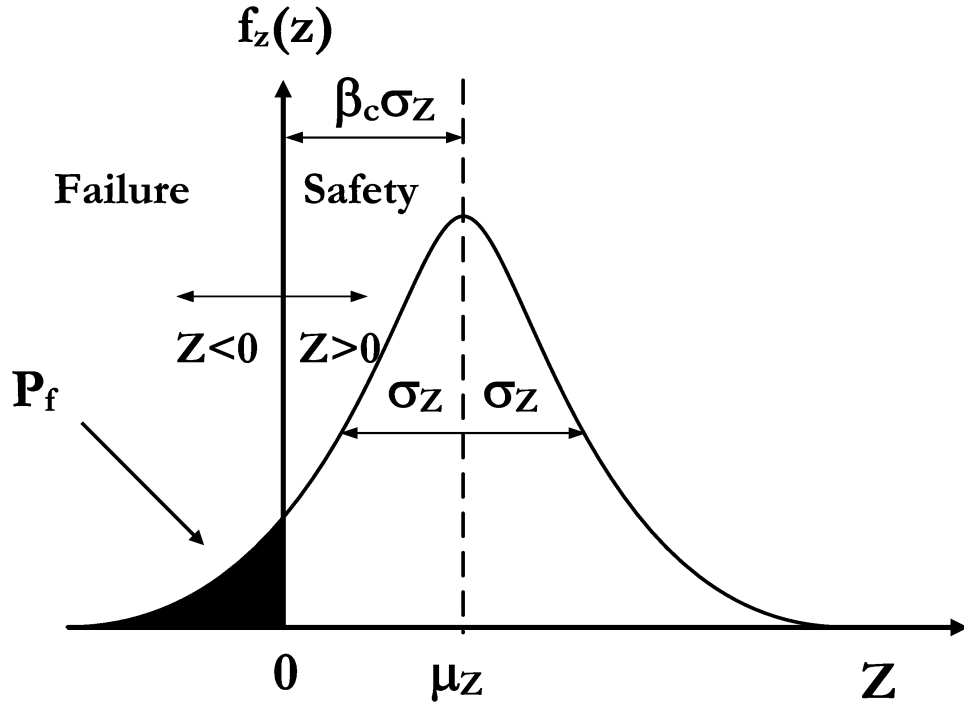


Figure 3.14: Distribution of safety margin, $Z = R - S$ (Melchers 2002)

$$\mu_Z \approx g(\mu_X) \quad (3.101)$$

$$\sigma_Z \approx \sqrt{\frac{1}{2} \sum_{i=1}^n \sum_{j=1}^n \frac{\partial g}{\partial x_i} \frac{\partial g}{\partial x_j} COV(x_i, x_j)} \quad (3.102)$$

where $COV(x_i, x_j)$ is the coefficient of variation for the random variables x_i and x_j . Also, a better estimation of the mean value of Z can be obtained from considering the square term in the Taylor series

$$\mu_Z = g(\mu_X) + \frac{1}{2} \sum_{i=1}^n \sum_{j=1}^n \frac{\partial^2 g}{\partial x_i \partial x_j} COV(x_i, x_j) \quad (3.103)$$

However, the second order variance requires obtaining the higher moments of the random variables, which may not be available in practical situations (Ang and Tang (1975) [79]).

Finally, the safety index (β_c), and the probability of failure (P_f) can be determined from eq.(3.87). Also, since the limit state function is linearized around the mean value, the safety index method is also known as the mean value first-order second-moment (MVFOSM). However, it is important to know that the estimation of the probability of failure using the safety index can only give accurate values for special cases, particularly, when the performance function is a simple addition or multiplication of the statistically independent random variables. Also, it gives different reliability values for the same design problem if the formulation of the performance function is changed to an equivalent formulation (i.e. this reliability calculation method lacks invariance). Thus, there was a need to develop some improved methods that avoid this problem. Yet, these improved methods are based on the safety index idea, which (from Eq. (3.87)) gives a qualitative measure of safety, in the sense that larger value of β_c means safer design and vice versa.

Hasofer and Lind reliability index (β_{HL})

The Hasofer and Lind (H-L) reliability index is one of the most widely used reliability calculation methods (Madsen et al., 1986; Haldar and Mahadevan 1995, 2000, Barakat et al., 1999, Der Kiureghian 2000, Melchers 2001 [3,80-84]). It is an improvement over the Cornell's safety index and it avoids its lack of invariance problem. The algorithm is presented for the calculation of reliability index for correlated Gaussian and non-Gaussian random variables in the following sections.

3.15 Correlated Gaussian random variables

The limit state function ($g(x)=0$) is written explicitly in terms of a vector of random variables ($X = \{x_i\}_{i=1}^n$). The limit state function separates acceptable performance (i.e. when $g(x) > 0$) from unacceptable performance (i.e. "failure" when $g(x) < 0$). Let X be mutually correlated Gaussian random variables. Covariance matrix of the correlated random variables x_1, x_2, \dots, x_n is $C_{ij} = \langle (x_i - \mu_i)(x_j - \mu_j) \rangle$, in

which $\langle \cdot \rangle$ is the expectation operator, μ_i and σ_i are mean and standard deviation of random variable x_i .

To determine the location of the most probable point of failure, the first step is to transform the set of original random variables ‘ X ’ into a Gaussian and correlated set of reduced variables ‘ $R = \{r_i\}_{i=1}^n$ ’ by $r_i = (x_i - \mu_i) / \sigma_i$, where r_i ’s are normally distributed with mean zero and unit standard deviation.

Covariance matrix of ‘ R ’ is $\rho_{ij} = \left\langle \left(\frac{x_i - \mu_i}{\sigma_i} \right) \left(\frac{x_j - \mu_j}{\sigma_j} \right) \right\rangle$ (which can also be called as the correlation coefficient matrix of X), where $|\rho_{ij}| \leq 1$, $i, j = 1 \text{ to } n$.

The required set of uncorrelated transformed variates can be obtained from ‘ R ’ by the transformation, $Y = T^T R$, where T is the transformation matrix can be obtained from the eigen value analysis of the correlation coefficient matrix of the original random variables ($[\rho_{ij}]$). In any case T must satisfy the equation given by $T^T [\rho_{ij}] T = [v]$, where $[v]$ is a diagonal matrix of the eigen values of $[\rho_{ij}]$. $Y = \{y_k\}_{k=1}^n$ is a set of uncorrelated random variables with ‘0’ mean and $\sqrt{v_k}$ is the standard deviation. Uncorrelated set of Gaussian random variables ‘ Y ’ can be transformed into a standard normal space ‘ $U = \{u_k\}_{k=1}^n$ ’ by $u_k = y_k / \sqrt{v_k}$, where u_k is independent of $u_j \forall k \neq j$ with mean ‘0’ and unit standard deviation.

By rearranging the terms in the above equations we can write random variable ‘ x_k ’ as follows:

$$x_k = \sigma_k \sum_{i=1}^n \Phi_{ki} \sqrt{v_i} u_i + \mu_k \quad (3.104)$$

where $k, i = 1, 2, \dots, n$

For uncorrelated random variables $\sqrt{v_k}=1$ and $\Phi_{ki}=1$

3.16 Calculation of reliability index

The performance function can be written as

$$g(u) = FS-1 \quad (3.105)$$

The basic formulation for FORM can be stated as follows:

$$\text{Find } \beta, \text{ which } \begin{cases} \text{minimizes} & \sqrt{u^T u} \\ \text{subjected to} & g(u) = 0 \end{cases} \quad (3.106)$$

This problem is modeled as a nonlinear constrained optimization problem which can be solved using the method of Lagrange multipliers and is given by,

$$\text{Lagrangian, } L = \sqrt{\sum_{i=1}^n u_i^2} + \lambda g(u) \quad (3.107)$$

where λ is the Lagrange multiplier. The stationary points of L can be found by solving the following set of equations $(\partial L / \partial u_i) = 0$ and $(\partial L / \partial \lambda) = 0$ (Arora 1989 [85]).

$$\frac{\partial L}{\partial u_j} = \frac{u_j}{\sqrt{\sum_{i=1}^n u_i^2}} + \lambda \frac{\partial g}{\partial u_j} = 0 \quad (3.108)$$

$$\text{where } \frac{\partial g}{\partial u_j} = \sum_{i=1}^n \frac{\partial g}{\partial x_i} \frac{\partial x_i}{\partial u_j} = \sum_{i=1}^n \left(\frac{\partial g}{\partial x_i} (\sigma_i) \right), \quad j = 1, 2, \dots \text{ to } n. \quad (3.109)$$

$$\frac{\partial L}{\partial \lambda} = g(u) = 0 \quad (3.110)$$

After simplification, Lagrange multiplier (λ) can be written as:

$$\lambda = \frac{1}{\sqrt{\sum_{j=1}^n \left\{ \sum_{i=1}^n \frac{\partial g}{\partial x_i}(\sigma_i) \right\}^2}} \quad \text{where } k = 1, 2, \dots \text{ to } n \quad (3.111)$$

Now the design point in the standard normal space (u_k) can be expressed as

$$u_k = -\beta \frac{\sum_{i=1}^n \frac{\partial g}{\partial x_k}(\sigma_i)}{\sqrt{\sum_{j=1}^n \left\{ \sum_{i=1}^n \frac{\partial g}{\partial x_i}(\sigma_i) \right\}^2}} = -\alpha_k \beta \quad \text{where } k = 1, 2, \dots \text{ to } n \quad (3.112)$$

Rearranging the above Eq. (3.103), we get

$$\sum_{j=1}^n u_k \left[\sum_{i=1}^n \frac{\partial g}{\partial x_k}(\sigma_i) \right] = -\beta \sqrt{\sum_{j=1}^n \left\{ \sum_{i=1}^n \frac{\partial g}{\partial x_k}(\sigma_i) \right\}^2} \quad (3.113)$$

$$\beta = \frac{-\sum_{j=1}^n u_k \left[\sum_{i=1}^n \frac{\partial g}{\partial x_k}(\sigma_i) \right]}{\sqrt{\sum_{j=1}^n \left\{ \sum_{i=1}^n \frac{\partial g}{\partial x_k}(\sigma_i) \right\}^2}} \quad (3.114)$$

Design point (x_k) can be written as

$$x_k = \sigma_k \sum_{i=1}^n (-\alpha_i \beta) + \mu_k \quad \text{where } k = 1, 2, \dots, n. \quad (3.115)$$

3.17 Non-Gaussian random variables

The Hasofer-Lind reliability index for non-normal variables are computed using transformation of non-normal to normal variables. Several transform models such as Rosenblatt transformation (Rosenblatt 1952), Nataf transformation (Nataf 1962), Rackwitz and Fiessler algorithm (Rackwitz and Fiessler 1976, 1978), Chen and Lind

(1983) [86- 90] are available. A widely used approach by Rackwitz and Fiessler (1976) [88] is described in the following section. The algorithm computes equivalent mean and standard deviation by imposing conditions that the cumulative distribution

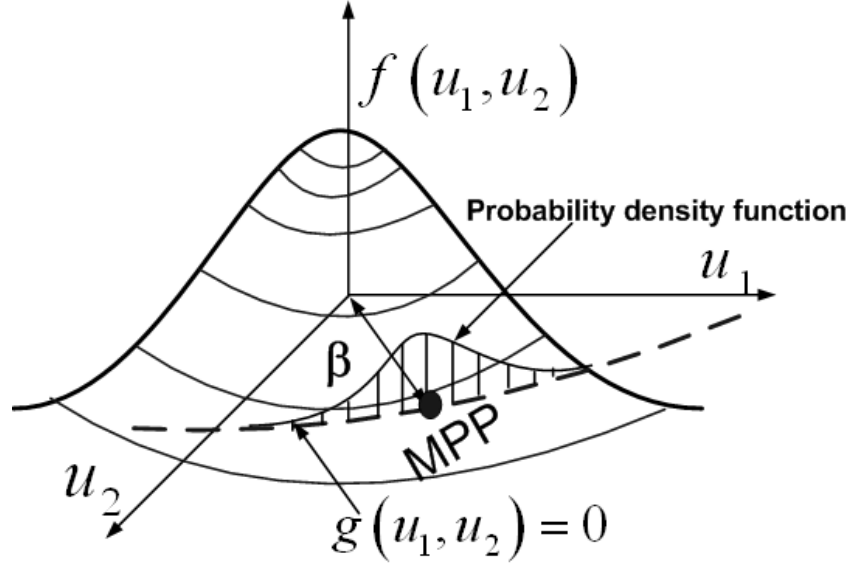


Figure 3.15: Two dimensional representation of design point on the failure boundary for the linear limit state function

function and the probability density functions of the actual variable and the equivalent normal variable are equal at the design points on the failure surface, that is at the checking point x_i^* ,

$$\Phi\left(\frac{x_i^* - \mu_{x_i}^N}{\sigma_{x_i}^N}\right) = F_{x_i}(x_i^*) \quad (3.116)$$

where $\mu_{x_i}^N$ and $\sigma_{x_i}^N$ are the mean and standard deviation of the equivalent normal variable at the checking point, and $F_{x_i}(x_i^*)$ is the cumulative distribution function of the original non-normal variables. Rearranging Eq. (3.107), we get

$$\mu_{x_i}^N = x_i^* - \Phi^{-1}\left[F_{x_i}(x_i^*)\right]\sigma_{x_i}^N \quad (3.117)$$

Equating probability density functions of the original variable and the equivalent normal variables at the checking points,

$$\frac{1}{\sigma_{X_i}^N} \phi \left(\frac{x_i^* - \mu_{X_i}^N}{\sigma_{X_i}^N} \right) = f_{X_i}(x_i^*) \quad (3.118)$$

where $\phi(\cdot)$ and $f_x(x_i^*)$ are the probability density functions of the equivalent standard normal and the original random variables. From Eq. (3.109),

$$\sigma_{X_i}^N = \frac{\phi \left\{ \Phi^{-1} \left[F_{X_i}(x_i^*) \right] \right\}}{f_{X_i}(x_i^*)} \quad (3.119)$$

Based on the known equivalent normal mean and standard deviation, β_{HL} can be obtained.

3.18 Most probable point of failure (MPP)

A major step in a FORM for reliability analysis is to determine the MPP. This is usually accomplished by using an optimization search algorithm. The minimum distance associated with the MPP (Fig.3.15) provides a measurement of safety or probability of failure. In the standard normal space, the point on the first order limit state function at which the distance from the origin is minimum is the Most Probable Point of failure (MPP) and the shortest distance corresponding to MPP is called as reliability index (β). In this case the limit state surface is approximated by a tangent plane at the design point that will eventually converge to the most probable point (MPP) of failure (Fig.3.15).

Fig. 3.16 illustrates the concept of reliability index and MPP search for a two variable case in the standard normal space. Finding the MPP and the reliability index is a minimization problem, which usually involves an iterative search process using FORM. Among the various possible values ($\beta_1, \beta_2, \beta_3, \beta_4, \beta_5$), the minimum β is identified.

Probability of failure is given by

$$P_f = P[g(u) < 0] = \Phi(-\beta) \quad (3.120)$$

where $\Phi(\cdot)$ is the cumulative distribution function (CDF) of the standard normal variate.

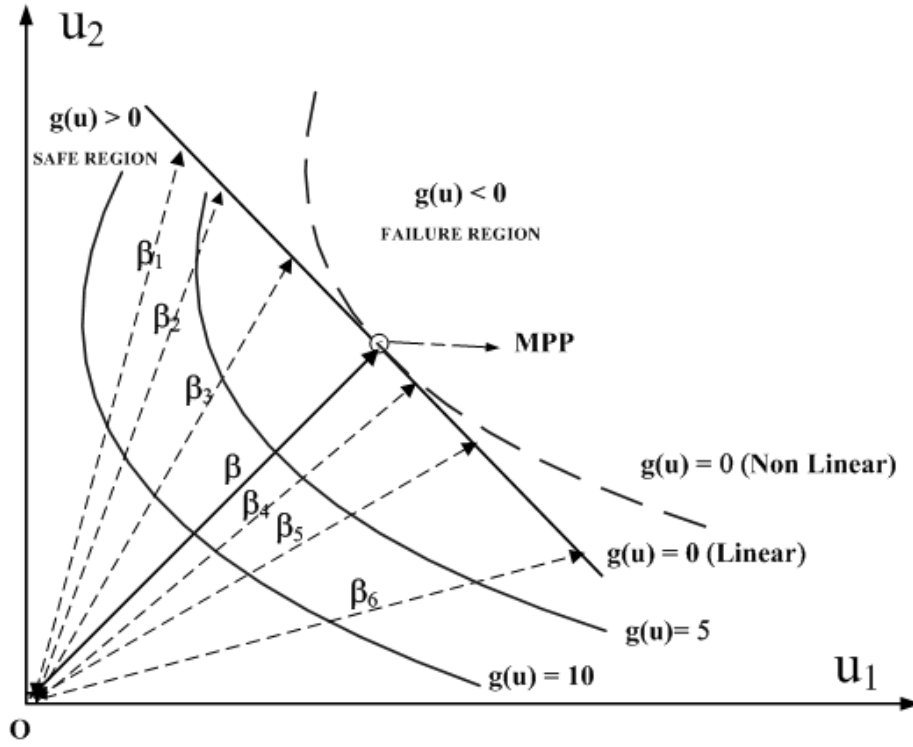


Figure 3.16: Identification of MPP in the reliability analysis (FORM)

The H-L reliability index gives an exact estimation for the design reliability for linear performance functions, and an acceptable approximation for most of the nonlinear performance functions as long as the radius of curvature of the performance function is large compared to magnitude of β .

3.19 Random variables considered in the present study

The parameters that are assumed to vary in the present study are the cohesion of the soil c , the angle of internal friction ϕ and the unit density of the soil γ . The mean and coefficient of variations of these parameters are available in the literature by various authors such as Phoon and Kulhawy (1999) [28] and Duncan (2000) [35] etc.

In this study, for reliability indices, the stability number $c/\gamma H$ is considered for calculations. When the values of mean and coefficient of variation of c , ϕ and γ are known, the coefficient of variation values for $c/\gamma H$ is calculated as follows

$$COV = \frac{\sigma}{\mu} \quad (3.121)$$

By the formula used for the variance of a fraction, the variance of $c/\gamma H$ can be written as

$$\sigma^2 \left(\frac{c}{\gamma H} \right) = \frac{\mu_{\gamma H}^2 \sigma_c^2 + \mu_c^2 \sigma_{\gamma H}^2}{\mu_{\gamma H}^4} \quad (3.122)$$

expanded as

$$\sigma^2 \left(\frac{c}{\gamma H} \right) = \frac{\mu_{\gamma H}^2 \mu_c^2 COV_c^2 + \mu_c^2 \mu_{\gamma H}^2 COV_{\gamma H}^2}{\mu_{\gamma H}^4} \quad (3.123)$$

which gives

$$\sigma \left(\frac{c}{\gamma H} \right) = \frac{\mu_c}{\mu_{\gamma H}} \sqrt{COV_c^2 + COV_{\gamma H}^2} \quad (3.124)$$

which can be written as

$$\sigma \left(\frac{c}{\gamma H} \right) = \mu \left(\frac{c}{\gamma H} \right) \sqrt{COV_c^2 + COV_{\gamma H}^2} \quad (3.125)$$

from which we obtain

$$COV \left(\frac{c}{\gamma H} \right) = \sqrt{COV_c^2 + COV_{\gamma H}^2} \quad (3.126)$$

Now, one will have the mean and coefficient of variation values for the parameters $c/\gamma H$ and ϕ .

In this study, the mean and variance of the parameters are taken in such a way that any combination of the values available in the literature will be a subset of the values taken in the study. The following are the values and their corresponding

Table 3.1: Random variables considered in the present study

Random Variable	Statistics		
	Mean	COV (%)	Distribution
$\frac{c}{\gamma H}$	0.1 to 0.5	10-30	Normal
ϕ	10 – 40°	5-20	Log-Normal

Thus the reliability indices are calculated for various methods by changing the factor of safety accordingly in the performance function

The following matrices (Fig.3.17–3.21) represent the minimum values of the reliability indices calculated for each point on the center grid for corresponding set of values of radii as slip circle parameters for all the methods of slices discussed previously. The least value in the entire grid is taken as the critical reliability index β_{OMS} , β_{Bishop} , $\beta_{Spencer}$, and β_{MP} for ordinary method of slices, Bishop's simplified method, Spencer method and Morgenstern – Price method respectively. The corresponding center is the critical center for the given slope.

NF	NF	NF	NF	NF	NF	NF	NF	NF	NF	NF
NF	NF	NF	NF	NF	NF	NF	NF	NF	NF	NF
NF	NF	NF	NF	NF	NF	NF	NF	NF	NF	NF
5.936	5.606	5.280	4.972	4.704	4.522	NF	NF	NF	NF	NF
7.385	7.041	6.674	6.287	5.883	5.478	5.102	4.819	4.797	5.357	6.124
7.493	7.183	6.855	6.511	6.152	5.782	5.415	5.073	4.809	4.773	5.424
8.535	8.345	8.157	7.976	7.805	7.657	7.549	7.511	7.598	7.927	8.532
9.929	9.865	9.819	9.794	9.803	9.861	9.988	10.217	10.599	10.678	11.768
11.441	11.486	11.559	11.669	11.826	12.045	12.343	12.749	13.300	14.054	15.121
13.756	13.878	14.030	14.221	14.458	14.754	15.122	NF	12.342	NF	NF
15.442	12.309	12.425	12.573	12.744	12.953	NF	NF	NF	NF	NF

Figure 3.17: Critical Reliability Indices for Ordinary Method of Slices

NF	NF	NF	NF	NF	NF	NF	NF	NF	NF	NF
NF	NF	NF	NF	NF	NF	NF	NF	NF	NF	NF
NF	NF	NF	NF	NF	NF	NF	NF	NF	NF	NF
5.999	5.681	5.370	5.078	4.829	4.667	NF	NF	NF	NF	NF
7.432	7.098	6.743	6.372	5.989	5.611	5.267	5.026	5.048	5.620	6.438
7.638	7.352	7.053	6.746	6.432	6.121	5.830	5.588	5.463	5.612	6.466
8.807	8.654	8.510	8.382	8.276	8.209	8.203	8.296	8.556	8.982	9.637
10.333	10.317	10.327	10.368	10.456	10.610	10.855	11.231	11.800	12.253	13.703
11.976	12.076	12.213	12.398	12.644	12.967	13.392	13.953	14.698	15.700	17.057
14.259	14.435	14.618	14.821	15.036	15.248	16.137	NF	NF	NF	NF
15.756	15.937	16.137	NF	NF	NF	NF	NF	NF	NF	NF

Figure 3.18: Critical Reliability Indices for Bishop's Simplified Method

NF	NF	NF	NF	NF	NF	NF	NF	NF	NF	NF
NF	NF	NF	NF	NF	NF	NF	NF	NF	NF	NF
NF	NF	NF	NF	NF	NF	NF	NF	NF	NF	NF
5.896	5.555	5.214	4.887	4.594	4.384	NF	NF	NF	NF	NF
7.364	7.013	6.636	6.236	5.814	5.384	4.971	4.640	4.571	5.185	5.975
7.432	7.109	6.766	6.402	6.018	5.616	5.209	4.815	4.493	4.423	5.303
8.426	8.217	8.006	7.798	7.594	7.406	7.249	7.150	7.170	7.445	7.995
9.771	9.684	9.611	9.554	9.524	9.536	9.607	9.769	10.073	9.920	10.946
11.244	11.264	11.308	11.385	11.504	11.678	11.925	12.271	12.755	13.427	14.341
13.667	13.778	13.919	14.098	14.325	14.612	14.974	NF	NF	NF	NF
15.579	15.730	15.918	16.115	NF	NF	NF	NF	NF	NF	NF

Figure 3.19: Critical Reliability Indices for Janbu Simplified Method

NF	NF	NF	NF	NF	NF	NF	NF	NF	NF	NF
NF	NF	NF	NF	NF	NF	NF	NF	NF	NF	NF
NF	NF	NF	NF	NF	NF	NF	NF	NF	NF	NF
5.992	5.674	5.361	5.068	4.818	4.655	NF	NF	NF	NF	NF
7.427	7.093	6.738	6.366	5.983	5.604	5.260	5.018	5.038	5.617	6.444
7.635	7.349	7.051	6.744	6.430	6.119	5.830	5.590	5.468	5.626	6.511
8.806	8.653	8.510	8.382	8.277	8.211	8.206	8.300	8.563	8.986	9.654
10.334	10.318	10.328	10.369	10.458	10.612	10.857	11.234	11.803	12.334	13.696
11.977	12.077	12.215	13.023	12.645	12.969	13.394	13.954	14.698	15.696	NF
14.260	14.435	14.616	14.818	15.011	15.641	16.136	NF	NF	NF	NF
15.752	15.932	16.108	NF	NF	NF	NF	NF	NF	NF	NF

Figure 3.20: Critical Reliability Indices for Spencer Method

NF	NF	NF	NF	NF	NF	NF	NF	NF	NF	NF
NF	NF	NF	NF	NF	NF	NF	NF	NF	NF	NF
NF	NF	NF	NF	NF	NF	NF	NF	NF	NF	NF
5.970	5.648	5.331	5.035	4.781	4.614	NF	NF	NF	NF	NF
7.412	7.075	6.717	6.341	5.953	5.569	5.220	4.973	4.989	5.567	6.398
7.613	7.324	7.023	6.713	6.396	6.081	5.787	5.544	5.419	5.578	6.474
8.784	8.630	8.485	8.355	8.249	8.181	8.176	8.270	8.535	8.968	9.659
10.314	10.297	10.307	10.347	10.436	10.590	10.836	11.215	11.790	12.331	13.718
11.959	12.059	12.196	13.010	12.628	12.952	13.379	13.942	14.690	15.699	NF
14.248	14.424	14.614	14.816	14.966	15.630	16.127	NF	NF	NF	NF
15.737	15.930	15.901	NF	NF	NF	NF	NF	NF	NF	NF

Figure 3.21: Critical Reliability Indices for Morgenstern-Price Method

Chapter 4

Reliability Analysis of Homogeneous Soil Slopes

4.1 Validation of the formulation

In order to ensure that the values obtained by the present formulation are acceptable, the results obtained are compared with some standard examples given in the literature.

Factor of Safety

Initially, the factor of safety values are compared to the values given in several literature works as detailed below.

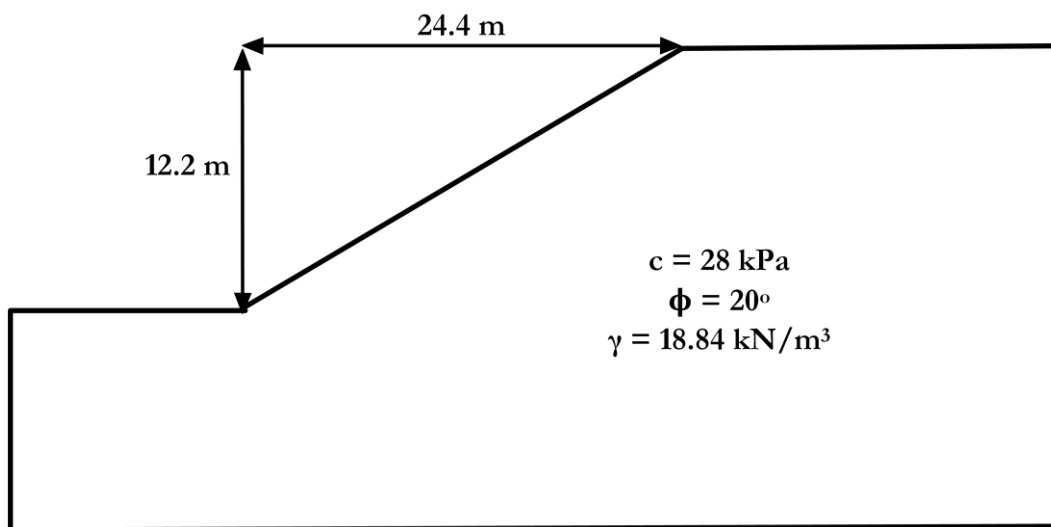


Figure 4.1: The geometry and soil properties of the slope from Bolton et al. (2003)

The first example considered was taken from Bolton et al. (2003) [91] as shown in Fig.4.1 with homogeneous cohesive soil. The comparison of the results found is shown in Table 4.1. The Janbu's Method gives lower factor of safety as it ignores

interslice shear forces and may violate moment equilibrium for the mass as a whole. While Spencer's method incorporates the interslice shear force by assuming a constant force angle and satisfies all equilibrium conditions. Hence Janbu's method generates factors of safety lower than Spencer's.

Table 4.1: The comparison of factors of safety obtained from the study with Bolton et al. (2003)

c (kPa)	$\phi(^{\circ})$	γ (kN/m ³)	FS _{Janbu}		FS _{Spencer}	
			Bolton et al.(2003)	Present Study	Bolton et al.(2003)	Present Study
28	20	18.84	1.832	1.8488	1.99	2.0182

The second example taken was from Zolfaghari et al. (2005) [92] as shown in Fig.4.2. It can be seen that when the values from the literature are compared to those obtained by the present study (Table 4.2), they are very close and hence acceptable.

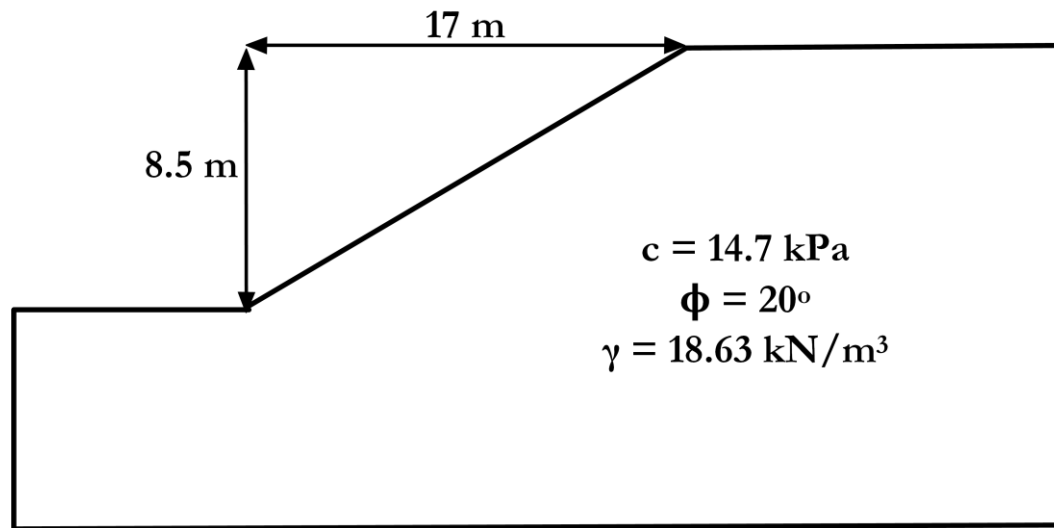


Figure 4.2: The geometry and soil properties of the slope from Zolfaghari et al. (2005)

Table 4.2: The comparison of factors of safety obtained from the study with Zolfaghari et al. (2005)

c (kPa)	$\phi(^{\circ})$	γ (kN/m ³)	FS _{Bishop}	
			Zolfaghari et al.(2005)	Present Study
14.7	20	18.632	1.74	1.76

Another example was taken from Malkawi et al. (2000) [65] (Fig.4.3) which uses MCSM optimization to calculate the factors of safety for a given slope of height 5m and 1V:2H slope angle.

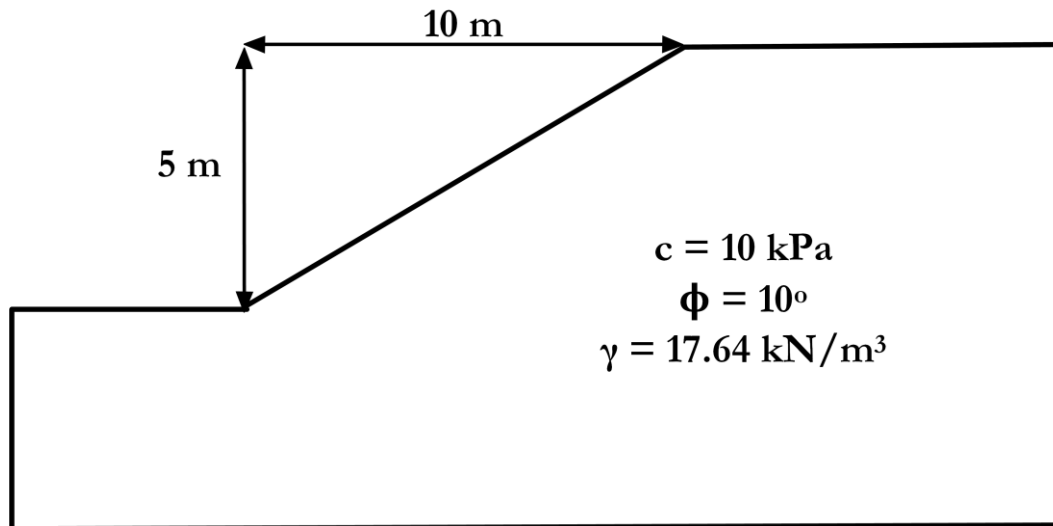


Figure 4.3: The geometry and soil properties of the slope from Malkawi et al. (2000)

Table 4.3 gives the summary of the comparison. It is observed that the present study slightly overestimates the factor of the safety which is deemed acceptable for the current technique used.

Table 4.3: The comparison of factors of safety obtained from the study with Malkawi et al. (2001)

c (kPa)	$\phi(^{\circ})$	$\gamma \text{ (kN/m}^3\text{)}$	FS _{MP}	
			Malkawi et al. (2000)	Present Study
10	10	17.64	1.338	1.351

Also, a set of values taken from Zhao et al. (2008) [70], for the slope geometry given in Fig.4.4, are compared to the values obtained from the present study in Table 4.4. It is observed the values obtained are comparable and hence acceptable.

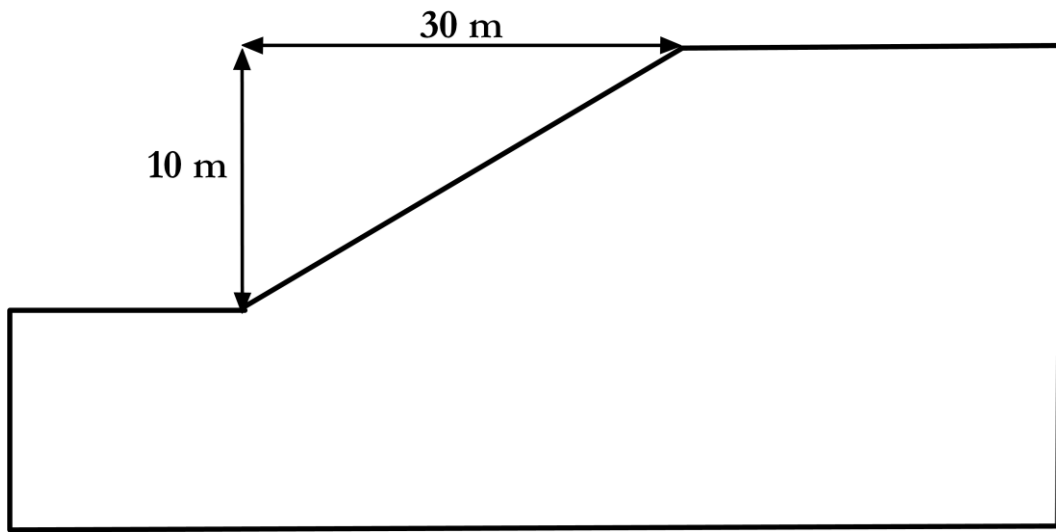


Figure 4.4: The geometry and soil properties of the slope from Malkawi et al. (2000)

Table 4.4: The comparison of factors of safety obtained from the study with Zhao et al. (2008)

c (kPa)	ϕ (°)	γ (kN/m ³)	FS _{Bishop}		FS _{Spencer}	
			Zhao et al. (2008)	Present	Zhao et al. (2008)	Present
13	16	18	1.734	1.758	1.733	1.758
13	16	20	1.813	1.822	1.811	1.822
13	20	22	1.907	1.902	1.905	1.903
15	16	20	1.760	1.786	1.758	1.786
15	18	22	1.842	1.854	1.84	1.854
15	20	18	2.126	2.148	2.124	2.147
17	16	22	1.780	1.806	1.778	1.806
17	18	18	2.079	2.107	2.077	2.108
17	20	20	2.141	2.164	2.139	2.164
15	18	20	1.904	1.923	1.902	1.923

Also, random examples were created in GeoStudio and the values obtained from the software are compared to the ones obtained by the present study as shown in Table 4.5.

Table 4.5: The comparison of factors of safety obtained from the study with GeoStudio examples

H (m)	α (°)	c (kPa)	ϕ (°)	γ (kN/m ³)	FSOMS		FS _{Bishop}		FS _{Janbu}		FS _{Spencer}		F _{MP}	
					Geostudio	Present Study	Geostudio	Present Study	Geostudio	Present Study	Geostudio	Present Study	Geostudio	Present Study
25	18.43	15	32	19	2.419	2.391	2.487	2.489	2.409	2.377	2.486	2.490	2.486	2.484
15	21.80	1	40	18	2.231	2.336	2.255	2.488	2.230	2.328	2.254	2.498	2.254	2.501
8	18.43	10	23	19	2.071	2.180	2.187	2.242	2.055	2.157	2.184	2.241	2.184	2.232
20	21.80	28	0	20	0.512	0.563	0.530	0.570	0.493	0.539	0.530	0.570	0.530	0.569
18	18.43	9	30	20	2.165	2.156	2.237	2.248	2.155	2.144	2.236	2.249	2.236	2.243
5	15.95	0	42	20	3.446	3.482	3.561	3.647	3.513	3.473	3.561	3.651	3.561	3.647

As it can clearly be seen that the values calculated from the present study are not significantly different to the values provided in the literature. Hence, it can be said that the formulation for the factor of safety is validated.

Reliability Indices

In a process similar to the factors of safety, the reliability indices obtained are also compared to the values available given by Zhao et al. (2008) [70] as given in Table 4.6 which uses a combination of SVM and FOSM. This is summarized as follows

Table 4.6: The comparison of reliability indices (β_{Bishop} , β_{Spencer}) obtained from Zhao et al. (2008) and calculated from the present study

COV (%)	β_{Bishop}				β_{Spencer}			
	Zhao et al. (2008)			Present FOSM	Zhao et al. (2008)			Present FOSM
	PEM	FOSM	SVM+ FOSM		PEM	FOSM	SVM+ FOSM	
5	11.120	10.820	10.740	11.638	11.120	10.950	11.030	11.633
10	5.590	5.410	5.370	5.819	5.590	5.470	5.510	5.816
15	3.750	3.610	3.580	3.879	3.730	3.650	3.680	3.878
20	2.830	2.700	2.690	2.910	2.690	2.740	2.760	2.908
25	2.290	2.160	2.150	2.328	2.280	2.190	2.210	2.327
30	1.930	1.800	1.790	1.940	1.920	1.820	1.840	1.939

* PEM : Point estimate method

* FOSM: First order second moment method

* SVM : Support vector Machine technique

From the Table 4.6 it can be seen that there is not much difference in the values of reliability indices calculated from the present study to those stated in the literature. Hence it can be said that the formulation for the calculation of Reliability Index has been validated.

4.2 Slip Circles Study

In order to study the effect of the geometric as well as the shear strength parameters of the soil, the values of the parameters are varied as follows.

Table 4.7: The ranges of the values used for the various parameters involved in the present study

Parameter	Range
$c/\gamma H$	0.1 - 0.5
ϕ	10 - 40°
$z = \tan^{-1}(\alpha)$	3 - 0.5
COV of ϕ	5 - 20%
COV of $c/\gamma H$	10 - 40%

The change in the magnitude and the position of critical reliability index and the critical slip circles is observed by drawing slip circles for the of all except one of the parameter value as fixed and the last one is varied continuously to observe its corresponding effect separately for the various methods of slices

Effect of slope angle α

- Figure 4.5 shows the effect of change in slope angle α on the critical slip surfaces for ordinary method of slices. A more magnified view is given by Fig.4.6 which shows the effect of change in slope angle on the shear bands for the ordinary method of slices.
- It can be observed that as the value of α increases, the volume of soil involved in the failure mechanism (and hence the location of the critical centers) is decreasing. This decrease is causes the normal force at the base of the slip

surface to decrease which in turn causes a corresponding decrease in the value of stability i.e. the reliability indices.

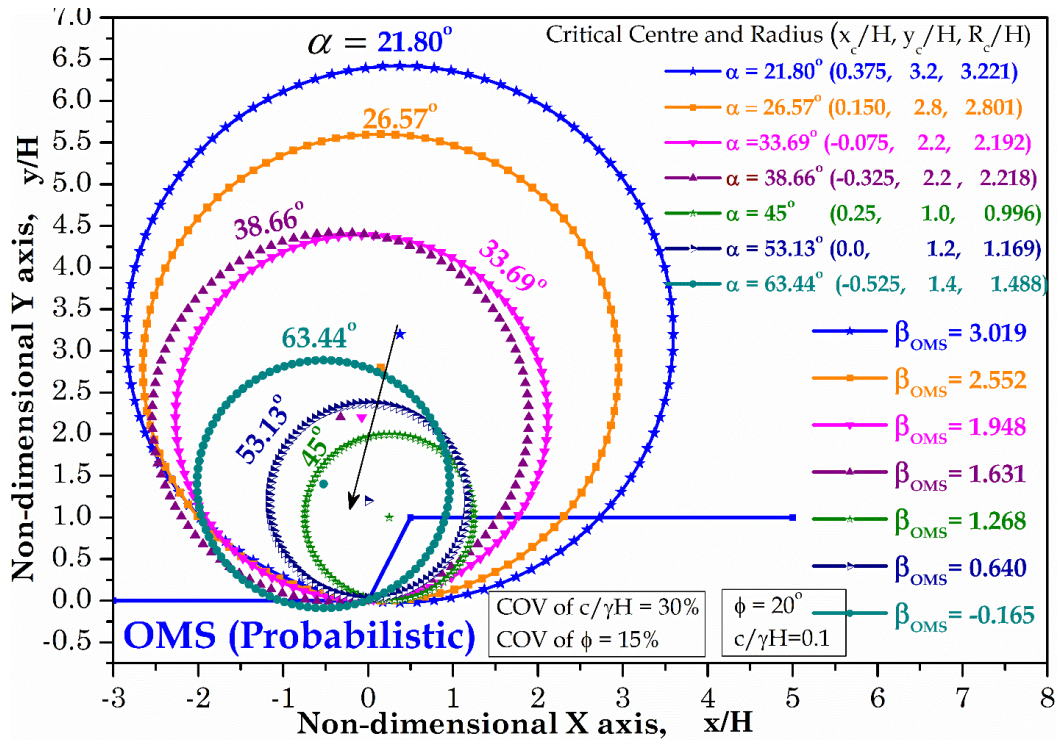


Figure 4.5: The effect of change in slope angle α on the critical slip surfaces for Ordinary Method of Slices

- In the case of Bishop's simplified method (Fig.4.7 and 4.8), the soil involved in $\alpha = 45^\circ >$ that involved in $\alpha = 53.13^\circ$. This behavior can be attributed to the possibility that a local minima is being chosen for that particular value instead of a global minima which causes the anomaly in the behavior. It may be eliminated by taken a finer grid or by changing the position of the generalized grids.
- Similarly the Fig 4.7 and Fig.4.8 show the effect of slope angle for Bishop's Simplified Method, Fig.4.9 and Fig.4.10 show the effect of slope angle for Spencer Method, and Fig.4.11 and Fig.4.12 show the effect of slope angle for Morgenstern-Price Method.

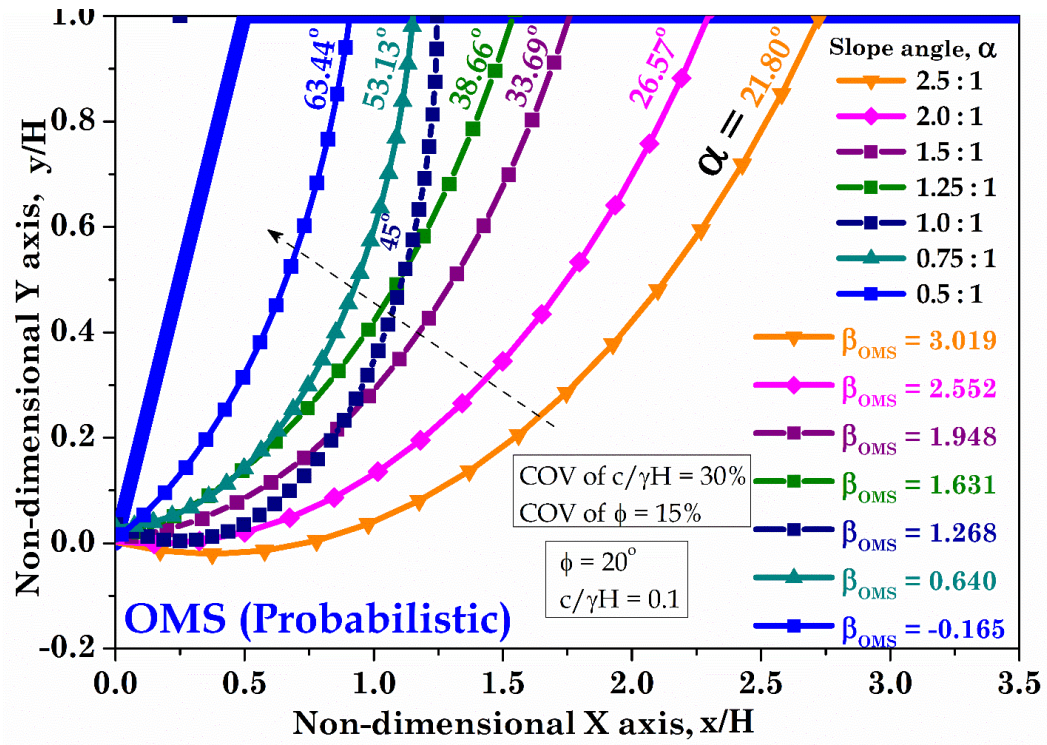


Figure 4.6: The effect of change in slope angle α on the shear bands for Ordinary Method of Slices

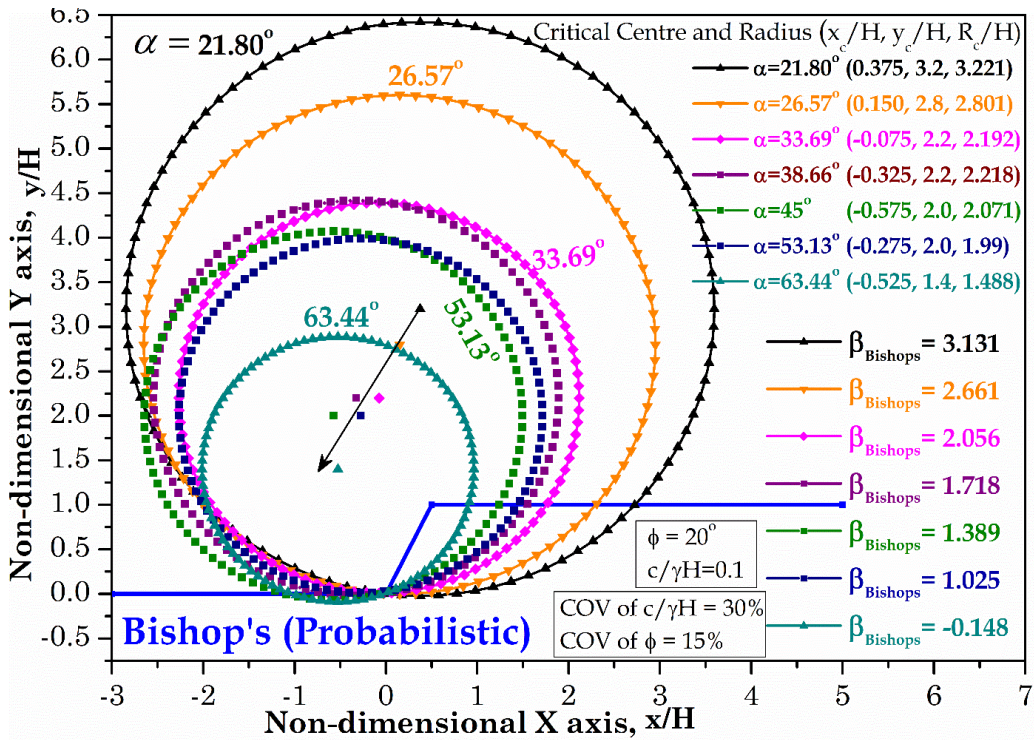


Figure 4.7: The effect of change in slope angle α on the critical slip surfaces for Bishop's Simplified Method

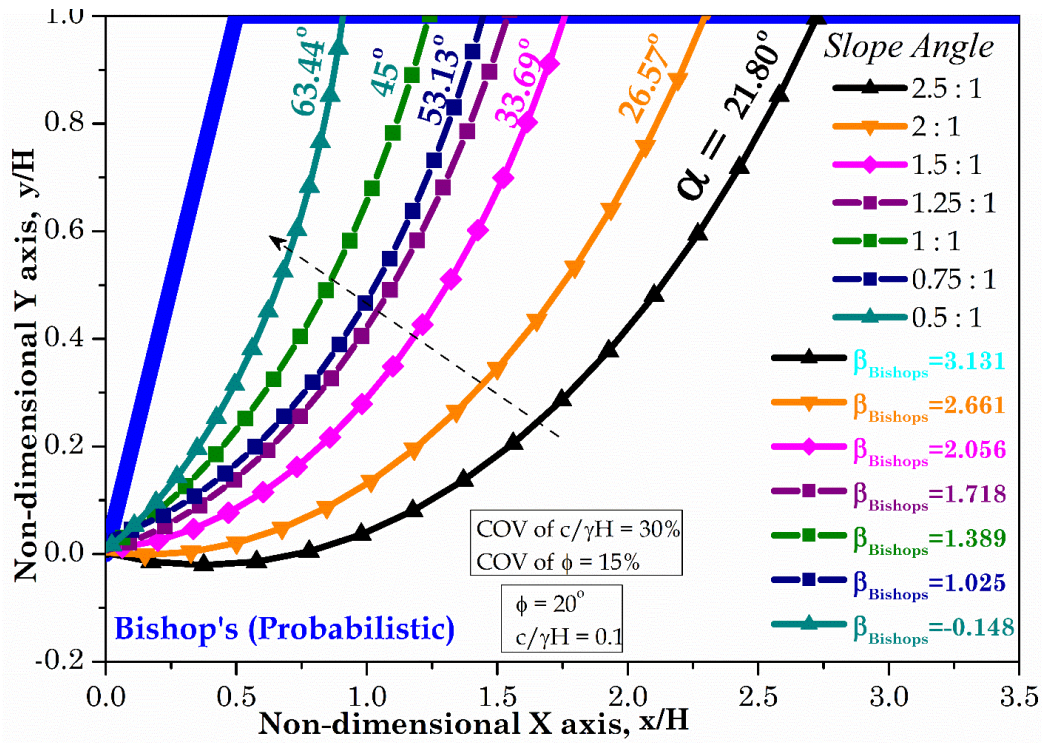


Figure 4.8: The effect of change in slope angle α on the shear bands for Bishop's Simplified Method

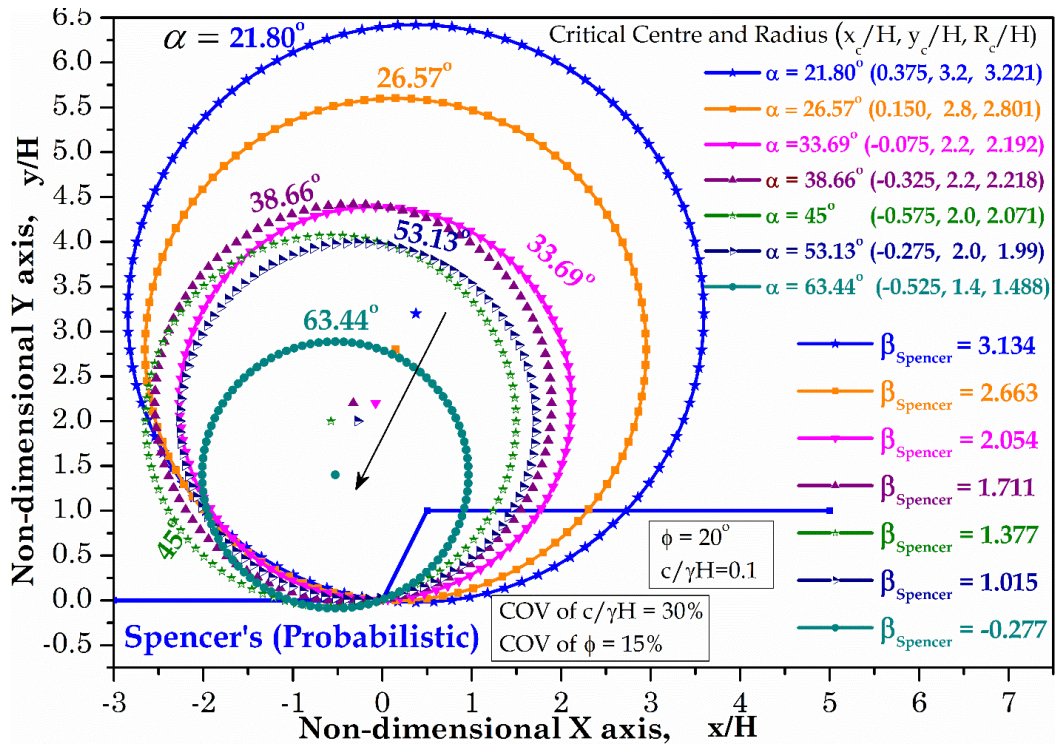


Figure 4.9: The effect of change in slope angle α on the critical slip surfaces for Spencer Method

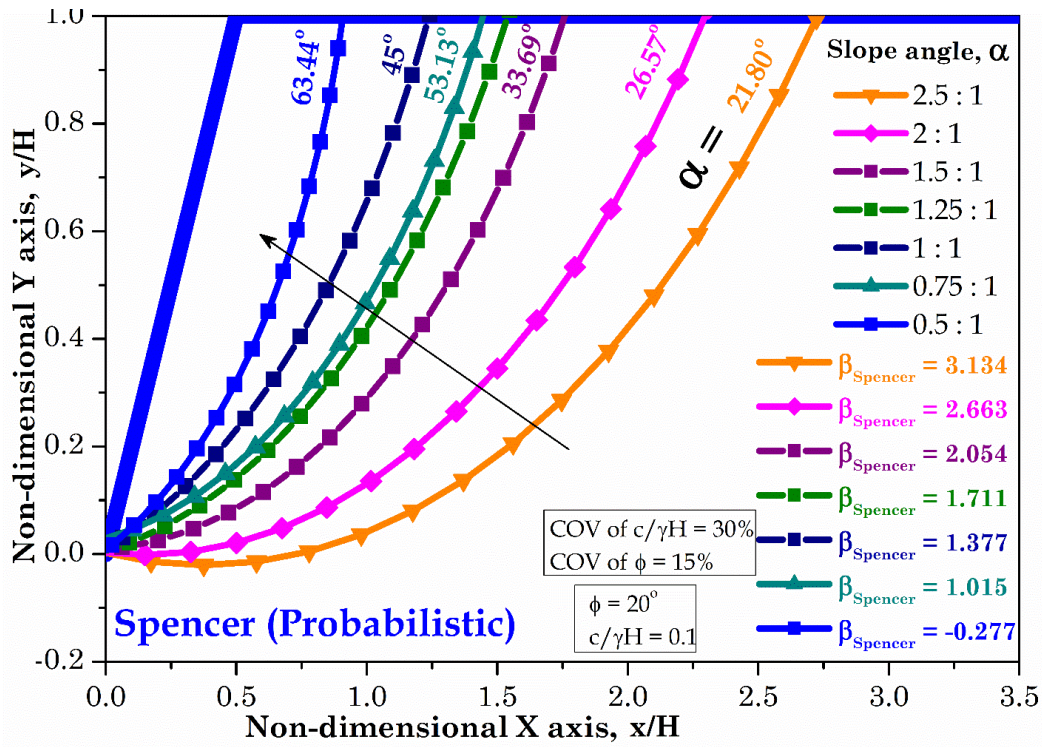


Figure 4.10: The effect of change in slope angle α on the shear bands for Spencer Method

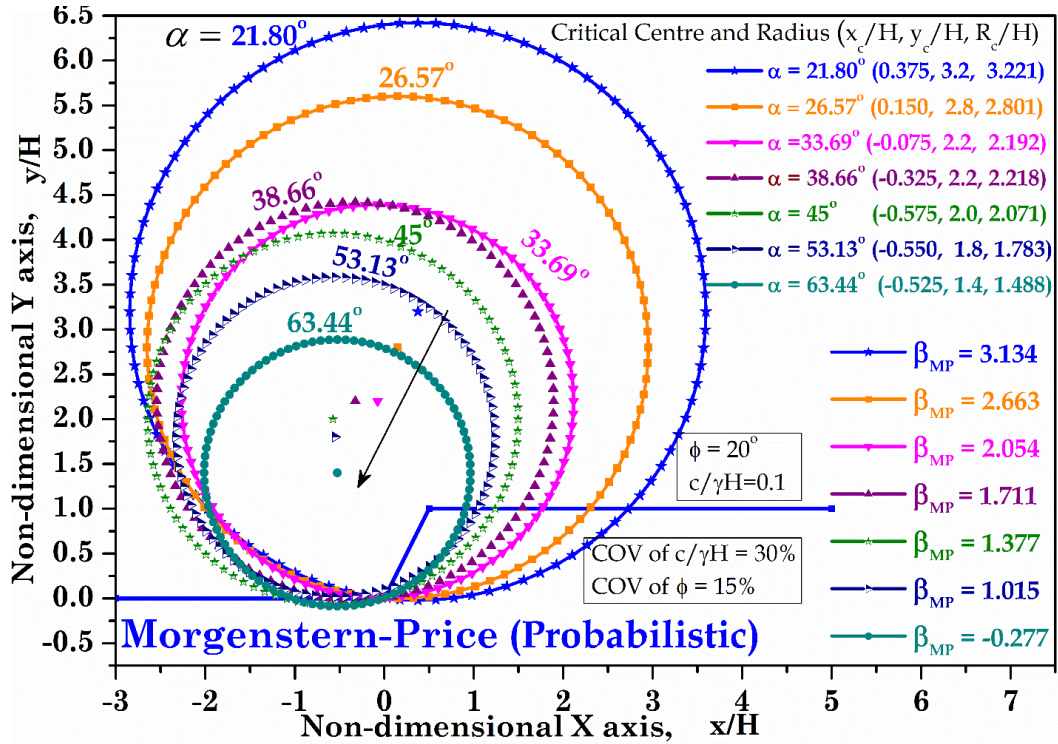


Figure 4.11: The effect of change in slope angle α on the critical slip surfaces for Morgenstern-Price Method

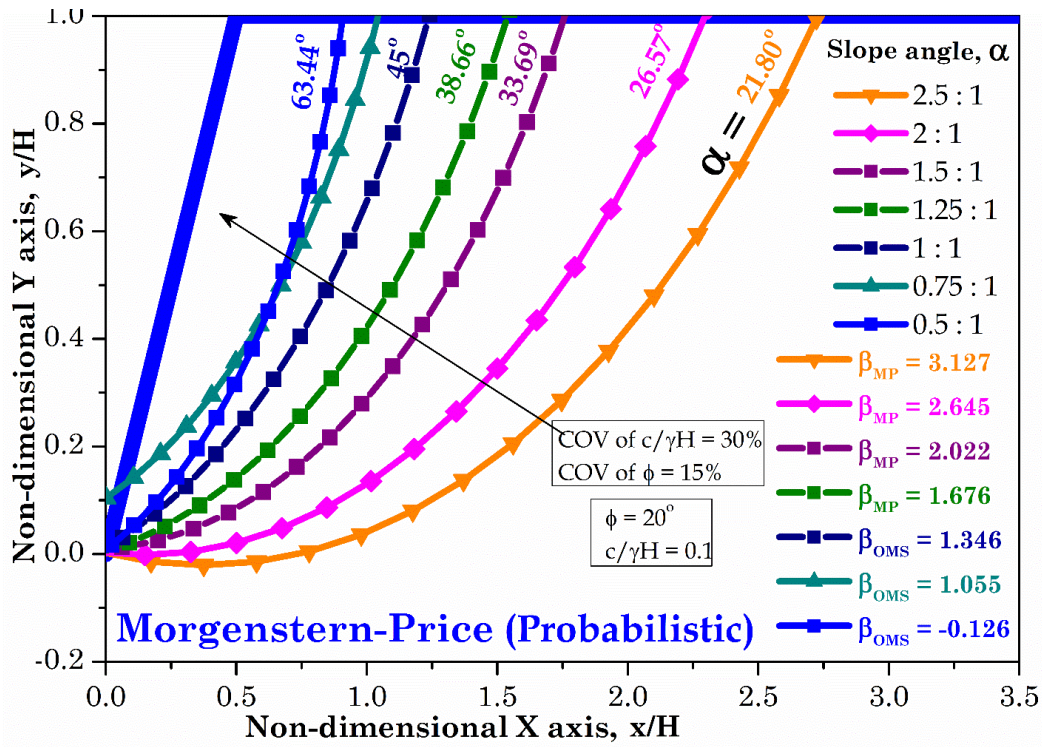


Figure 4.12: The effect of change in slope angle α on the shear bands for Morgenstern-Price Method

Effect of stability number $c/\gamma H$

- The effect of the stability number $c/\gamma H$ on the slip surfaces, is considered by fixing the rest of the parameters and changing $c/\gamma H$ gradually over its range of 0.1 to 0.5 at an interval of 0.1.
- Figure 4.13 and Fig 4.14 show the effect of these changes on the positions of the slip circles and on the shear bands formed for the Ordinary Method of Slices.
- An increase in $c/\gamma H$ value implies that either the resistance parameter c of the soil increases, making the slope stronger in resistance or the load coming on the slope is less which increases the stability. Either of the actions result in increase of stability causing an increase in the value of reliability index β . With an increase in stability, there is decrease in the volume of soil involved in failure as well which causes a change in the position of slip circles, but not it is bit very significant.

- Similar behavior is seen when Bishop's simplified method, Spencer method and Morgenstern-Price method is used. (Fig 4.15 - 4.20)

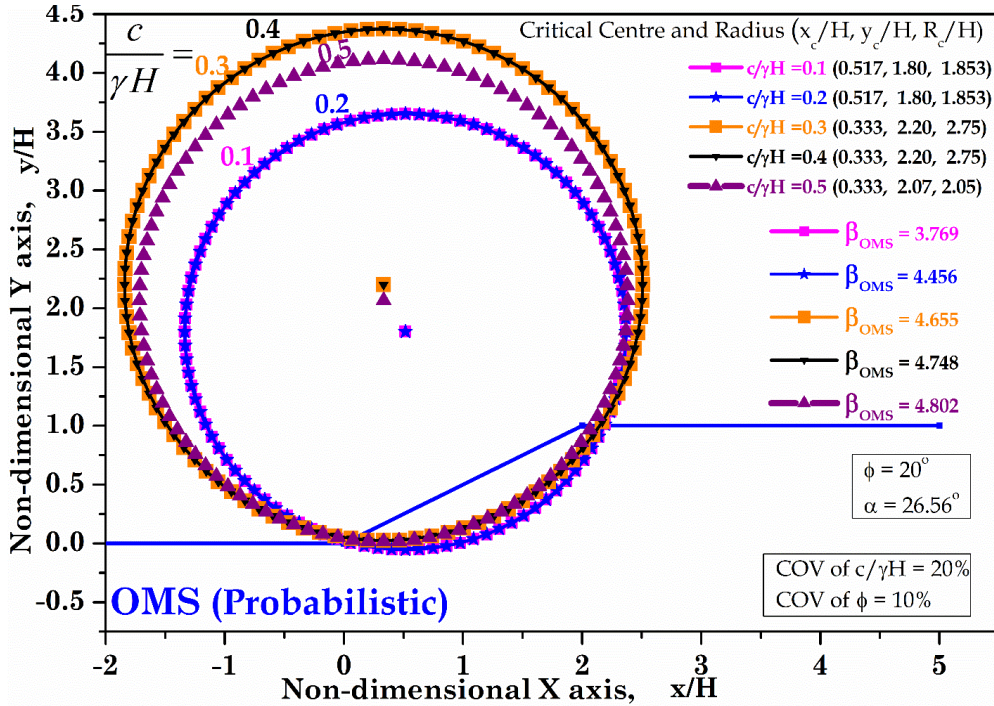


Figure 4.13: The effect of change in $c/\gamma H$ on the critical slip surfaces for Ordinary Method of Slices

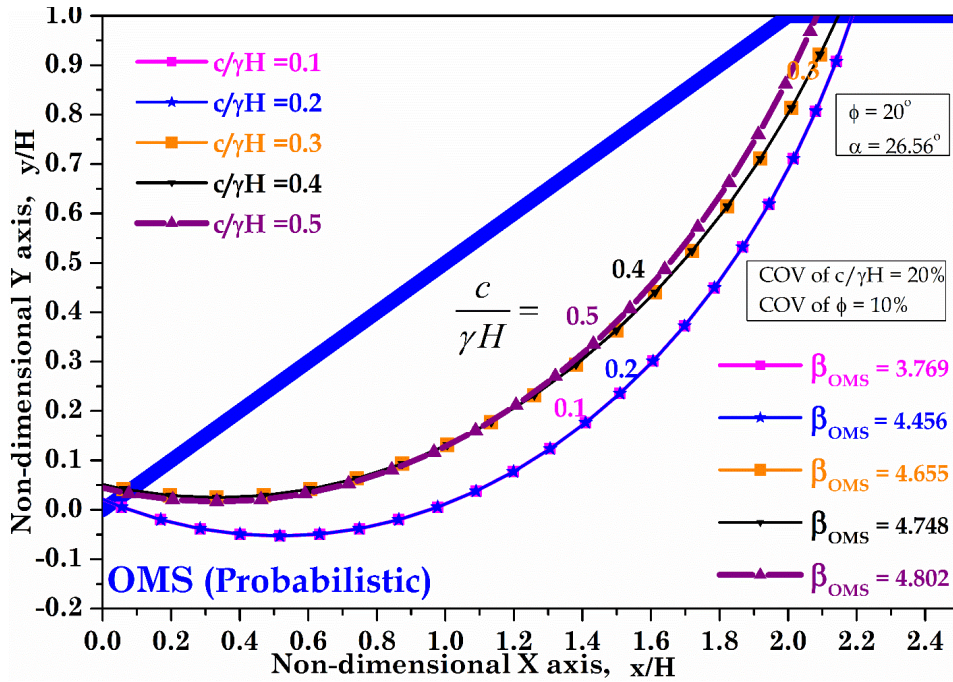


Figure 4.24: The effect of change in $c/\gamma H$ on the shear bands for Ordinary Method of Slices

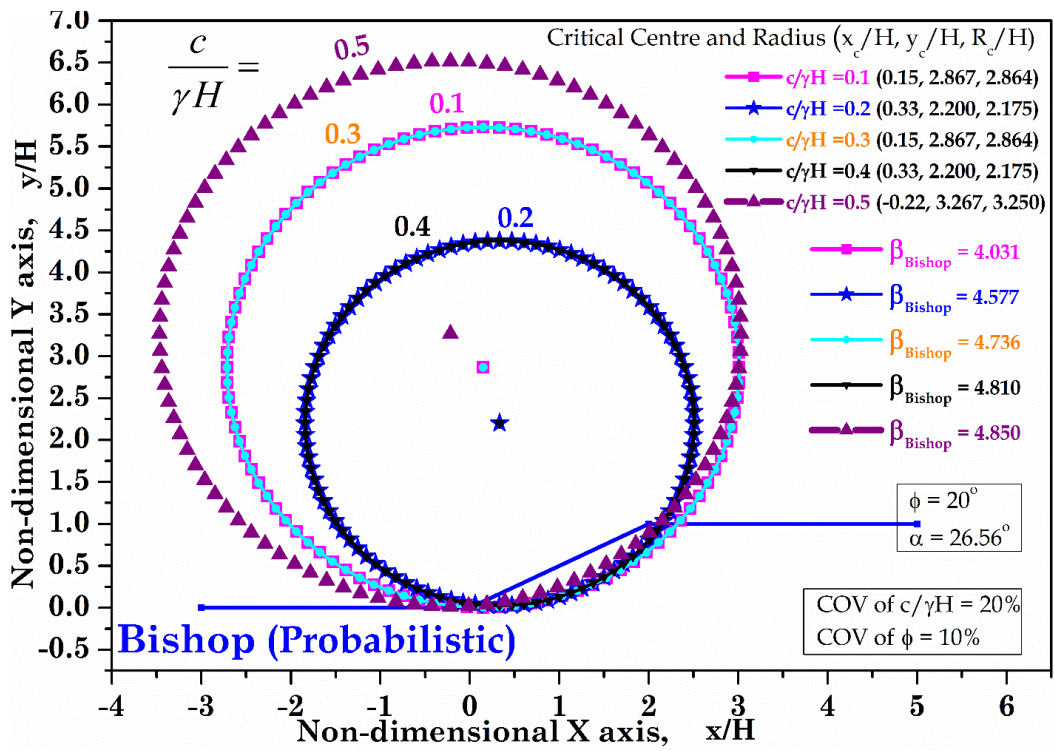


Figure 4.35: The effect of change in $c/\gamma H$ on the critical slip surfaces for Bishop's Simplified Method

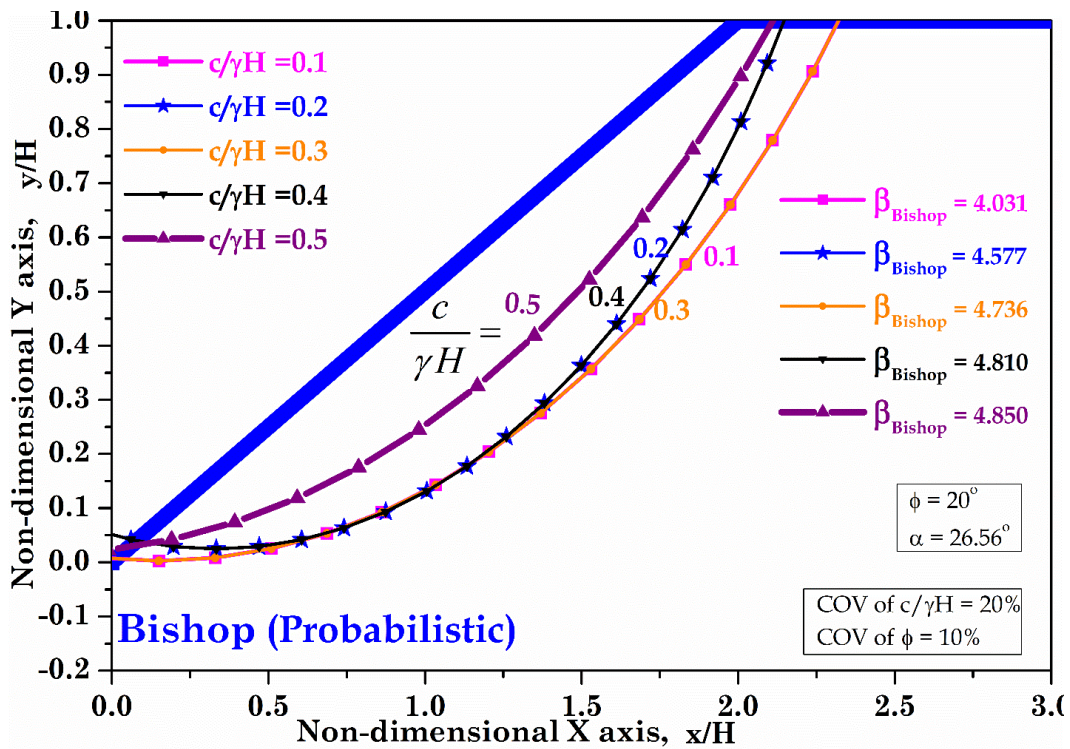


Figure 4.46: The effect of change in $c/\gamma H$ on the shear bands for Bishop's Simplified Method

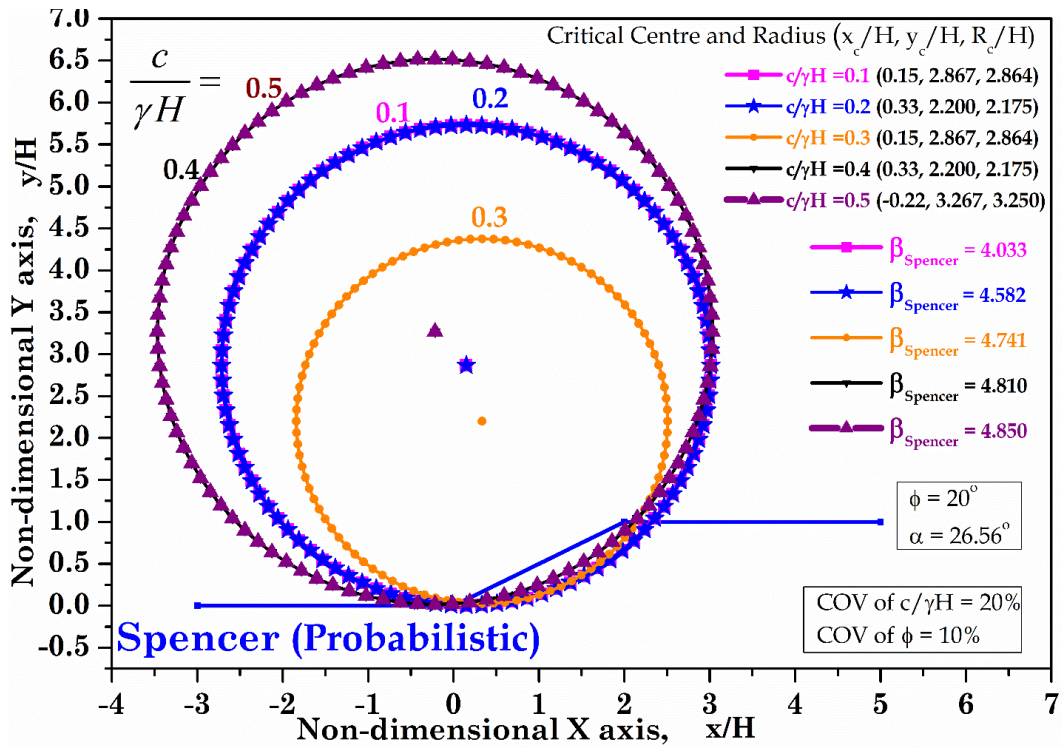


Figure 4.57: The effect of change in $c/\gamma H$ on the critical slip surfaces for Spencer Method

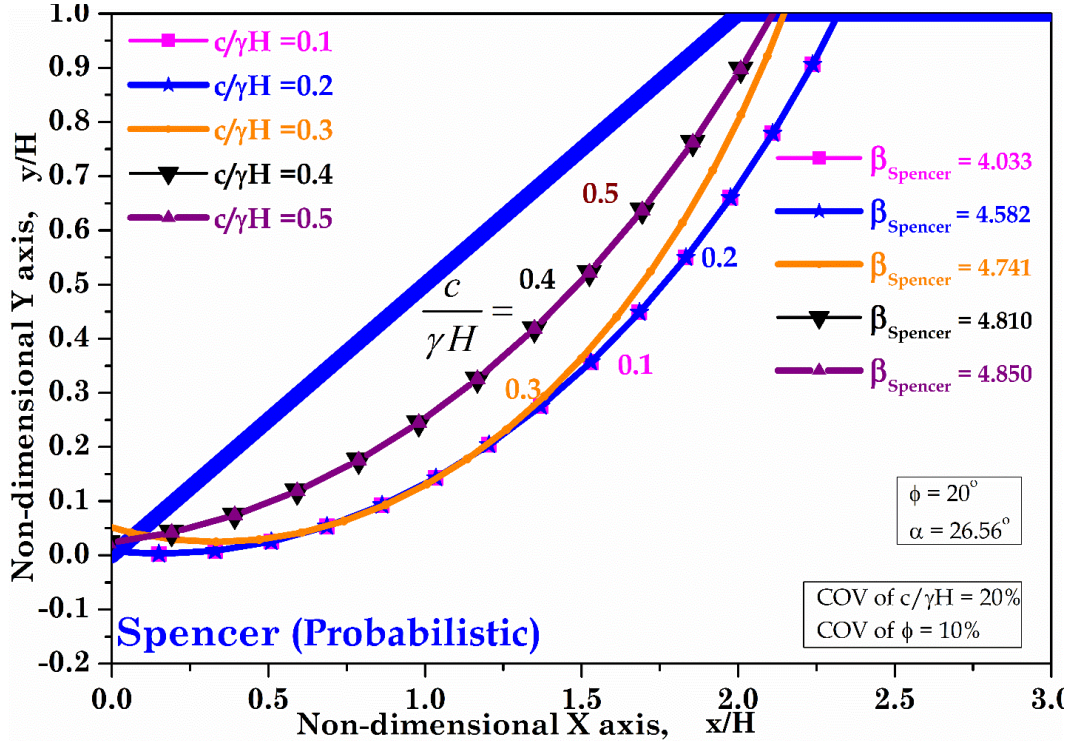


Figure 4.68: The effect of change in $c/\gamma H$ on the shear bands for Spencer Method

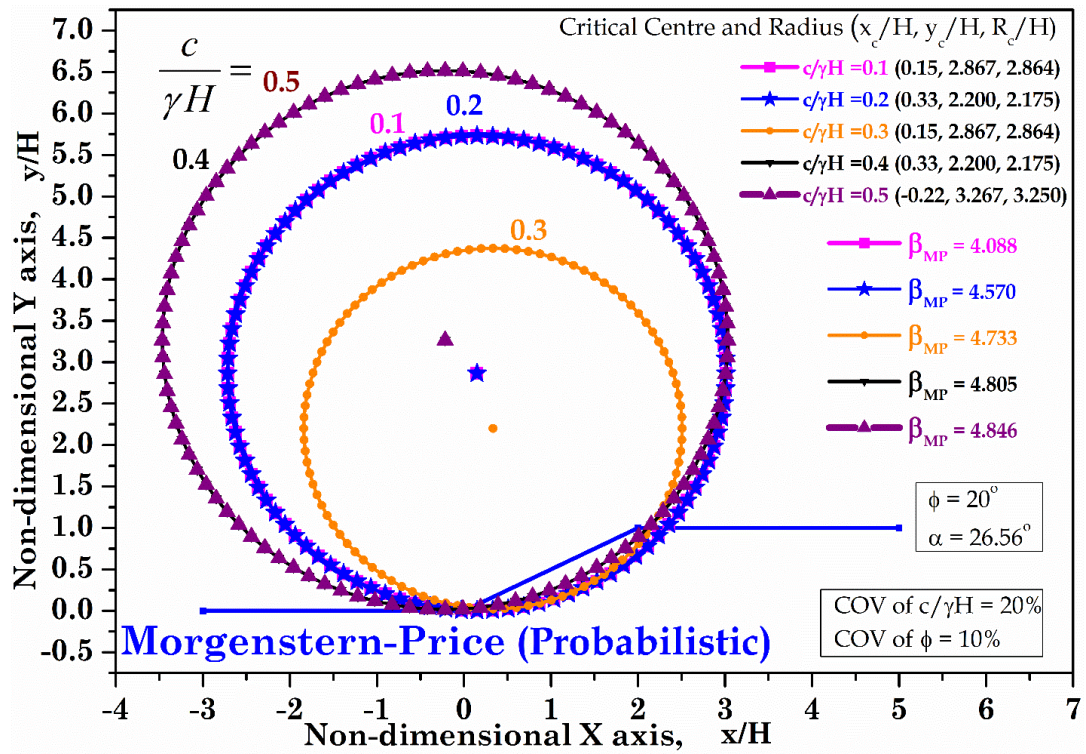


Figure 4.79: The effect of change in $c/\gamma H$ on the critical slip surfaces for Morgenstern-Price Method

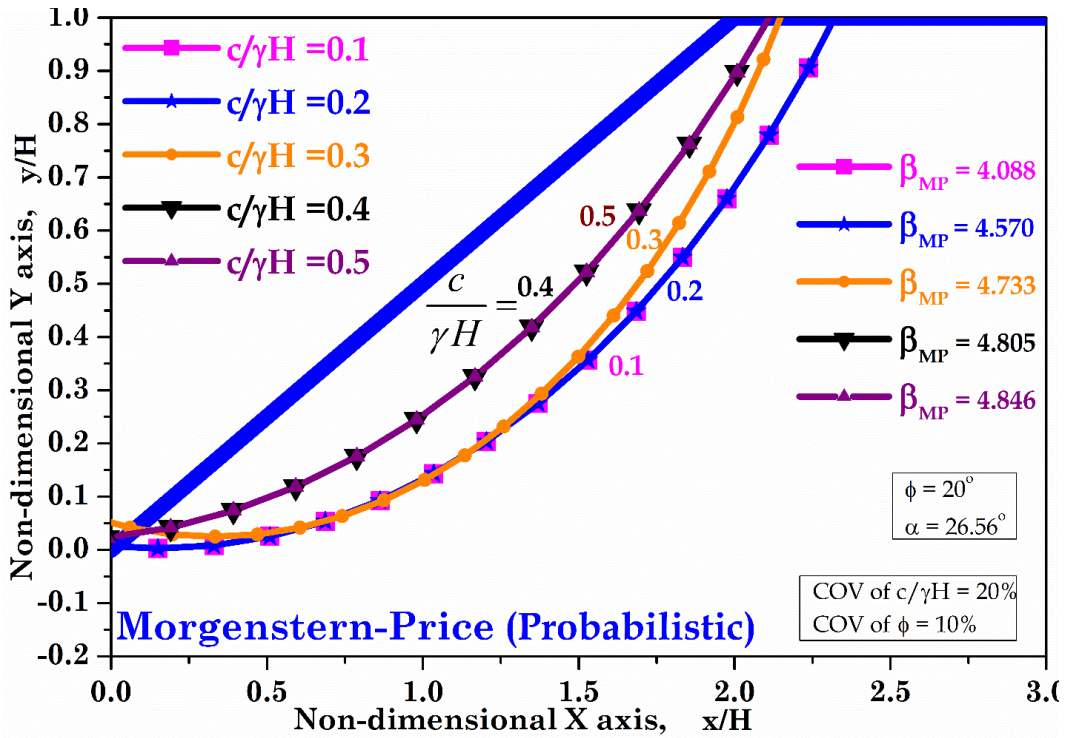


Figure 4.20: The effect of change in $c/\gamma H$ on the shear bands for Morgenstern-Price Method

Effect of COV of $c/\gamma H$

- In an effort to observe the how the change in the COV of $c/\gamma H$ causes a change in the slip surface positions as well as the reliability indices, similar charts are drawing in which all the other parameters involved except the COV of $c/\gamma H$ are kept constant as it is varied over the values of 10-40% at an interval of 10%.
- Figure 4.21 and Fig.4.22 represent the slip circles and the shear band positions for observing the effect of COV of $c/\gamma H$ by Ordinary method of slices.
- It can be seen that as the uncertainty associated with $c/\gamma H$ increases, there is a significant decrease in the value of reliability index. The critical centers move away from the soil, decreasing the volume of soil involved in the failure but the movement is not too much and stabilizes quickly.
- The critical surface fall on the positive side of the variability of $c/\gamma H$ i.e. the critical surface is being calculated when the mean value of COV of $c/\gamma H$ is decreasing.
- Similarly Fig.4.23 to Fig.4.28 give the same for the rest of the methods of slices.

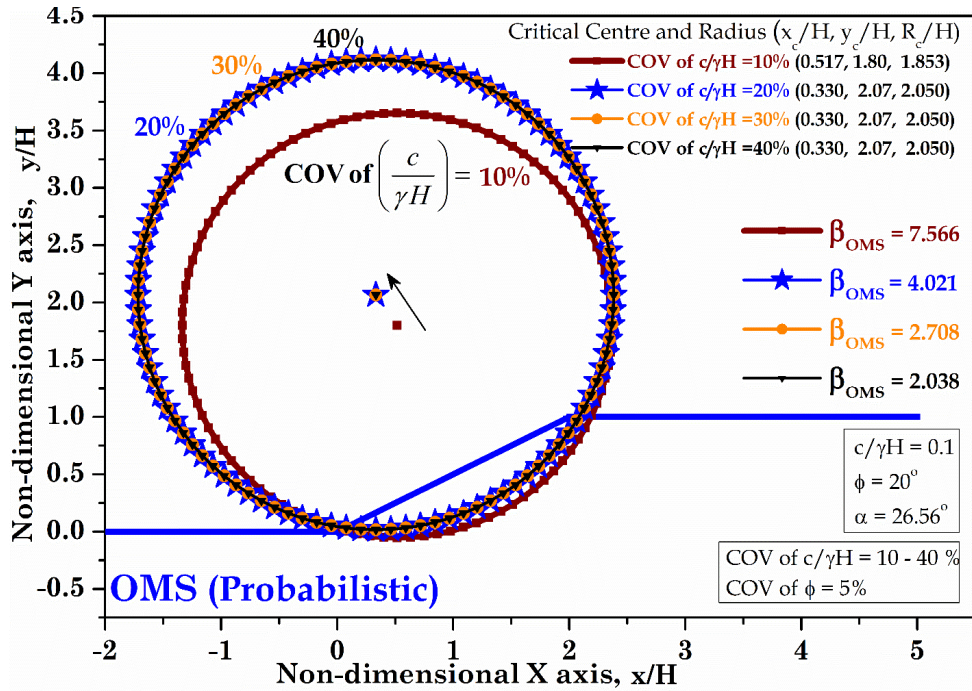


Figure 4.21: The effect of change in COV of $c/\gamma H$ on the critical slip surfaces for Ordinary Method of Slices

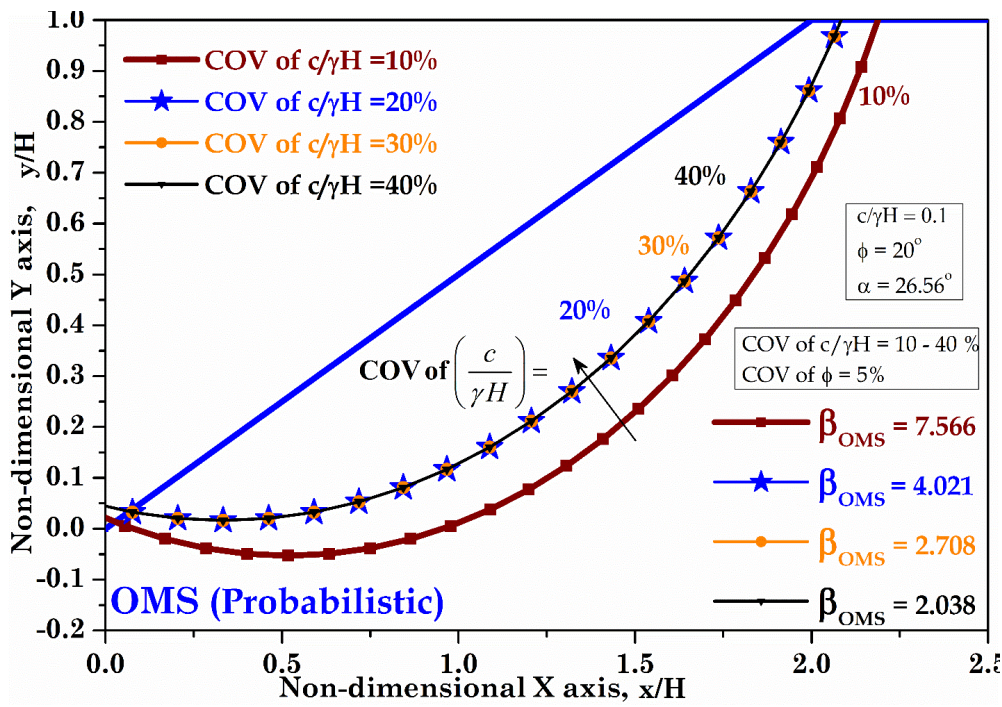


Figure 4.22: The effect of change in COV of $c/\gamma H$ on the shear bands for Ordinary Method of Slices

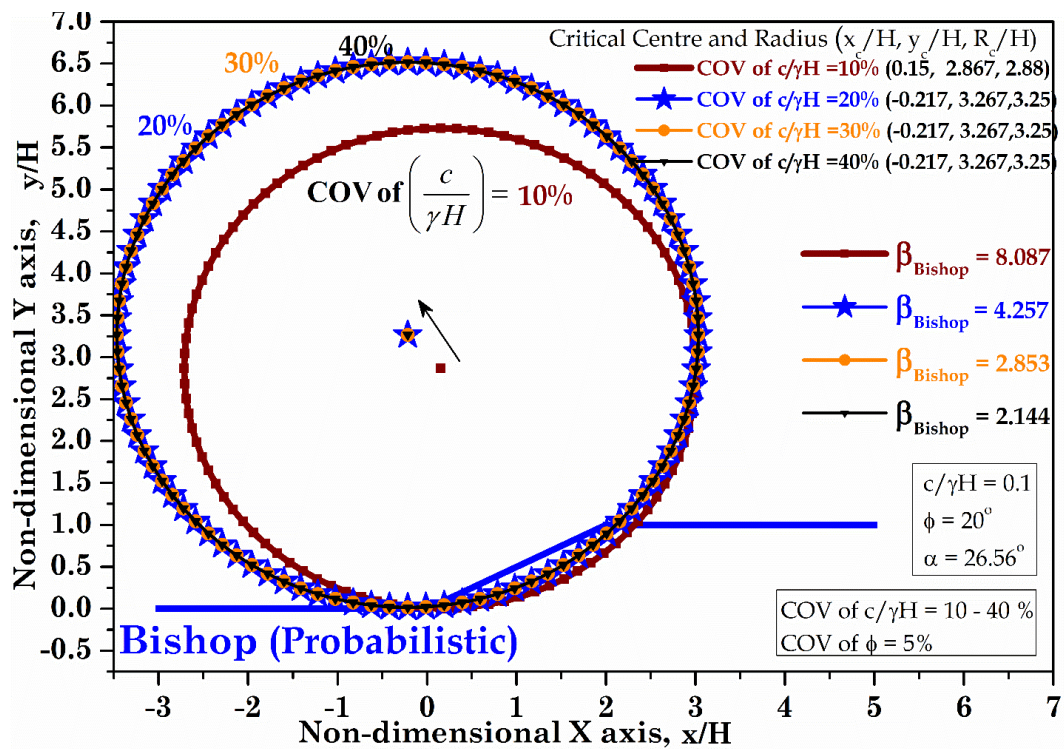


Figure 4.23: The effect of change in COV of $c/\gamma H$ on the critical slip surfaces for Bishop's Simplified Method

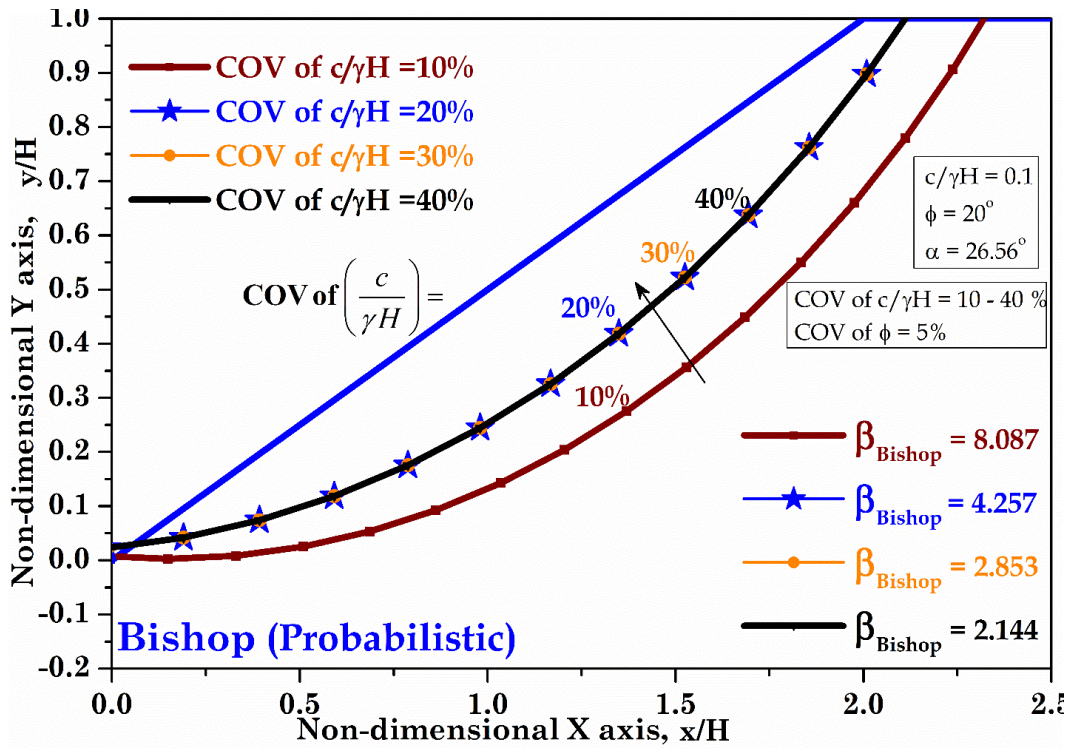


Figure 4.24: The effect of change in COV of $c/\gamma H$ on the shear bands for Bishop's Simplified Method

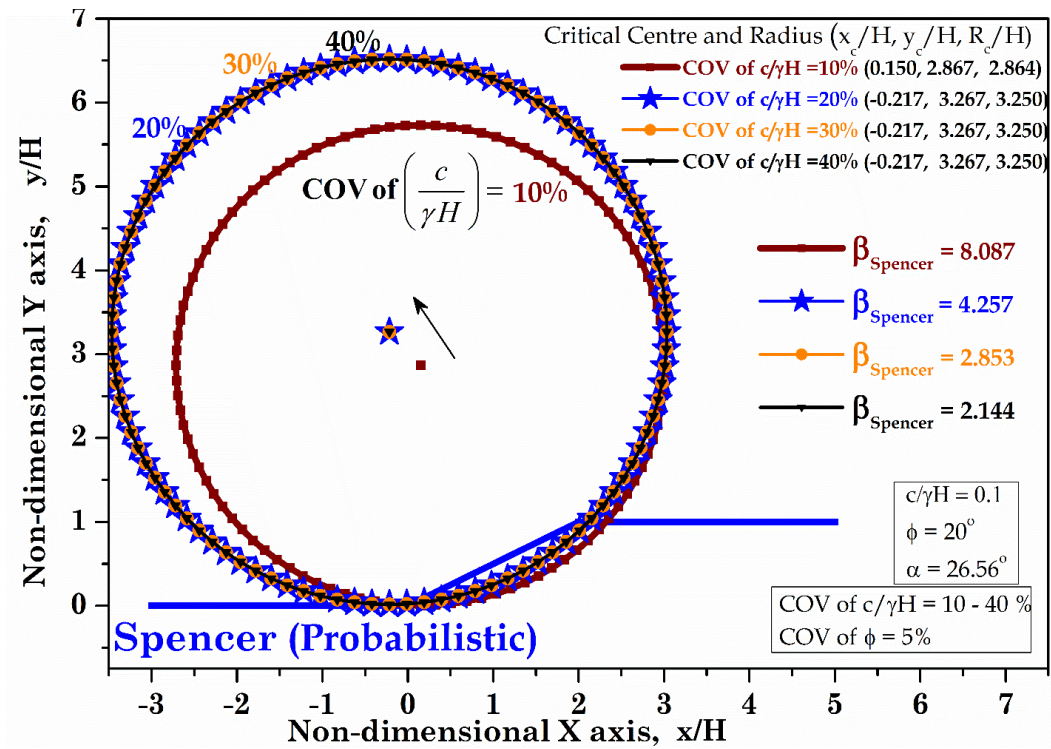
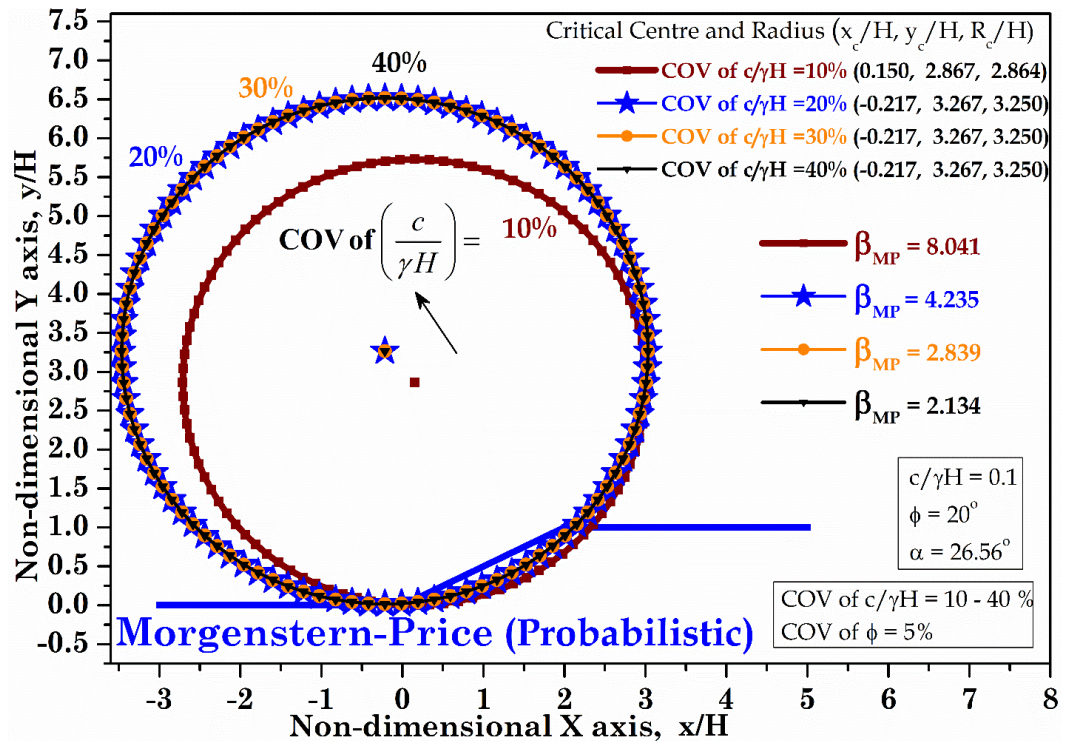
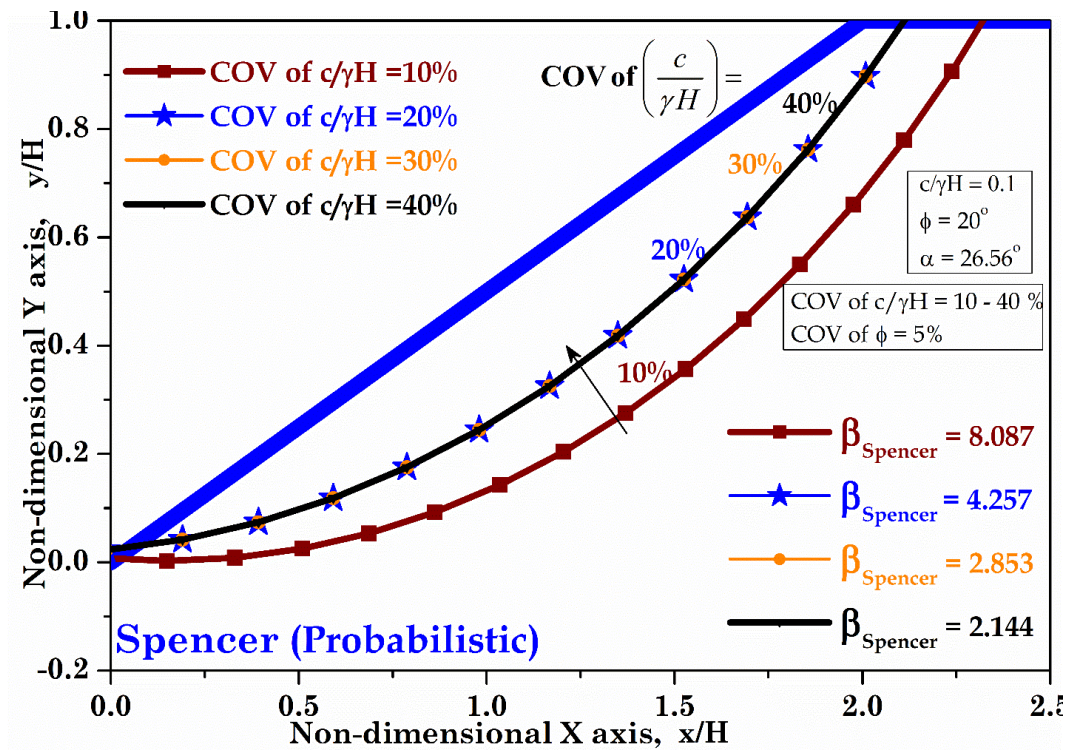


Figure 4.25: The effect of change in COV of $c/\gamma H$ on the critical slip surfaces for Spencer's Probabilistic Method



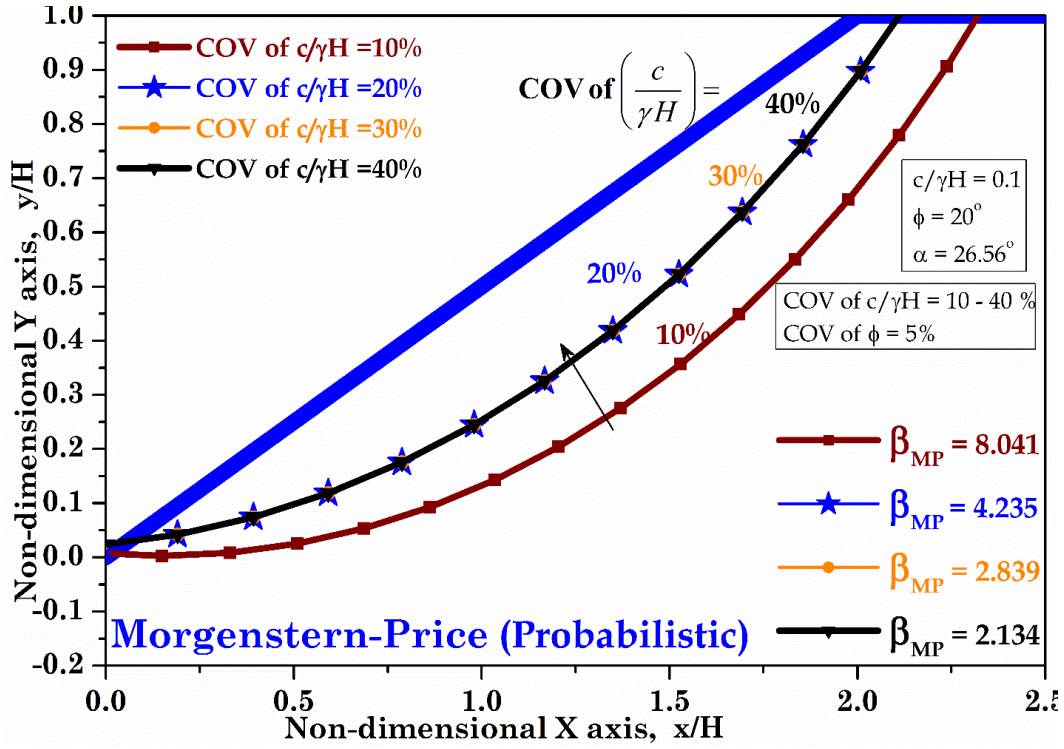


Figure 4.28: The effect of change in COV of $c/\gamma H$ on the shear bands for Morgenstern-Price Method

Effect of angle of internal friction ϕ

- Similar to above procedure, to observe how the angle of internal friction ϕ affects the reliability indices and the slip circles formation, the other parameters are kept constant and the angle of internal friction ϕ is varied over the range of $10-40^\circ$ at an interval of 10° .
- As ϕ increases, the resistance to failure increases, which increases the reliability indices. Even though there is an overall increase in the stability of the slope, the volume of soil involved in failure increases with increasing ϕ , though not very significantly.
- Figure 4.29 and Fig.4.30 represent the slip circles and the shear band positions for observing the effect of angle of internal friction ϕ by ordinary method of slices. Similarly Fig.4.31 and Fig.4.32 give the same for the rest of the methods of slices as there is not much significant difference in the slip circle positions but the values of β are heavily influenced by the method used.

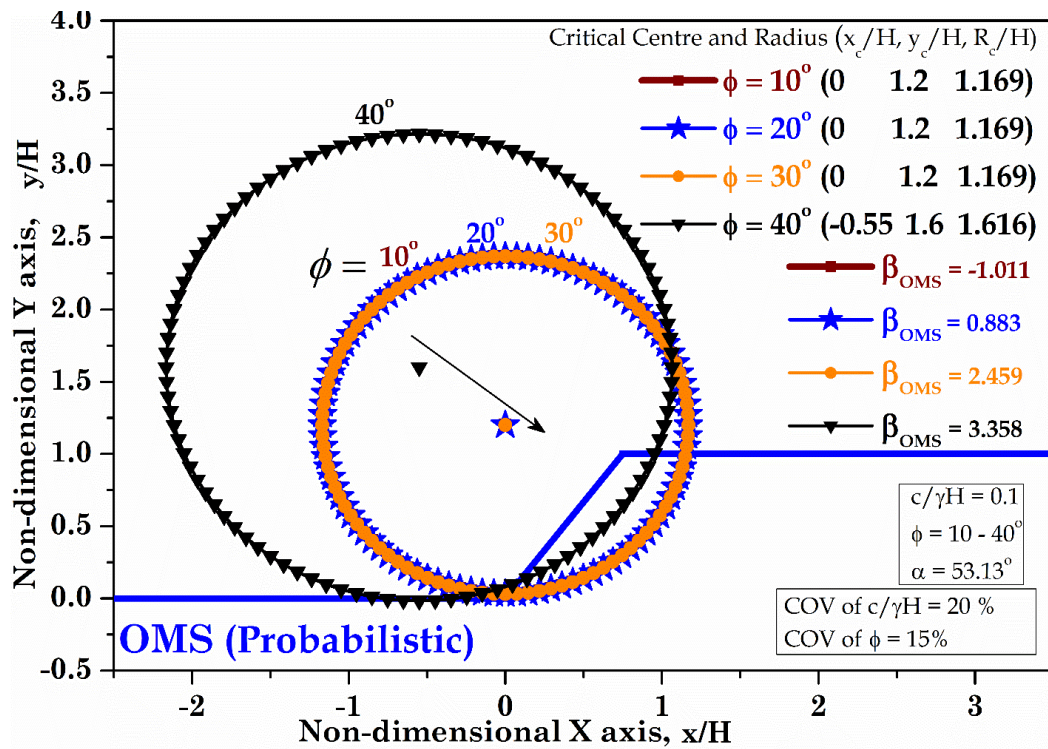


Figure 4.29: The effect of change in ϕ on the critical slip surfaces for Ordinary Method of Slices

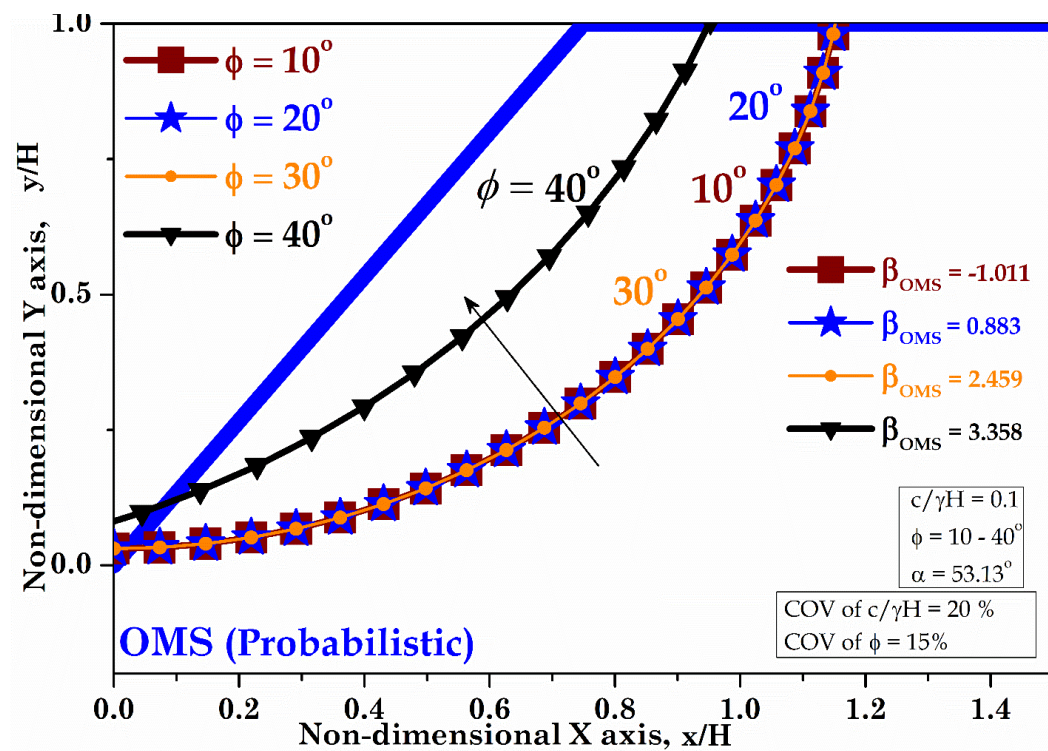


Figure 4.30: The effect of change in ϕ on the shear bands for Ordinary Method of Slices

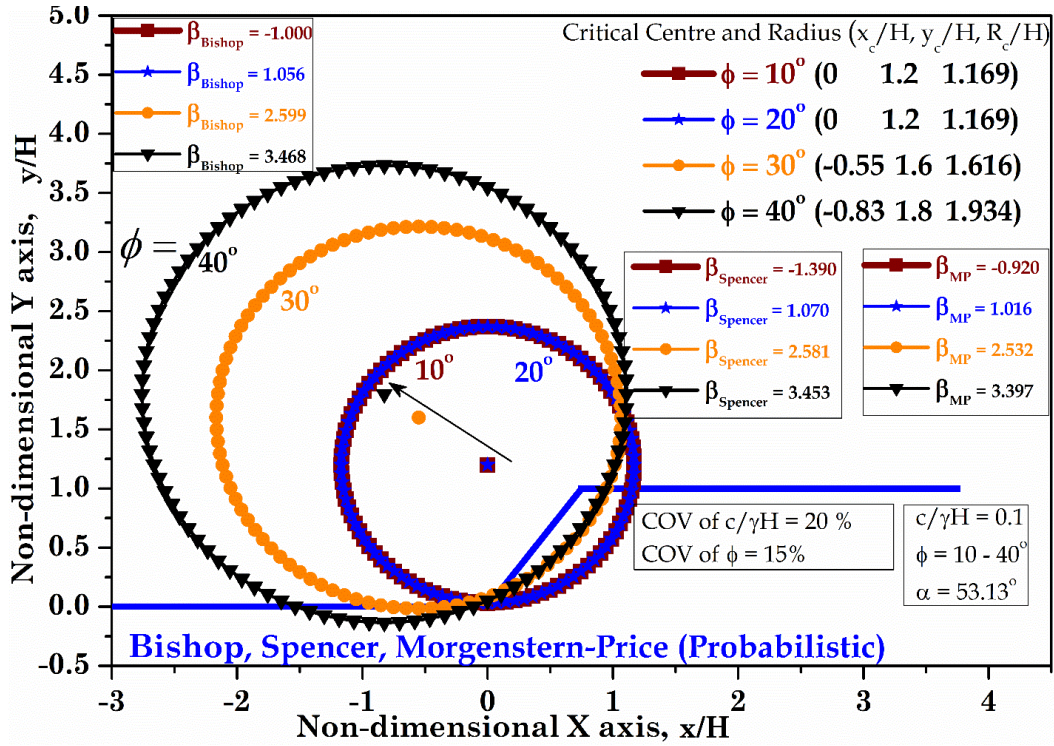


Figure 4.31: The effect of change in ϕ on the critical slip surfaces for Bishop's Simplified, Spencer and Morgenstern-Price Method

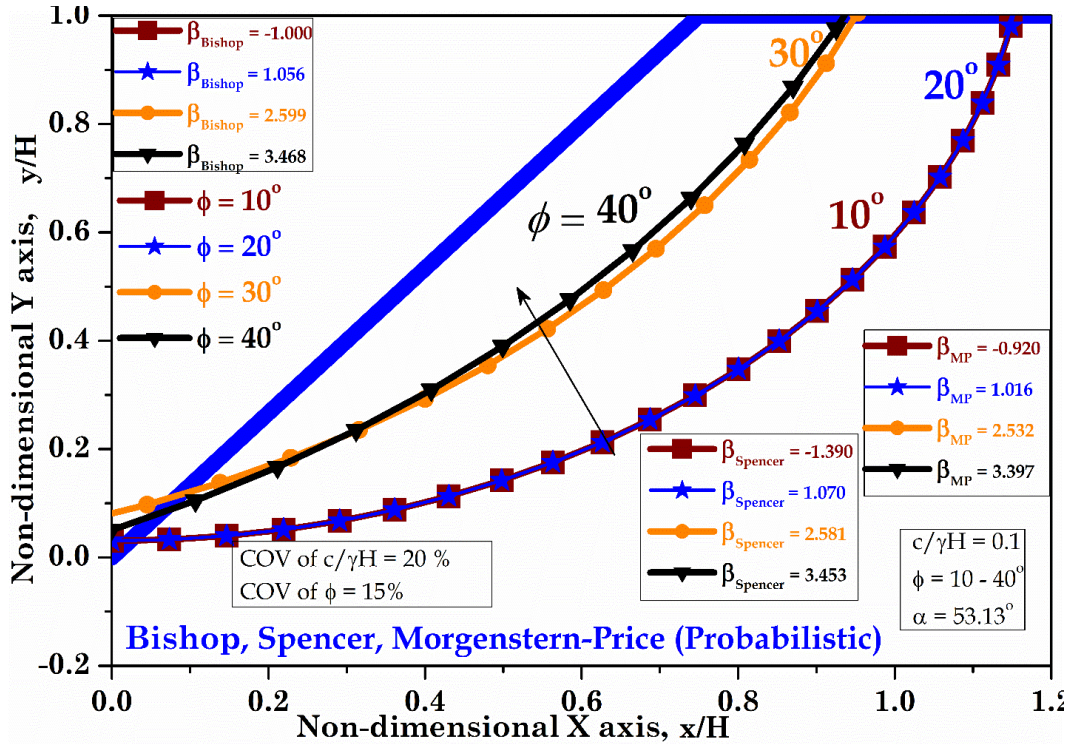


Figure 4.32: The effect of change in ϕ on the shear bands Bishop's Simplified, Spencer and Morgenstern-Price Method

Effect of COV of ϕ

- This effect is observed by changing the COV of ϕ over the range of 5-20% at 5% intervals and keeping the other parameters as constant.
- Increase in variability of the resisting parameter ϕ causes decrease in β 's involved. There is not much change in values of the reliability indices but a significant change in position of the critical slip surfaces is observed.
- The critical centres, as COV of ϕ increases, move towards the soil, increasing the volume of soil involved in the failure of the slope. The critical surface fall on the negative side of the variability of ϕ i.e. the critical slip surfaces are calculated when there is decrease in the values of ϕ .
- Figure 4.33 and Fig.4.34 show the effect of change in slope angle α on the critical slip surfaces and on the shear bands for Ordinary Method of Slices.
- Similarly the Fig.4.35 – 4.40 show the same for Bishop's Simplified Method, for Spencer Method, and for Morgenstern-Price Method respectively.

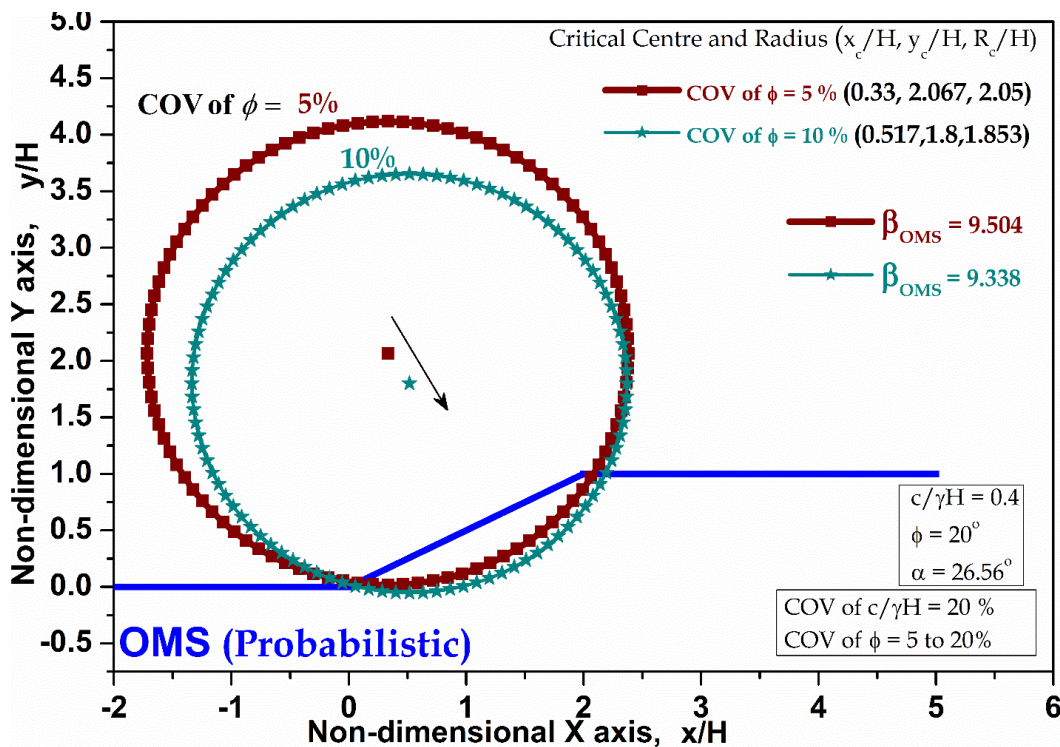


Figure 4.33: The effect of change in COV of ϕ on the critical slip surfaces for Ordinary Method of Slices

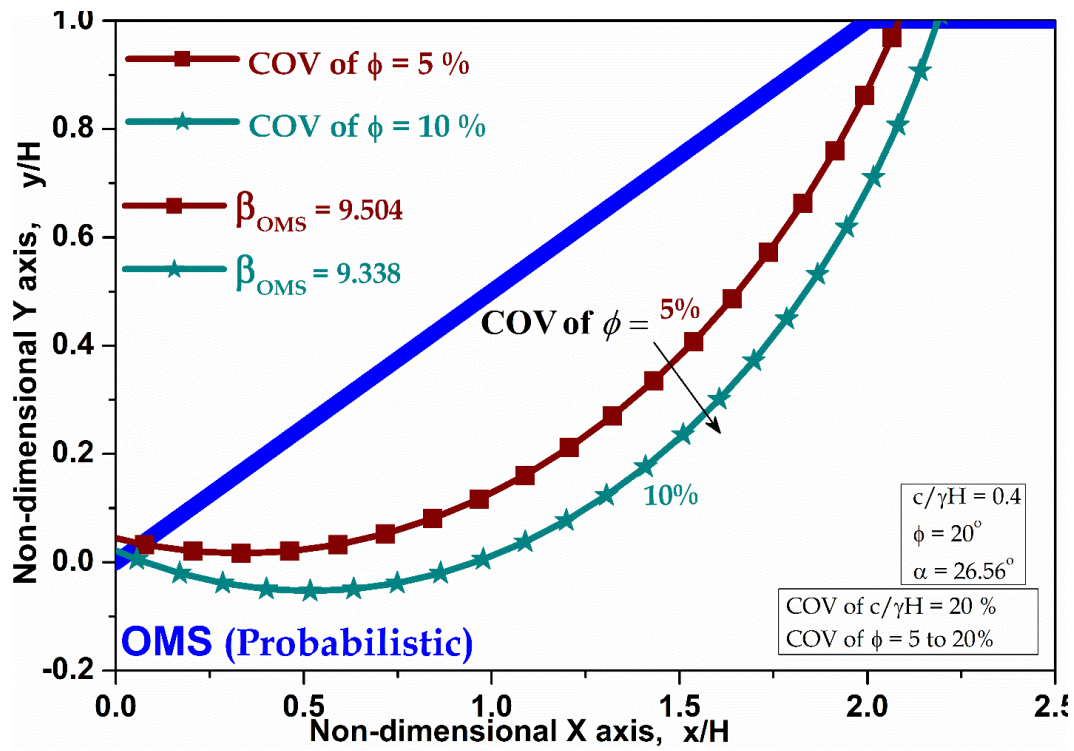


Figure 4.34: The effect of change in COV of ϕ on the shear bands for Ordinary Method of Slices

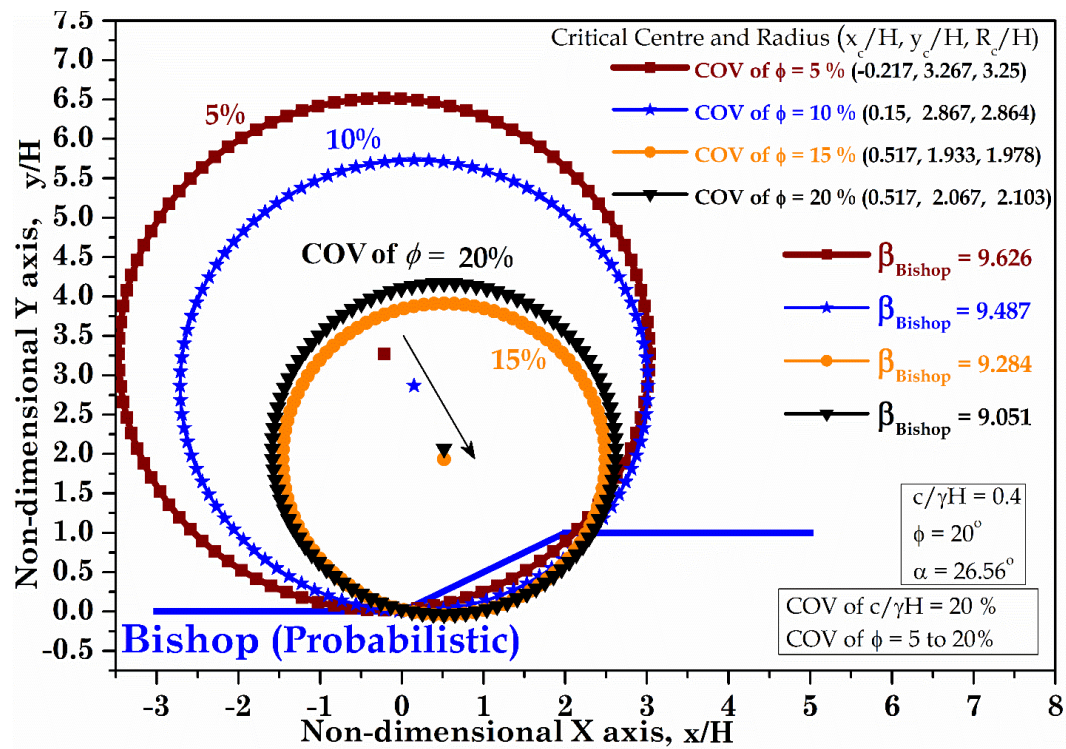


Figure 4.35: The effect of change in COV of ϕ on the critical slip surfaces for Bishop's Simplified Method

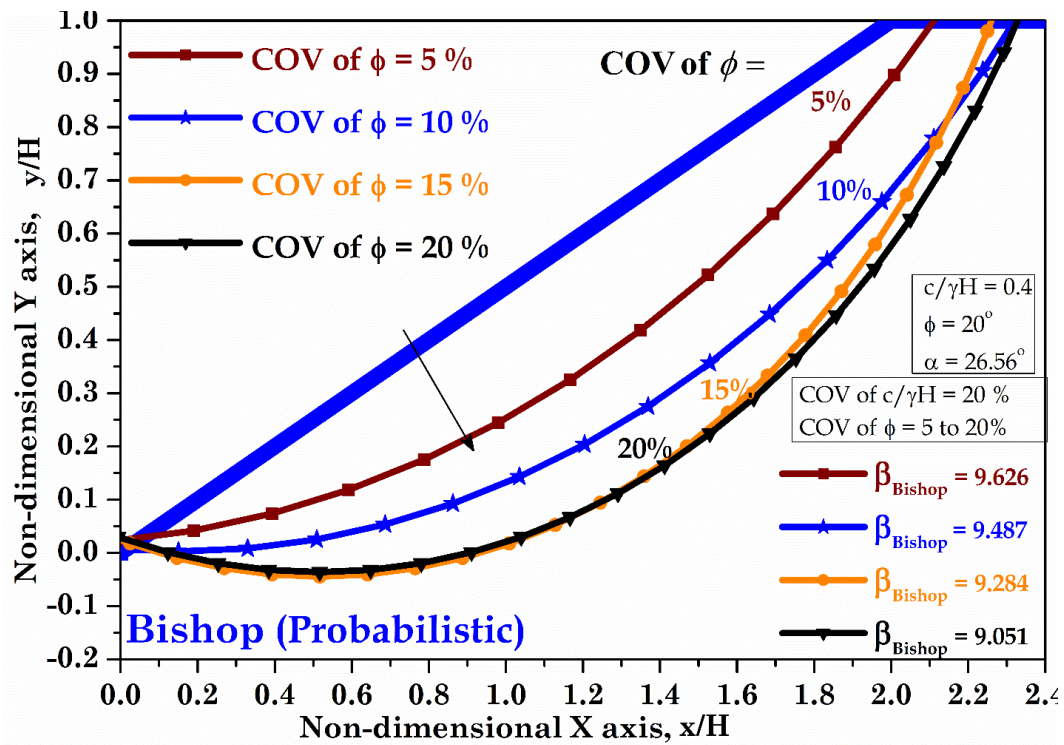


Figure 4.36: The effect of change in COV of ϕ on the shear bands for Bishop's Simplified Method

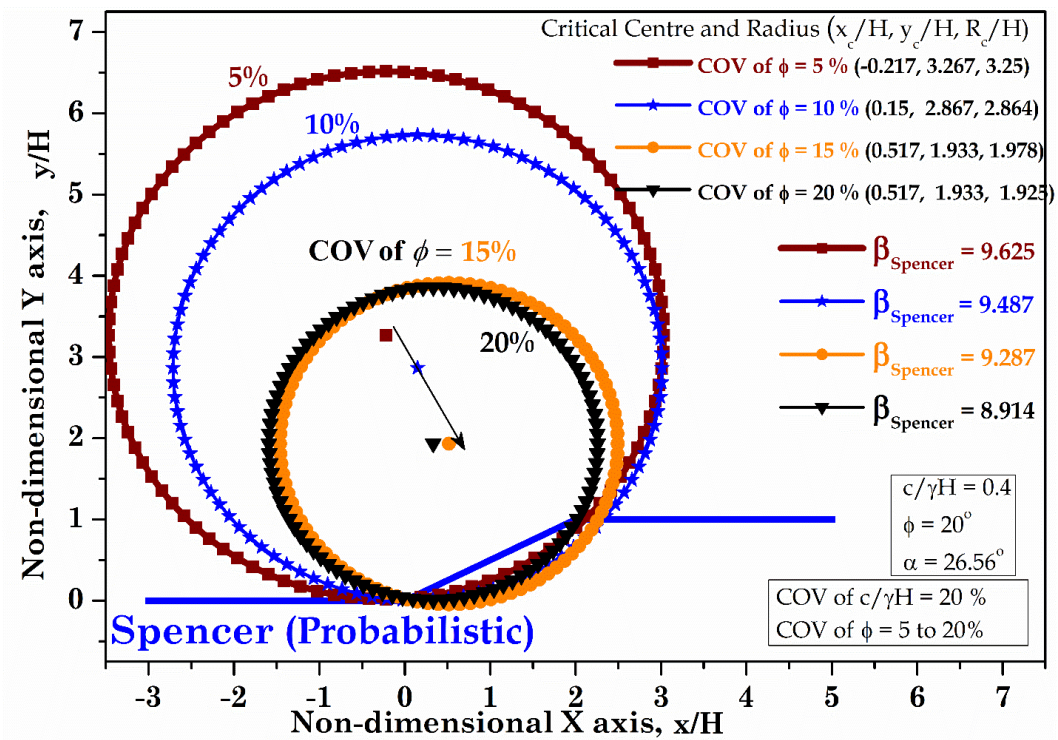


Figure 4.37: The effect of change in COV of ϕ on the critical slip surfaces for Spencer Method

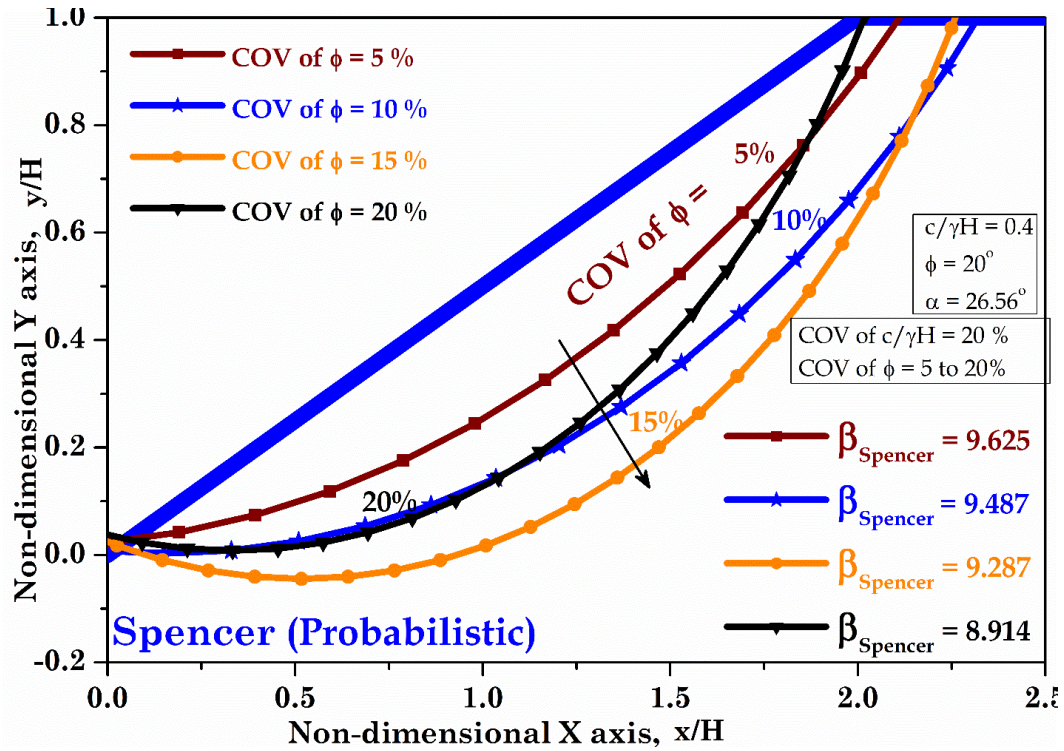


Figure 4.38: The effect of change in COV of ϕ on the shear bands for Spencer Method

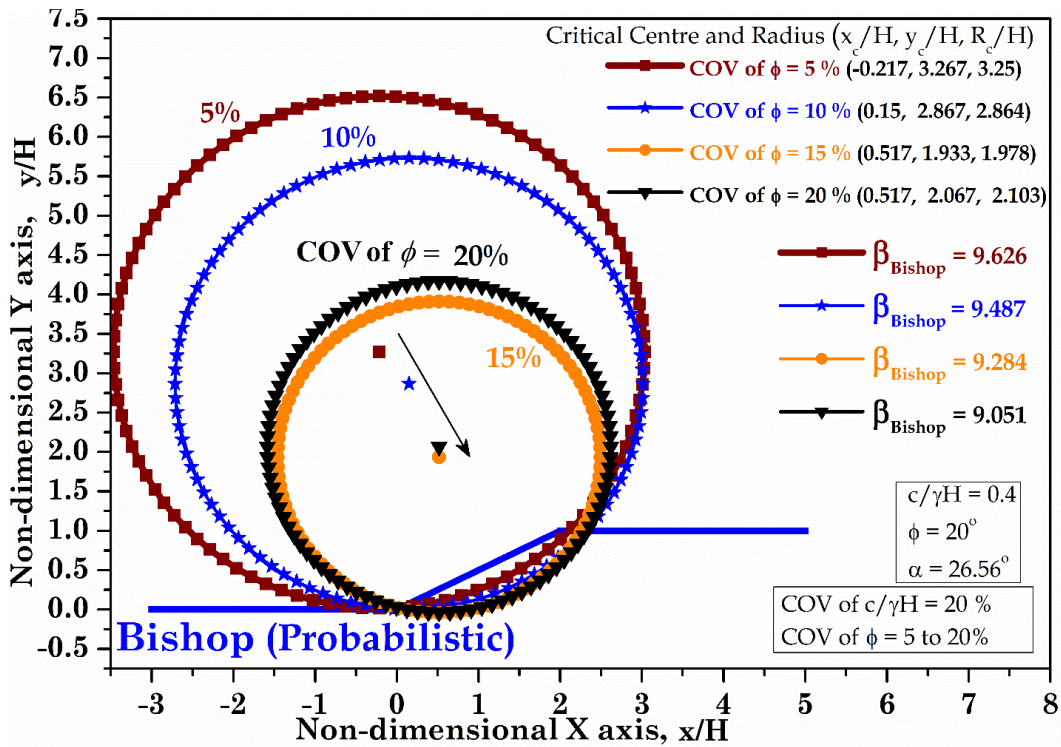


Figure 4.39: The effect of change in COV of ϕ on the critical slip surfaces for Morgenstern-Price Method

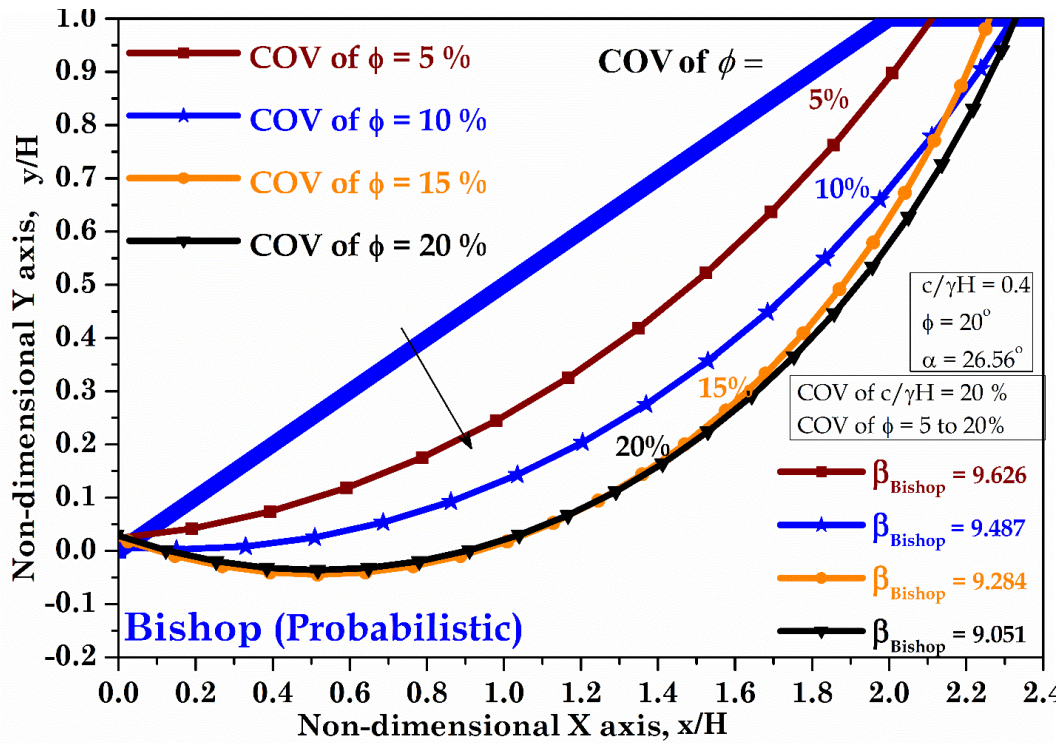


Figure 4.40: The effect of change in COV of ϕ on the shear bands for Morgenstern-Price Method

Thus deductions have been made on the effect of the varying parameters on the magnitude of reliability Indices and also the allocation of the critical centers and their critical slip surfaces.

4.3 Design Charts

The reliability indices were calculated for the various combinations of all the parameters involved and also over the different method of slices. These values are summarized by proposing the design charts for the Ordinary, Bishops, Spencer and Morgenstern-Price method. These charts can be used for calculating the reliability indices for any given homogenous slope as long as they possess the characteristics defined in the charts.

The reliability indices are called as good or bad based on the classification given by USACE (1997). USACE gave the tolerable values of Reliability Indices (β) for different performance levels as shown in Table 4.8. The design charts are based on these values.

Table 4.8: The classification of Reliability Indices as given by USACE (1997)

Target Reliability Indices		
Expected Performance Level	β	Probability of Unsatisfactory Performance
High	5	0.0000003
Good	4	0.00003
Above Average	3	0.001
Below Average	2.5	0.006
Poor	2	0.023
Unsatisfactory	1.5	0.07
Hazardous	1	0.16

For each design chart, the values of the stability number $c/\gamma H$, the angle of internal friction ϕ and the method of slope stability used in deriving the reliability index is kept constant and the rest of the parameters i.e. the slope angle α , the COV of $c/\gamma H$ and COV of ϕ are varied.

4.4 Design Charts for Ordinary Method of Slices

- In Fig 4.41, the values of reliability indices obtained by the ordinary method of slices are given. The values of the parameters considered are $c/\gamma H = 0.1$ and $\phi = 10^\circ$ are fixed and the rest are varied over their respective ranges as given in Table 4.7. The following observations can be made.
- When the COV of ϕ is constant, as the COV of $c/\gamma H$ increases from 10% to 40%, a clear decrease in the reliability index value is observed owing to the fact that there is an increase in the variability of the parameters. Similarly, as COV of ϕ increases from 5% to 20%, there is decrease in the maximum reliability index of for each variation.
- It can also be observed that the slopes having angles beyond 45° or so cannot exist because they are beyond hazardous i.e. they cannot sustain.
- Also, it is clear that the values with high variability and steeper slopes fall in the hazardous zones, but as the variability decreases and the slope is more geometrically stable, the reliability of the slope increases.
- When the COV of $\phi = 5\%$ and COV of $c/\gamma H$ increases from 10% to 40%, slope having their inclinations in the range of $30 - 45^\circ$ are mostly hazardous in their reliability and should be avoided. Almost all the slope with inclinations lesser

than 25° have acceptable levels of performance despite of the variation in the soil properties.

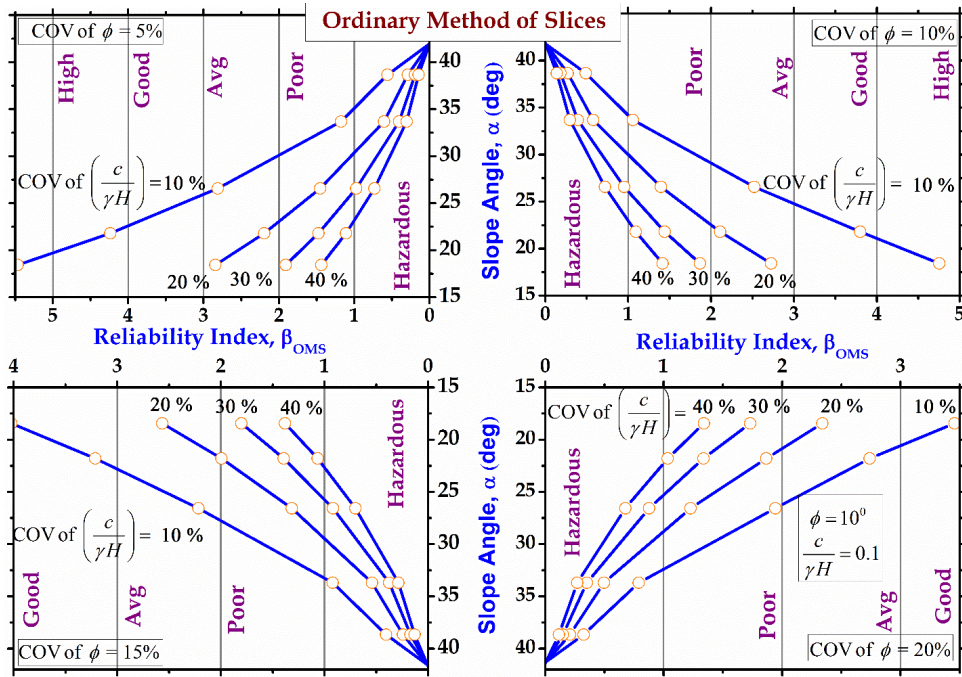


Figure 4.41: Design charts for $c/\gamma H=0.1$ and $\phi=10^\circ$ for Ordinary Method of Slices

Similar observations can be made for Fig.4.42 – 4.60 for ordinary method of slices, Figs.4.61 – 4.80 for Bishop's simplified method, Fig.4.81– 4.100 for Spencer method and Fig.4.101 – 4.120 for Morgenstern –Price method.

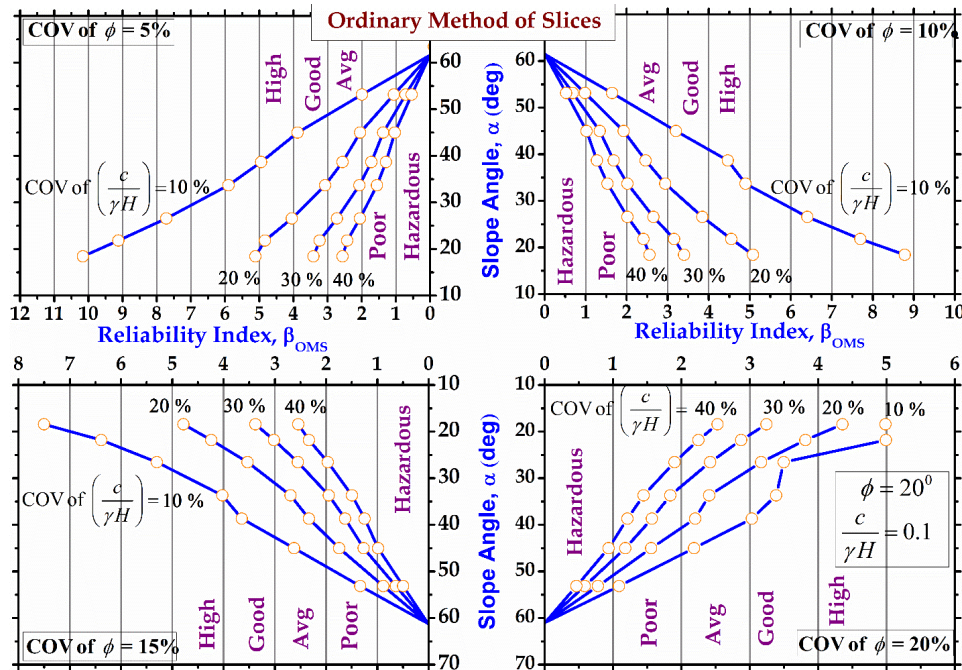


Figure 4.42: Design charts for $c/\gamma H=0.1$ and $\phi=20^\circ$ for Ordinary Method of Slices

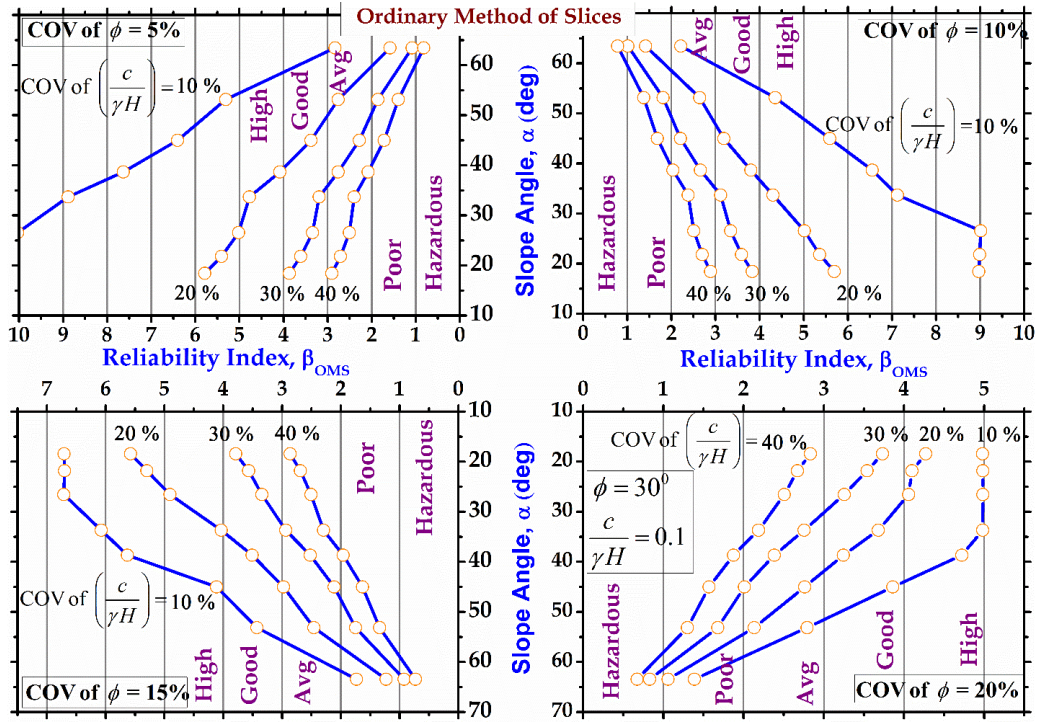


Figure 4.43: Design charts for $c/\gamma H = 0.1$ and $\phi = 30^\circ$ for Ordinary Method of Slices

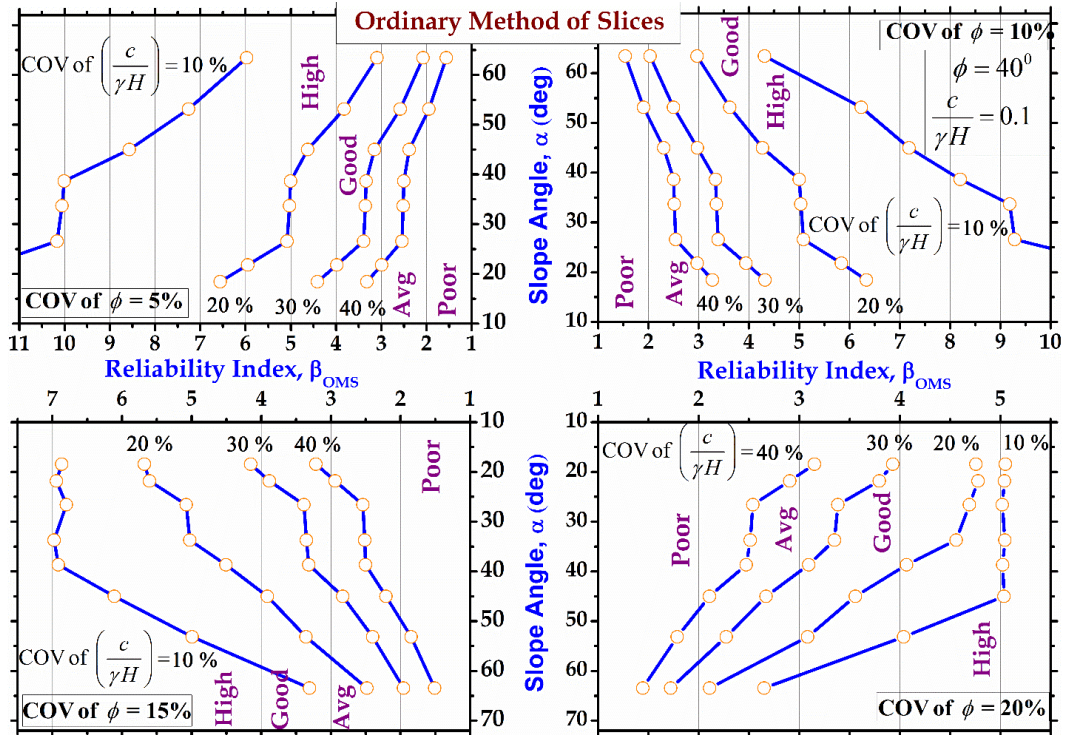


Figure 4.44: Design charts for $c/\gamma H = 0.1$ and $\phi = 40^\circ$ for Ordinary Method of Slices

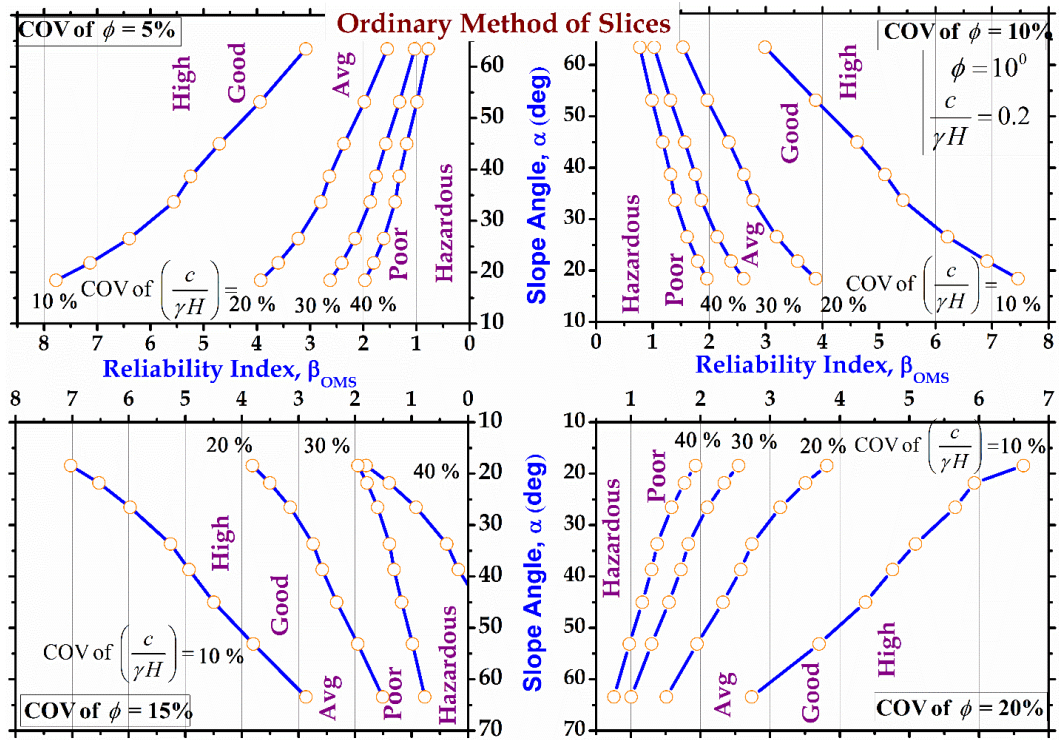


Figure 4.45: Design charts for $c/\gamma H=0.2$ and $\phi=10^\circ$ for Ordinary Method of Slices

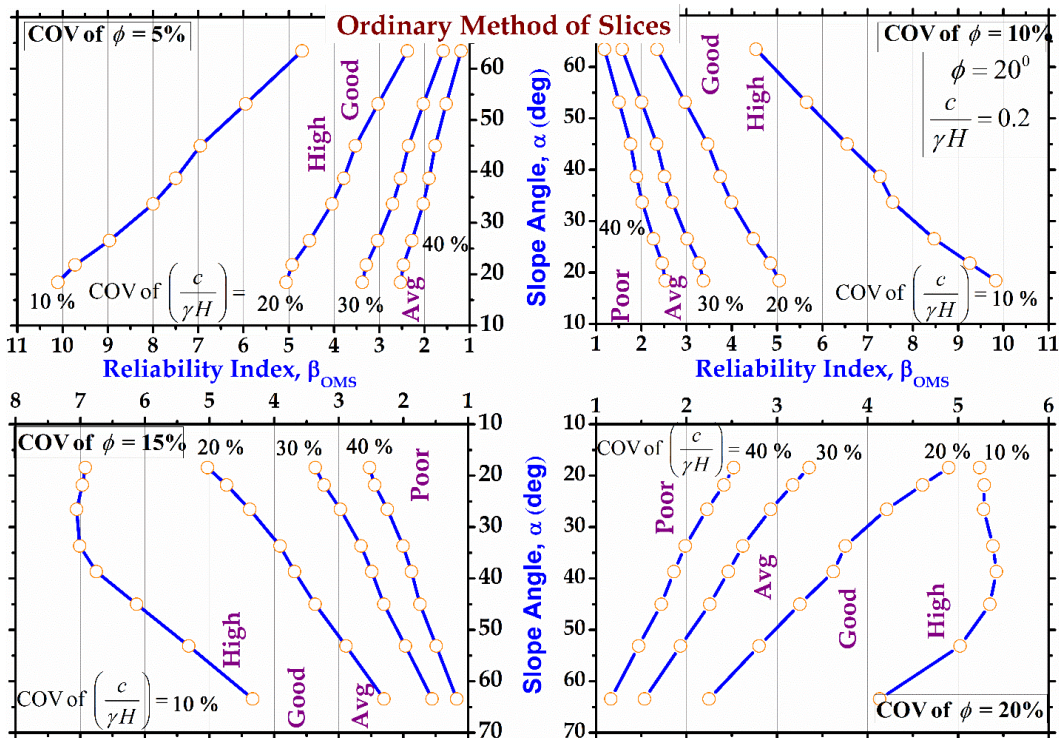


Figure 4.46: Design charts for $c/\gamma H=0.2$ and $\phi=20^\circ$ for Ordinary Method of Slices

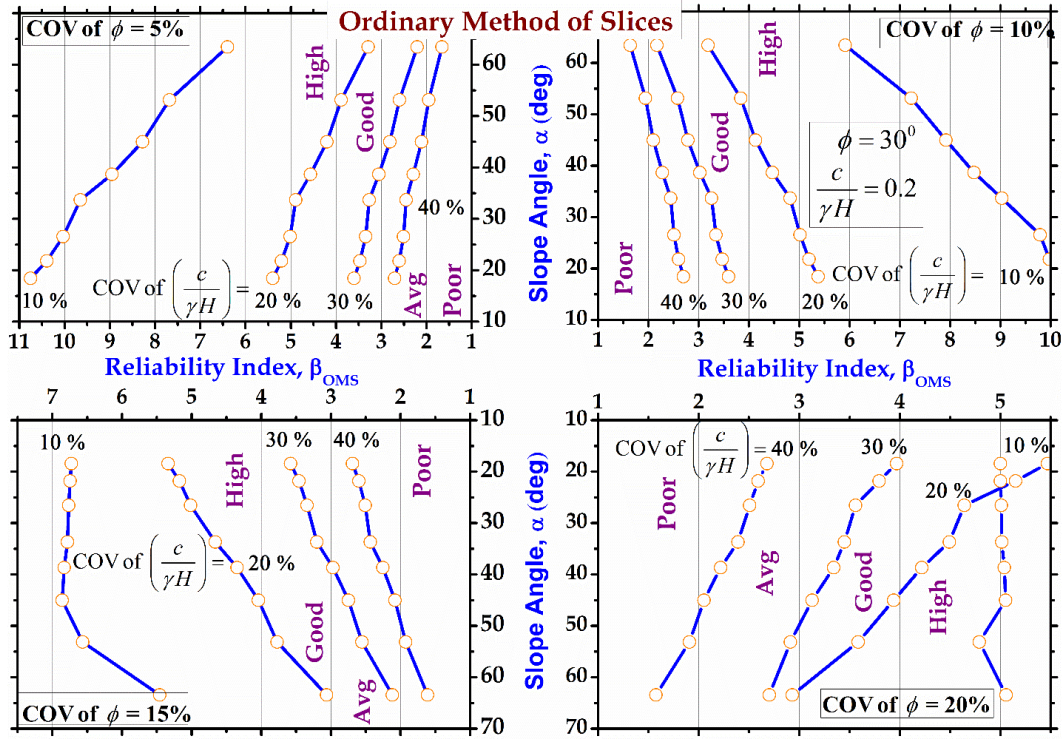


Figure 4.47: Design charts for $c/\gamma H = 0.2$ and $\phi = 30^\circ$ for Ordinary Method of Slices

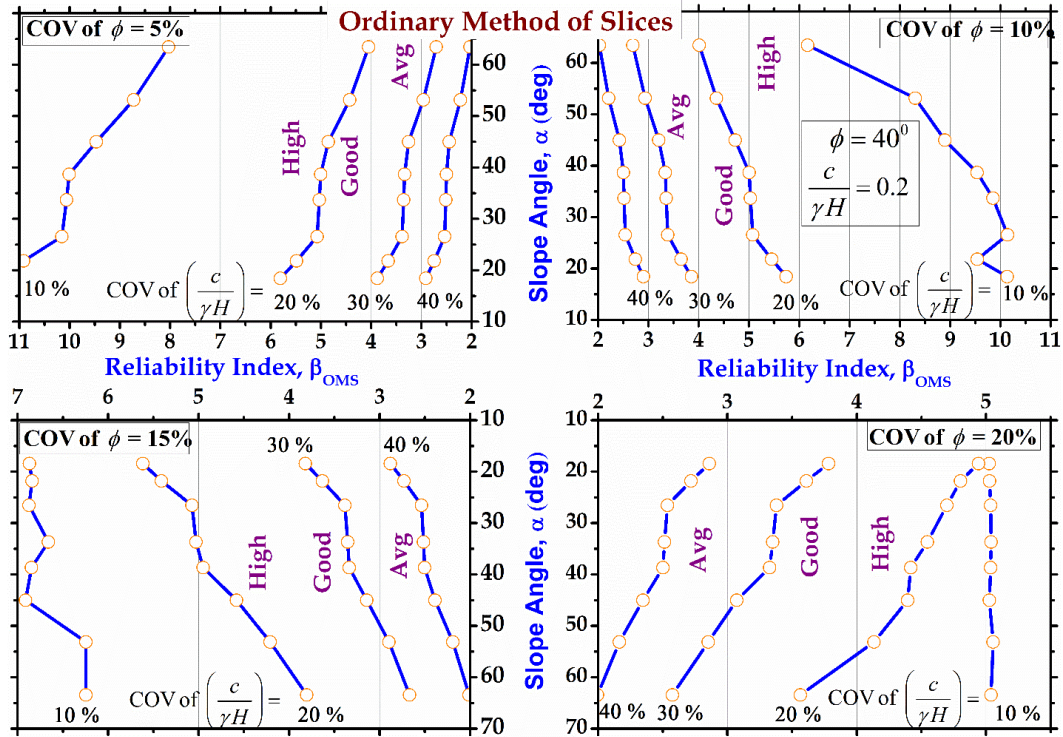


Figure 4.48: Design charts for $c/\gamma H = 0.2$ and $\phi = 40^\circ$ for Ordinary Method of Slices

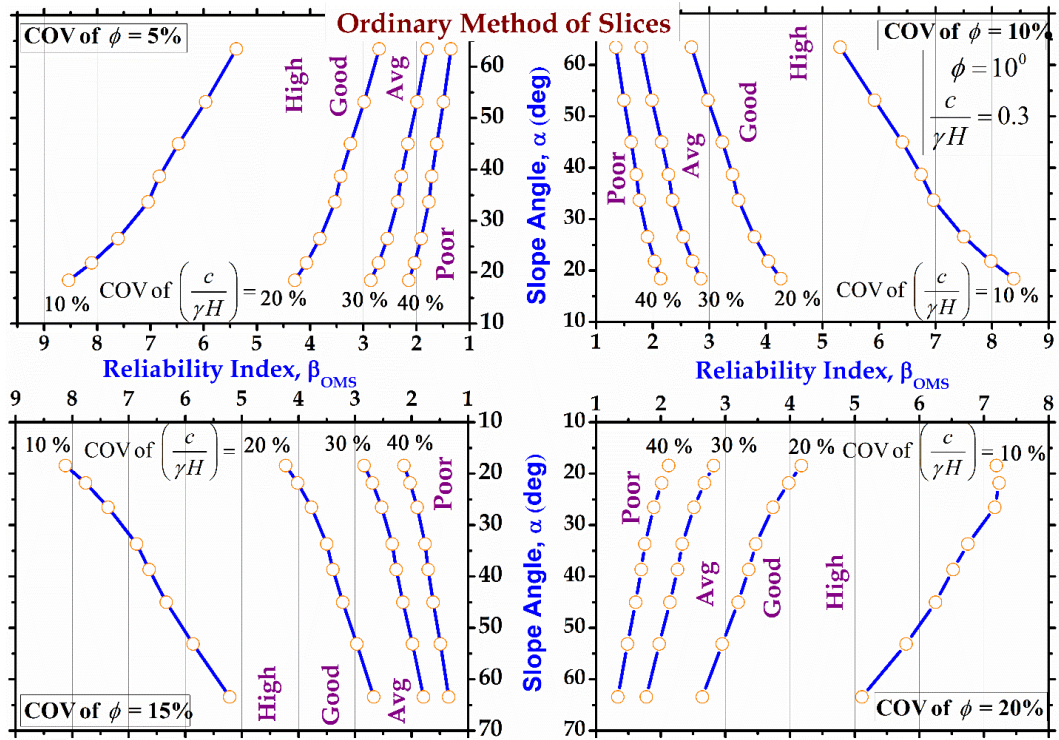


Figure 4.49: Design charts for $c/\gamma H=0.3$ and $\phi=10^\circ$ for Ordinary Method of Slices

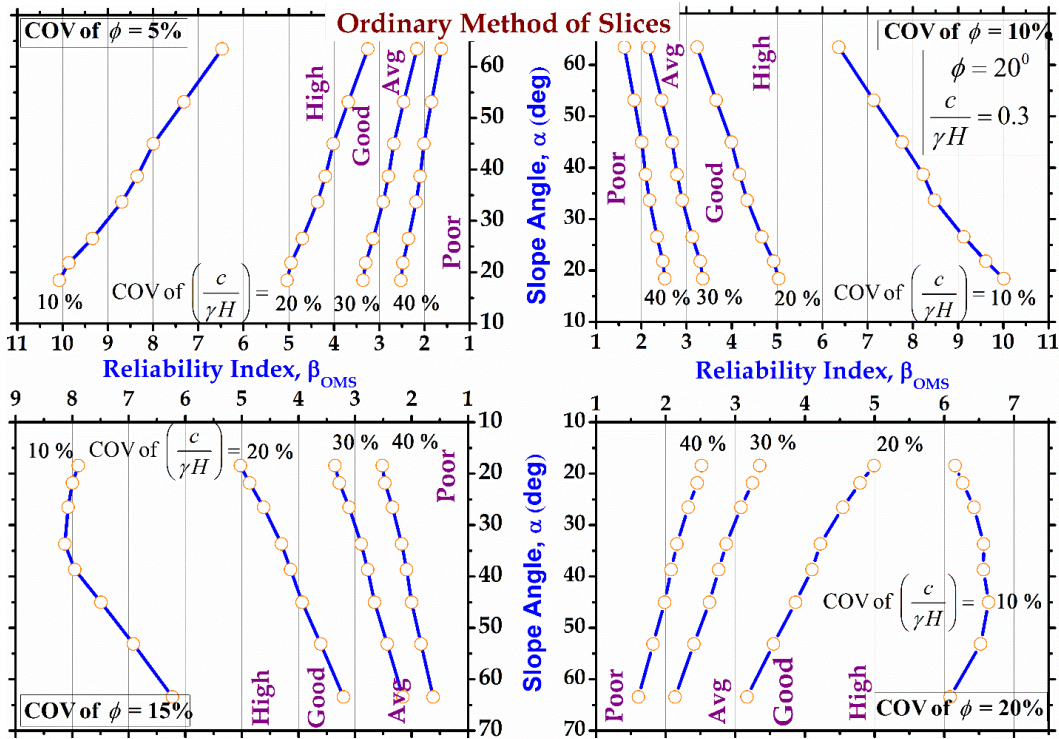


Figure 4.50: Design charts for $c/\gamma H=0.3$ and $\phi=20^\circ$ for Ordinary Method of Slices

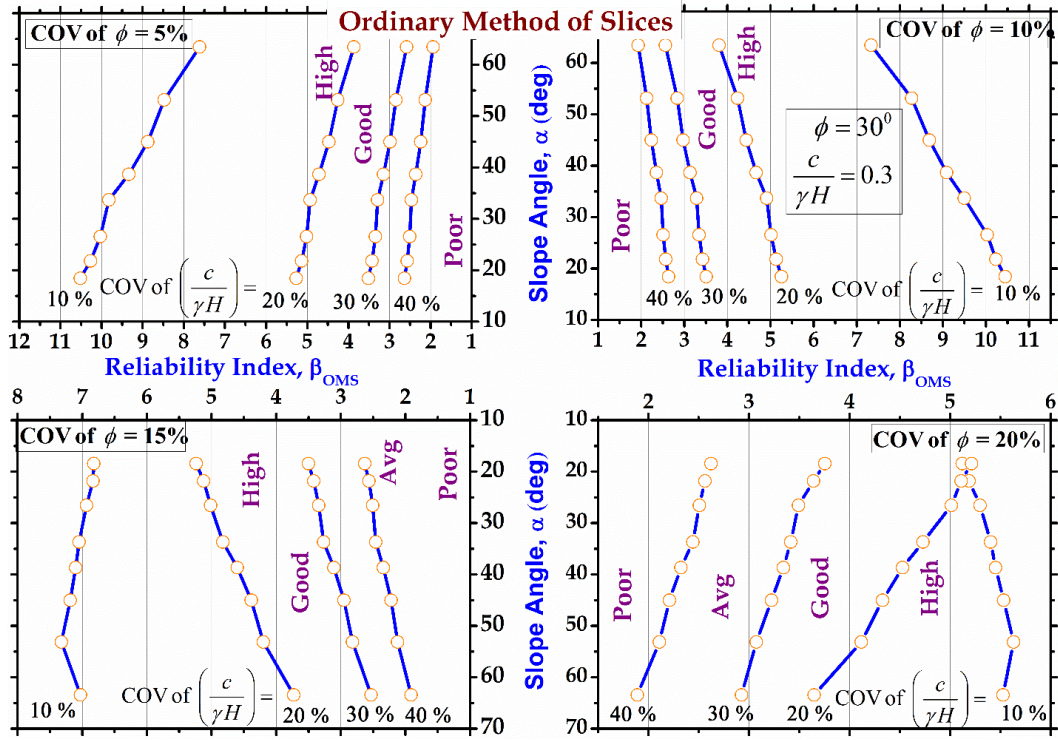


Figure 4.51: Design charts for $c/\gamma H = 0.3$ and $\phi = 30^\circ$ for Ordinary Method of Slices

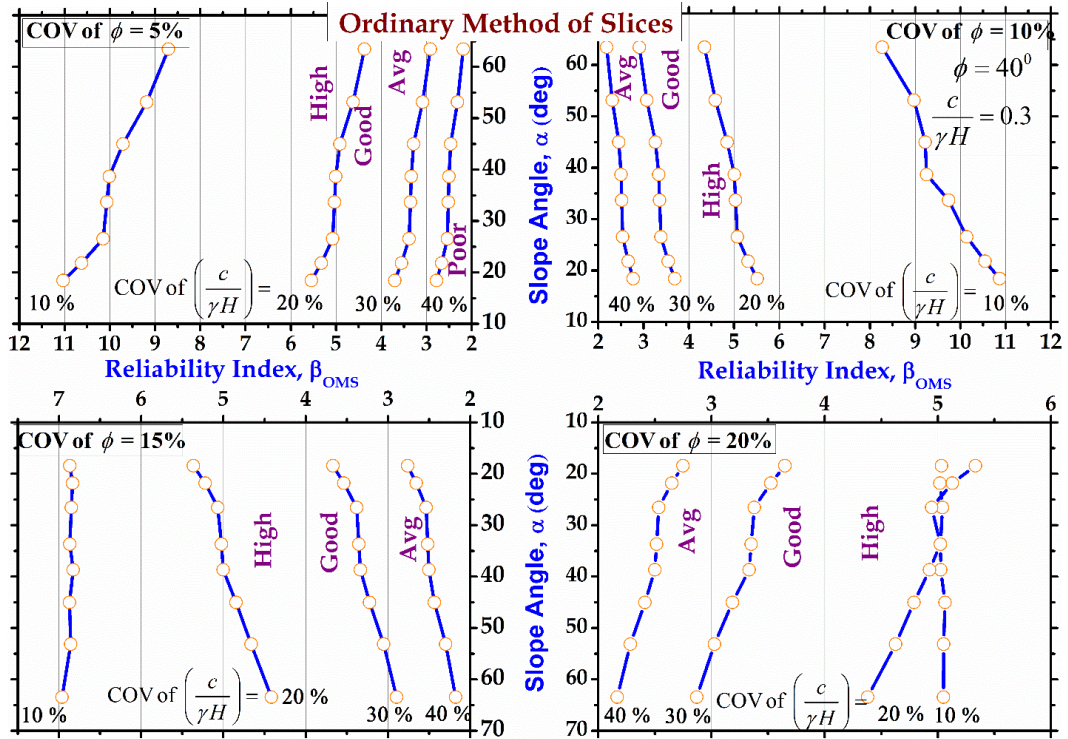


Figure 4.52: Design charts for $c/\gamma H = 0.3$ and $\phi = 40^\circ$ for Ordinary Method of Slices

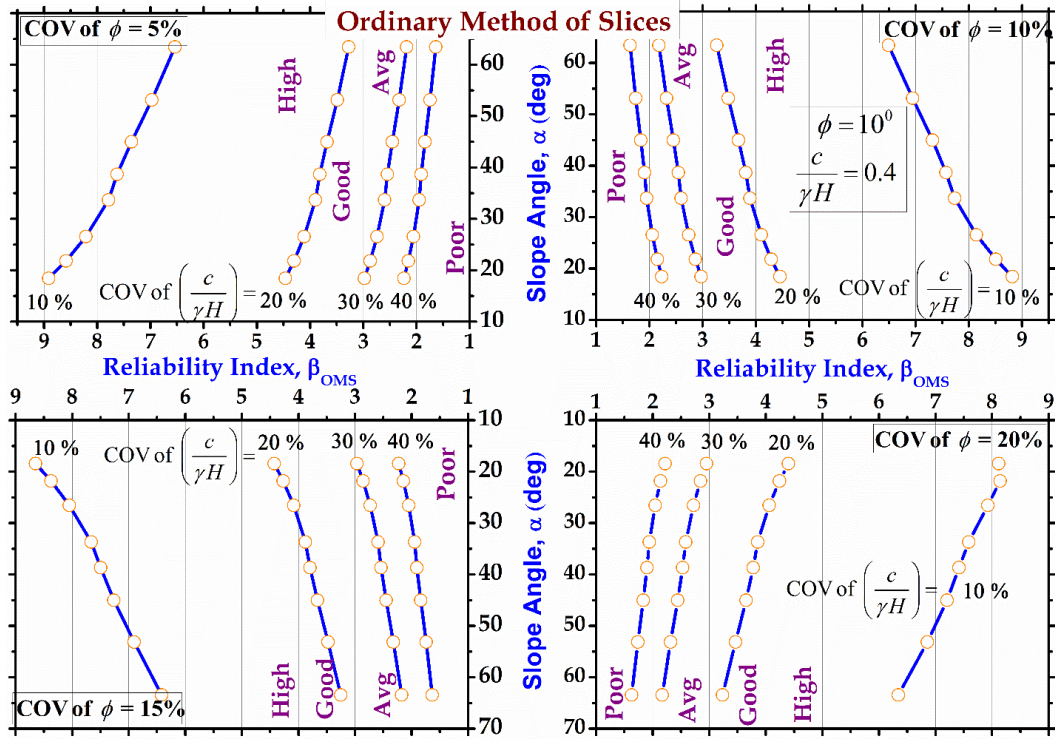


Figure 4.53: Design charts for $c/\gamma H=0.4$ and $\phi=10^\circ$ for Ordinary Method of Slices

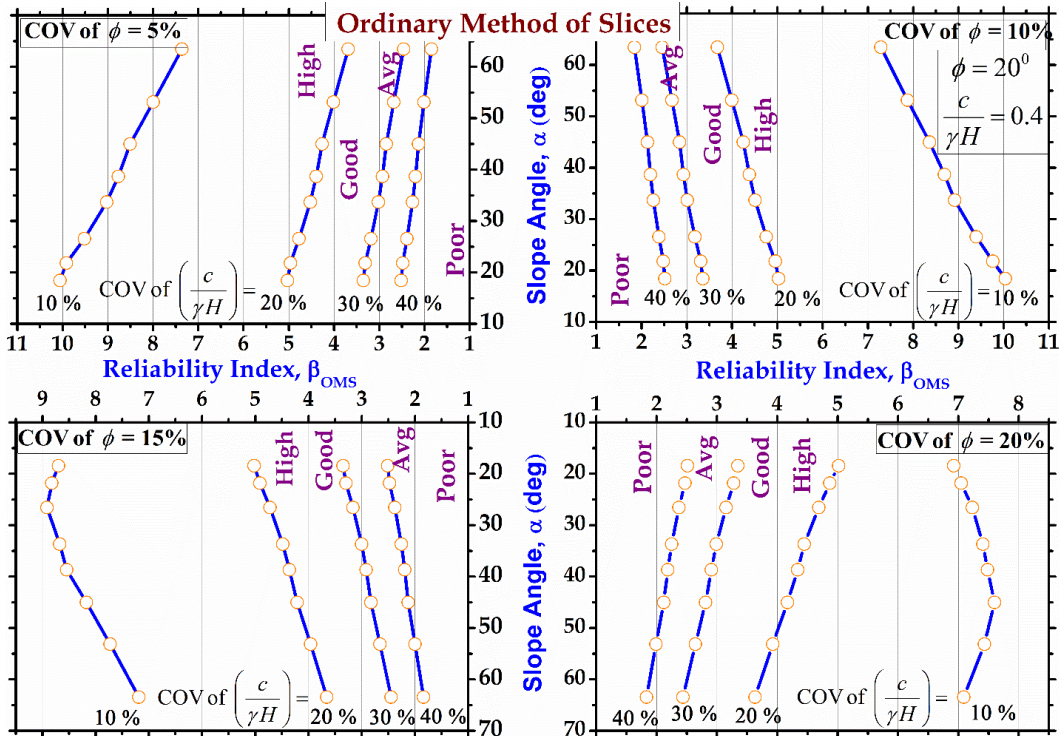


Figure 4.54: Design charts for $c/\gamma H=0.4$ and $\phi=20^\circ$ for Ordinary Method of Slices

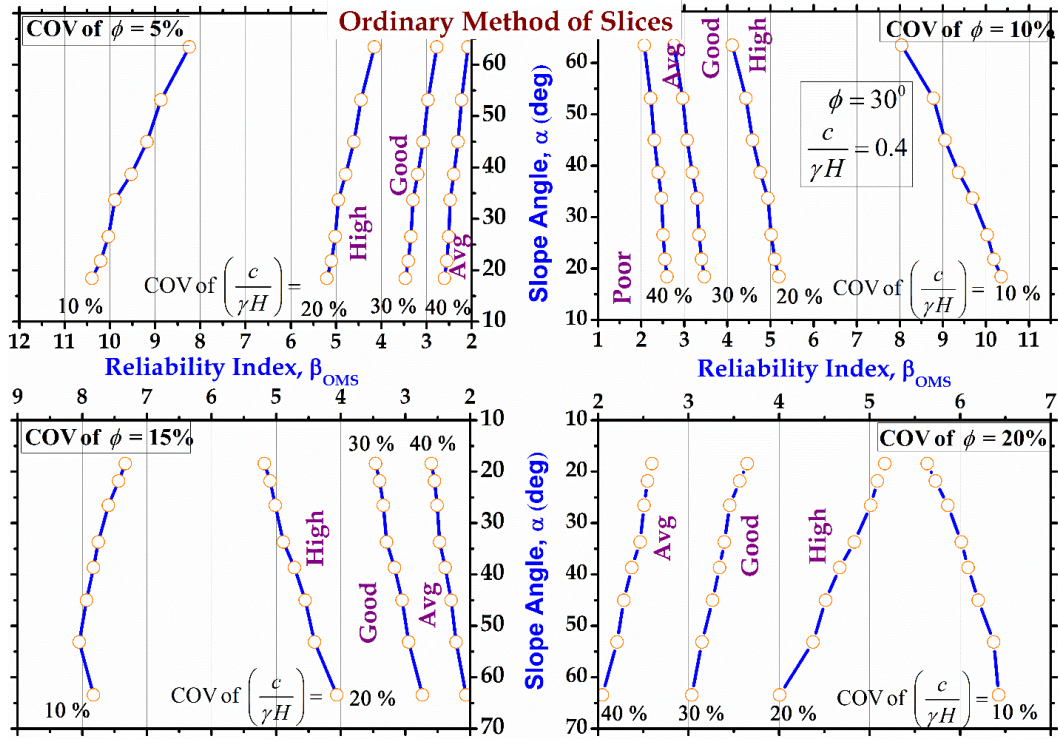


Figure 4.55: Design charts for $c/\gamma H = 0.4$ and $\phi = 30^\circ$ for Ordinary Method of Slices

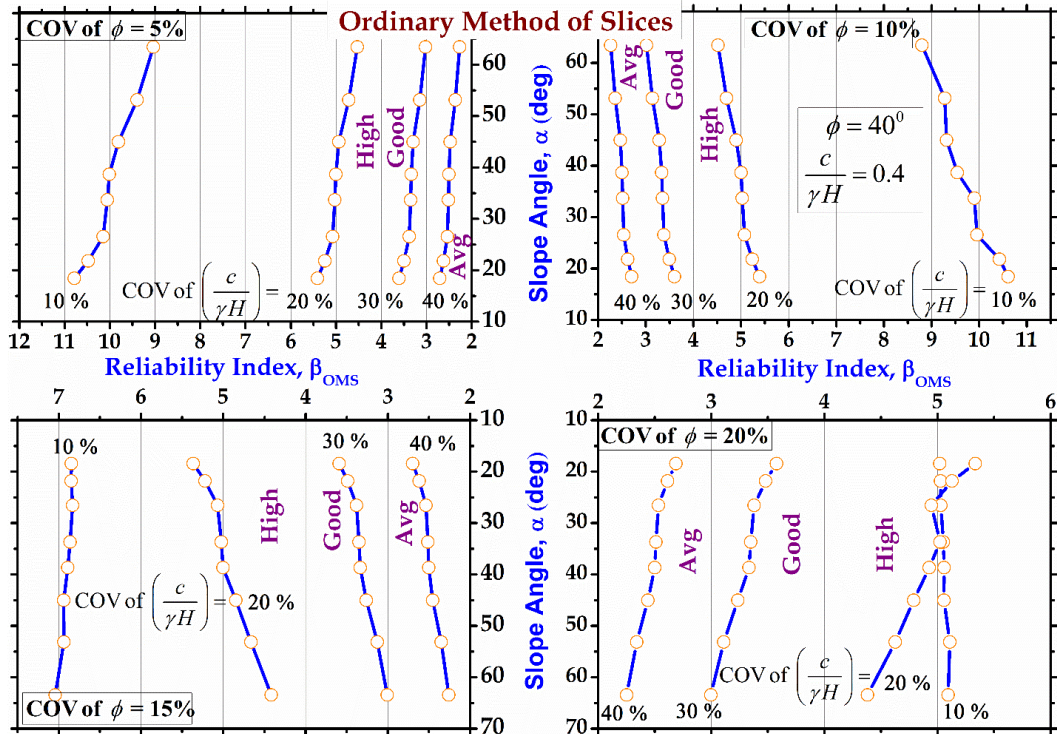


Figure 4.56: Design charts for $c/\gamma H = 0.4$ and $\phi = 40^\circ$ for Ordinary Method of Slices

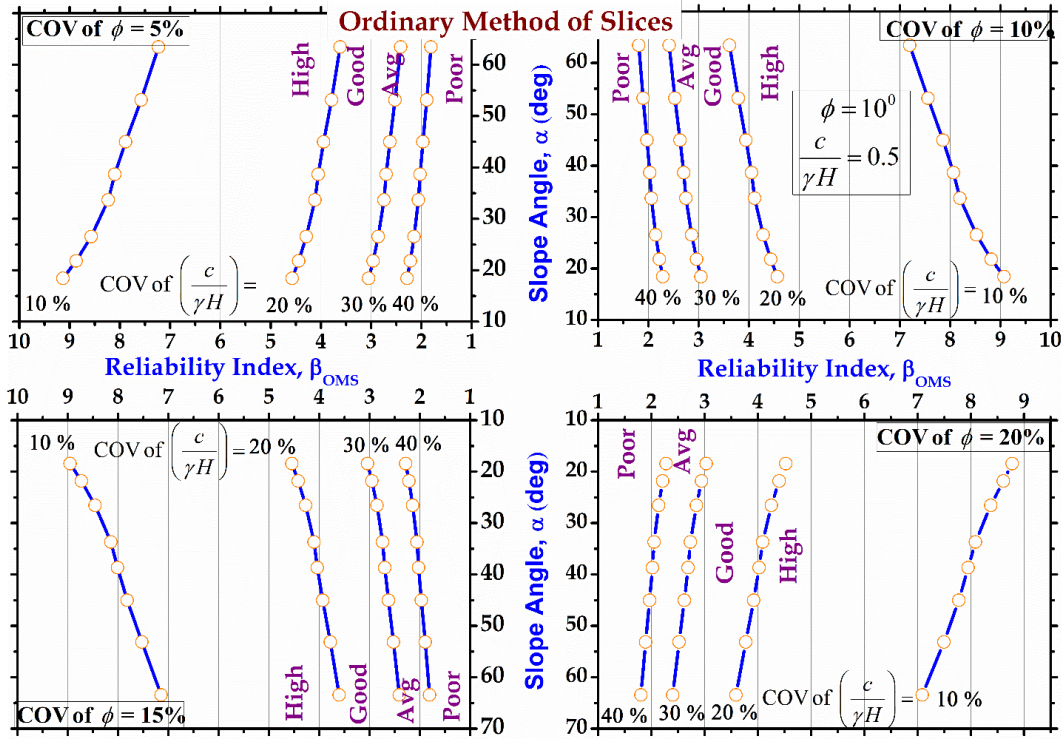


Figure 4.57: Design charts for $c/\gamma H = 0.5$ and $\phi = 10^\circ$ for Ordinary Method of Slices

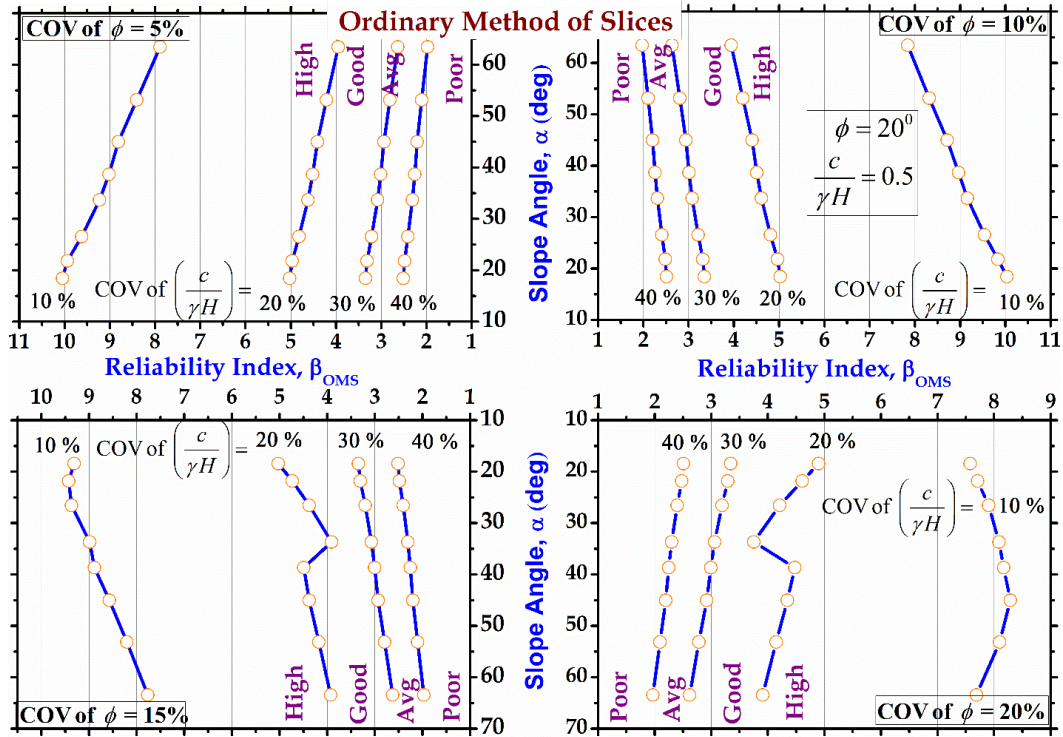


Figure 4.58: Design charts for $c/\gamma H = 0.5$ and $\phi = 20^\circ$ for Ordinary Method of Slices

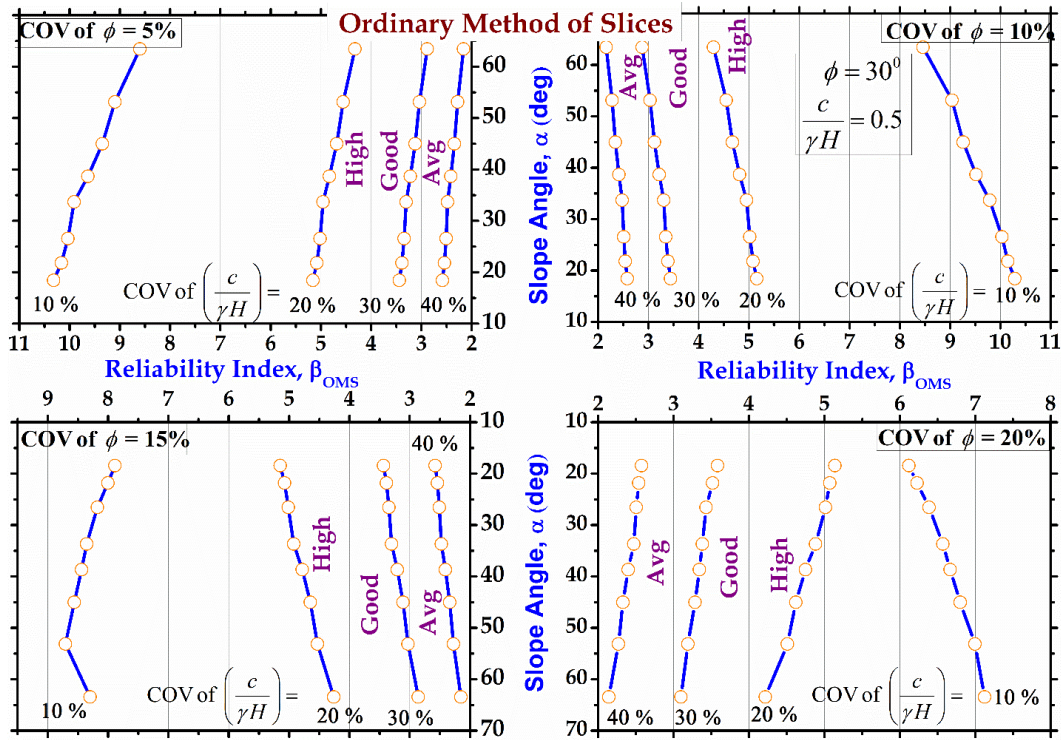


Figure 4.59: Design charts for $c/\gamma H=0.5$ and $\phi=30^\circ$ for Ordinary Method of Slices

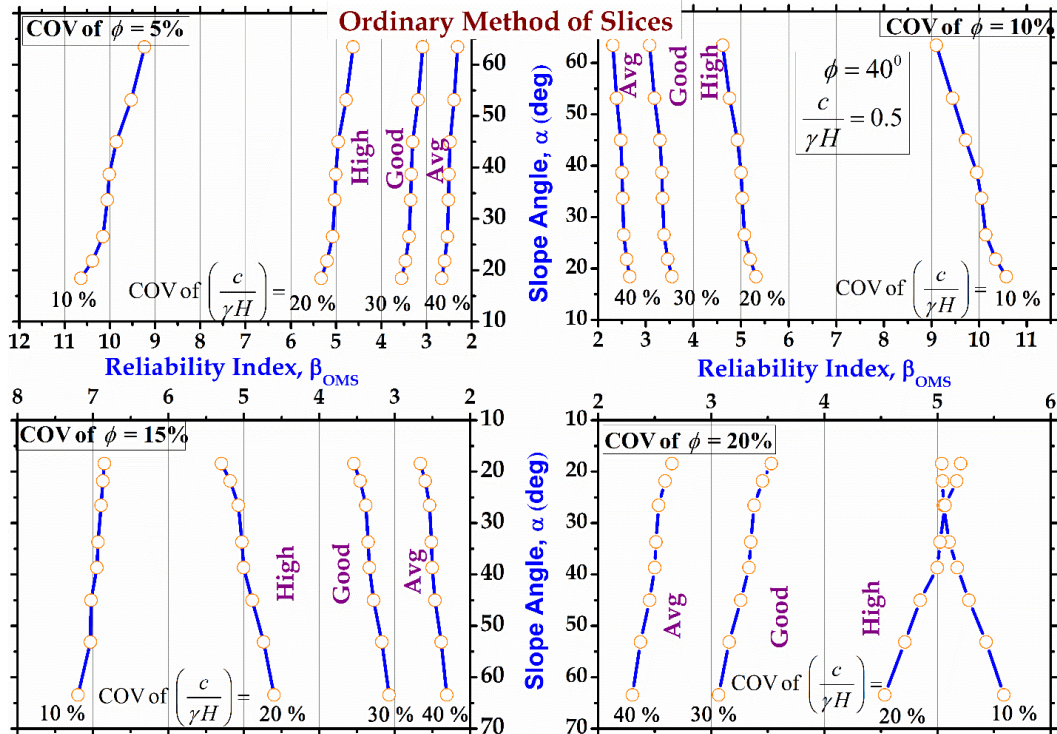


Figure 4.60: Design charts for $c/\gamma H=0.5$ and $\phi=40^\circ$ for Ordinary Method of Slice

4.5 Design Charts for Bishop's Simplified Method

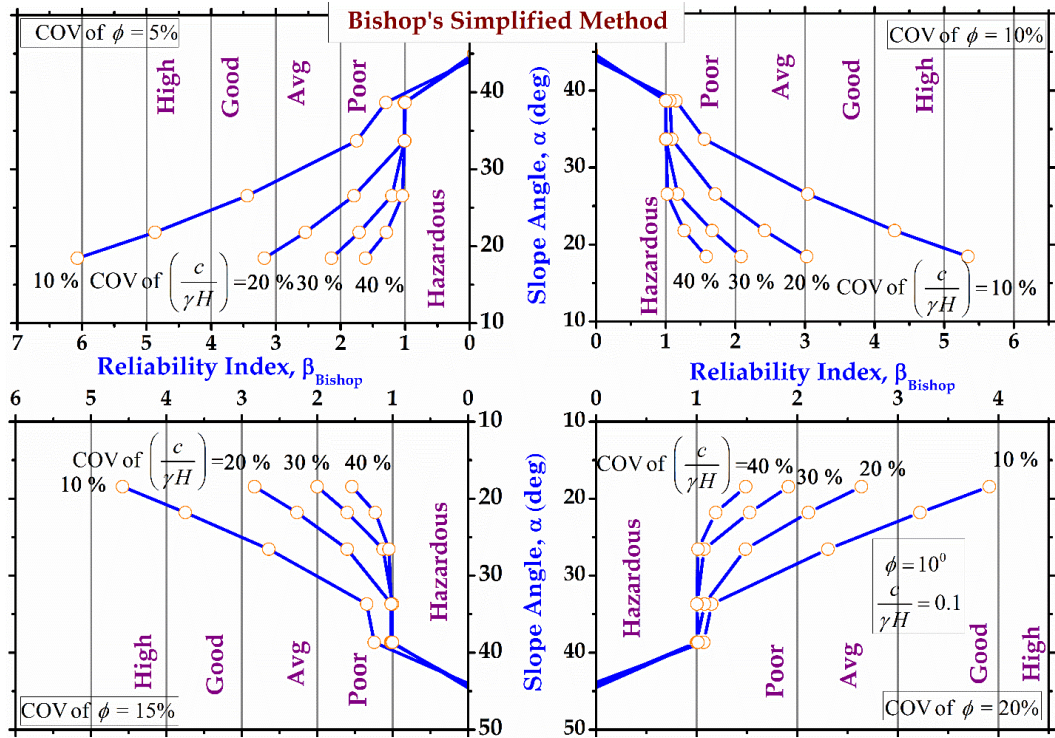


Figure 4.61: Design charts for $c/\gamma H = 0.1$ and $\phi = 10^\circ$ for Bishop's Simplified Method

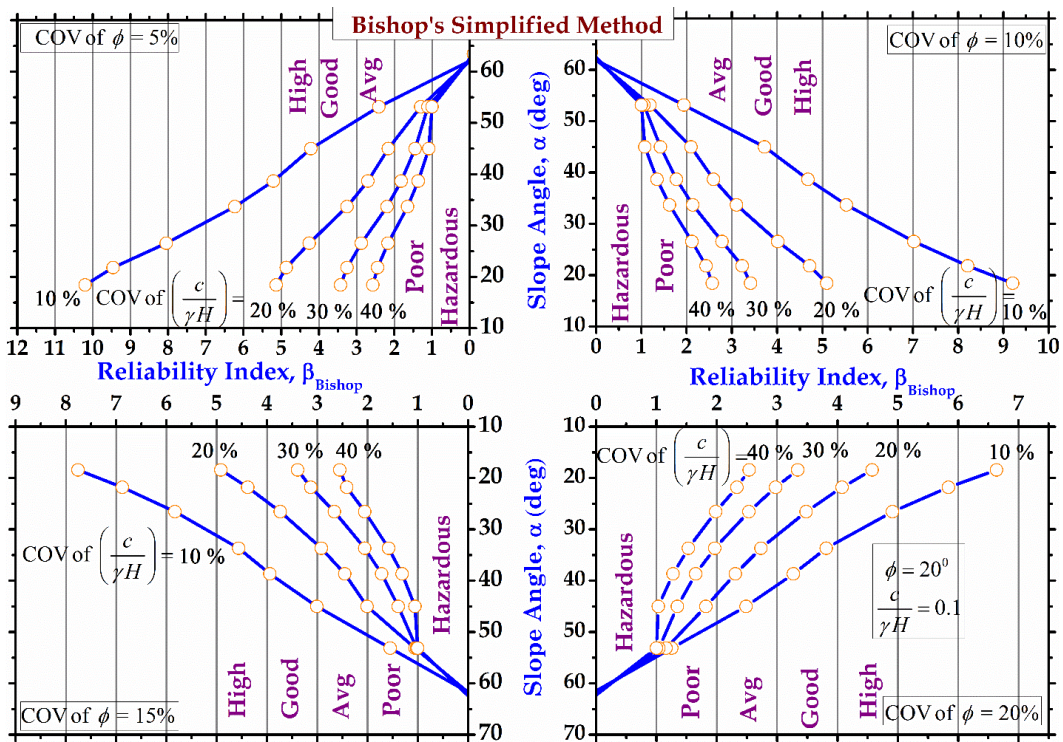


Figure 4.62: Design charts for $c/\gamma H = 0.1$ and $\phi = 20^\circ$ for Bishop's Simplified Method

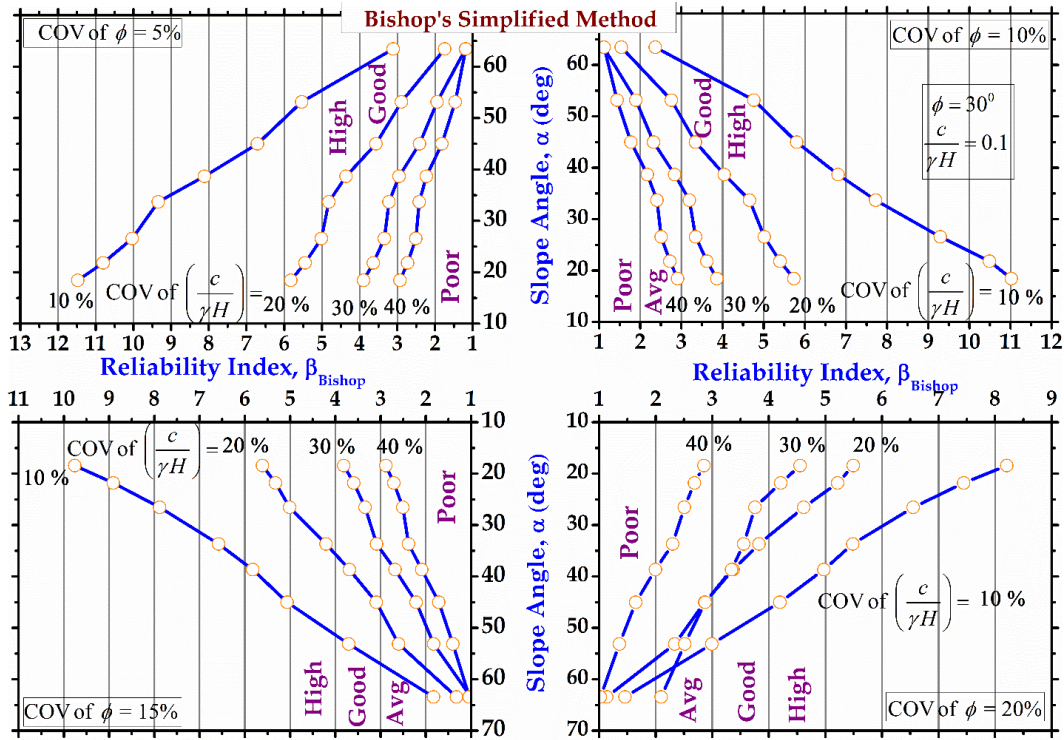


Figure 4.63: Design charts for $c/\gamma H=0.1$ and $\phi=30^\circ$ for Bishop's Simplified Method

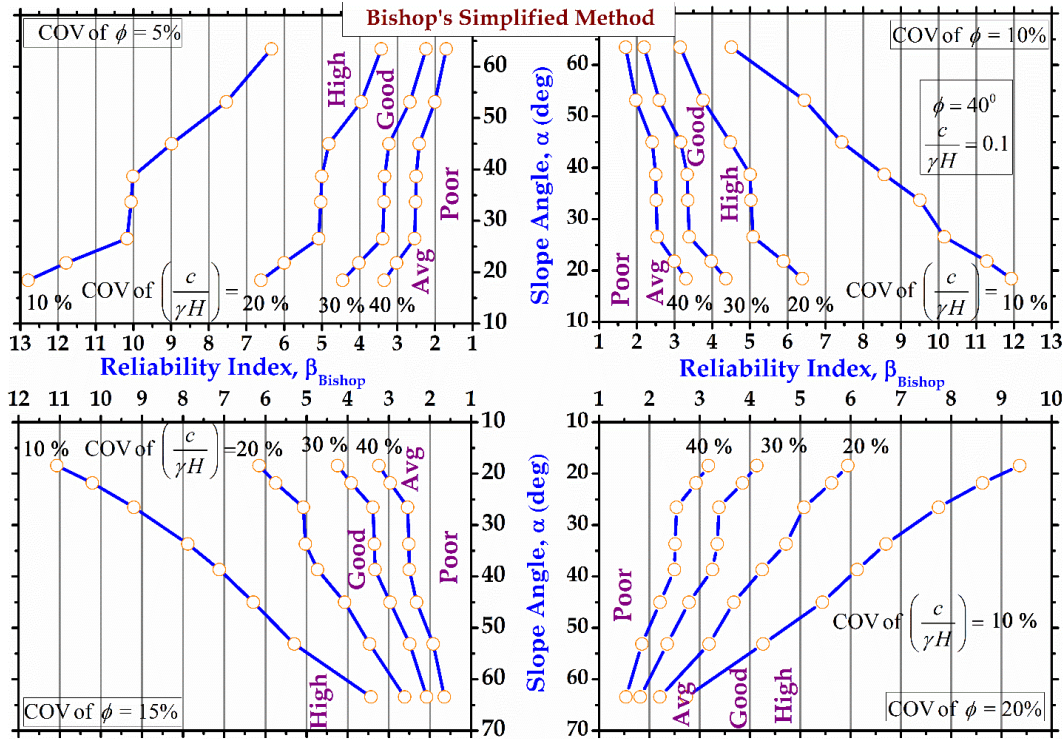


Figure 4.64: Design charts for $c/\gamma H=0.1$ and $\phi=40^\circ$ for Bishop's Simplified Method

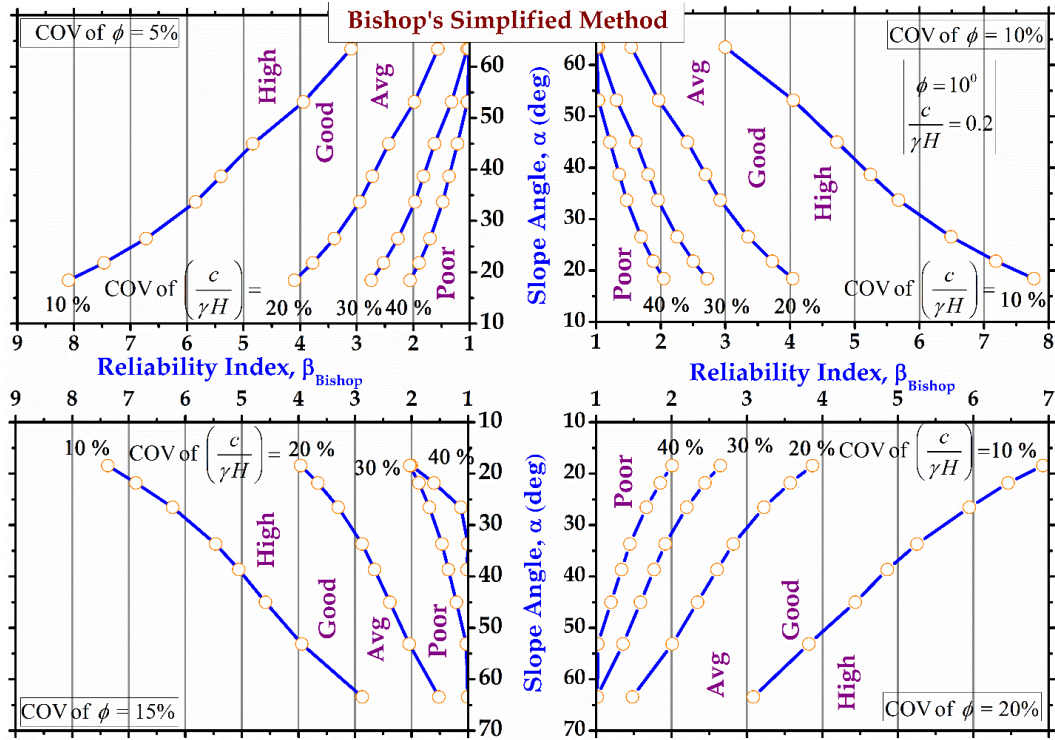


Figure 4.65: Design charts for $c/\gamma H=0.2$ and $\phi=10^\circ$ for Bishop's Simplified Method

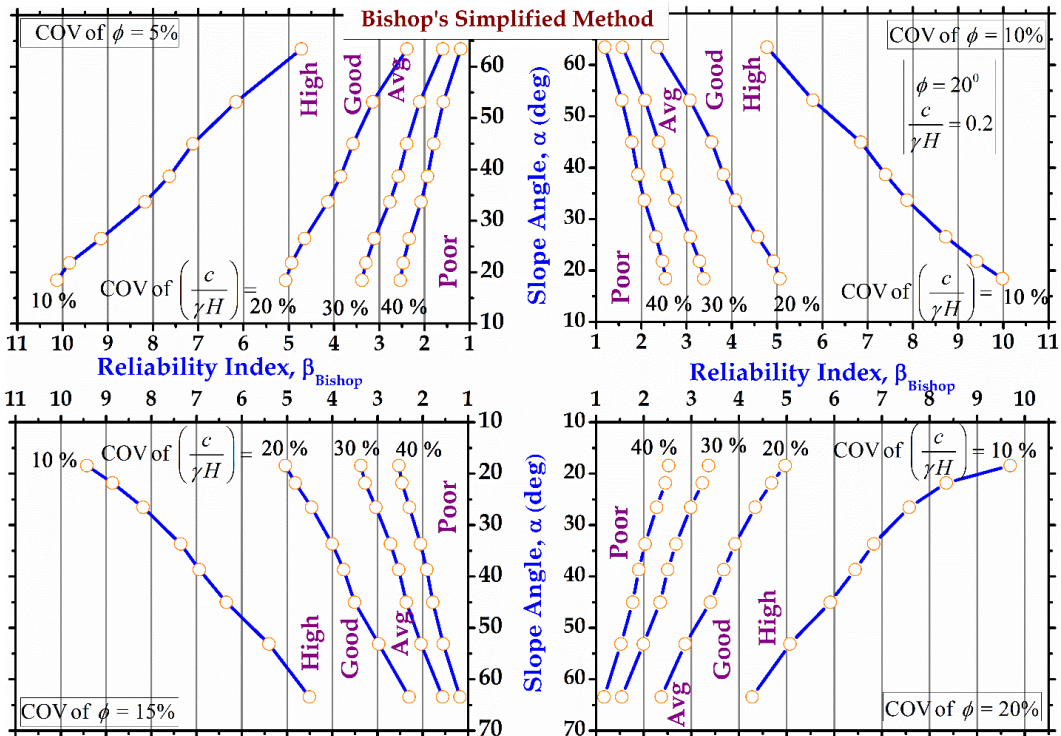


Figure 4.66: Design charts for $c/\gamma H=0.2$ and $\phi=20^\circ$ for Bishop's Simplified Method

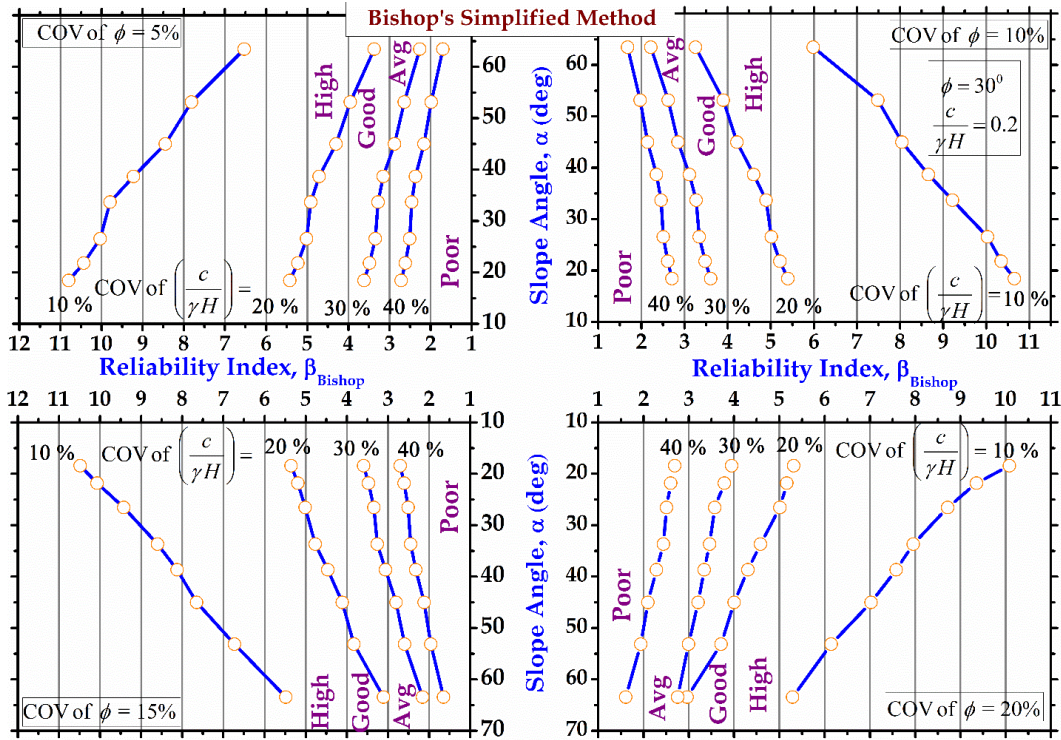


Figure 4.67: Design charts for $c/\gamma H=0.2$ and $\phi=30^\circ$ for Bishop's Simplified Method

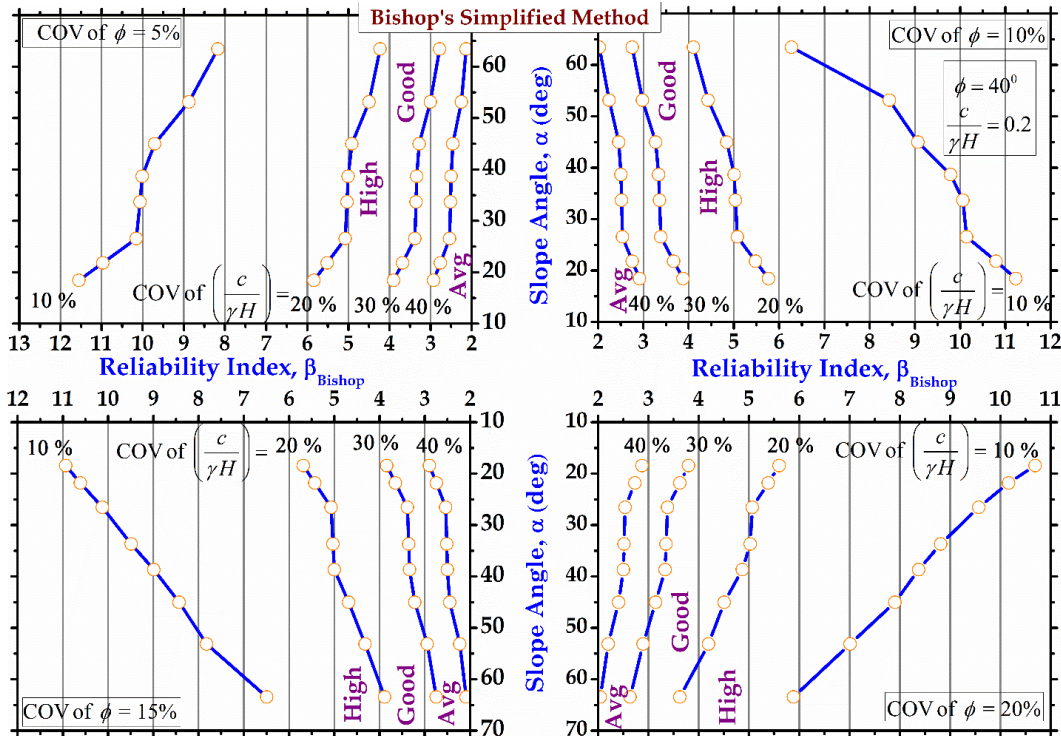


Figure 4.68: Design charts for $c/\gamma H=0.2$ and $\phi=40^\circ$ for Bishop's Simplified Method

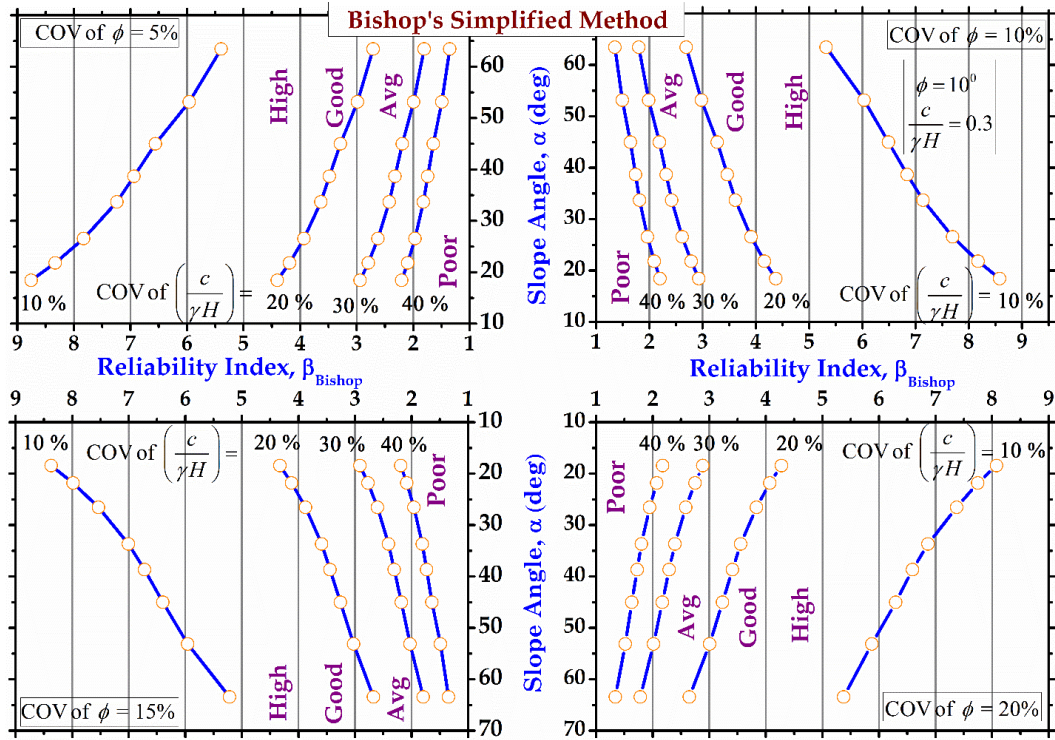


Figure 4.69: Design charts for $c/\gamma H=0.3$ and $\phi=10^\circ$ for Bishop's Simplified Method

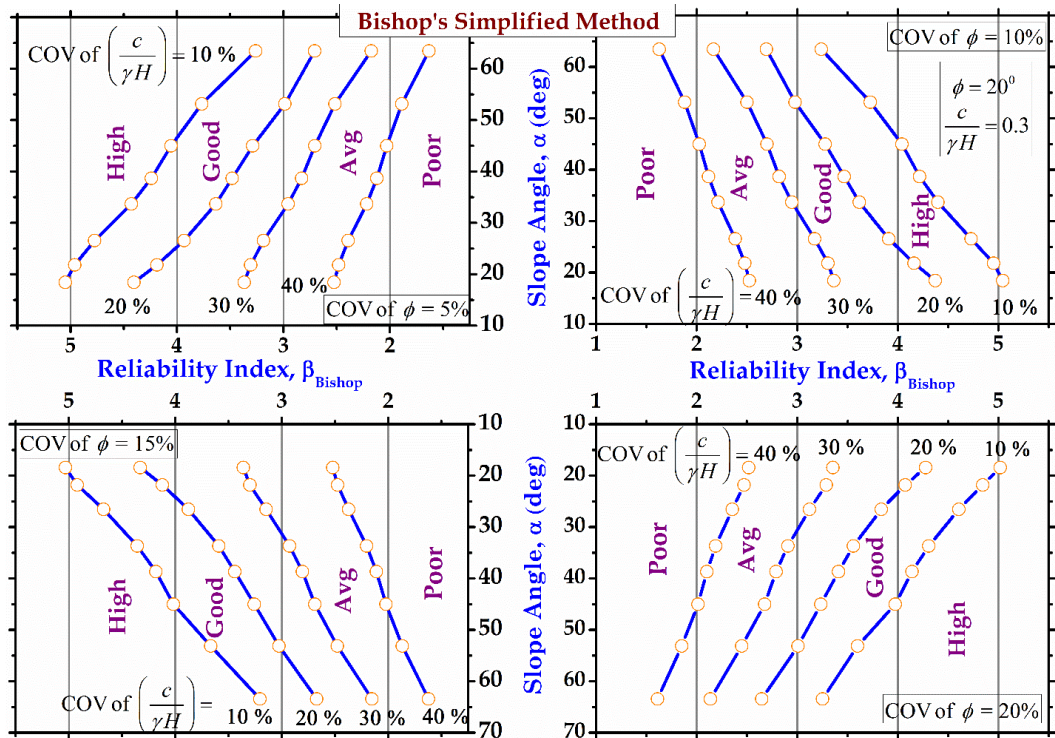


Figure 4.70: Design charts for $c/\gamma H=0.3$ and $\phi=20^\circ$ for Bishop's Simplified Method

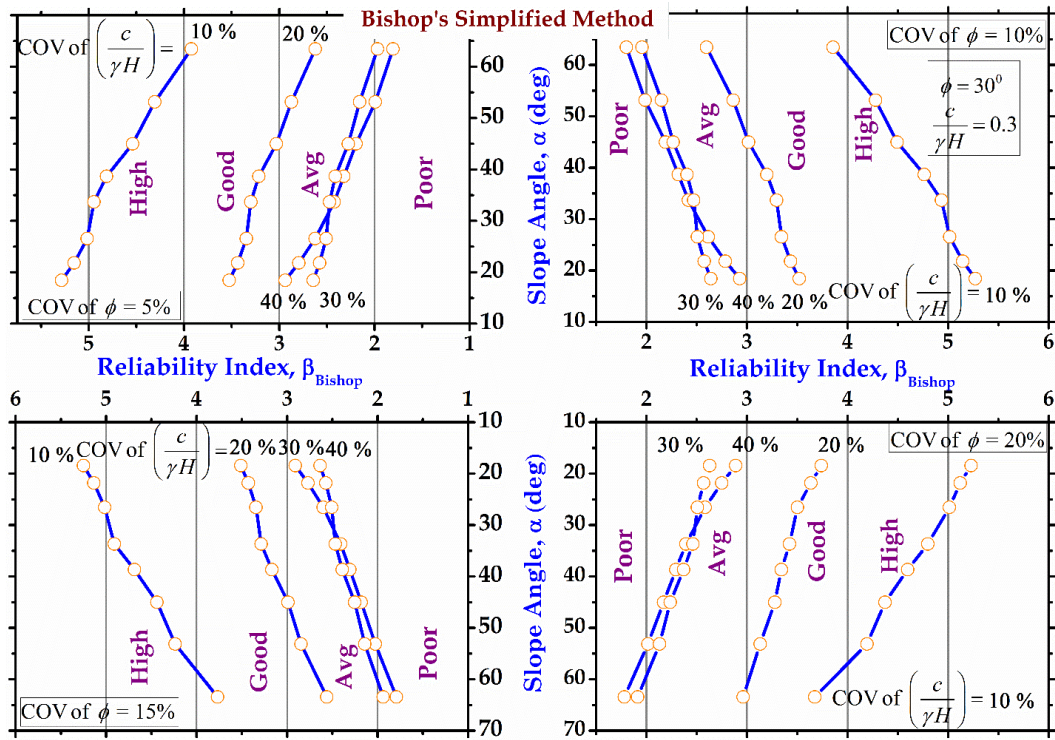


Figure 4.71: Design charts for $c/\gamma H=0.3$ and $\phi=30^\circ$ for Bishop's Simplified Method

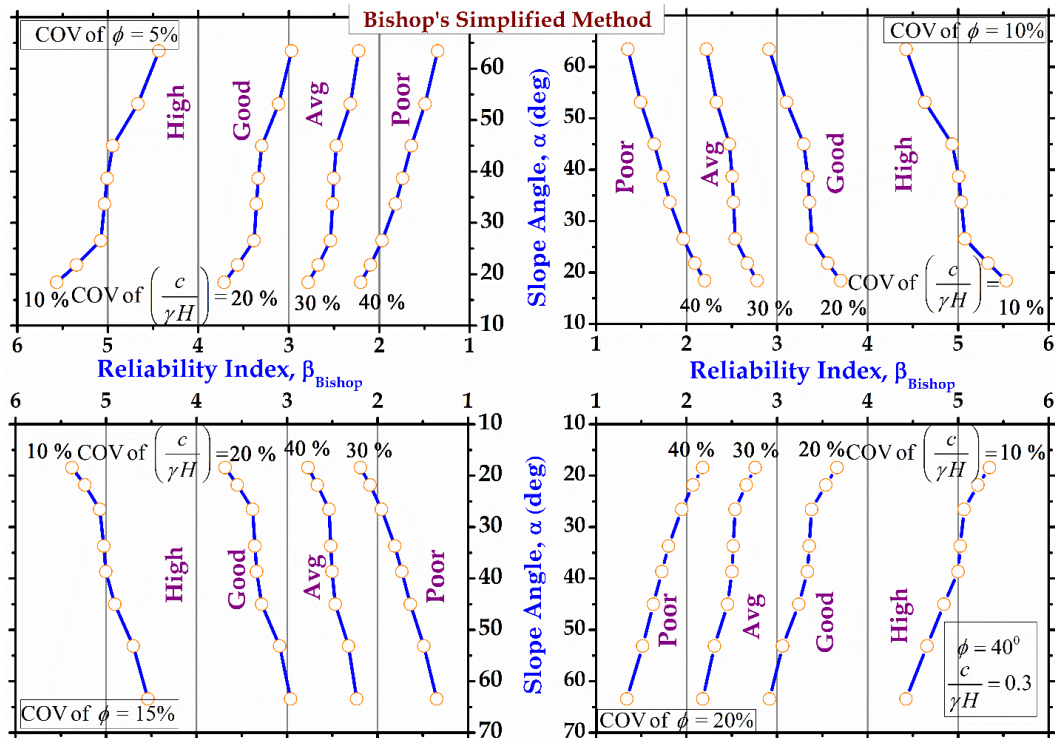


Figure 4.72: Design charts for $c/\gamma H=0.3$ and $\phi=40^\circ$ for Bishop's Simplified Method

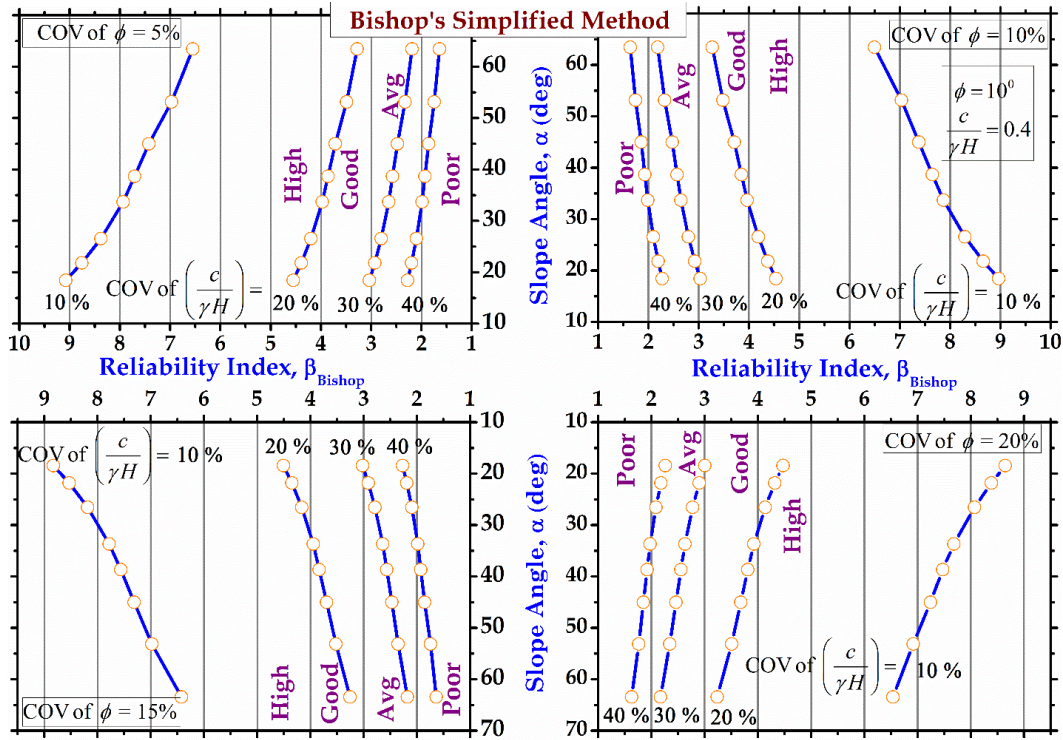


Figure 4.73: Design charts for $c/\gamma H=0.4$ and $\phi=10^\circ$ for Bishop's Simplified Method

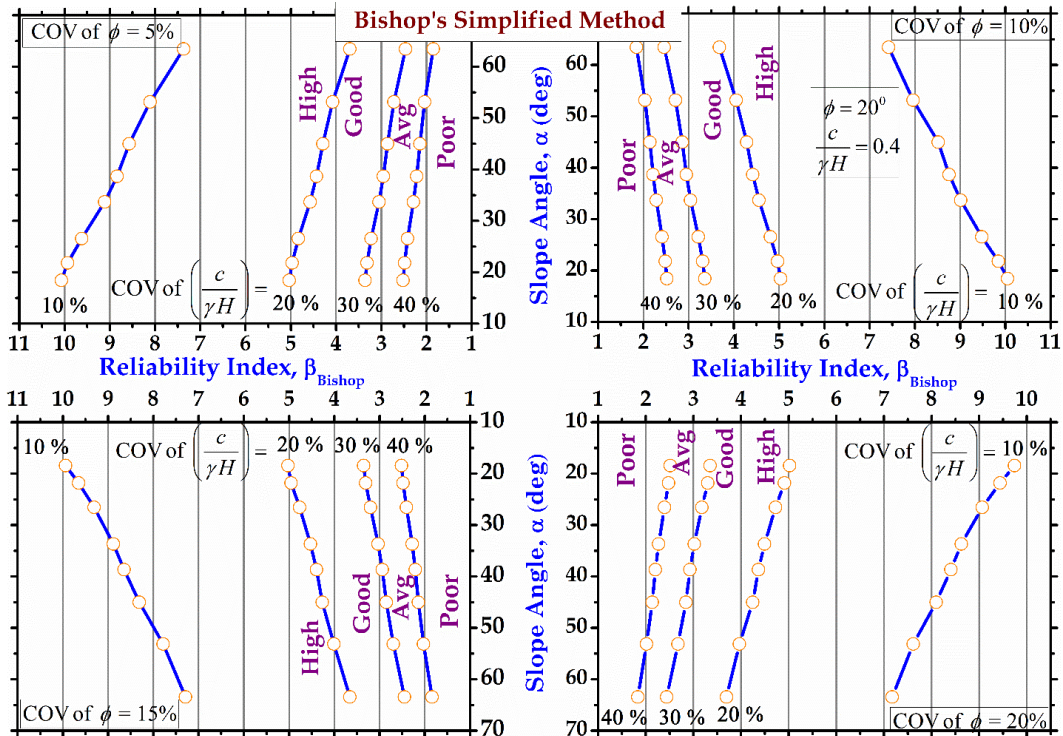


Figure 4.74: Design charts for $c/\gamma H=0.4$ and $\phi=20^\circ$ for Bishop's Simplified Method

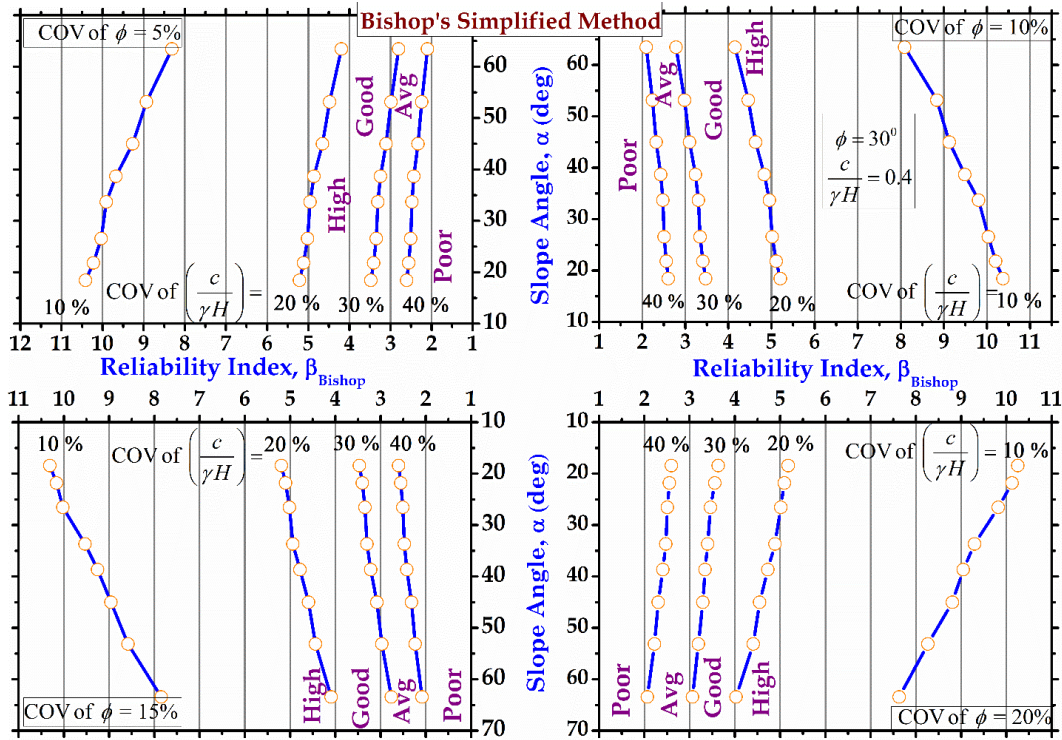


Figure 4.75: Design charts for $c/\gamma H=0.4$ and $\phi=30^\circ$ for Bishop's Simplified Method

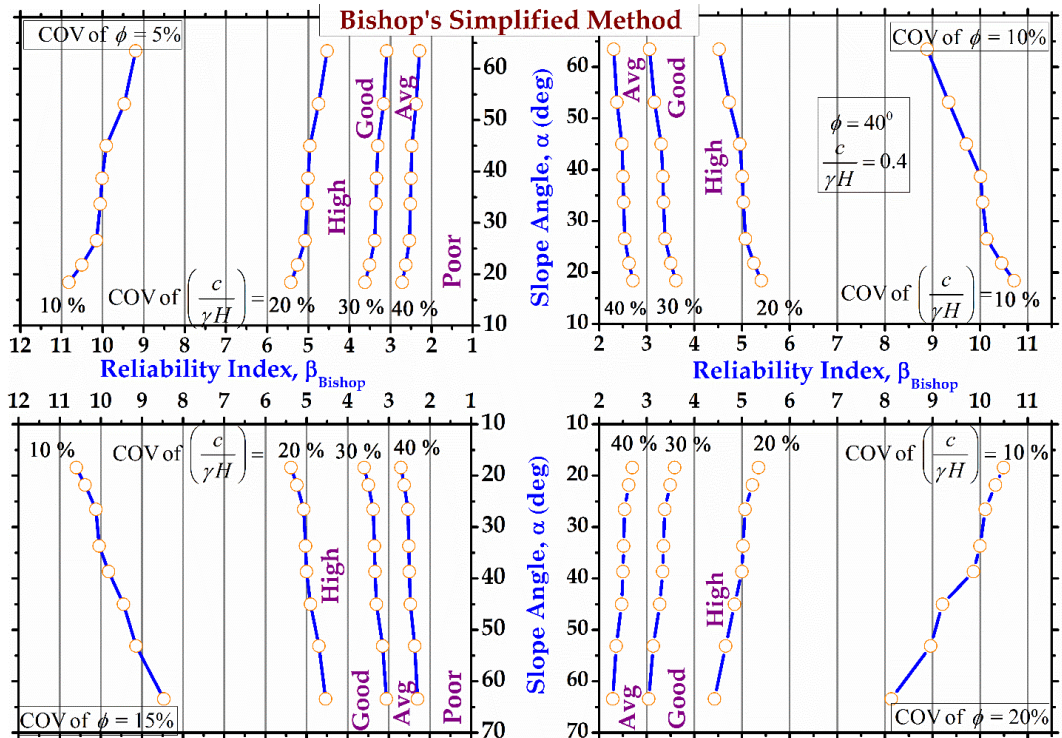


Figure 4.76: Design charts for $c/\gamma H=0.4$ and $\phi=40^\circ$ for Bishop's Simplified Method

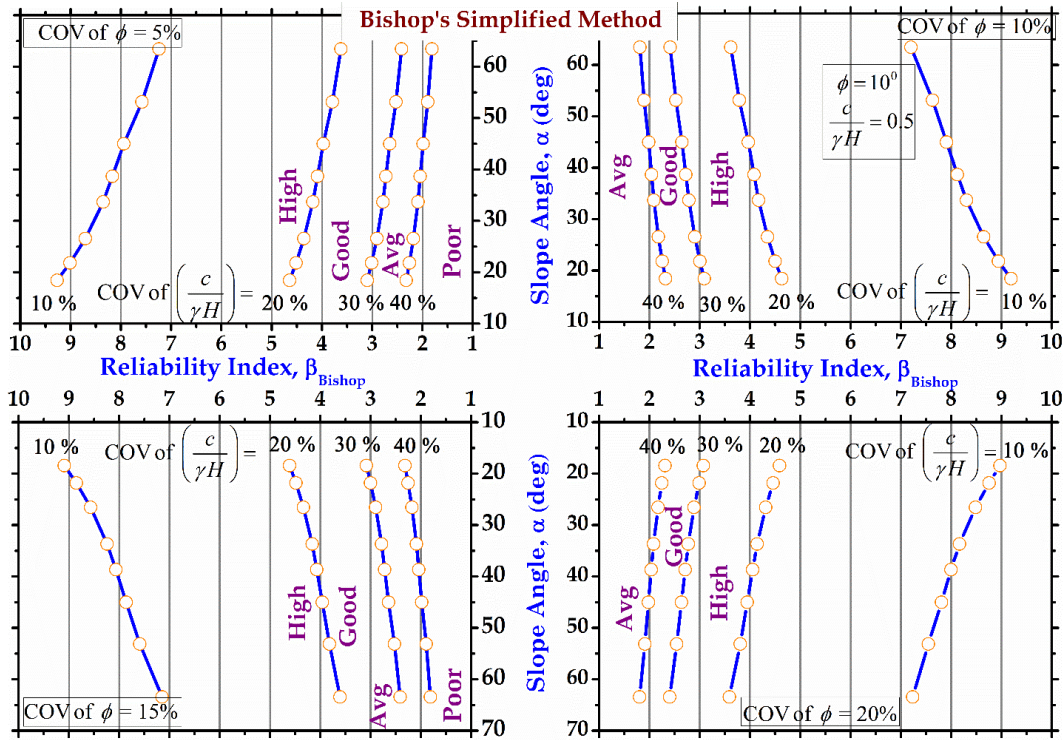


Figure 4.77: Design charts for $c/\gamma H = 0.5$ and $\phi = 10^\circ$ for Bishop's Simplified Method

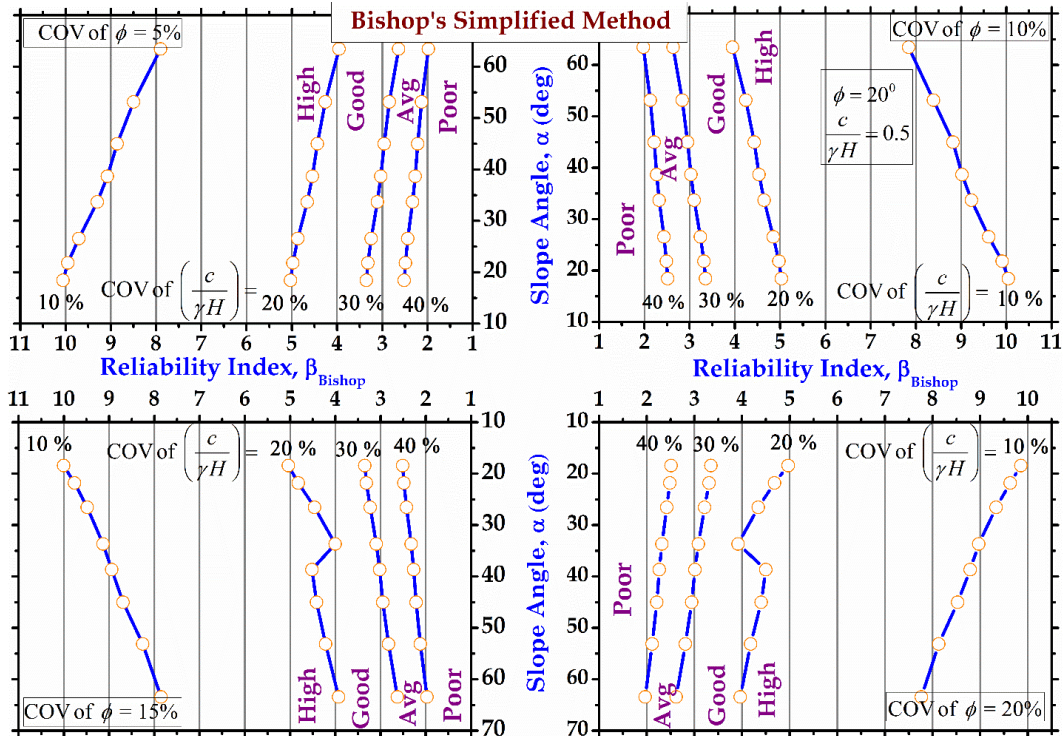


Figure 4.78: Design charts for $c/\gamma H = 0.5$ and $\phi = 20^\circ$ for Bishop's Simplified Method

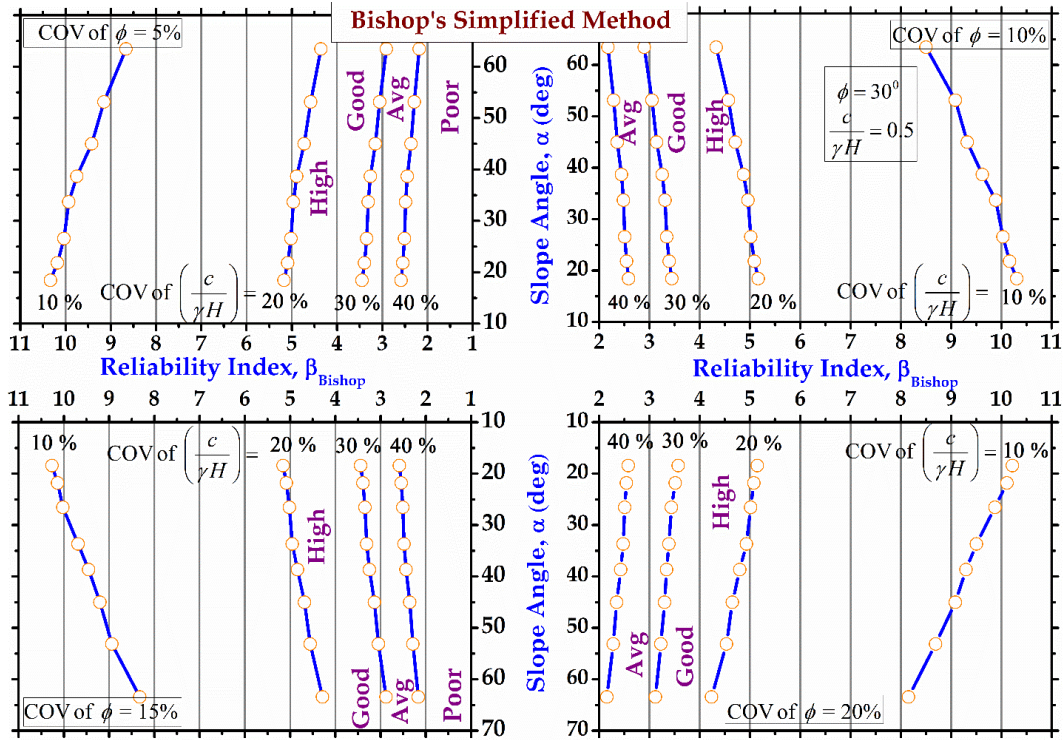


Figure 4.79: Design charts for $c/\gamma H=0.5$ and $\phi=30^\circ$ for Bishop's Simplified Method

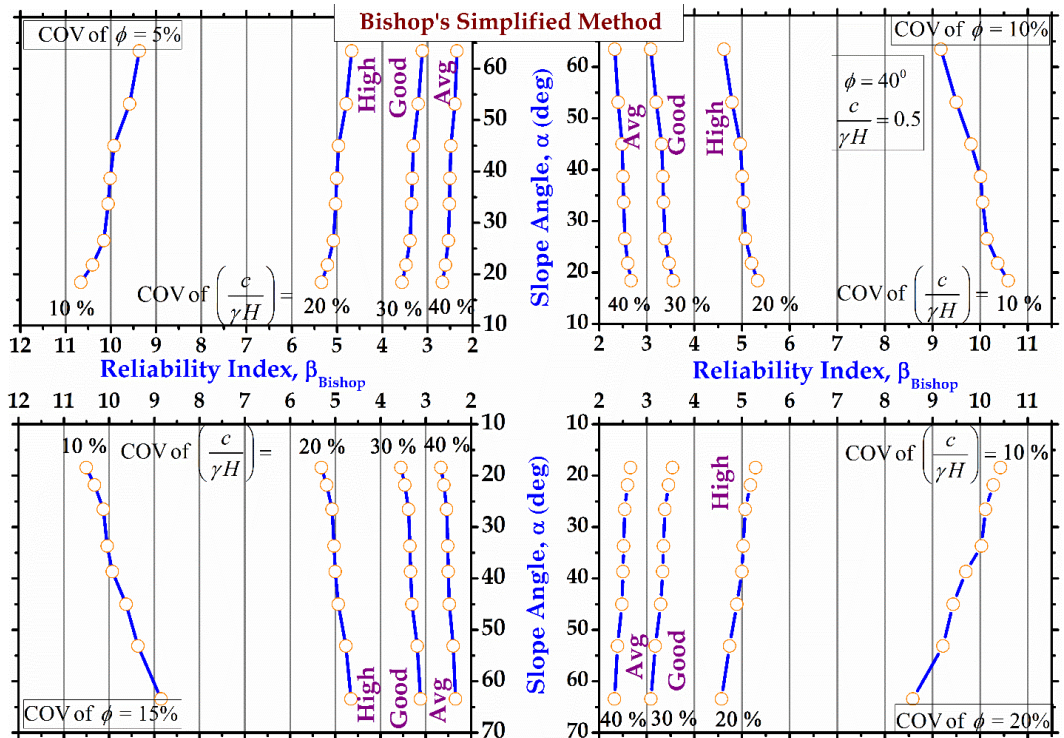


Figure 4.80: Design charts for $c/\gamma H=0.5$ and $\phi=40^\circ$ for Bishop's Simplified Method

4.6 Design Charts for Spencer Method

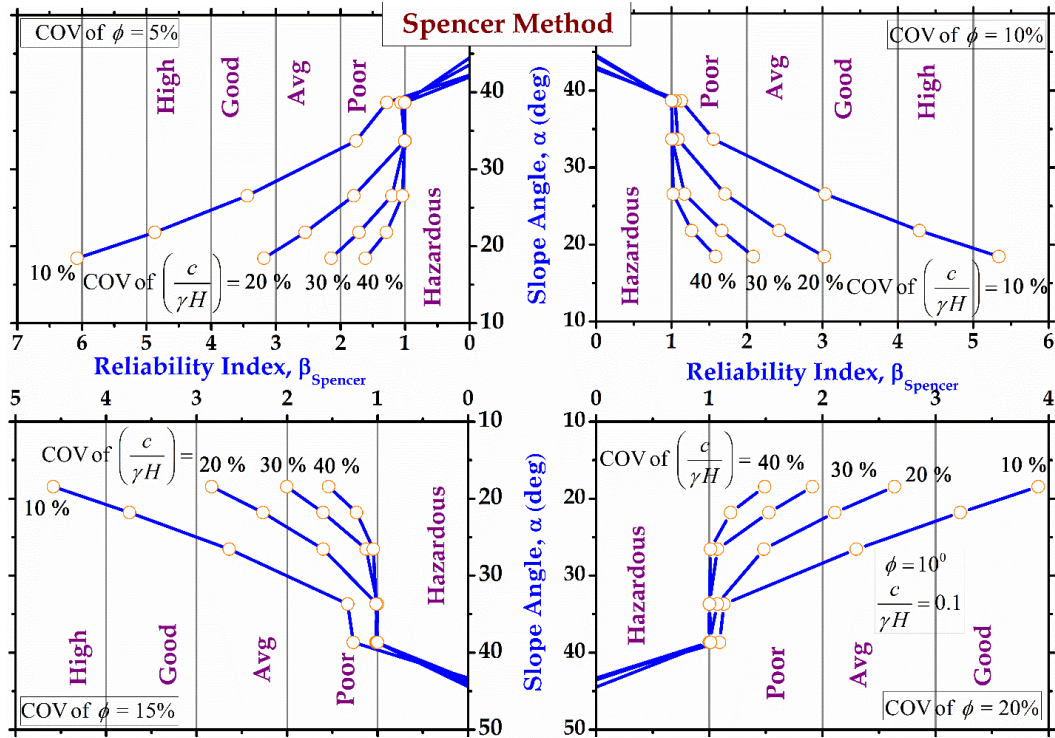


Figure 4.81: Design charts for $c/\gamma H = 0.1$ and $\phi = 10^\circ$ for Spencer Method

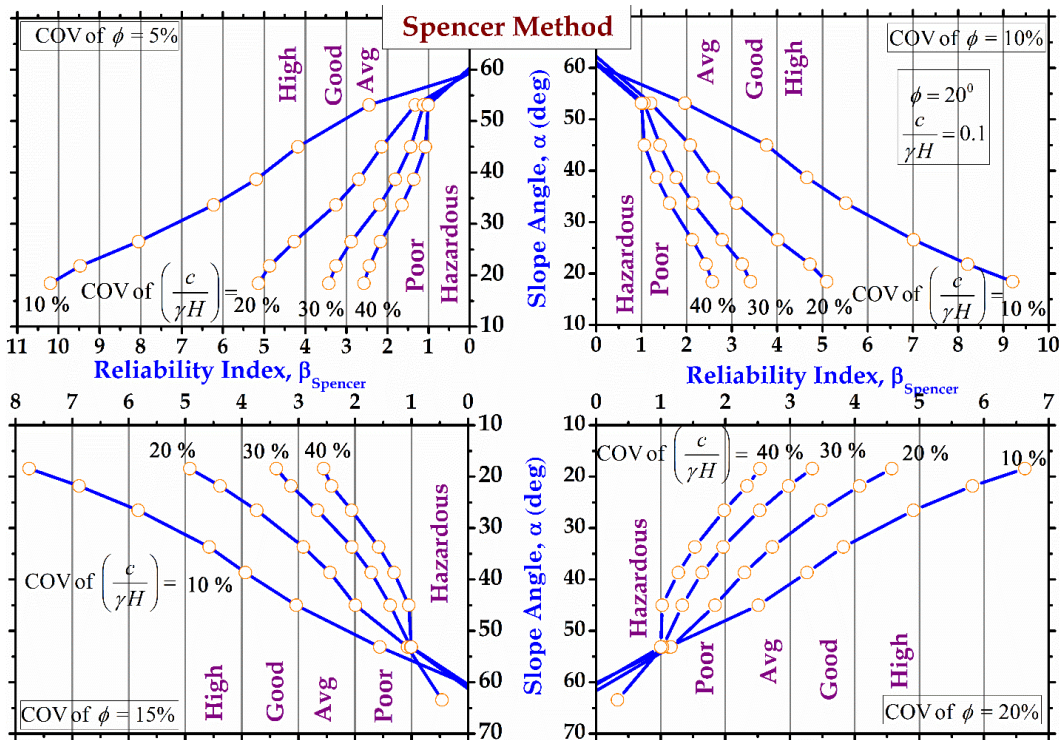


Figure 4.82: Design charts for $c/\gamma H = 0.1$ and $\phi = 20^\circ$ for Spencer Method

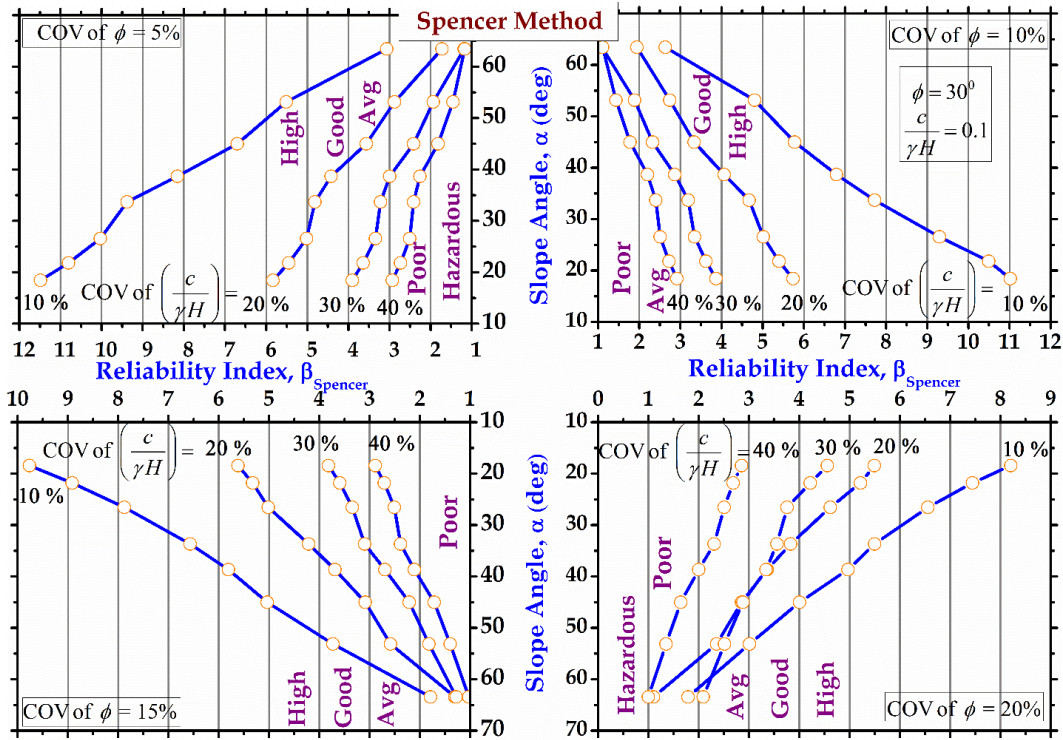


Figure 4.83: Design charts for $c/\gamma H = 0.1$ and $\phi = 30^\circ$ for Spencer Method

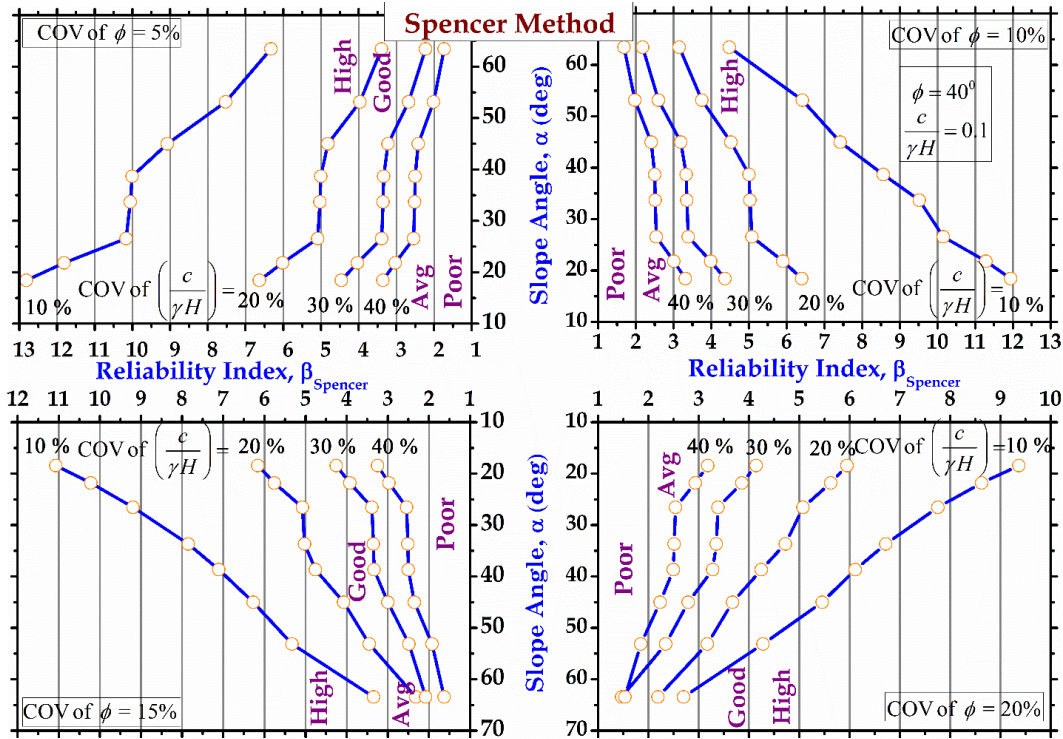


Figure 4.84: Design charts for $c/\gamma H = 0.1$ and $\phi = 40^\circ$ for Spencer Method

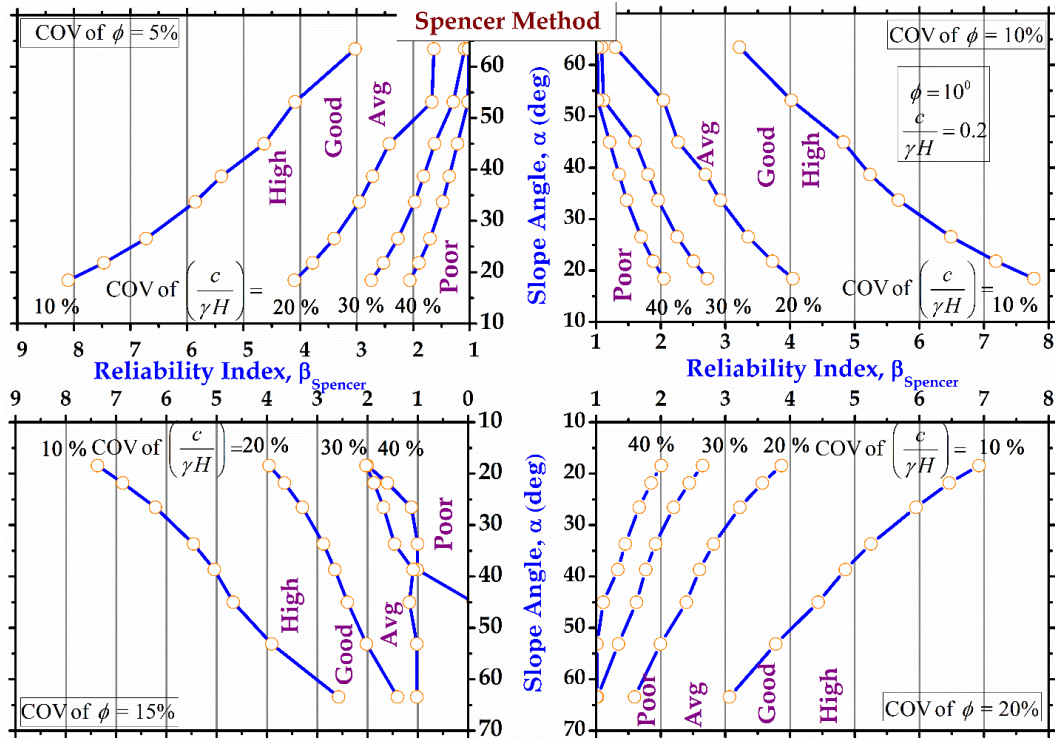


Figure 4.85: Design charts for $c/\gamma H = 0.2$ and $\phi = 10^\circ$ for Spencer Method

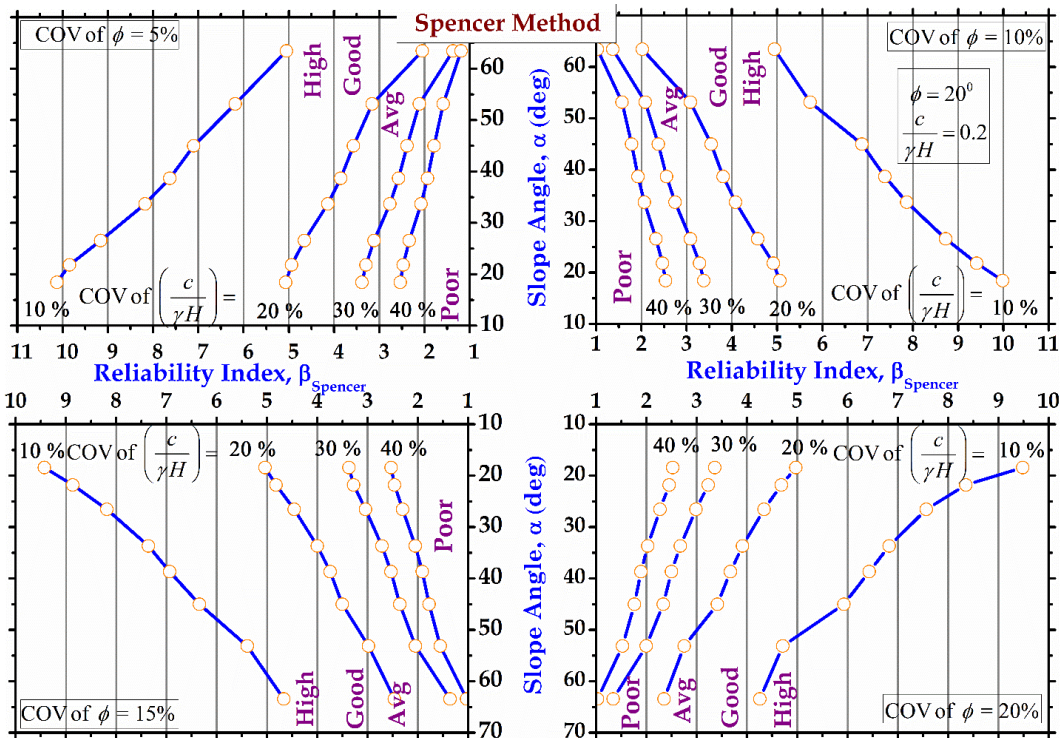


Figure 4.86: Design charts for $c/\gamma H = 0.2$ and $\phi = 20^\circ$ for Spencer Method

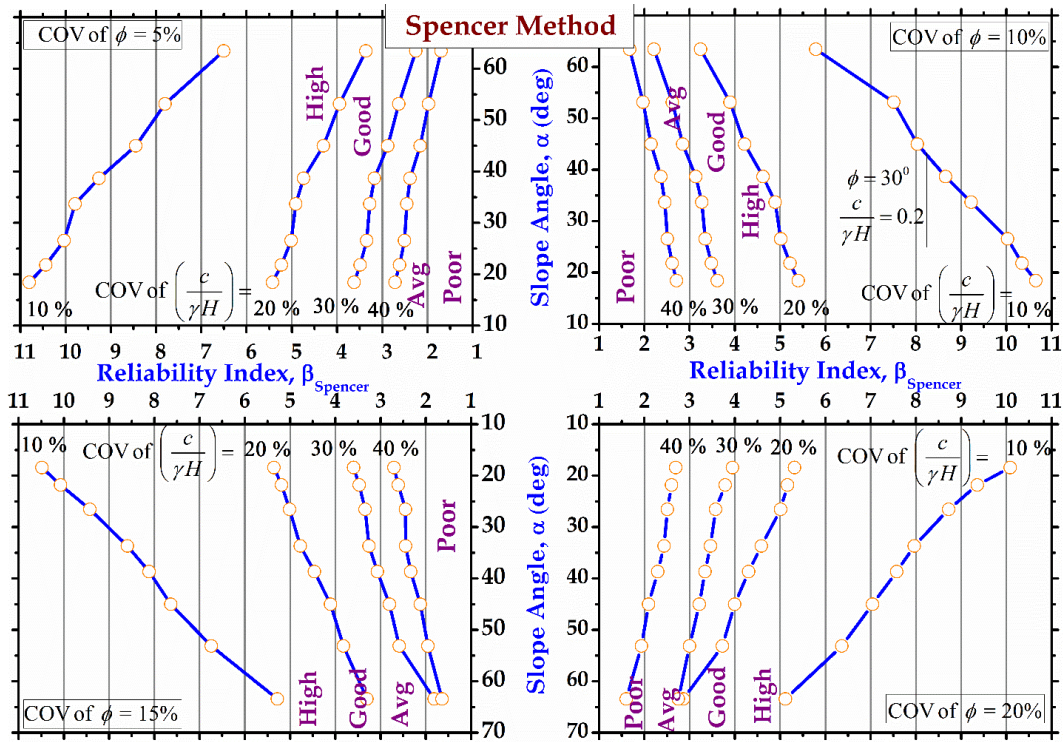


Figure 4.87: Design charts for $c/\gamma H = 0.2$ and $\phi = 30^\circ$ for Spencer Method

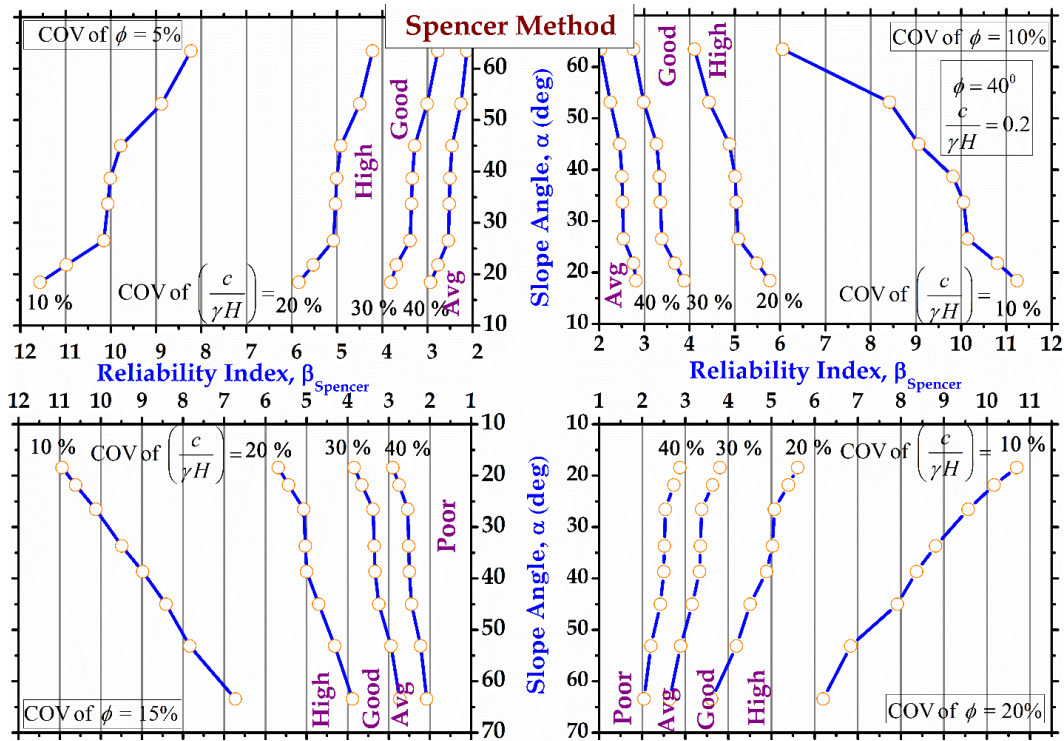


Figure 4.88: Design charts for $c/\gamma H = 0.2$ and $\phi = 40^\circ$ for Spencer Method

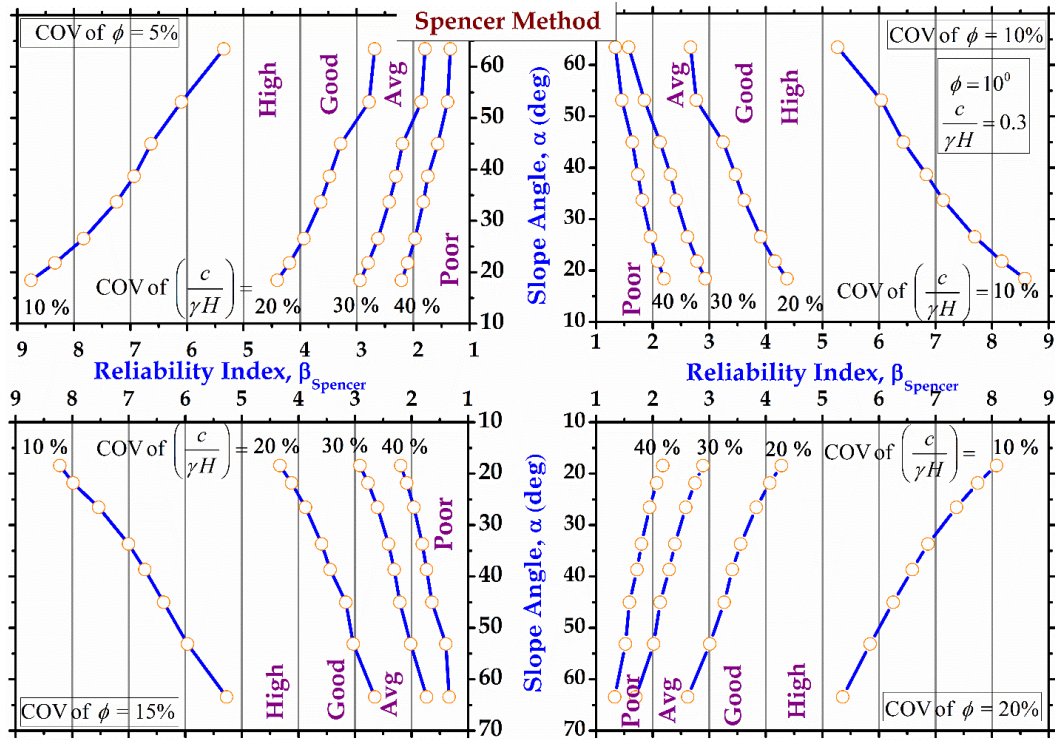


Figure 4.89: Design charts for $c/\gamma H = 0.3$ and $\phi = 10^\circ$ for Spencer Method

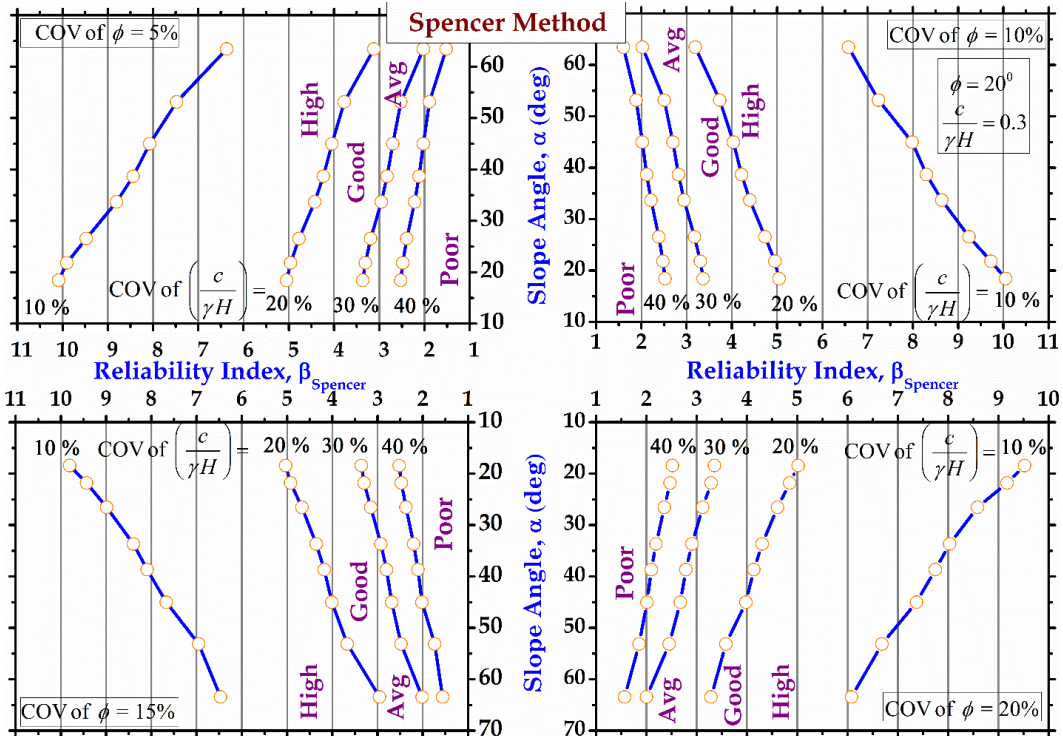


Figure 4.90: Design charts for $c/\gamma H = 0.3$ and $\phi = 20^\circ$ for Spencer Method

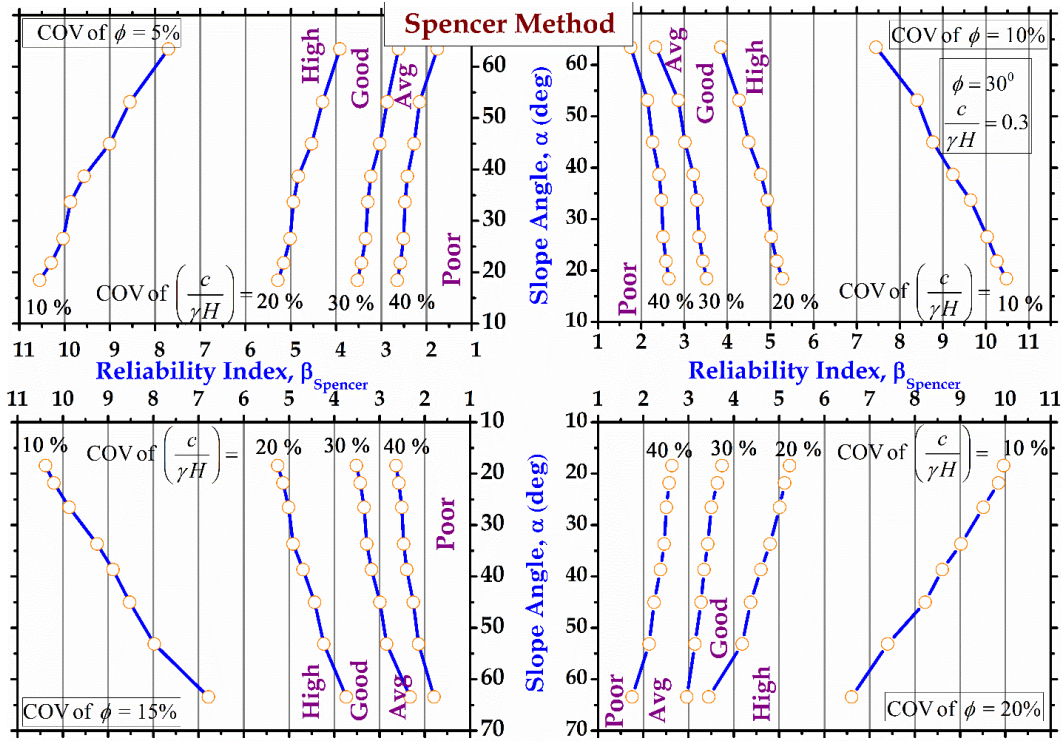


Figure 4.91: Design charts for $c/\gamma H = 0.3$ and $\phi = 30^\circ$ for Spencer Method

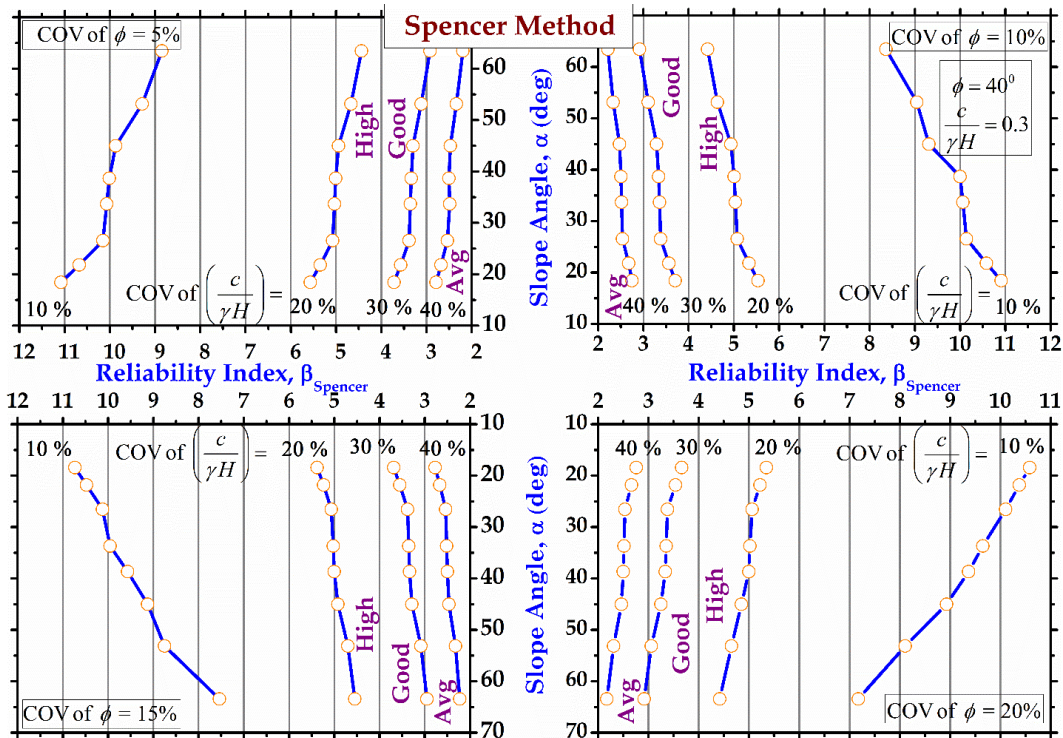


Figure 4.92: Design charts for $c/\gamma H = 0.3$ and $\phi = 40^\circ$ for Spencer Method

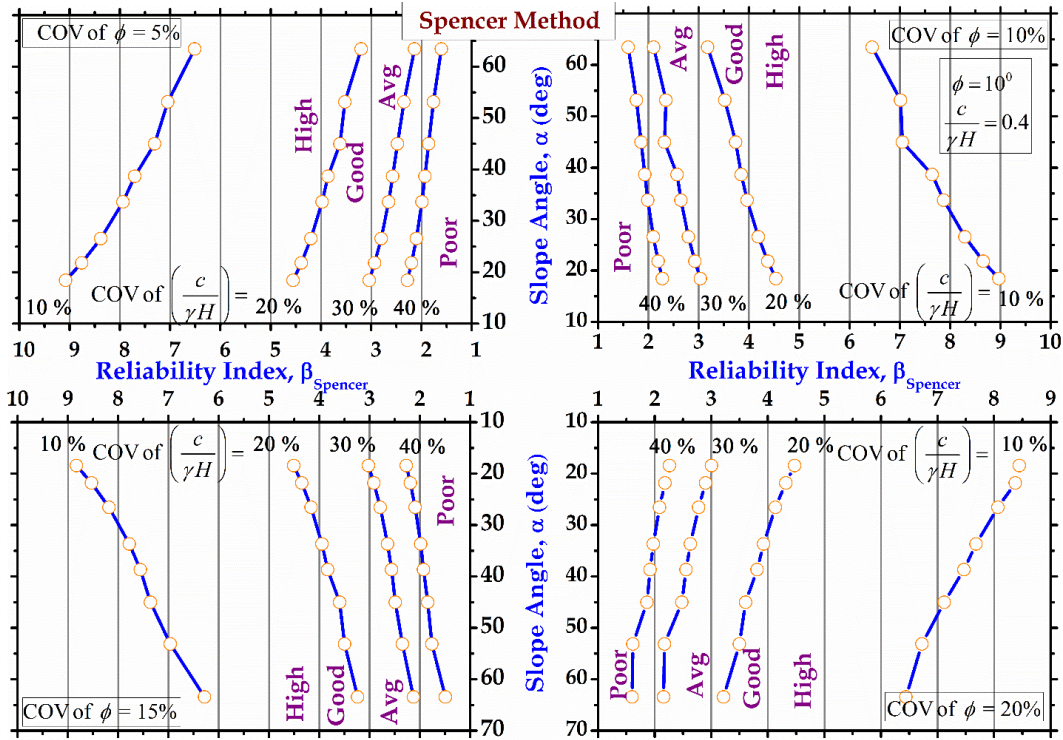


Figure 4.93: Design charts for $c/\gamma H=0.4$ and $\phi=10^\circ$ for Spencer Method

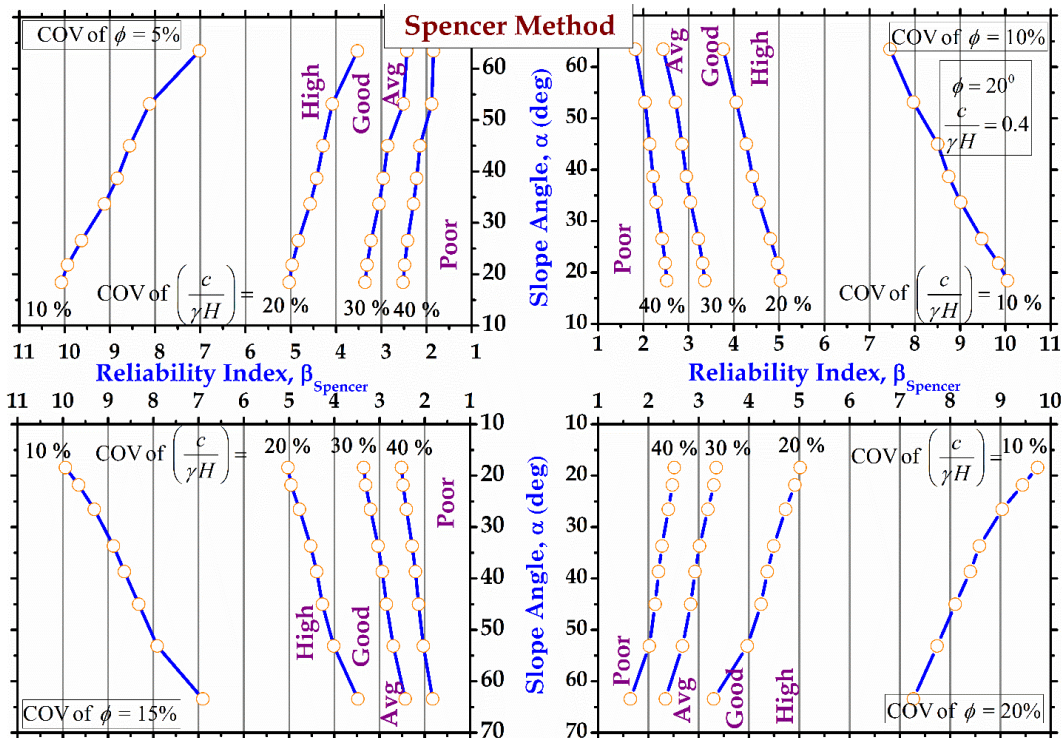


Figure 4.94: Design charts for $c/\gamma H=0.4$ and $\phi=20^\circ$ for Spencer Method

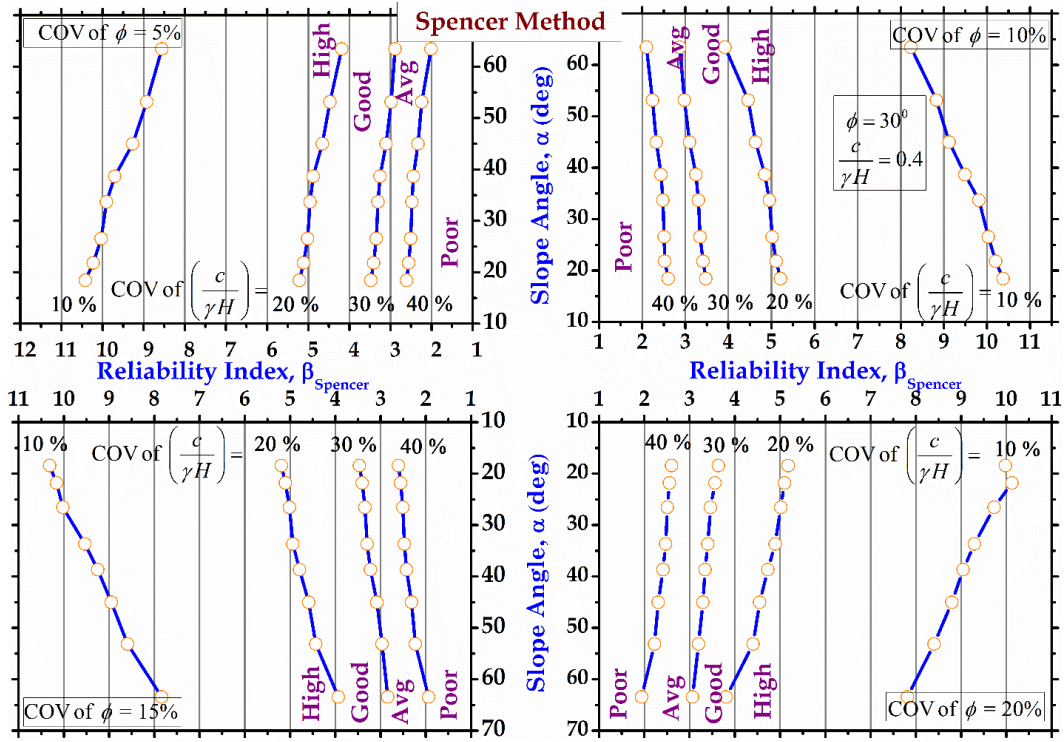


Figure 4.95: Design charts for $c/\gamma H = 0.4$ and $\phi = 30^\circ$ for Spencer Method

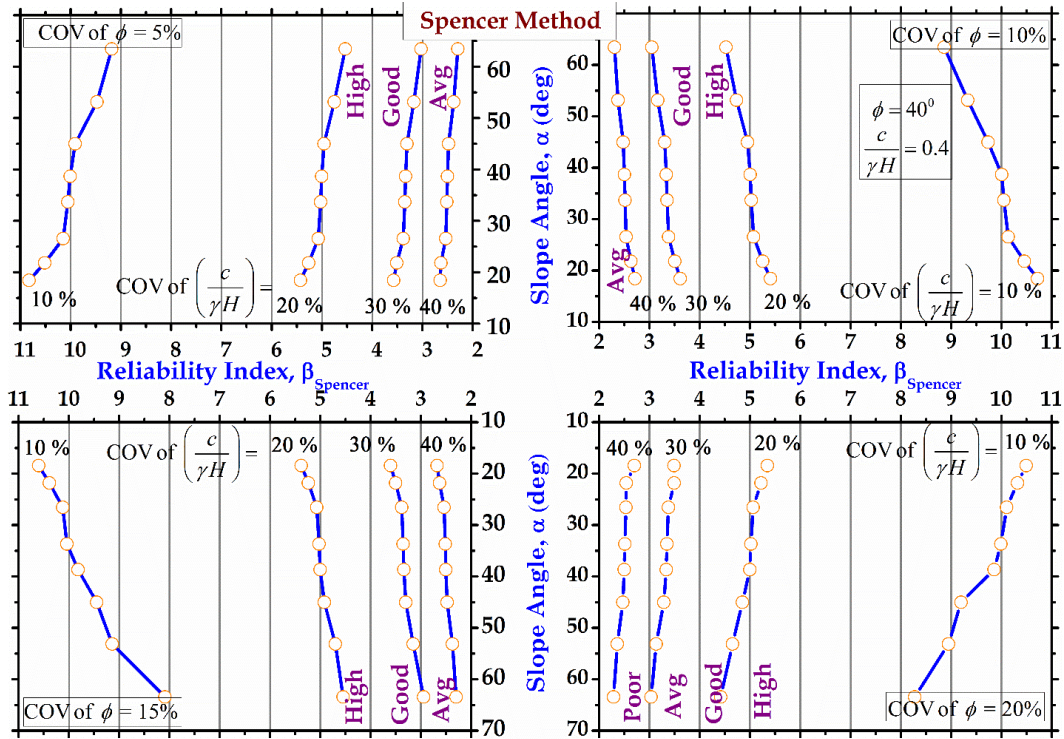


Figure 4.96: Design charts for $c/\gamma H = 0.4$ and $\phi = 40^\circ$ for Spencer Method

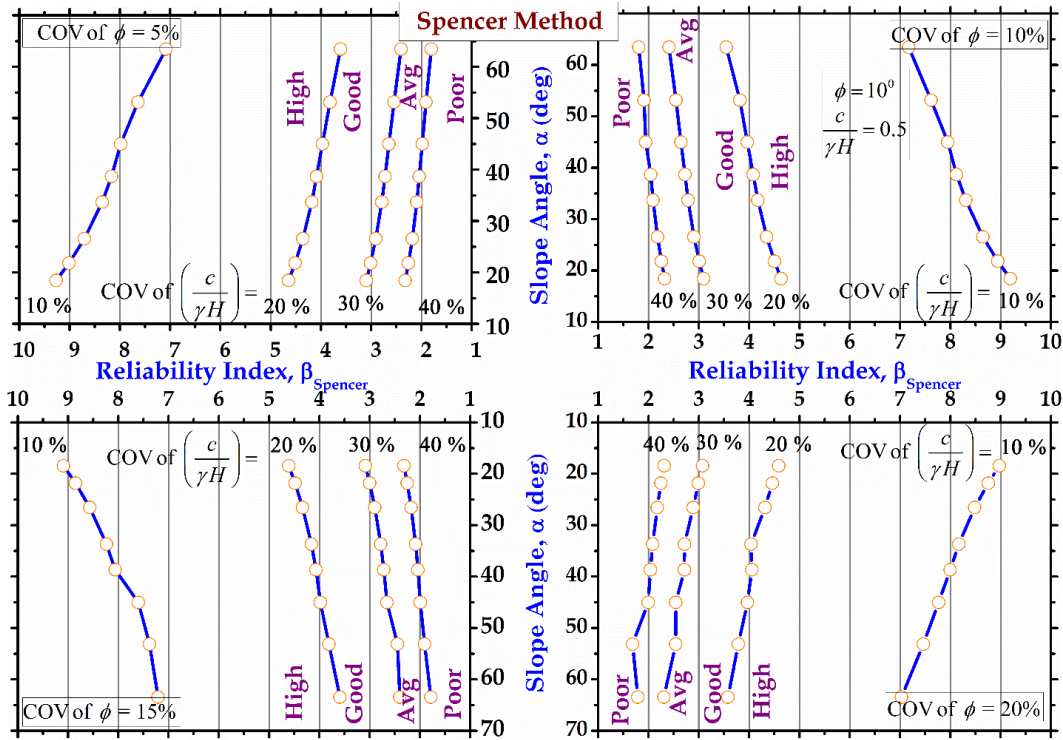


Figure 4.97: Design charts for $c/\gamma H=0.5$ and $\phi=10^\circ$ for Spencer Method

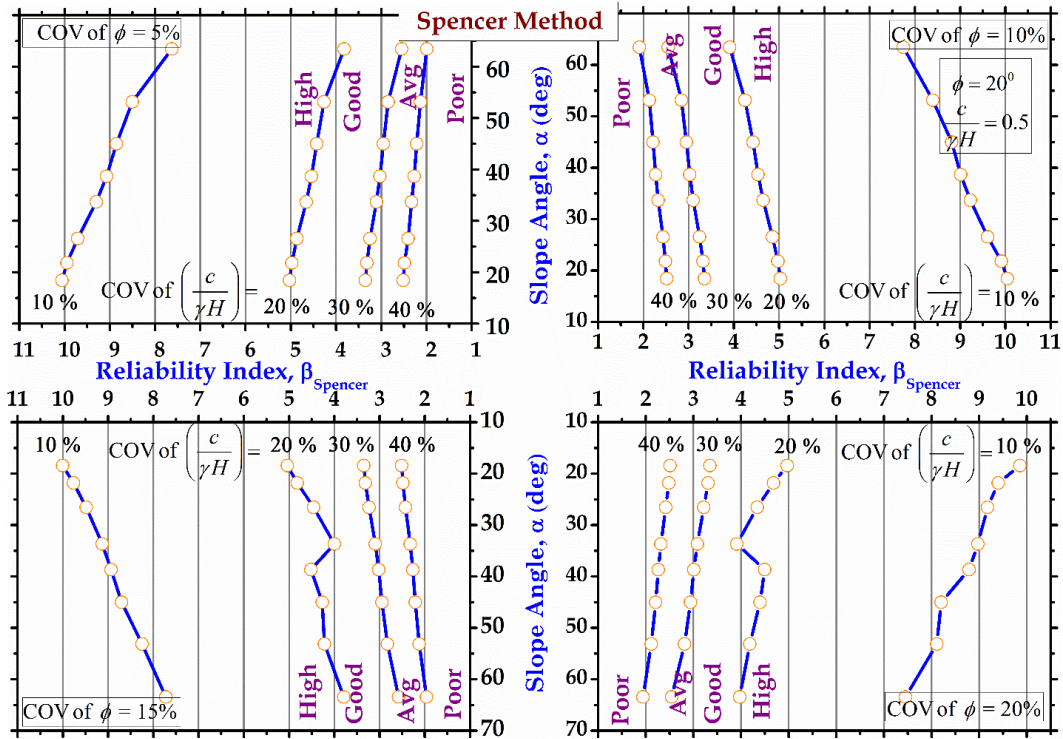


Figure 4.98: Design charts for $c/\gamma H=0.5$ and $\phi=20^\circ$ for Spencer Method

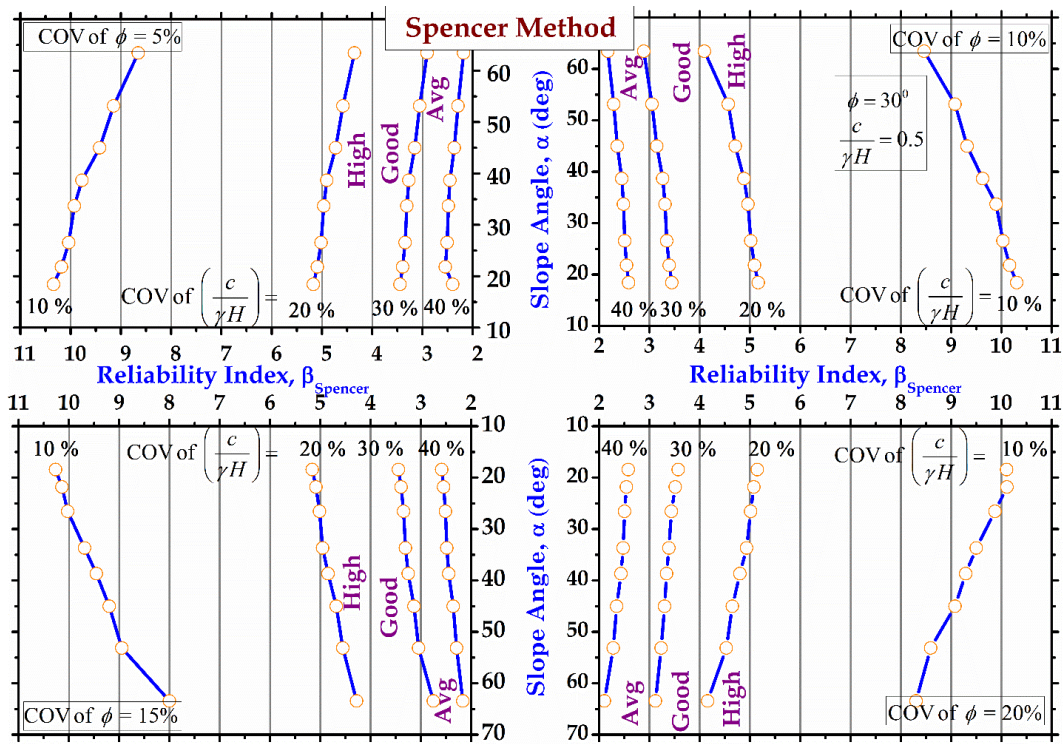


Figure 4.99: Design charts for $c/\gamma H = 0.5$ and $\phi = 30^\circ$ for Spencer Method

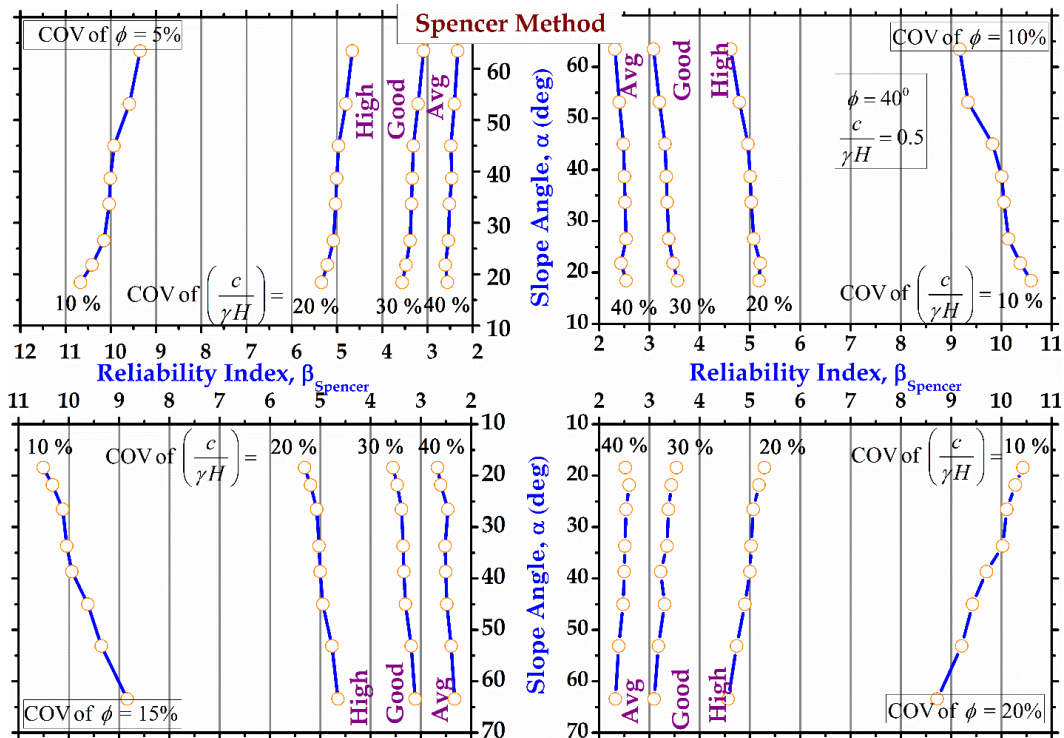


Figure 4.100: Design charts for $c/\gamma H = 0.5$ and $\phi = 40^\circ$ for Spencer Method

4.7 Design Charts for Morgenstern-Price Method

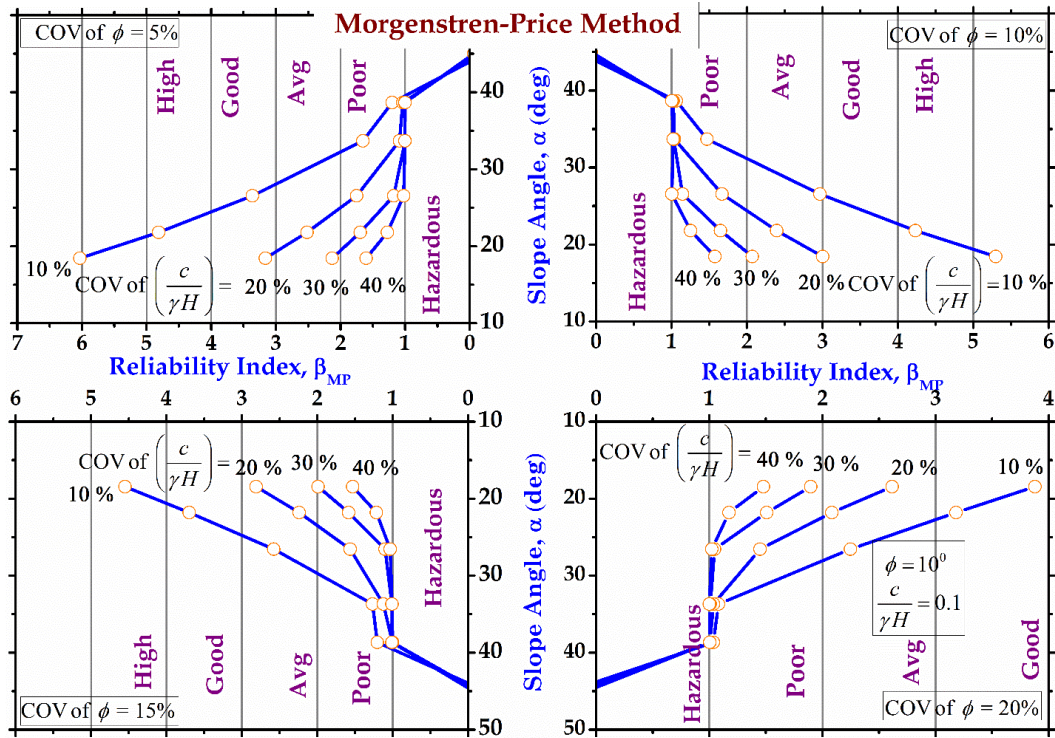


Figure 4.101: Design charts for $c/\gamma H=0.1$ and $\phi=10^\circ$ for Morgenstern-Price Method

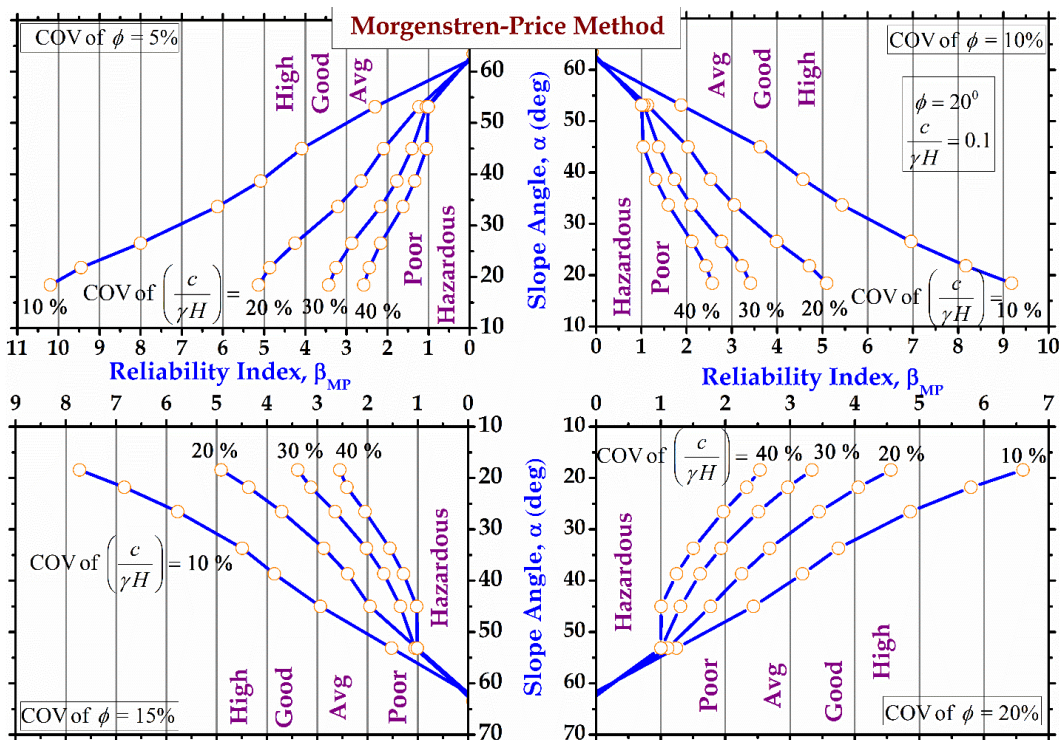


Figure 4.102: Design charts for $c/\gamma H=0.1$ and $\phi=20^\circ$ for Morgenstern-Price Method

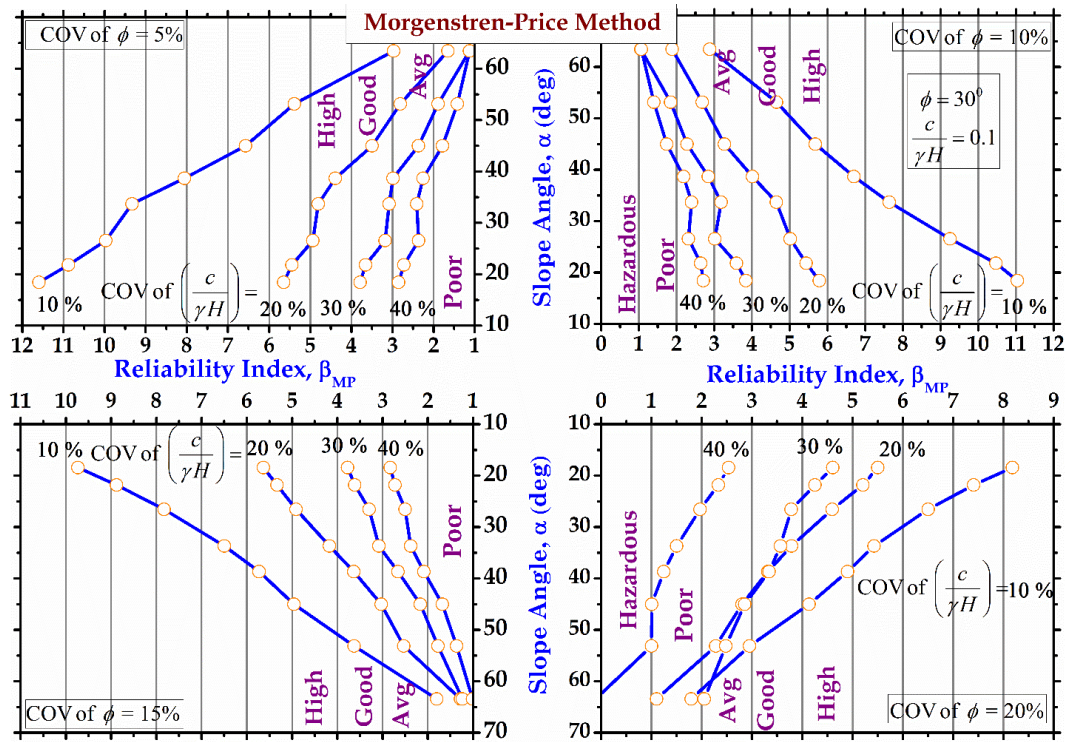


Figure 4.103: Design charts for $c/\gamma H=0.1$ and $\phi=30^\circ$ for Morgenstern-Price Method

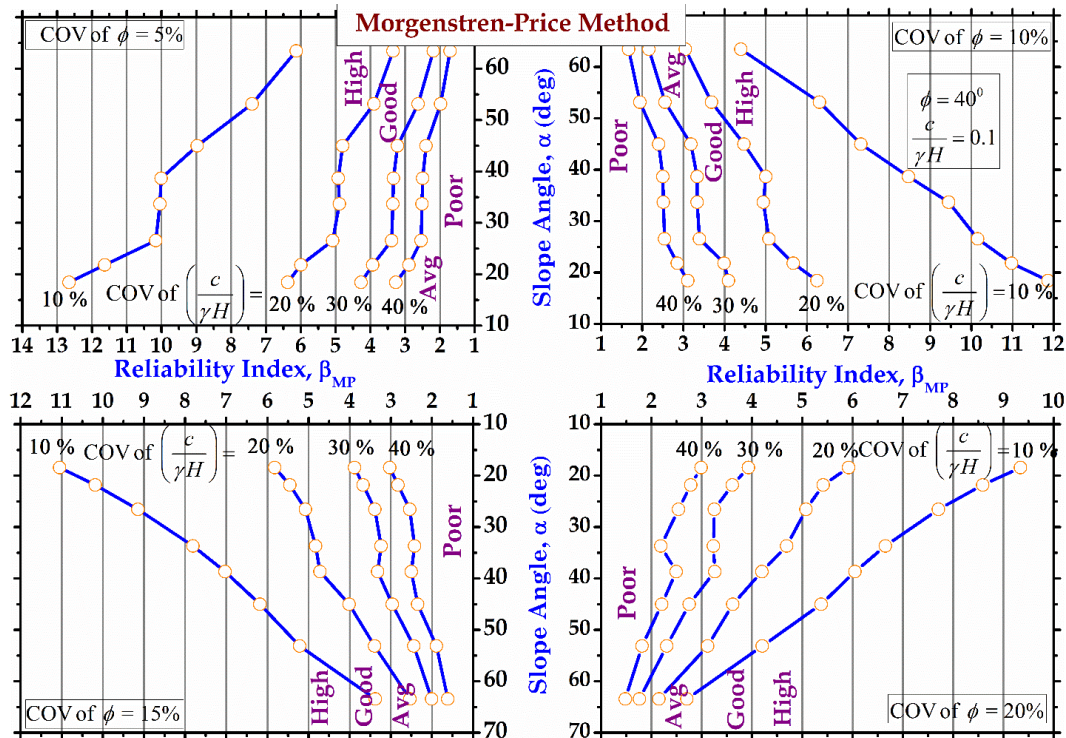


Figure 4.104: Design charts for $c/\gamma H=0.1$ and $\phi=40^\circ$ for Morgenstern-Price Method

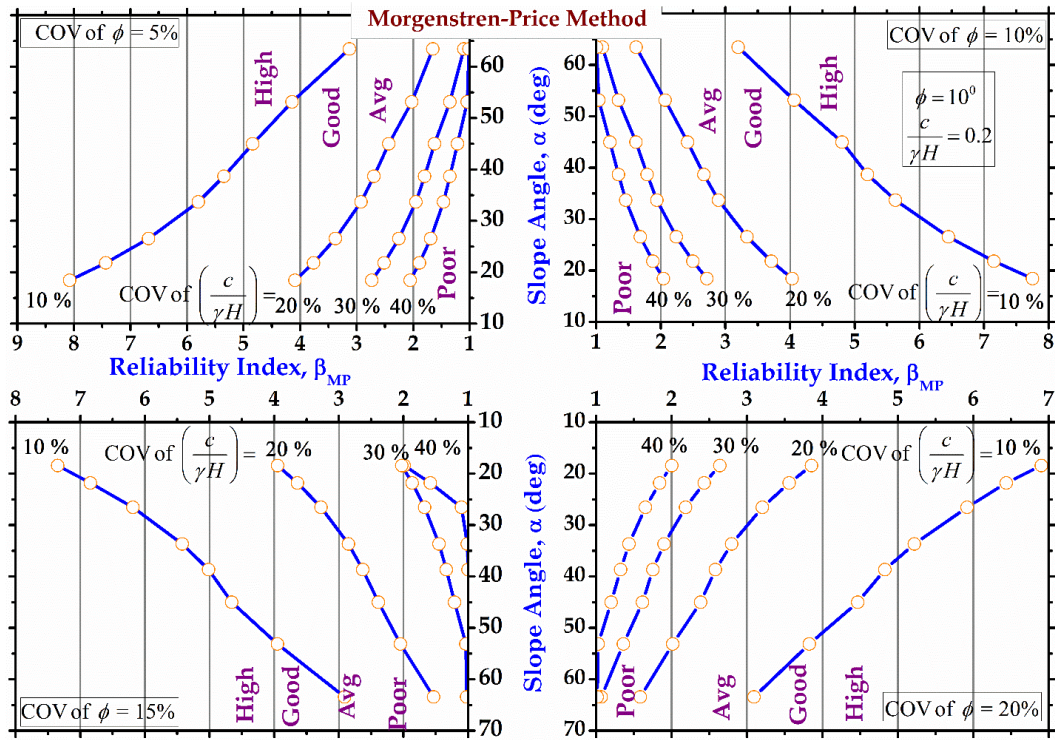


Figure 4.105: Design charts for $c/\gamma H = 0.2$ and $\phi = 10^\circ$ for Morgenstern-Price Method

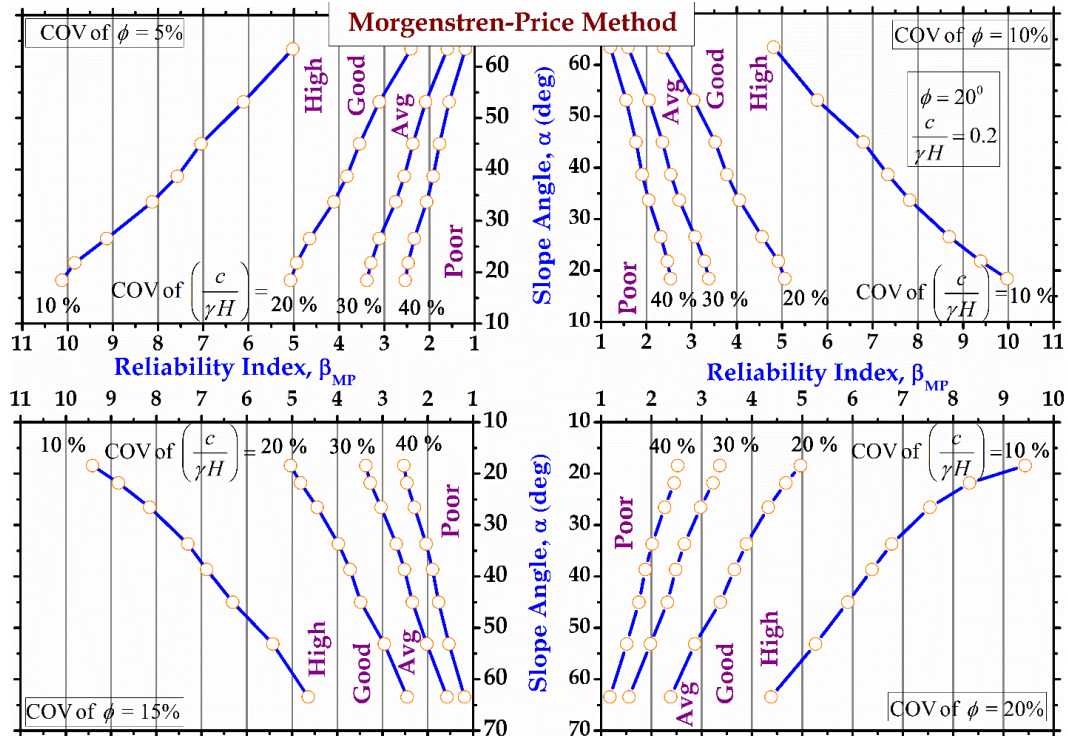


Figure 4.106: Design charts for $c/\gamma H = 0.2$ and $\phi = 20^\circ$ for Morgenstern-Price Method

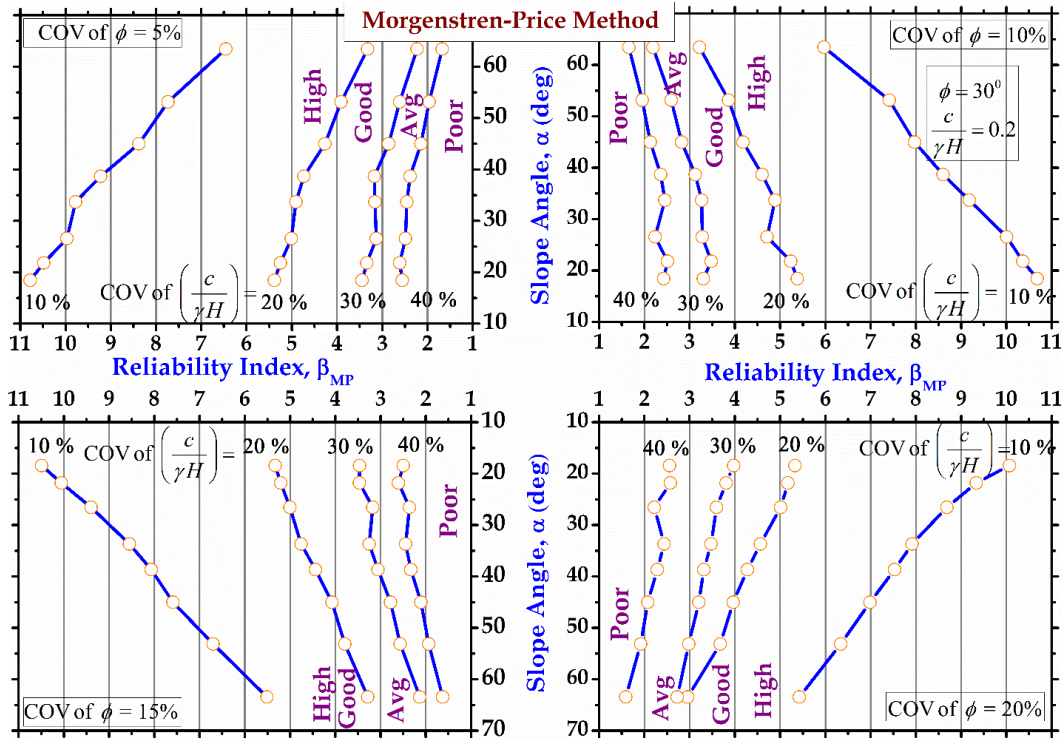


Figure 4.107: Design charts for $c/\gamma H = 0.2$ and $\phi = 30^\circ$ for Morgenstern-Price Method

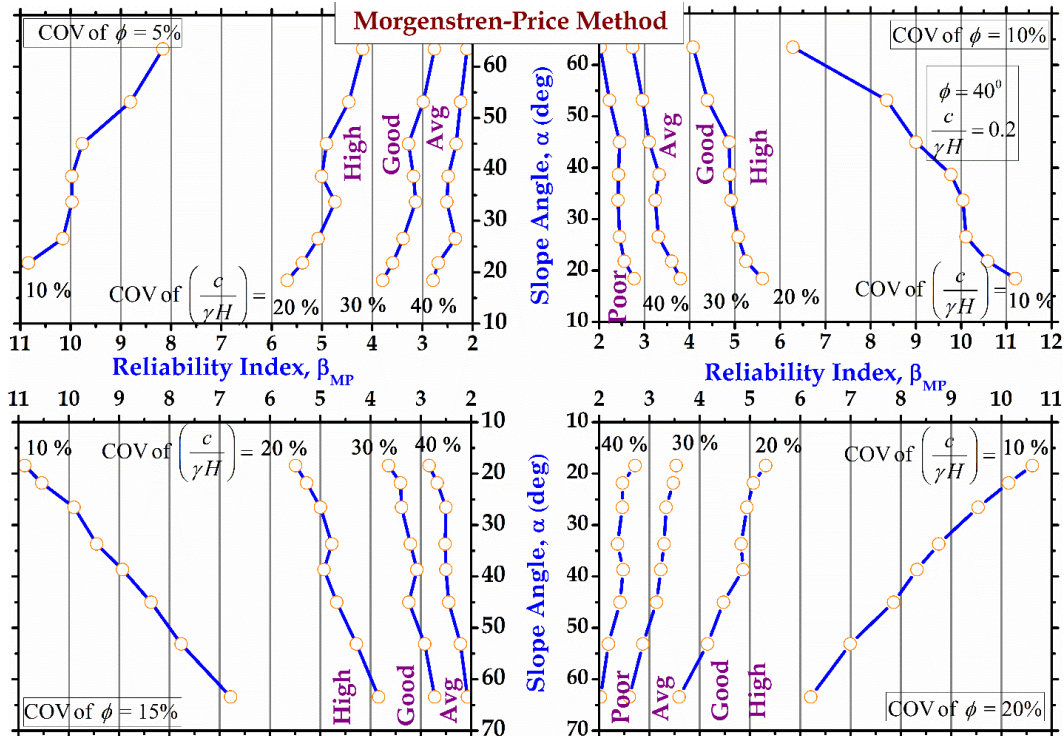


Figure 4.108: Design charts for $c/\gamma H = 0.2$ and $\phi = 40^\circ$ for Morgenstern-Price Method

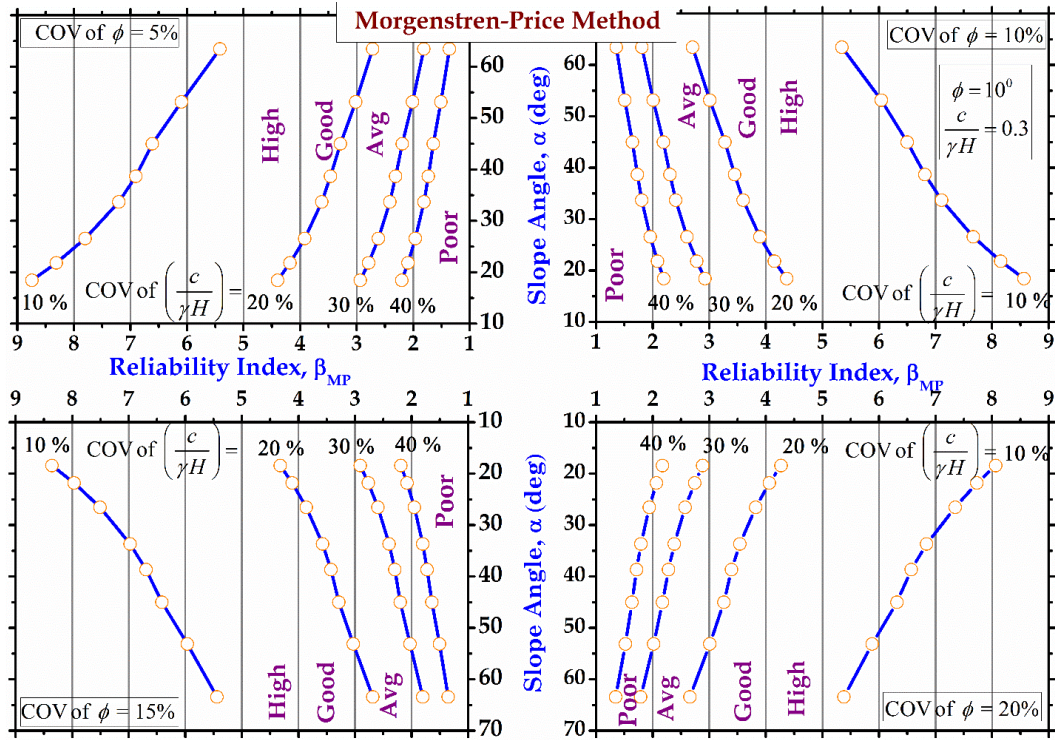


Figure 4.109: Design charts for $c/\gamma H = 0.3$ and $\phi = 10^\circ$ for Morgenstern-Price Method

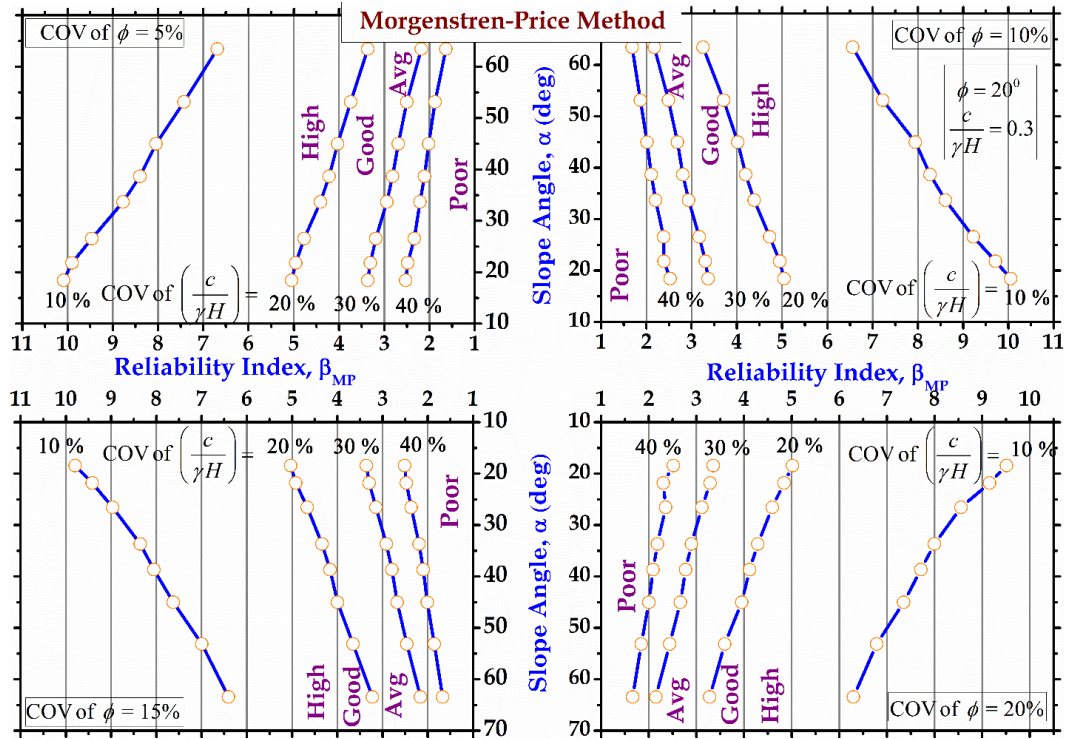


Figure 4.110: Design charts for $c/\gamma H = 0.3$ and $\phi = 20^\circ$ for Morgenstern-Price Method

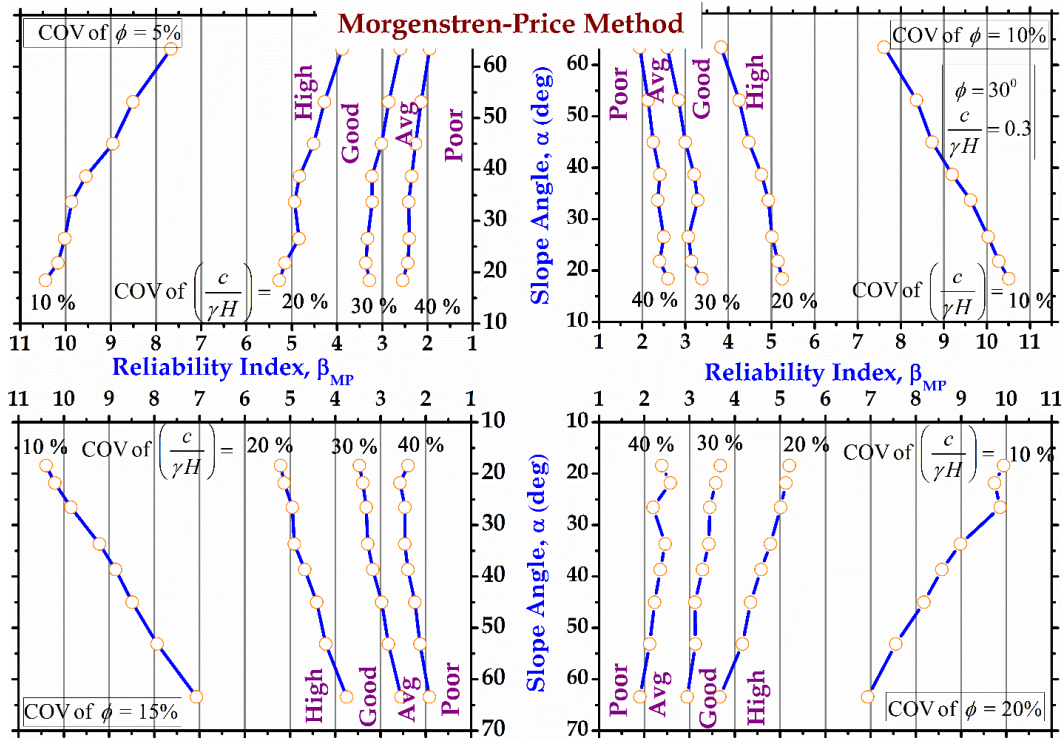


Figure 4.111: Design charts for $c/\gamma H = 0.3$ and $\phi = 30^\circ$ for Morgenstern-Price Method

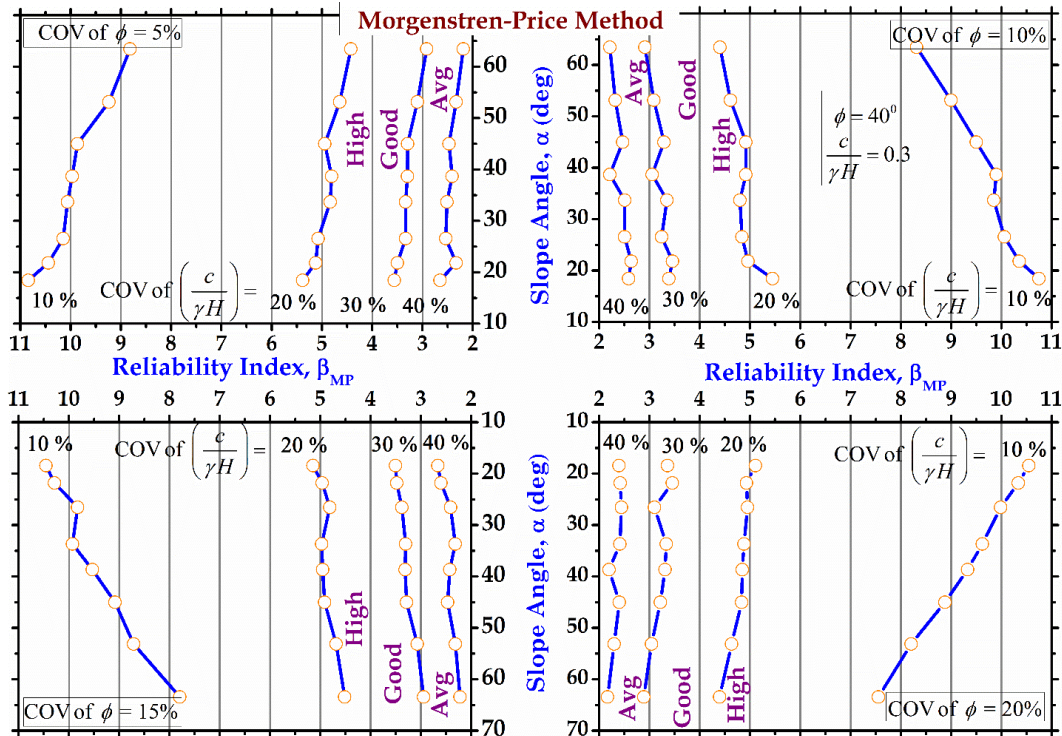


Figure 4.112: Design charts for $c/\gamma H = 0.3$ and $\phi = 40^\circ$ for Morgenstern-Price Method

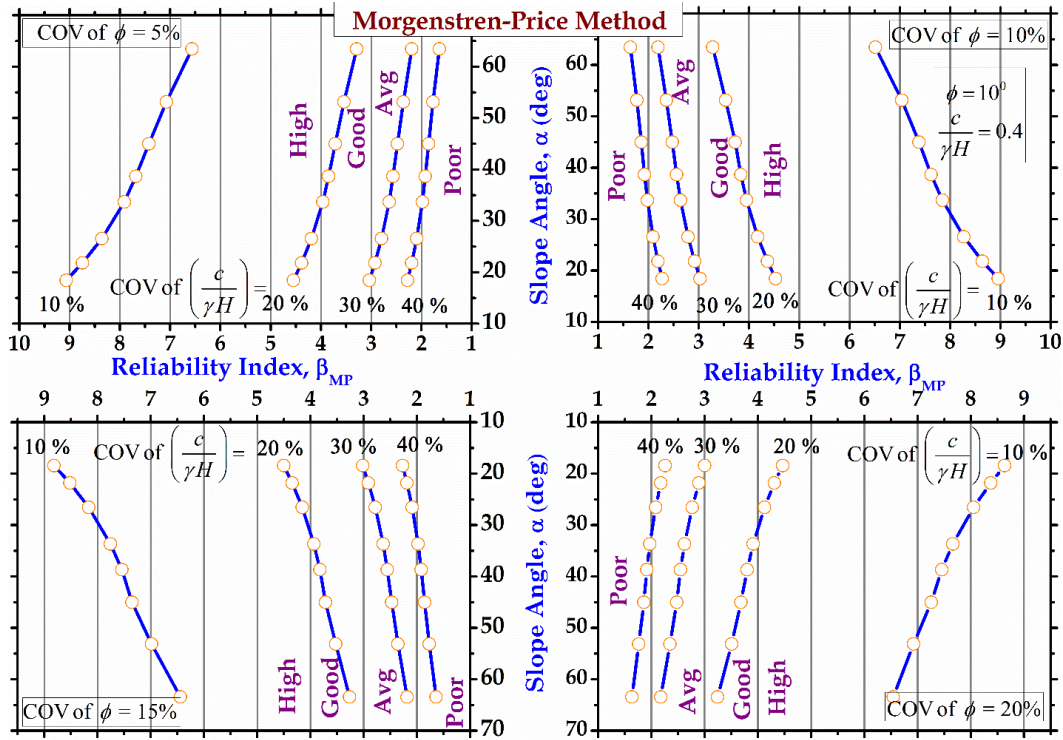


Figure 4.113: Design charts for $c/\gamma H = 0.4$ and $\phi = 10^\circ$ for Morgenstern-Price Method

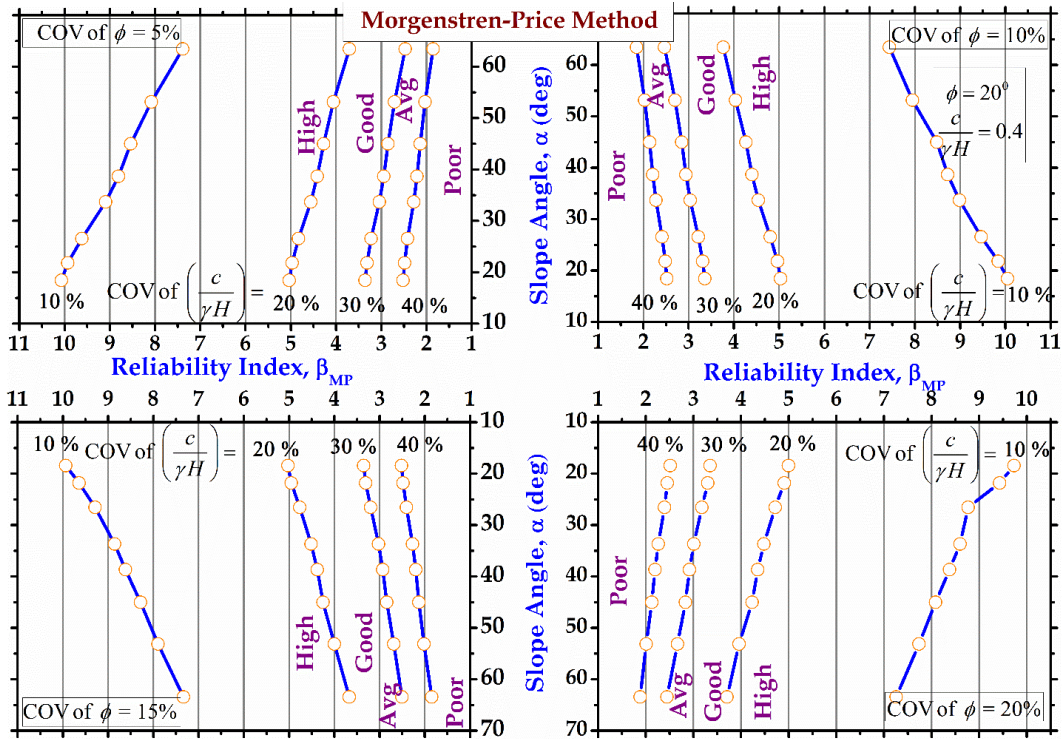


Figure 4.114: Design charts for $c/\gamma H = 0.4$ and $\phi = 20^\circ$ for Morgenstern-Price Method

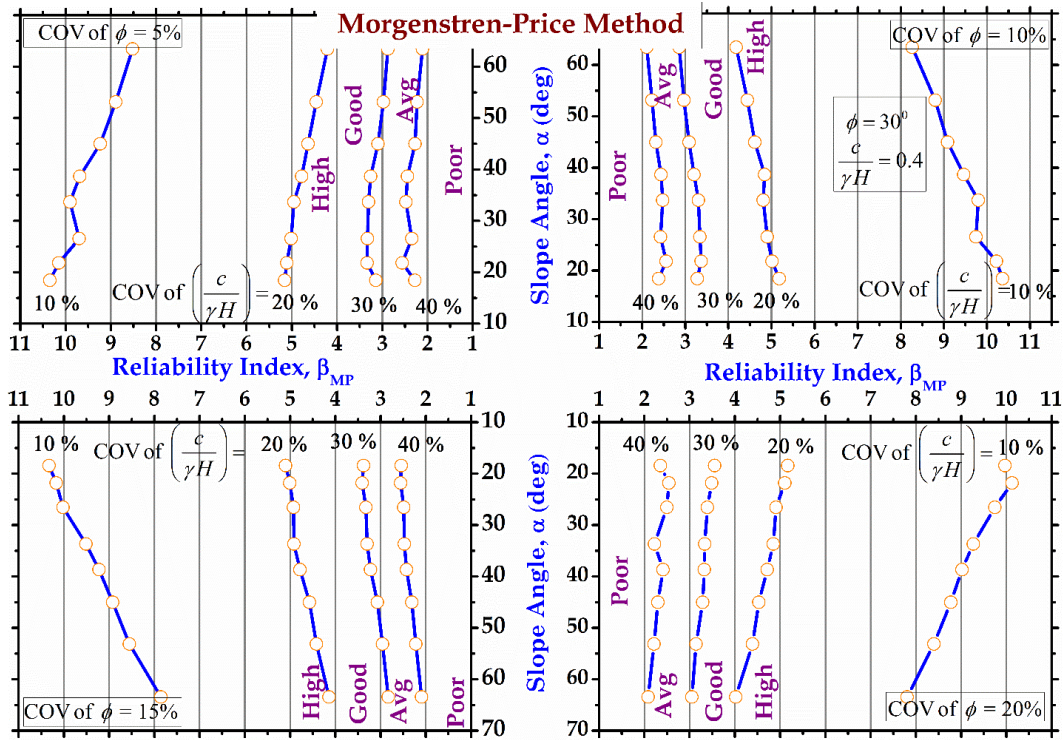


Figure 4.115: Design charts for $c/\gamma H = 0.4$ and $\phi = 20^\circ$ for Morgenstern-Price Method

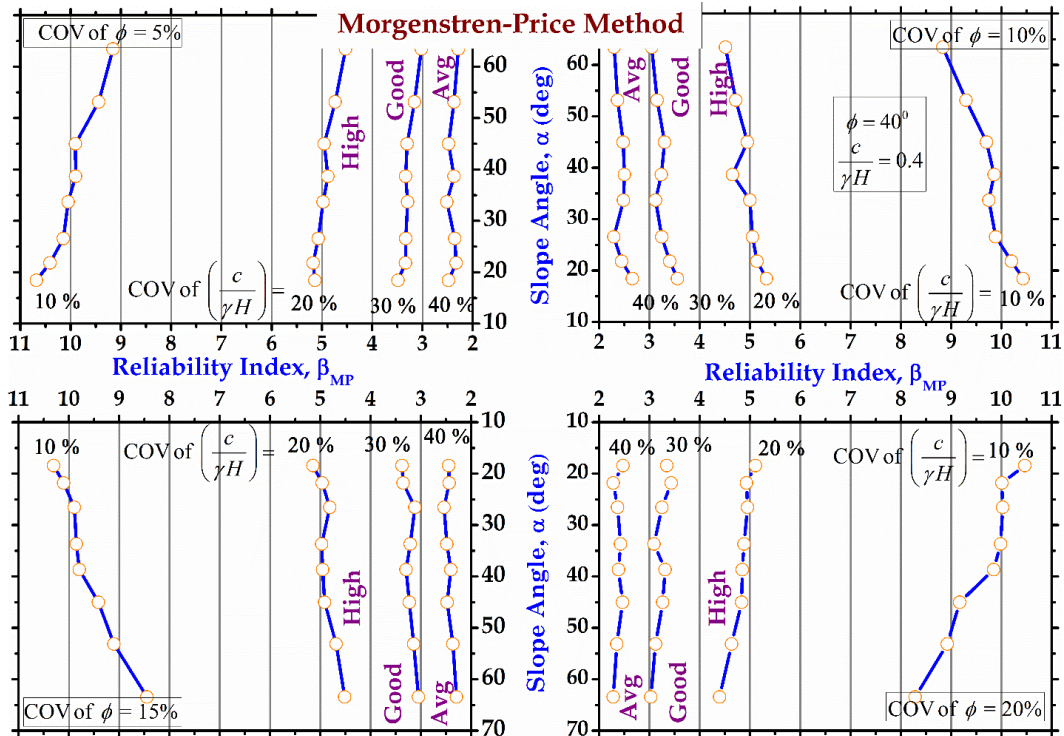


Figure 4.116: Design charts for $c/\gamma H = 0.4$ and $\phi = 40^\circ$ for Morgenstern-Price Method

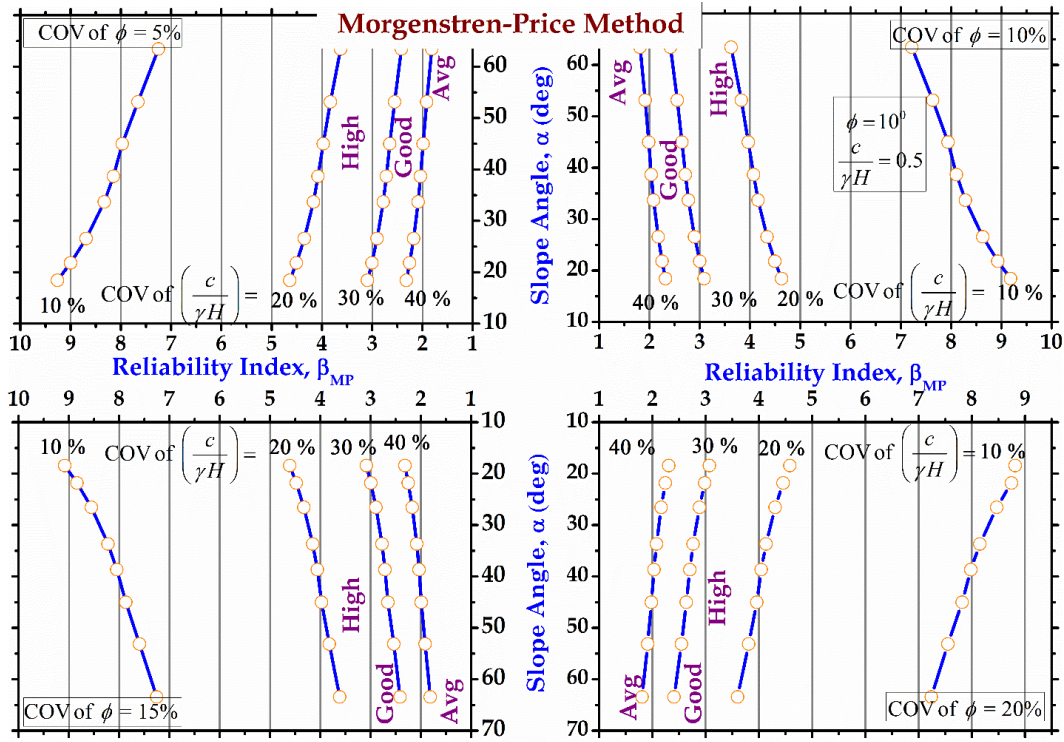


Figure 4.117: Design charts for $c/\gamma H = 0.5$ and $\phi = 10^\circ$ for Morgenstern-Price Method

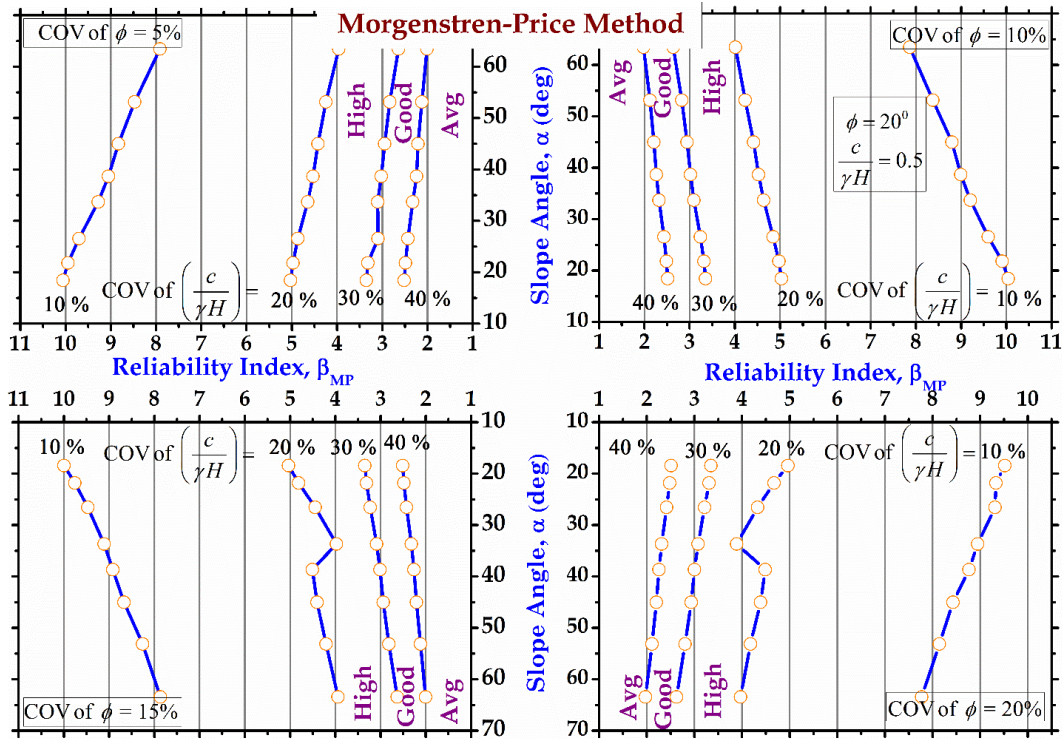


Figure 4.118: Design charts for $c/\gamma H = 0.5$ and $\phi = 10^\circ$ for Morgenstern-Price Method

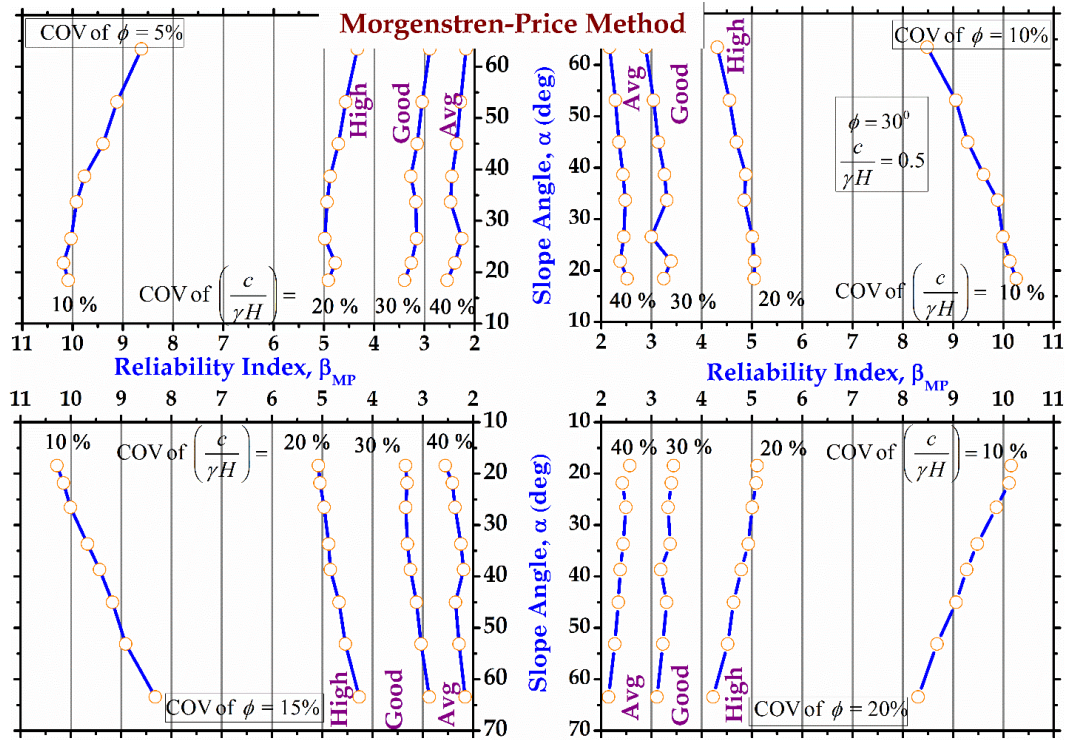


Figure 4.119: Design charts for $c/\gamma H=0.5$ and $\phi=30^\circ$ for Morgenstern-Price Method

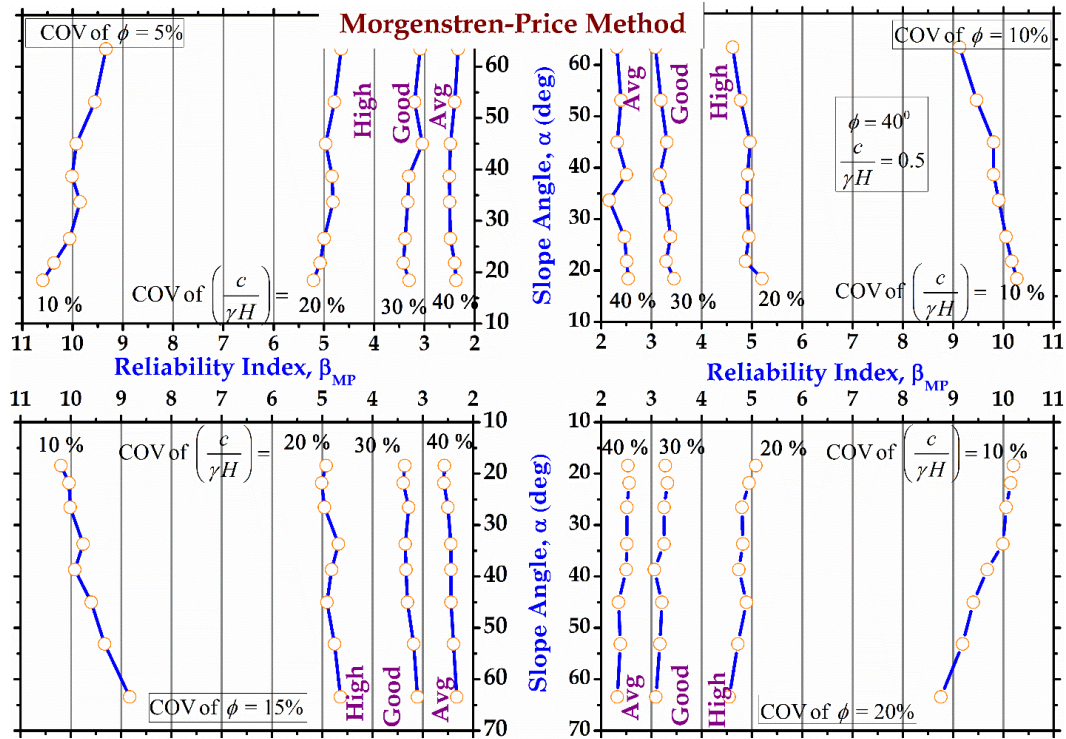


Figure 4.120: Design charts for $c/\gamma H=0.5$ and $\phi=40^\circ$ for Morgenstern-Price Method

4.8 Design Example

Consider an example which has the following parameters

H : The height of the soil mass in m = 5

α : angle of slope with horizontal in degrees = 26.56

c : the value of cohesion of the fill in kPa = 9.8

ϕ : angle of internal cohesion in degrees = 10

γ : unit weight of the fill in kN/m³ = 17.64

COV($c/\gamma H$) : Co-efficient of Variation of $c/\gamma H$ = 10%

COV(ϕ) : Co-efficient of Variation of ϕ = 10%

This example gives a $c/\gamma H$ of 0.11.

As the charts provided are for the values of which gives $c/\gamma H$ equal to 0.1 and 0.2, the value for 0.11 is obtained by recognizing the corresponding values for $\phi = 10^\circ$, COV($c/\gamma H$) = 10% and COV(ϕ) = 10% from these two charts and then interpolating them to the value of $c/\gamma H = 0.11$.

The values of Reliability Indices obtained are

$$\beta_{OMS} = 2.888 \quad \beta_{Bishop} = 3.38 \quad \beta_{Spencer} = 3.381 \quad \beta_{MP} = 3.314$$

The value of the reliability for the ordinary method of slices is the least while the one's from the β from the other methods are in the least comparable.

Morgenstern – Price method value can be taken to be most accurate parameter to depict the reliability of the slope as it takes into account the sinusoidal interslice forces.

It can be observed that the slope has an above average performance with the current variability as all the reliability indices are more than 3.0 except for ordinary method of slices.

Chapter 5

Pore Water Pressure and Layered Soil Slopes

5.1 Pore Water Pressure

The presence of water table has significant effect on the stability of slopes due to the presence of seepage force through the structure, which affects the behavior of the slope. Also effective shear stress parameters must be used in the calculation of factor of safety in the presence of water table.

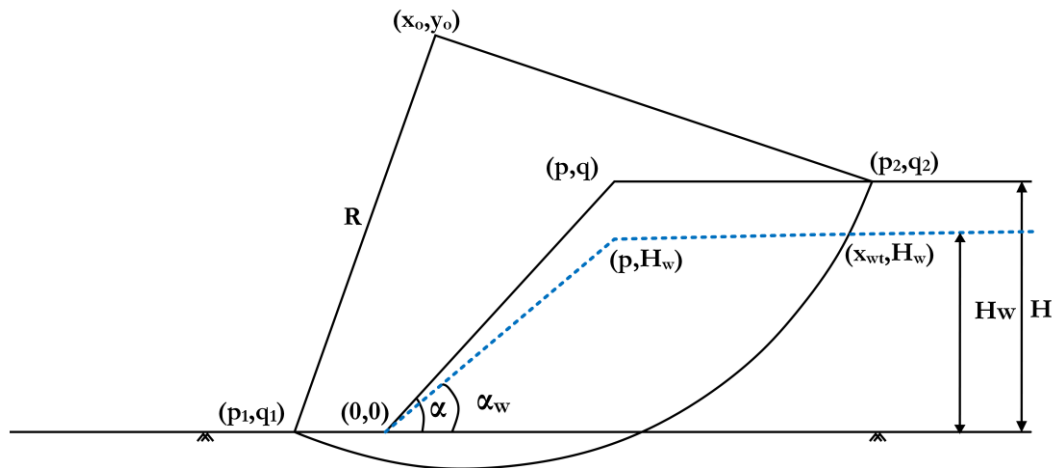


Figure 5.1: The geometry and parameters used for factor of safety using pore water pressure calculations

Equations of factor of safety with steady seepage

The various factor of safety equations used previously do not take into account the presence of water table. An attempt has been made to integrate pore water pressure in the present study.

The various equations for factor of safety are now to be modified in order to accommodate the seepage forces coming on the slope and hence into the calculation of the slice information.

The average pore water pressure, u_i , at the base of each slice can be defined as

$$u_i = \gamma_w h_{wi} \quad (5.1)$$

where h_{wi} = height of the water table at the base of the i^{th} slice

The total force caused by the pore water pressure at the bottom of the i^{th} slice is equal to

$$U_i = u_i dl_i \quad (5.2)$$

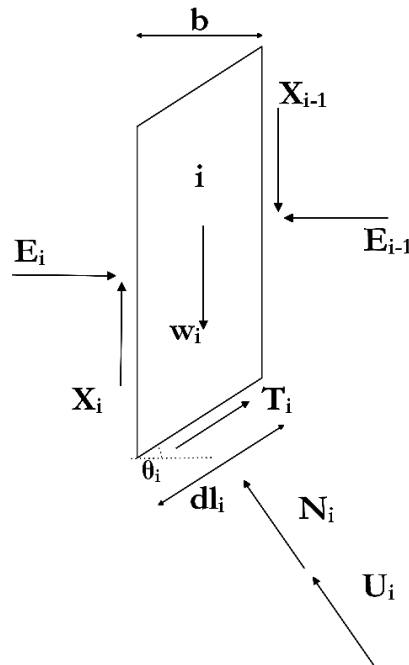


Figure 5.2: The forces acting on a slice in presence of water table

The equations of the factors of safety take on the following forms

$$FS_{OMS} = \frac{\sum (cdl_i + (W_i \cos \theta_i - udl_i \cos^2 \theta_i) \tan \phi)}{\sum W_i \sin \theta_i} \quad (5.3)$$

$$FS_{Bishop} = \frac{\sum \left[\frac{cdl_i + (W_i - udl_i \cos \theta_i) \tan \phi}{m} \right]}{\sum W_i \sin \theta_i} \quad (5.4)$$

$$F_m = \frac{M_r}{M_d} = \frac{\sum_{i=1}^n (cdl_i + N'_i \tan \phi) R}{\sum_{i=1}^n w_i h_{off_i}} \quad (5.5)$$

$$F_f = \frac{F_r}{F_d} = \frac{\sum_{i=1}^n T_{i,lim}}{\sum_{i=1}^n T_i} = \frac{\sum_{i=1}^n (cdl_i + N'_i \tan \phi) \times \cos \theta_i}{\sum_{i=1}^n (N'_i + U_i) \sin \theta_i} \quad (5.6)$$

where

$$N'_i = \frac{w_i + X_i - X_{i-1} - U_i \cos \theta_i - \frac{cdl_i \sin \theta_i}{F}}{\cos \theta_i + \frac{\tan \phi \sin \theta_i}{F}}$$

$$E_i = E_{i-1} - (N'_i + U_i) \sin \theta_i + T_i \cos \theta_i$$

Formulation in MATLAB

The calculation of the width of the slices is lightly different from before in the sense that the areas between the slices are divided based on the x-coordinate of the slices.

The value x_{wt} which is the x-coordinate of the point at which the slip surface meets the water table, is calculated by substituting the y-coordinate as water table height H_w in the circle equation given by eq. 3.19.

Then, the areas between the entry p_2 and x_{wt} , x_{wt} and p , p and 0 and 0 and exit p_1 are all divided separately into a n_1, n_2, n_3, n_4, n_5 number of slices such that we get different widths for slices in different areas. The total number of slices is taken as 30. These widths are then fed into program as before.

The parameter to be measured and calculated in addition to the ones obtained previously is the average height of the water table for each slice hw_i , which is calculated as follows.

The midpoints of the base of the slices (mbx_i, mby_i) (Fig.5.3) are calculated as

$$mbx_i = \frac{x_{i+1} + x_i}{2} \quad (5.7)$$

$$mby_i = \frac{y_{i+1} + y_i}{2} \quad (5.8)$$

Now, as we proceed from left to right along the slices, depending on the position of the slice in relation to the water table, hw changes as follows. If

$$p_2 > x_{i+1} > x_{wt} \Rightarrow hw_i = 0 \quad (5.9)$$

$$x_{wt} > x_{i+1} > p \Rightarrow hw_i = Hw - mby_i \quad (5.10)$$

$$p > x_{i+1} > 0 \Rightarrow hw_i = (mbx_i \tan \alpha_w) - mby_i \quad (5.11)$$

$$0 > x_{i+1} > p_1 \Rightarrow hw_i = 0 - mby_i \quad (5.12)$$

If the slip circle exits after the toe i.e. the exit point lies on the slope, the n_6 part and their corresponding parameters are all taken as equal to 0 and the above calculations are made and their corresponding values are assigned.

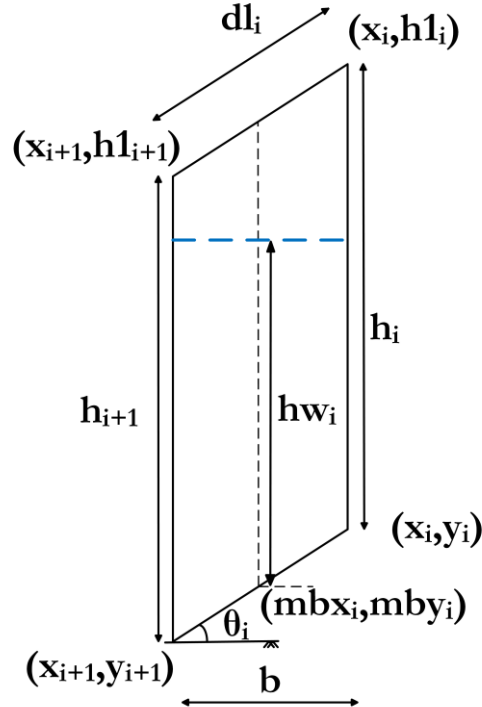


Figure 5.3: The calculation of the water head for a slice

Thus, once the hw_i 's (Fig.5.3) are calculated, the pore water pressure component can be calculated corresponding and the factor of safety values are obtained.

The changes to include water table calculations were made only for the Ordinary Method of Slices and the Bishops Simplified Method.

The comparison of the values for an example with slope properties taken from Malkawi et al., (2008) [93] and calculated in GeoStudio is shown in Table 5.1. It is seen that there is no significant difference between the values stated in literature and those calculated from the present study.

Table 5.1. The comparison of the values obtained from GeoStudio to those calculated by the present study for the presence of water table

H (m)	α (°)	Hw (m)	α_w(°)	c (kPa)	ϕ(°)	γ (kN/ m³)	FSOMS		FS_{Bishop}		β_{OMS}	β_{Bishop}
							Malkawi (2008)	Present Study	Malkawi (2008)	Present Study		
50	26.6	40	21.8	30	30	18	1.71	1.76	1.81	1.82	9.58	10.23

5.2 Layered Soil Slope

Naturally occurring slope might be homogenous or layered in terms of the formation of the slope. Stratified deposits are very common in nature especially with a weak layer perched in between strong layers.

Man-made slopes, especially in landfills and certain types of earthen embankments can also be considered as layered soil slopes. Hence it is essential to analyze the performance of such slopes in order to have a well-rounded study.

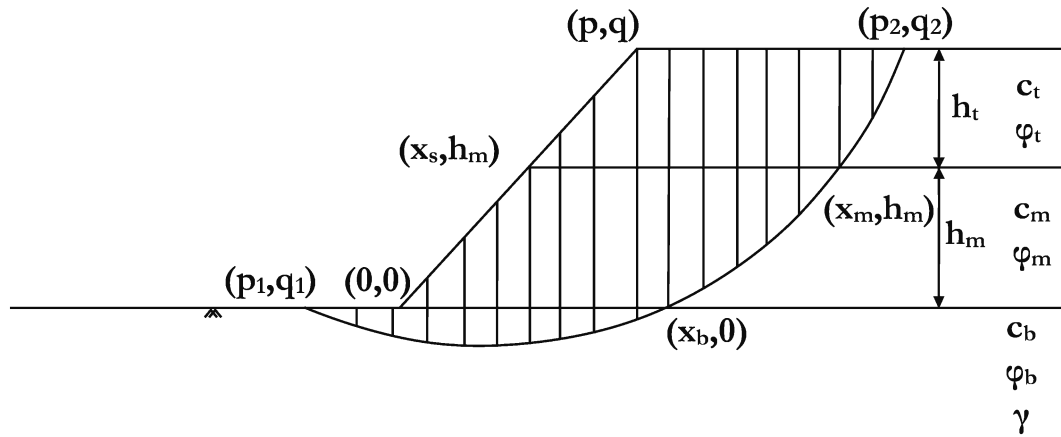


Figure 5.4: Three Layered soil slope showing the parameters used in determination of factor of safety

For the purpose of this study, a slope having three layers is taken into consideration. The supporting base of the slope is assumed to have properties c_b , ϕ_b . A second layer above that, having properties c_m , ϕ_m and a height of h_m , makes up the lower part of the slope. The top layer of the slope has its properties as c_t , ϕ_t and of h_t in height. The entire slope is will have a uniform density of γ .

Calculation of factor of safety for layered soils

For multilayered slopes, the difference is in the way the weights of the slices are calculated. For example, a given slice in slip surface, depending on its position in the slope may contain all the three soils, only top two layers of the slope or just the top layer of the slope. Thus the values of c and ϕ taken into consideration for the calculation of its weight depend on the position of the slice.

In order to avoid having slices which fall in between two layers, the slice widths are decided in a way that all the slices start or end exactly at the junction of two layers. Hence determination of the points of intersection of the slip circle with these layer boundaries is to be done.

The x-coordinates, x_m and x_b , of the points of intersection can be calculated by substituting the layer heights as the y-coordinates in the slip circle equation (eq. 3.19.) i.e., h_m and 0 respectively.

The point x_s is the x-coordinate of the point where the middle layer meets the slope which can be calculated by using the slope equation (eq. 3.18) and substituting the value of $y = h_m$ in it.

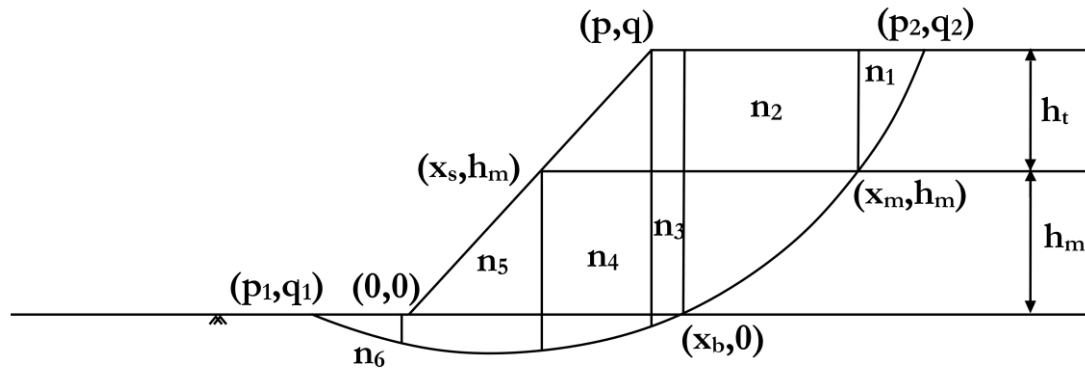


Figure 5.5: Three Layered soil slope showing the division of the slices to determine corresponding c and ϕ

Once these are determined, then the areas between p_2 and x_m , x_m and x_b , x_b and x_s , x_s and p , p and 0 and 0 and p_1 are divided into n_1 , n_2 , n_3 , n_4 , n_5 , n_6 number of slices separately. The total number of slices is taken as 30. This results in different widths for the slices in different areas. These widths are then fed into program as before.

It is important to judge which value of c and ϕ go into the calculation of a particular slice 'i', which again depends on the position of the slice.

Say the area between p_2 and x_m is divided into n_1 number of slices, then all these n_1 slices lie only in the top layer of the soil, hence the corresponding shear strengths parameters for these slices would be c_t and ϕ_t . This is done as follows

$$p_2 < x_{i+1} < x_m \Rightarrow c_i = c_t \text{ and } \phi_i = \phi_t \quad (5.13)$$

$$x_m < x_{i+1} < x_b \Rightarrow c_i = c_m \text{ and } \phi_i = \phi_m \quad (5.14)$$

If $x_b > p$ then

$$p < x_{i+1} < p_1 \Rightarrow c_i = c_b \text{ and } \phi_i = \phi_b \quad (5.15)$$

else

$$p < x_{i+1} < p_1 \Rightarrow c_i = c_b \text{ and } \phi_i = \phi_b \quad (5.16)$$

If the slip circle exits after the toe i.e. the exit point lies on the slope, the n_5 and n_6 parts and their corresponding parameters are all taken as equal to 0 and the above calculations are made and their corresponding values are assigned.

Thus, we can then feed the corresponding c and ϕ of each slice into the previous formulation in order to obtain the factors of safety.

The factor of safety equations can be written as

$$F_f = \frac{\sum_{i=1}^n T_{i,\text{lim}}}{\sum_{i=1}^n T_i} = \frac{\sum_{i=1}^n \left(\frac{c_i}{\gamma H} dl_i + N_i \tan \phi_i \right) \cos \theta_i}{\sum_{i=1}^n N_i \sin \theta_i} \quad (5.17)$$

$$F_m = \frac{\sum_{i=1}^n \left(\frac{c_i}{\gamma H} dl_i + N_i \tan \phi_i \right)}{\sum_{i=1}^n w_i h_{\text{off}_i}} \quad (5.18)$$

In case of layered soil slope, the present formulation has been developed to calculate the only the factors of safety. This formulation can be used to further expansion to reliability calculations as shown previously for homogeneous slopes.

The comparison of the values for a random example generated in GeoStudio and those obtained from the present study is shown in Table 5.2.

Table 5.2. The comparison of the values obtained from GeoStudio to those calculated by the present study for three layered soil slope

c_t (kPa)	ϕ_t (°)	h_t (m)	c_m (kPa)	ϕ_m (°)	h_m (m)	c_b (kPa)	ϕ_b (°)	γ (kN/m ³)	FS _{OMS}		FS _{Bishop}		FS _{Spencer}		FS _{Mp}	
									Geostudio	Present Study	Geostudio	Present Study	Geostudio	Present Study	Geostudio	Present Study
15	20	5	17	21	4.15	35	28	19	1.76	1.73	1.84	1.85	1.84	1.85	1.84	1.83

It is seen that there is no significant difference between the values generated by GeoStudio and those calculated from the present study.

References

- [1] Peck, R. B. (1969). A man of judgment, 2nd R. P. Davis, Lecture on the Practice of Engineering, West Virginia University Bulletin.
- [2] Basha, B. M., and G. L. S. Babu. "Target reliability-based optimisation for internal seismic stability of reinforced soil structures." *Géotechnique* 62.1 (2011): 55-68.
- [3] Madsen, H. O., S. Krenk, and N. C. Lind. "Methods of structural reliability." (1986).
- [4] Bishop, A. W., The Use of Slip Circles in Stability Analysis of Slopes. *Geotechnique*, 1955: Vol. 5.
- [5] Janbu, N. "Stability analysis of Slopes with Dimensionless Parameters." Thesis for the Doctor of Science in the Field of Civil Engineering, Harvard University Soil Mechanics Series, No. 46, 1954a.
- [6] Lowe, John, and Leslie Karafiath. "Stability of earth dams upon drawdown." *Proc. 1st Pan-Am Conf. On Soil Mech. And Founf. Engrg.*, Mexico City, 2, 537. Vol. 552. 1960.
- [7] Spencer, E. "A method of analysis of the stability of embankments assuming parallel inter-slice forces." *Geotechnique* 17.1 (1967): 11-26.
- [8] Morgenstern, N. R. and Price, V. E., The Analysis of the Stability of General Slip Surfaces. *Geotechnique*, 1965: Vol. 15, No. 1 pp. 77-93.
- [9] Zhu, N.L., 2003. Way to determine stable slope angle of furrow pits considering size effects of rock mass. *Journal of Wuhan University of Technology*, 25(4):38-40 (in Chinese)
- [10] Fredlund, D. G., & Krahn, J. "Comparison of slope stability methods of analysis." *Canadian Geotechnical Journal*, 14.3, 1977: 429-439.
- [11] Phoon, Kok-Kwang, and Fred H. Kulhawy. "Characterization of geotechnical variability." *Canadian Geotechnical Journal* 36.4 (1999): 612-624.
- [12] Lumb, Peter. "The variability of natural soils." *Canadian Geotechnical Journal* 3.2 (1966): 74-97.

- [13] Tan, C.P. Donald, I.B. and Melchers, R.E. (1993). Probabilistic Slope Stability Analysis - State-of-the-Art, Proceedings of the Conference on Probabilistic Methods in Geotechnical Engineering, Canberra, Australia. pp. 89-110.
- [14] Lambe, T. William, and Robert V. Whitman. "Soil Mechanics, SI Version, J." (1979): 553.
- [15] Lumb, P. "Application of statistics in soil mechanics." Soil Mechanics New Horizons. IK Lee, ed (1974).
- [16] Höeg, Kaare, and Ramesh P. Murarka. "Probabilistic analysis and design of a retaining wall." Journal of the Geotechnical Engineering Division 100.3 (1974): 349-366.
- [17] Singh, A. (1971). "How reliable is the factor of safety in foundation engineering?" First International Conference on Applications of Statistics and Probability in Soil and Structural Engineering, Hong Kong, Hong Kong University Press: 389–424.
- [18] Schultze, E. "Some aspects concerning the application of statistics and probability to foundation structures." Proceeding of the 2nd International Conference on the Applications of Statistics and Probability in Soil and Structure Engineering, Aachen, Germany. 1975.
- [19] Ingles, O. G. and Noble, C. S. (1975). "The evaluation of base course materials." Soil Mechanics-Recent Developments. Valliappan, S., Hain, S. J. and Lee, I. K. Sydney, Unisearch Ltd.: 399–410.
- [20] Minty, E. J., Smith, R. B. and Pratt, D. N. (1979). "Interlaboratory testing variability assessed for a wide range of NSW soil types." Third International Conference on Applications of Statistics and Probability in Soil and Structural Engineering, Sydney: 221–235.
- [21] Corotis, R. B., Azzouz, A. S. and Krizek, R. (1975). "Statistical evaluation of soil index properties and constrained modulus." Second International Conference on Applications of Statistics and Probability in Soil and Structural Engineering, Aachen: 273–294.
- [22] Stamatopoulos, A. C. and Kotzias, P. C. (1975). "The relative value of increasing number of observations." Second International Conference on

Applications of Statistics and Probability in Soil and Structural Engineering, Aachen. 495–510.

- [23] Sherwood, P. T. (1970). "An examination of the reproducibility of soil classification and compaction tests." Symposium on Quality Control of Road Works, Centre d'Etudes Techniques de l'Equipement
- [24] Otte, E. (1978). "A Structural Design Procedure for Cement Treated Layers in Pavements." DSc (Eng), Civil Engineering, University of Pretoria.
- [25] Morse, R. K. (1971). "The importance of proper soil units for statistical analysis." First International Conference on Applications of Statistics and Probability in Soil and Structural Engineering, Hong Kong, Hong Kong University Press: 347–355.
- [26] Seed, H. B. and Peacock, W. H. (1971). "Test procedure for measuring soil liquefaction characteristics." Journal of the Soil Mechanics and Foundations Division, ASCE 97(SM8): 1099–1119.
- [27] Harr, M. E. (1984). "Reliability-based design in civil engineering." 1984 Henry M. Shaw Lecture, Dept. of Civil Engineering, North Carolina State University, Raleigh, N.C.
- [28] Phoon, Kok-Kwang, and Fred H. Kulhawy. "Evaluation of geotechnical property variability." Canadian Geotechnical Journal 36.4 (1999): 625-639.
- [29] Lacasse, S., and F. Nadim. "Model uncertainty in pile axial capacity calculations." Offshore Technology Conference. Offshore Technology Conference, 1996.
- [30] Wolff, T. F. (1996). "Probabilistic slope stability in theory and practice." Uncertainty in the Geologic Environment, Madison, WI, ASCE: 419–433.
- [31] Lacasse, Suzanne, and Farrokh Nadim. "Uncertainties in characterising soil properties." Publikasjon-Norges Geotekniske Institutt 201 (1997): 49-75.
- [32] Chakraborty, S., and S. S. Dey. "A stochastic finite element dynamic analysis of structures with uncertain parameters." International Journal of Mechanical Sciences 40.11 (1998): 1071-1087.
- [33] Lutes, Loren D., Shahram Sarkani, and Shuang Jin. "Response variability of an SSI system with uncertain structural and soil properties." Engineering Structures 22.6 (2000): 605-620.

- [34] Popescu, R., Prevost, J. H., and Deodatis, G. (1998). "Spatial variability of soil properties: two case studies," Proceedings, Geotechnical Earthquake Engineering and Soil Dynamics III, Seattle, Washington, pp. 568-579.
- [35] Duncan, J. Michael. "Factors of safety and reliability in geotechnical engineering." *Journal of geotechnical and geoenvironmental engineering* 126.4 (2000): 307-316.
- [36] Larsson, Stefan, Håkan Stille, and Lars Olsson. "On horizontal variability in lime-cement columns in deep mixing." *Geotechnique* 55.1 (2005): 33-44.
- [37] Ditlevsen, O. (1997). "Structural reliability codes for probabilistic design – a debate paper based on elementary reliability and decision analysis concepts." *Structural Safety*, 19(3): 253–270.
- [38] Tang, Wilson H. "Uncertainties in offshore axial pile capacity." *Foundation Engineering@ sCurrent Principles and Practices*. ASCE, 1989.
- [39] Der Kiureghian, A. and De Stefano, M. (1991). "Efficient algorithm for second-order reliability analysis." *Journal of Engineering Mechanics*, ASCE 117(12): 2904–2923.
- [40] O, Eze E., Adeyemi G. O, and Fasanmade P. A. "Variability in Some Geotechnical Properties of Three Lateritic Sub-Base Soils Along Ibadan Oyo Road." *IOSR Journal of Applied Geology and Geophysics IOSRJAGG* 2.5 (2014): 76-81. Web.
- [41] Fellenius, W. "Calculations of the Stability of Earth Dams." In *Proceedings of the Second Congress of Large Dams*. Washington D. C, 1936: Vol. 4, pp. 445-63.
- [42] Janbu, N., L. Bjerrum, and B. Kjaernsli. "Soil mechanics applied to some engineering problems." *Norwegian Geotechnical Institute. Publication 16* (1956).
- [43] Janbu, Nilmar. *Shear strength and stability of soils*. Norges geotekniske institutt, 1973.
- [44] Fredlund, D. G., Krahn, J., & Pufahl, D. E. "The relationship between limit equilibrium slope stability methods." In *Proceedings of the*

International Conference on Soil Mechanics and Foundation Engineering (1981): 409-416.

- [45] Fredlund, D. G. "Analytical methods for slope stability analysis." Proceedings of the 4th International Symposium on Landslides. s. l.:[sn], 1984: 229-250.
- [46] Yamagami, T., and Y. Ueta. "Search for critical slip lines in finite element stress fields by dynamic programming." Proceedings of the 6th International Conference on Numerical Methods in Geomechanics. Innsbruck. 1988.
- [47] Farias, M. M., and D. J. Naylor. "Safety analysis using finite elements." Computers and Geotechnics 22.2 (1998): 165-181.
- [48] Zou, Jin-Zhang, David J. Williams, and Wen-Lin Xiong. "Search for critical slip surfaces based on finite element method." Canadian Geotechnical Journal 32.2 (1995): 233-246.
- [49] Greco, Venanzio R. "Efficient Monte Carlo technique for locating critical slip surface." Journal of Geotechnical Engineering 122.7 (1996): 517-525.
- [50] Malkawi, AI Husein, Waleed F. Hassan, and Sarada K. Sarma. "An efficient search method for finding the critical circular slip surface using the Monte Carlo technique." Canadian Geotechnical Journal 38.5 (2001): 1081-1089.
- [51] Cheng, Y. M., et al. "Particle swarm optimization algorithm for the location of the critical non-circular failure surface in two-dimensional slope stability analysis." Computers and Geotechnics 34.2 (2007): 92-103.
- [52] Cheng, Y. M., et al. "Determination of the critical slip surface using artificial fish swarms algorithm." Journal of geotechnical and geoenvironmental engineering 134.2 (2008): 244-251.
- [53] van der Meij, R., and J. B. Sellmeijer. "A genetic algorithm for solving slope stability problems: From Bishop to a free slip plane." Numerical Methods in Geotechnical Engineering:(NUMGE 2010) (2000): 345.

- [54] Zhu, D. Y., et al. "A new procedure for computing the factor of safety using the Morgenstern-Price method." *Canadian geotechnical journal* 38.4 (2001): 882-888.
- [55] Zhu, D. Y., et al. "A concise algorithm for computing the factor of safety using the Morgenstern Price method." *Canadian geotechnical journal* 42.1 (2005): 272-278.
- [56] Cheng, Y. M., Z. H. Zhao, and Y. J. Sun. "Evaluation of interslice force function and discussion on convergence in slope stability analysis by the lower bound method." *Journal of geotechnical and geoenvironmental engineering* 136.8 (2010): 1103-1113.
- [57] Christian, John T., Charles C. Ladd, and Gregory B. Baecher. "Reliability applied to slope stability analysis." *Journal of Geotechnical Engineering* 120.12(1994): 2180-2207.
- [58] Tang, W. H., ed., (1995). *Probabilistic Methods in Geotechnical Engineering*. Washington, DC, National Academy Press.
- [59] Wu, Tien H., and Leland M. Kraft. "Safety analysis of slopes." *Journal of the Soil Mechanics and Foundations Division* 96.2 (1970): 609-630.
- [60] Yong, R. N., et al. "Application of risk analysis to the prediction of slope instability." *Canadian Geotechnical Journal* 14.4 (1977): 540-553.
- [61] Li, K. S., and P. Lumb. "Probabilistic design of slopes." *Canadian Geotechnical Journal* 24.4 (1987): 520-535.
- [62] Oka, Yoneo, and Tien H. Wu. "System reliability of slope stability." *Journal of Geotechnical Engineering* 116.8 (1990): 1185-1189.
- [63] Chowdhury, R. N., and D. W. Xu. "Geotechnical system reliability of slopes." *Reliability Engineering & System Safety* 47.3 (1995): 141-151.
- [64] Hassan, Ahmed M., and Thomas F. Wolff. "Search algorithm for minimum reliability index of earth slopes." *Journal of Geotechnical and Geoenvironmental Engineering* 125.4 (1999): 301-308.
- [65] Malkawi, Abdallah I. Husein, Waleed F. Hassan, and Fayez A. Abdulla. "Uncertainty and reliability analysis applied to slope stability." *Structural Safety* 22.2 (2000): 161-187.

- [66] El-Ramly, H., N. R. Morgenstern, and D. M. Cruden. "Probabilistic slope stability analysis for practice." *Canadian Geotechnical Journal* 39.3 (2002): 665-683.
- [67] Low, B. K. "Practical probabilistic slope stability analysis." *Proceedings, soil and rock America* 2 (2003): 2777-84.
- [68] Bhattacharya, G., et al. "Direct search for minimum reliability index of earth slopes." *Computers and Geotechnics* 30.6 (2003): 455-462.
- [69] Xue, Jian-Feng, and Ken Gavin. "Simultaneous determination of critical slip surface and reliability index for slopes." *Journal of Geotechnical and Geoenvironmental Engineering* 133.7 (2007): 878-886.
- [70] Zhao, Hong-bo. "Slope reliability analysis using a support vector machine." *Computers and Geotechnics* 35.3 (2008): 459-467.
- [71] Cho, Sung Eun. "Probabilistic stability analyses of slopes using the ANN-based response surface." *Computers and Geotechnics* 36.5 (2009): 787-797.
- [72] Bhattacharya, G., & Dey, S. "Reliability Evaluation of Earth Slopes by First Order Reliability Method." In *Proceedings of Indian Geotechnical Conference – 2010, GEOTrendz, IGS Mumbai Chapter & IIT Bombay* 2010.
- [73] Wang, Yu, Zijun Cao, and Siu-Kui Au. "Efficient Monte Carlo simulation of parameter sensitivity in probabilistic slope stability analysis." *Computers and Geotechnics* 37.7 (2010): 1015-1022.
- [74] Griffiths, D. V., Jinsong Huang, and Gordon A. Fenton. "Probabilistic infinite slope analysis." *Computers and Geotechnics* 38.4 (2011): 577-584.
- [75] Rickard, O.C., & Sitar, N. "bSLOPE: A Limit Equilibrium Slope Stability Analysis Code for iOS." *Geotechnical Engineering Report No. UCB/GT/12-01, Department of Civil and Environmental Engineering, UC Berkeley, Berkeley, CA* 2012.
- [76] Duncan, J. Michael, Stephen G. Wright, and Thomas L. Brandon. *Soil strength and slope stability*. John Wiley & Sons, 2014.

- [77] Nash, David. "Comparative Review of Limit Equilibrium Methods of Stability Analysis." *Slope Stability: Geotechnical Engineering and Geomorphology*. John Wiley and Sons New York. 1987. p 11-75, 43 fig, 6 tab, 70 ref. (1987).
- [78] Ang, Alfredo H-S., and Wilson H. Tang. *Probability concepts in engineering planning and design*. 1984.
- [79] ANG H-S, Alfredo, and H. Wilson TANG. *Probability Concepts in Engineering Planning And Design*. Vol. 1, Basic Principles. 1975.
- [80] Haldar, Achintya, and Sankaran Mahadevan. "First-order and second-order reliability methods." *Probabilistic structural mechanics handbook*. Springer US, 1995. 27-52.
- [81] Haldar, Achintya, and Sankaran Mahadevan. *Probability, reliability, and statistical methods in engineering design*. John Wiley & Sons, Incorporated, 2000.
- [82] Barakat, Samer A., Abdallah I. Husein Malkawi, and H. Tahat Ra'ed. "Reliability-based optimization of laterally loaded piles." *Structural safety* 21.1 (1999): 45-64.
- [83] Der Kiureghian, A. "The geometry of random vibrations and solutions by FORM and SORM." *Probabilistic Engineering Mechanics* 15.1 (2000): 81-90.
- [84] Melchers, Robert E. "On the ALARP approach to risk management." *Reliability Engineering & System Safety* 71.2 (2001): 201-208.
- [85] Arora, Jasbir S. *Introduction to Optimization*. McGraw-Hill, New York (1989).
- [86] Rosenblatt, Murray. "Remarks on a multivariate transformation." *The annals of mathematical statistics* (1952): 470-472.
- [87] Nataf, Andre. "Statistique mathematique-determination des distributions de probabilites dont les marges sont donnees." *Comptes Rendus Hebdomadaires Des Seances De L Academie Des Sciences* 255.1 (1962): 42.

- [88] Fiezler, Bernd, Rainer Hawranek, and Rüdiger Rackwitz. Numerische Methoden für probabilistische Bemessungsverfahren und Sicherheitsnachweise. LKI, 1976.
- [89] Rackwitz, Rüdiger. "Reliability analysis—a review and some perspectives." *Structural safety* 23.4 (2001): 365-395.
- [90] Chen, X., and N. C. Lind. "Fast probability integration by three-parameter normal tail approximation." *Structural Safety* 1.4 (1983): 269-276.
- [91] Bolton, Hermanus, Gerhard Heymann, and Albert Groenwold. "Global search for critical failure surface in slope stability analysis." *Engineering Optimization* 35.1 (2003): 51-65.
- [92] Zolfaghari, Ali R., Andrew C. Heath, and Paul F. McCombie. "Simple genetic algorithm search for critical non-circular failure surface in slope stability analysis." *Computers and geotechnics* 32.3 (2005): 139-152.
- [93] Malkawi, Abdallah I. Husein, Waleed F. Hassan, and Sarada K. Sarma. "Global search method for locating general slip surface using Monte Carlo techniques." *Journal of geotechnical and geoenvironmental engineering* 127.8 (2001): 688-698.